

УДК 539.374

Doi: 10.31772/2712-8970-2021-22-2-218-226

Для цитирования: Постановка задачи оптимизации структуры аппаратно-программного комплекса системы управления реального времени / С. Н. Ефимов, В. А. Терсков, О. Ю. Серикова, А. В. Попова // Сибирский аэрокосмический журнал. 2021. Т. 22, № 2. С. 218–226. Doi: 10.31772/2712-8970-2021-22-2-218-226.

For citation: Efimov S. N., Terskov V. A., Serikova O. Y., Popova A. V. Statement of the problem of optimization of the structure information processing computer appliances for real-time control systems. *Siberian Aerospace Journal*. 2021, Vol. 22, No. 2, P. 218–226. Doi: 10.31772/2712-8970-2021-22-2-218-226.

Постановка задачи оптимизации структуры аппаратно-программного комплекса системы управления реального времени

С. Н. Ефимов^{1*}, В. А. Терсков¹, О. Ю. Серикова², А. В. Попова¹

¹Сибирский государственный университет науки и технологий имени академика М. Ф. Решетнева
Российская Федерация, 660037, г. Красноярск, просп. им. газ. «Красноярский рабочий», 31

²Красноярский институт железнодорожного транспорта –
филиал Иркутского государственного университета путей сообщения
Российская Федерация, 660028, г. Красноярск, ул. Новая Заря, 2

*E-mail: efimov@bk.ru

В статье приведена постановка задачи оптимизации структуры аппаратно-программных комплексов, предназначенных для систем управления реального времени, применяемых, в том числе, в ракетно-космической отрасли. Кроме того, изучены особенности данной задачи, влияющие на выбор методов оптимизации. Делается вывод, что данная задача может быть эффективно решена с использованием эволюционных методов оптимизации.

Существующие модели производительности позволяют определять минимальную аппаратную конфигурацию многопроцессорного вычислительного комплекса. Предложенный в данной статье подход позволяет находить конфигурации, обладающие аппаратной избыточностью (по сравнению с минимальной конфигурацией), но, за счёт этого, имеющие большую вероятность нахождения в состояниях, обеспечивающих производительность, достаточную для достижения целей функционирования проектируемой системы управления реального времени. Описанный подход является более гибким, чем простое дублирование всех аппаратных компонентов минимальной конфигурации, что может быть использовано для уменьшения затрат на создание и эксплуатацию проектируемой системы управления.

Предложенная модель может быть использована для оптимизации производительности многопроцессорных аппаратно-программных комплексов систем управления реального времени. При этом нужно учитывать, что ресурсы, выделенные на создание и эксплуатацию аппаратно-программного комплекса, всегда ограничены. Поэтому целесообразно рассматривать задачу оптимизации производительности как многокритериальную: одним критерием будет производительность, а другим – затраты на создание аппаратно-программного комплекса.

Ключевые слова: аппаратно-программный комплекс, модель, производительность, системы управления реального времени, теория массового обслуживания.

Statement of the problem of optimization of the structure information processing computer appliances for real-time control systems

S. N. Efimov^{1*}, V. A. Terskov¹, O. Y. Serikova², A. V. Popova¹

¹Reshetnev Siberian State University of Science and Technology
31, Krasnoyarskii rabochii prospekt, Krasnoyarsk, 660037, Russian Federation

²Krasnoyarsk Institute of Railway Transport, branch of the Irkutsk State University of Communications
2, Novaya Zarya St., Krasnoyarsk, 660028, Russian Federation

*E-mail: efimov@bk.ru

The article presents the problem of optimizing the structure of information processing computer appliances for real-time control systems used, among other things, in the rocket and space industry. In addition, the features of this problem that affect the choice of optimization methods are studied. It's concluded that this problem can be effectively solved using evolutionary optimization methods.

Existing performance models allow you to determine the minimum hardware configuration of a multiprocessor computing system. The approach proposed in this article allows us to find configurations that have hardware redundancy (compared to the minimum configuration), but, due to this, have a greater probability of being in states that provide performance sufficient to achieve the goals of functioning of the designed real-time control system. The described approach is more flexible than simply duplicating all hardware components of the minimum configuration, which can be used to reduce the cost of creating and operating the designed control system.

The proposed model can be used to optimize the performance of multiprocessor hardware and software complexes of real-time control systems. At the same time, it should be taken into account that the resources allocated for the creation and operation of the hardware and software complex are always limited. Therefore, it is advisable to consider the problem of performance optimization as a multi-criterion: one criterion will be performance, and the other-the cost of creating a hardware and software complex.

Keywords: Computer appliance, model, performance, real-time system, queuing theory.

Introduction

A real-time system (RTS) is a hardware and software complex (HSC) that solves the problems of controlling various processes in conditions of time constraints.

Many modern control systems are real-time systems for which performance is a critical parameter: the control action must be developed in the required time, otherwise it becomes useless. This class of control systems includes, for example, control systems used in the rocket and space industry, air traffic control systems or technological process control systems. [1; 2].

Such control systems are hardware and software complexes that are a set of hardware and software that work together to accomplish a given task.

Requirements for the performance of computing systems used in real-time control systems are constantly increasing due to the increasing complexity of control objects.

Increasing the speed of computing technology has traditionally gone in two ways: increasing the clock frequency of processors and developing multiprocessor systems. Today, we can state that the possibilities of increasing the clock frequency have been exhausted, which is due to physical limitations [3]. This means that real-time control systems will inevitably be created on the basis of multiprocessor computing systems.

It is important to understand that the hardware performance requirements for real-time control systems are determined by the software that is used to generate the control action. Special requirements

are also imposed on the software of real-time control systems related to the need to ensure that the correct control action is obtained in a strictly defined time. Therefore it is advisable to study the performance of multiprocessor computing systems in close connection with the functioning of software.

For the design of multiprocessor hardware and software systems, a model of their performance is needed, which would make it possible to determine the speed of architecture options without experimentation, which can be extremely time-consuming and require significant costs.

The existing models of performance of multiprocessor computing systems [4–6] do not take into account the possibility of hardware failures and its recovery. In practice, when designing hardware and software complexes of control systems real-time, this aspect cannot be ignored, since a decrease in performance due to the failure of one of the processors can lead to the impossibility of generating a control action in the required time, which is unacceptable for real-time systems.

Performance model and formulation of the optimization problem

We consider a more general performance model, which includes additional states in which not all processors and buses are healthy, as well as transitions between states corresponding to processor and bus failures, as well as their recovery. The computing system is considered as a queuing system (QS).

The investigated HSC consists of N types of processors containing by M_i ($i = 1, 2, \dots, N$) processors of each type with the average execution time of one instruction T_{0i} . Processors are combined with RAM via N_1 buses. The service time of a request from a processor of the i type is τ_i . It is assumed that the time interval between any two adjacent claims obeys the Poisson distribution law with the parameter ν_i . The total flow of failures from processors of all types and interface buses also obeys the Poisson distribution law with the parameter λ_i . In addition, when evaluating the performance of a computing system, it is assumed that the time interval between two adjacent services obeys an exponential distribution law with the parameter μ_i , and the recovery time of buses and processors of the i type obeys the exponential law with the parameter ξ_i .

The states in which the considered system can be will be denoted as $a_{n, m_1, m_2, \dots, m_N, j_1, j_2, \dots, j_N}^{k, l}$. In this case, $(N_1 - n)$ interface buses are in good order and participate in the computational process, and n are faulty and are restored, $(M_1 - m_1)$ processors of the first type are serviceable and participate in the computational process, while m_1 are defective and are being restored, $(M_2 - m_2)$ processors of the second type are serviceable and participate in the computational process, and m_2 are faulty and restored, ..., $(M_N - m_N)$ processors of the N type are in good order and participate in the computational process, and m_N are faulty and restored. The system contains j_1 requests from processors of the first type, j_2 requests from processors of the second type, ..., j_N requests from processors of N type, k buses are busy with servicing, and l requests are in queues for servicing.

Due to the ordinariness of the streams of memory accesses, memory servicing of processors, failures and recovery of hardware components, transitions are possible only between states that differ in the value of only one index, and this index can either increase or decrease by one.

Composing the system of Kolmogorov – Chapman equations [7] according to the general rules for queuing systems, we obtain a system of linear differential equations for the probabilities of states in which the system can be.

Equating the derivatives to zero in this system, we obtain a system of linear algebraic equations for the probabilities of states in a stationary mode.

Solving the system with one of the numerical methods of linear algebra, we obtain the values of the probabilities of various states that can be used to determine any performance characteristics of the analyzed system [8].

In order for the failures of software elements to be considered statistically independent, like failures of various pieces of equipment, these elements must be developed independently [9]. This approach to critical software development is called multiversion programming (*N*-version programming) [10]. It is easy to understand that the performance of software developed using this approach increases with an increase in the number of different versions and an increase in the performance of their runtime environment [11].

Obviously by increasing the number of redundant hardware and software components, the system performance can be brought to any a given level [12]. However, such systems can be too expensive to develop and / or operate. Therefore performance models must be complemented by cost models. The cost of building hardware comes down to adding up the costs of the components. Models for estimating the costs of creating fault-tolerant software take into account the costs of developing multi-version software, labor costs of personnel employed at different stages of the software life cycle, etc. [13; 14].

The constructed models allow one to proceed to the formalization of the problem of choosing the optimal architecture options for multiprocessor hardware and software complexes of real-time control systems. In this case, two groups of criteria are obvious:

- performance criteria that must be maximized (the probability of being in a state in which performance is sufficient to generate a control action, etc.);
- cost criteria to be minimized (system cost, system development cost, operating cost, repair cost, etc.).

In this case, constraints will be imposed on the variable tasks, for example, in terms of energy consumption, speed, etc. To simplify the task, the cost criteria can be translated into constraints, since for all cost characteristics of the system, as a rule, there are upper bounds set by the customer of the system management. Having singled out the leader among the performance criteria, we get a one-criterion conditional optimization problem with a set of essential constraints, into which the rest of the criteria will go. In addition, there will be a set of natural constraints (for example, the number of hardware components is an integer and positive number).

We consider the type of variables in our optimization problem. In this case, we will assume given the maximum number of processor types N and software versions K , the maximum and minimum possible number of processors of each type and buses (for processors m_i^+ and m_i^- , respectively, $i=1, \dots, N$, and for buses n^+ and n^-). Let us denote by m_i the number of processors of the i type included in the structure of the hardware-software complex ($i = 1, \dots, N$), by n - the number of buses, and by k - the number of software versions. It is not difficult to see that the variables of our optimization problem (k, m_i, n) are integer, that is, we have a discrete optimization problem.

Let us give a formal record of the posed problem of optimizing the structure of a hardware-software complex with multiversion software for real-time control systems:

$$\begin{aligned}
 & R_0(m_1, \dots, m_N, n, k) \rightarrow \max, \\
 \text{under conditions} \quad & R_l(m_1, \dots, m_N, n, k) \geq R_l^0, l = 1, \dots, L_R, \\
 & C_l(m_1, \dots, m_N, n, k) \leq C_l^0, l=1, \dots, L_C, \\
 & m_i^- \leq m_i \leq m_i^+, i = 1, \dots, N, \\
 & n^- \leq n \leq n^+, \\
 & 1 \leq k \leq K.
 \end{aligned}$$

In this problem, the following designations are adopted: R_0 is the leading criterion for evaluating performance; $R_l, l = 1, \dots, L_R$, are secondary performance evaluation criteria; $C_l, l = 1, \dots, L_C$, - cost estimation criteria; R_l^0, C_l^0 - maximum permissible levels of criteria converted to restrictions.

When designing the optimal structure of the hardware-software complex one cannot focus on the maximum performance of special processors, but it is necessary to choose it so as to ensure the maximum performance of the entire hardware-software complex as a whole. For the formal statement of the problem, this means that the values of the average execution time of one instruction T_{0i} by processors of the i type cannot be constant, but must also be included in the number of optimization variables. Moreover, the parameters of the system v_i and μ_i become functions of T_{0i} , that is, $v_i = v_i(T_{0i})$, $\mu_i = \mu_i(T_{0i})$. This leads to a significant complication of the optimization problem, turning it into a two-level first hierarchical task:

$$(R_0^*(T_{01}, \dots, T_{0i}, T_{0N}), R_l^*(T_{01}, \dots, T_{0i}, T_{0N}), C_l^*(T_{01}, \dots, T_{0i}, T_{0N})) \rightarrow \text{extr},$$

где R_0^* , R_l^* и C_l^* is optimization problem solution.

First of all, it should be noted that the space of possible solutions is discrete, since the configuration of the hardware-software complex is determined by the number of processors of various types and RAM buses, which can only be integers. At the same time, the power of the search space grows rapidly with the increase in the number of processor types.

If we roughly estimate the power of the optimization space, then we get the total number of possible configurations more than $1,6 \cdot 10^{20}$. At the same time, significant restrictions will not significantly reduce the number of search points.

A significant problem for solving the resulting optimization problem is created by the method of calculating objective functions (criteria), which are mostly given algorithmically.

There are all the signs of a complex optimization problem: algorithmically specified functions, different types of problem variables, a variable number of sought variables, a large search area for an optimal solution.

When solving such optimization problems, evolutionary optimization algorithms have proven themselves well [15–18]. Therefore, the study of the effectiveness of evolutionary algorithms when optimizing the structure of hardware and software complexes of real-time control systems can be indicated as a possible direction for further research.

Conclusion

The existing performance models make it possible to determine the minimum hardware configuration of a multiprocessor computing complex. The approach proposed in this article makes it possible to find configurations that have hardware redundancy (compared to the minimum configuration), but, due to this, have a high probability of being in states that provide performance sufficient to achieve the goals of functioning of the designed real-time control system. The described approach is more flexible than simple duplication of all hardware components of the minimum configuration, which can be used to reduce the cost of creating and operating the designed control system.

The proposed model can be used to optimize the performance of multiprocessor hardware and software complexes of real-time control systems. It should be borne in mind that the resources allocated for the creation and operation of the hardware and software complex are always limited. Therefore, it is advisable to consider the problem of performance optimization as a multi-criteria one: one criterion will be performance, and the other will be the cost of creating a hardware-software complex.

Thus, this article presents the formulation of the problem of optimizing the structure of hardware and software complexes with multiversion software designed for real-time control systems. In the

future, it is proposed to investigate the effectiveness of using evolutionary optimization methods to solve this problem.

Библиографические ссылки

1. Васильев В. А., Легков К. Е., Левко И. В. Системы реального времени и области их применения // Информатика и космос. 2016. № 3. С. 68–70.
2. Buttazzo G. Hard Real-Time Computing Systems: Predictable Scheduling Algorithms and Applications. New York, NY, Springer. 2011.
3. Sutter H. The free lunch is over: A fundamental turn toward concurrency in software // Dr. Dobbs's Journal. 2005. 30(3) [Электронный ресурс]. URL: <http://www.gotw.ca/publications/concurrency-ddj.htm> (дата обращения: 11.03.2021).
4. Liu Wang, Xiao Li, Shanghong Li Research on the Performance of Robot Multiprocessor Control System Based on BS Structure Digital Media // Microprocessors and Microsystems. 2020. Vol. 75. P. 103067.
5. Ефимов С. Н., Терсков В. А. Реконфигурируемые вычислительные системы обработки информации и управления. Красноярск : КРИЖТ ИрГУПС, 2013. 249 с.
6. Костров Б. В., Мартышкин А. И. Исследование структурной организации и оценка производительности многопроцессорных вычислительных систем с общей шиной // Известия Тульского гос. ун-та. Технич. науки. 2018. Вып. 2. С. 152–162.
7. Вентцель А. Д. Курс теории случайных процессов. М. : Наука, 1996. 400 с.
8. Бахвалов Н. С., Жидков Н. П., Кобельков Г. М. Численные методы. М. : БИНОМ. Лаборатория знаний, 2004. 636 с.
9. Липаев В. В. Экономика производства программных продуктов. М. : СИНТЕГ, 2011. 358 с.
10. Использование метода роя частиц для формирования состава мультиверсионного программного обеспечения / И. В. Ковалев, Е. В. Соловьев, Д. И. Ковалев и др. // Приборы и системы. Управление, контроль, диагностика. 2013. № 3. С. 1–6.
11. К вопросу реализации мультиверсионной среды исполнения бортового программного обеспечения автономных беспилотных объектов средствами операционной системы реального времени / И. В. Ковалев, В. В. Лосев, М. В. Сарамуд и др. // Вестник СибГАУ. 2017. Т. 18, № 1. С. 58–61.
12. Efimov S. N., Tyapkin V. N., Dmitriev D. D., Terskov V. A. Methods of Assessing the Characteristics of the Multiprocessor Computer System Adaptation Unit // Journal of Siberian Federal University. Mathematics & Physics. 2016. No. 9 (3). P. 288–295.
13. Глазова М. А. Модель СОСОМО II: анализ и пути усовершенствования // Экономика, статистика и информатика. 2008. № 3. С. 63–67.
14. Шеенок Д. А., Кукарцев В. В. Прогнозирование стоимости разработки систем с программной избыточностью // Известия Волгоградского гос. технич. ун-та. 2013. № 14 (117). С. 101–105.
15. Тархов Д. А., Радченко Д. С. Распределенные алгоритмы оптимизации // Современные информационные технологии и ИТ-образование. 2015. Том 11, № 2. С. 404–408.
16. Semenkina O. E., Popov E. A., Seminkin E. S. Cooperative self-configuring nature-inspired algorithm for a scheduling problem // IOP Conference Series: Materials Science and Engineering. 2021. P. 12080.
17. Goldberg D. E. Genetic algorithms in search, optimization, and machine learning, Reading, MA: Addison-Wesley Professional. 1989.

18. Полякова А. С., Липинский Л. В., Семенкин Е. С. Автоматизированная система формирования состава коллектива многокритериальным генетическим алгоритмом. М. : Роспатент. 2020. № государственной регистрации программы для ЭВМ RU 2020663770 от 22.10.2020.

References

1. Vasil'ev V. A., Legkov K. E., Levko I. V. [The real-time systems and applications]. *Informaciya i kosmos*. 2016, No. 3, P. 68–70. (In Russ.)
2. Buttazzo G. *Hard Real-Time Computing Systems: Predictable Scheduling Algorithms and Applications*. New York, NY, Springer. 2011.
3. Sutter H. The free lunch is over: A fundamental turn toward concurrency in software // *Dr. Dobbs's Journal*. 2005, No. 30 (3). Available at: <http://www.gotw.ca/publications/concurrency-ddj.htm> (accessed: 11.03.2021).
4. Liu Wang, Xiao Li, Shanghong Li Research on the Performance of Robot Multiprocessor Control System Based on BS Structure Digital Media. *Microprocessors and Microsystems*. 2020, Vol. 75, P. 103067.
5. Efimov S. N., Terskov V. A. *Rekonfiguriruyemye vychislitel'nye sistemy obrabotki informacii i upravleniya* [Reconfigurable computing systems for information processing and management]. Krasnoyarsk, KRIZHT IrGUPS Publ., 2013, 249 p.
6. Kostrov B. V., Martyshkin A. I. [Investigation of the structural organization and performance evaluation of multiprocessor computing systems with a common bus]. *Izvestiya Tul'skogo gosudarstvennogo universiteta. Tekhnicheskie nauki*. 2018, Vol. 2, P. 152–162. (In Russ.)
7. Wentzel A. D. *Kurs teorii sluchajnyh processov* [Course of the theory of random processes]. Moscow, Nauka Publ., 1996, 400 p.
8. Bakhvalov N. S., Zhidkov N. P., Kobelkov G. M. *Chislennyye metody* [Numerical methods]. Moscow, BINOM. Laboratoriya znaniy Publ., 2004, 636 p.
9. Lipaev V. V. *Ekonomika proizvodstva programmnyh produktov* [The economics of the software engineering]. Moscow, SINTEG Publ., 2011, 358 p.
10. Kovalev I. V., Solov'ev E. V., Kovalev D. I. et al. [Application of particle swarm optimization to design of N-version software composition]. *Pribory i sistemy. Upravlenie, kontrol', diagnostika*. 2013, No. 3, P. 1–6. (In Russ.)
11. Kovalev I. V., Losev V. V., Saramud M. V. et al. [On the issue of implementing a multiversion execution environment for on-board software of autonomous unmanned objects by means of a real-time operating system]. *Vestnik SibGAU*. 2017, Vol. 18, No. 1, P. 58–61. (In Russ.)
12. Efimov S. N., Tyapkin V. N., Dmitriev D. D., Terskov V. A. Methods of Assessing the Characteristics of the Multiprocessor Computer System Adaptation Unit. *Journal of Siberian Federal University. Mathematics & Physics*. 2016, No. 9 (3), P. 288–295.
13. Glazova M. A. [COCOMO II Model: Analysis and Improvement]. *Ekonomika, statistika i informatika*. 2013, No. 14 (117), P. 101–105. (In Russ.)
14. Sheenok D. A., Kukarcev V. V. [Forecasting the cost of developing systems with software redundancy]. *Izvestiya Volgogradskogo gosudarstvennogo tekhnicheskogo universiteta*. 2018, Vol. 2, P. 152–162. (In Russ.)
15. Tarhov D. A., Radchenko D. S. [Distributed optimization algorithms]. *Sovremennyye informacionnyye tekhnologii i IT-obrazovanie*. 2015, Vol. 11, No. 2, P. 404–408. (In Russ.)

16. Semenkina O. E., Popov E. A., Semenko E. S. Cooperative self-configuring nature-inspired algorithm for a scheduling problem. *IOP Conference Series: Materials Science and Engineering*. 2021, P. 12080.
17. Goldberg D. E. Genetic algorithms in search, optimization, and machine learning, Reading, MA: Addison-Wesley Professional. 1989.
18. Polyakova A. S., Lipinskiy L. V., Semenko E. S. *Avtomatizirovannaya sistema formirovaniya sostava kollektiva mnogokriterial'nym geneticheskim algoritmom* [An automated system for forming the composition of a team using a multicriteria genetic algorithm]. Moscow, Rospatent, 2020, No. gosudarstvennoj registracii programmy dlya EVM [state registration of a computer program] RU 2020663770. (In Russ.)

© Ефимов С. Н., Терсков В. А., Серикова О. Ю., Попова А. В., 2021

Ефимов Сергей Николаевич – кандидат технических наук, доцент, доцент кафедры информационно-управляющих систем; Сибирский государственный университет науки и технологий имени академика М. Ф. Решетнева. E-mail: efimov@bk.ru.

Терсков Виталий Анатольевич – доктор технических наук, профессор, профессор кафедры информационно-управляющих систем; Сибирский государственный университет науки и технологий имени академика М. Ф. Решетнева. E-mail: terskovva@mail.ru.

Серикова Олеся Юрьевна – аспирант; Красноярский институт железнодорожного транспорта – филиал Иркутского государственного университета путей сообщения. E-mail: olesyaserik@mail.ru.

Попова Анастасия Валерьевна – магистрант; Сибирский государственный университет науки и технологий имени академика М. Ф. Решетнева. E-mail: nasty.popowa@yandex.ru.

Efimov Sergei Nikolaevich – Cand. Sc., assistant professor, department of informational and control systems; Reshetnev Siberian State University of Science and Technology. E-mail: efimov@bk.ru.

Terskov Vitalii Anatolyevich – Dr. Sc., professor, department of informational and control systems; Reshetnev Siberian State University of Science and Technology. E-mail: terskovva@mail.ru.

Serikova Olesya Yuryevna – graduate student; Krasnoyarsk Institute of Railway Transport, branch of the Irkutsk State University of Communications. E-mail: olesyaserik@mail.ru.

Popova Anastasiya Valer'evna – master's degree student; Reshetnev Siberian State University of Science and Technology. E-mail: nasty.popowa@yandex.ru.

УДК 658.5:629.78

Doi: 10.31772/2712-8970-2021-22-2-227-243

Для цитирования: Картамышев А. С., Черныш Б. А. Разработка эффективной системы информационной поддержки принятия управленческих решений на предприятиях ракетно-космической отрасли // Сибирский аэрокосмический журнал. 2021. Т. 22, № 2. С. 227–243. Doi: 10.31772/2712-8970-2021-22-2-227-243.

For citation: Kartamyshev A. S., Chernysh B. A. Development of an effective system of information support for management decision-making at the enterprises of the rocket and space industry. *Siberian Aerospace Journal*. 2021, Vol. 22, No. 2, P. 227–243. Doi: 10.31772/2712-8970-2021-22-2-227-243.

Разработка эффективной системы информационной поддержки принятия управленческих решений на предприятиях ракетно-космической отрасли

А. С. Картамышев^{1*}, Б. А. Черныш²

¹АО «Информационные спутниковые системы» имени академика М. Ф. Решетнева»
Российская Федерация, 662972, г. Железногорск Красноярского края, ул. Ленина, 52

²Сибирский государственный университет науки и технологий имени академика М. Ф. Решетнева
Российская Федерация, 660037, г. Красноярск, просп. им. газ. «Красноярский рабочий», 31

*E-mail: kartam@iss-reshetnev.ru

В статье рассматривается роль информационных технологий на промышленных предприятиях ракетно-космической отрасли, приводятся результаты анализа научных источников по организации систем информационной поддержки для принятия управленческих решений, анализ существующих методик построения управленческого учета на предприятиях и способов его автоматизации. Делаются выводы о недостаточной проработанности изученных решений, как с точки зрения логики организации учета, так и с технической точки зрения. Определяются основные задачи системы информационной поддержки, методы формирования эффективного управленческого учета и цели его внедрения. Предлагается подход к созданию системы информационной поддержки в виде надстроенной управляющей базы данных в виде OLAP-решения, посредством которой интегрируются функциональные информационные системы и строится детализированный управленческий учет, связанный с бухгалтерским и налоговым учетами в единую систему в едином информационном пространстве. Описываются преимущества внедрения предлагаемой системы, позволяющей проводить всесторонний ретроспективный и оперативный анализ текущего состояния протекающих на предприятии процессов с денежной оценкой средствами SQL с высокой степенью доверия к данным. Оговариваются принципы создания элементов информационной системы для последующего эффективного план-факт анализа и выработки управленческих решений. Приводится схема организации единого информационного пространства и системы, обеспечивающей информационную поддержку процессов управления предприятием, рассматриваются основные информационные потоки. Описывается логика поддержания процесса формирования структурированного хранилища данных при автоматизации финансово-экономической части АСУП на базе представляемого способа организации данных, позволяющая увязать управленческий, бухгалтерский и налоговый учеты с одним источником актуальных данных, создавая при это эффективное OLAP-решение. Приводится наглядный пример организации данных в виде увязки средствами БД отражений первичных документов предлагаемым способом, обеспечивающим возможность оперативного анализа дебиторской и кредиторской задолженности и осуществления предварительного финансового контроллинга. Приводятся

примеры интерфейсов пользователя из разработанной системы информационной поддержки, построенной на описываемых способах организации данных. Делаются выводы об эффективности предлагаемого решения.

Ключевые слова: система информационной поддержки принятия управленческих решений, интеграция, единое информационное пространство, финансовый контроллинг, OLAP-решение.

Development of an effective system of information support for management decision-making at the enterprises of the rocket and space industry

A. S. Kartamyshev^{1*}, B. A. Chernysh²

¹JSC Academician M. F. Reshetnev "Information Satellite Systems"
52, Lenin St., Zheleznogorsk, Krasnoyarsk region, 662972, Russian Federation

²Reshetnev Siberian State University of Science and Technology
31, Krasnoyarskii rabochii prospekt, Krasnoyarsk, 660037, Russian Federation

*E-mail: kartam@iss-reshetnev.ru

The article examines the role of information technology at industrial enterprises of the rocket and space industry, provides the results of the analysis of scientific sources to organize information support systems for making management decisions, an analysis of existing methods for constructing management accounting at enterprises and methods of its automation. Conclusions are made about the insufficient elaboration of the studied solutions, both from the point of view of the logic of the organization of accounting, and from a technical point of view. The main tasks of the information support system, methods of forming effective management accounting and the goals of its implementation are determined. An approach to create an information support system in the form of a built-in control database in the form of an OLAP solution is proposed, through which functional information systems are integrated, and detailed management accounting related to accounting and tax accounting is built into a single system in a single information space. The article describes the advantages of implementing the proposed system, which allows for a comprehensive retrospective and operational analysis of the current state of the processes occurring at the enterprise with a monetary value using SQL tools with a high degree of confidence in the data. The principles of creating elements of the information system for the subsequent effective plan-fact analysis and development of management decisions are discussed. A diagram of the organization of a single information space and a system that provides information support for enterprise management processes is given, the main information flows are considered. The logic of maintaining the process of forming a structured data warehouse is described, while automating the financial and economic part of the automated control system based on the presented method of organizing data, which allows to link management, accounting and tax accounting with one source of relevant data, while creating an effective OLAP solution. An illustrative example of the organization of data in the form of linking the reflections of primary documents by means of a database using the proposed method, which provides the possibility of operational analysis of receivables and payables and the implementation of preliminary financial controlling, is given. The research provides examples of user interfaces from the developed information support system based on the described methods of data organization. Conclusions are made about the effectiveness of the proposed solution.

Keywords: information support system for making management decisions, integration, unified information space, financial controlling, OLAP solution.

Introduction

The prerequisite to implement economic activities (EA) is the application of information technology (IT) at the industrial enterprises to automate design processes, production management, logistic activities, financial economic and accounting processes. Successful automation of enterprise management system increases the efficiency of the management, stimulates labour productivity due to accelerating the information exchange in agreeing various issues, transiting to digital document workflow, reducing the influence of the human factor and the possibility of automated standard decision making. Information systems (IS) and processes at enterprises should be interdependent, since currently, it is impossible to provide workflow and management accounting without information support. IS ensures the fulfillment of the set goal satisfying numerous requirements for the production and accounting process, and not only records the results of business processes (BP) [1].

The relevance of the study in this article is determined due to the search for solutions to improve the efficiency of enterprise management in the rocket and space industry (RSI) within the state defense orders and high uncertainty.

An effective information support to the management process is required to make informed, relevant economic decisions based on reliable information from various sources, formed by means of accounting and analytical support for management processes, structured and supported according to certain rules.

Research analysis

The targeted research has demonstrated that the purpose of IP management is to provide consumers with appropriate relevant information in a certain subject area in the form of up-to-date information products [2].

Considering that the subject data of various processes are distributed over their functional IS, and management decisions are determined due to analyzing the financial and economic state of the enterprise and the ongoing processes, developing systems of information support management based on current economic data, connected in a database with the production process; the current economic data are available at any time. The process requires a data management tool for EA, integrated with functional IS containing the results of this activity, thereby forming management accounting (MA) at the enterprise [3].

In the sources [4–14], the methodology to construct MA mainly consists in determining the sequence of actions from the accounting audit to recommendations to automate the processes described and regulated before, which ultimately allow obtaining various mid-assessment of information necessary for making management decisions. However, there is a lack of clearly described solutions to organizing MA information support at large enterprises. One of the most important conclusions made as a result of the analysis is the need for MA obtaining data both on the planned performance of the enterprise and on the actual ones in the form of accumulated costs in case the required results are achieved. The purpose to develop information support to MA is to manage costs to control the cost of production. MA organization should be based on the management policy principles and consider enterprise features.

MA automation means a method of technical systematization of information into a single database with collecting, processing and transmitting the required information, which could be used to compile both accounting and management reporting, its measurement and evaluation of the results obtained. The analysis of sources [4–14] in the field of management accounting automation showed the following.

1. The proposed solutions based on accounting data are ineffective due to a significant information time lag concerning the fact of business transactions (BT), insufficient for managerial conclusions of analysis reflected in accounting entries, however, these data on work in progress (WIP) are not connected with the sales objects, affecting the cost of production. Fig.1 introduces a conventional approach to MA organization.

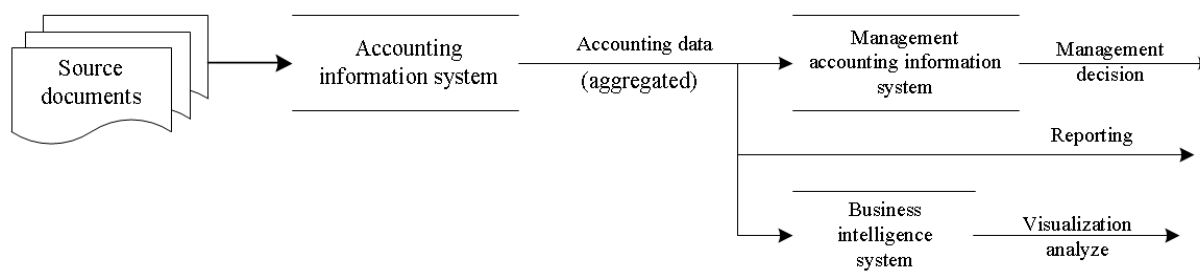


Рис. 1. Общий подход к организации УУ

Fig. 1. General approach to the organization of management accounting

2. MA automation problem is mainly solved by developing a parallel A autonomous MA system in an economic entity, which will certainly results in data discrepancies and distrust to information. Such solutions require very high qualifications of employees who process primary documents, since they are responsible for the correct distribution of the primary data across the MA registers. Large enterprises obtain employees working with primary documents being ordinary registrars and, as a rule, not having such skills when entering documents into the accounting system.

3. There are no ready-made solutions meeting the needs of companies in the rocket and space industry in the literature studied; on the contrary, there is a statement that such software has not yet been developed to be adapted for accounting, tax and management accounting simultaneously, this forces enterprises to use a whole set of tools, which is often inconvenient due to database incompatibility [14]. Among the many different programs and local solutions, the visibility (traceability) of the MA goals, the stages of their achievement with reference to the objects of control are lost.

Most of the scientists researching the problem of MA organization [4–14] conclude that it is necessary to build IS and their inherent information flows to store data to be considered as an OLAP system and be able to continuously compare the current data with the planned values of economic indicators tied to the objects of control and accounting. However, even such an approach to MA automation can contain hidden problems: processed and consolidated data, rather than primary data, can be overloaded, which can lead to distortion of information obtained on the basis of created data marts. In addition, accounting data is generated according to the rules and, for the accounting needs, they are unacceptable for operational decisions due to a delay. And, finally, the most important drawback of all approaches to the MA automation based on accounting data is the accounting records the performed BT and beautiful pictures in the BI system will show what a manager has not done, and they will use these data only to prepare a solution for the future, if the same conditions are created.

The most important accounting principles for MA is the availability of operational information about the real state of affairs rather than the document registration in the accounting system [8]. Accounting and MA automation does not only significantly increase the efficiency of the accounting department, but also reduces the likelihood of errors, improves the quality and efficiency of reporting by embedding mechanisms for BT visual reflection into the software [9].

In the rocket and space industry the main tasks to automate information support systems of enterprise management are:

- time-efficient analysis of receivables and payables;
- preliminary financial controlling (both at the stage of agreeing the payment requirement and creating a payment document);
- time-efficient tax accounting;
- organization of related management, accounting and tax accounting;
- management of the production cost in the form of accounting, controlling and managing production costs, decomposed by the price structure;
- connection of management accounting with PDM and PLM systems for accounting of technical results of activities to help detail work in progress to accounting objects.

In order to comply with the law, to ensure the ability to manage the life cycle (LC) of the manufactured products and their impact on the economy, developing information support systems become necessary for the processes occurring at the enterprise according to the regulatory authority requirements to accounting. The regulations to maintain separate management, accounting and tax accounting at an enterprise determine the conditions for the functionality of management information and control system (MICS), for the processes of structuring, transforming and storing information in a form meeting the requirements of regulatory documents and regulatory agencies for enterprise reporting, as well as suitable for analyzing statistical data. The tool for recording and analyzing data on EA should be able to integrate with functional IS, where the activity results are planned and considered. Up-to-date information about any individual item of the product should be available automatically in various views. Such an integrated IS should make compatible the processes of development and production of technology with the economics of these processes and can be used at enterprises as a PLM system. Fig.2 introduces MA main aspects.

The entire chain of processes from letting a contract to delivering finished products is accompanied by primary documents, the data of which are subject to mandatory accounting and tax accounting. The quality of information support to MA depends on the created opportunity to analyze the data of these documents in various aspects and with the least time serving the information consumer's interests. At large enterprises, with a large number of primary documents without an effective MA system, quickly finding results on constantly emerging issues is very difficult.

Analyzing standards, methods and experience in developing information support tools inevitably leads to an understanding the need for a transition to process management [15–19]. The most suitable and practical technology, combined with the principles of CALS/IPS, is the methodology to describe information flows in the IDEF0 notation and the Workflow technology of workflow management, supporting the BPMN notation [19]. A resolved issue can be considered the availability of BP description tools developed in the Russian Federation with the support of notations allowing to create detailed business models and generate regulations to implement processes in the covered areas of activity and of performers' job descriptions .

The management methodology, based on using the principles and developing information support for this, forms understanding of MA continuity and the quality management system (QMS) of an enterprise [17]. For managers to unambiguously understand a set of control objects and economic aspects of financial and economic activities (FEA), it is necessary to develop a corporate enterprise management system in a single information space (SIS) using one control database, with an unambiguous identification of accounting objects and primary documents associated with their life cycle.

Fig.3 demonstrates the principle of organizing information flows among the main functional systems and information consumers, the principle to which one should strive for MA purposes [18].

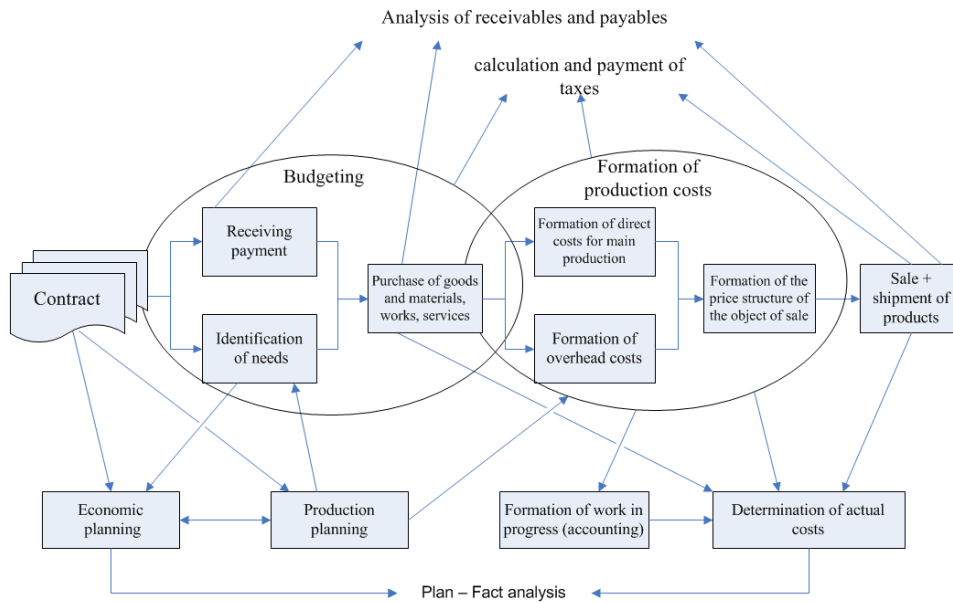


Рис. 2. Аспекты управленческого учета

Fig. 2. Aspects of management accounting

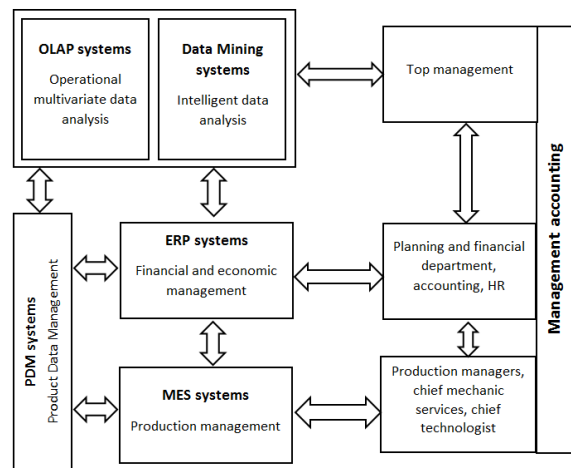


Рис. 3. Организация информационных потоков УУ как элемент СМК

Fig. 3. Organization of information flows of management accounting as an element of a quality management system

Developing MA information support

The most realistic and effective, and simultaneously, the most difficult way to develop MA information support is to develop MA database in the form of a SIS, in which the storage and accounting of the data of the main primary documents will be organized immediately in the form of an OLAP-solution that excludes the consolidation and overloading of primary data, and using the same structured array for the accounting and tax accounting. Realizing the solution will be effective through a built-in database and interfaces corresponding to MA goals, providing the processes developed for MA formation and their information flows. The data arrays formed by the solution are easily integrat-

ed with the necessary functional IS at the database level, as a result of which the linkage of subject IS with the economic system is organized, on the basis of which most management decisions are made.

Enterprise management, in addition to technical aspects, should be considered as a system of inter-related processes, where economic indicators (direct costs, payroll, overhead costs, budget, financing, etc.) act as controlled parameters. The result (feedback) to the deviation of the actual indicators from the planned ones will be a balanced management decision. For an effective MA, it is necessary to develop a methodology to store data for time-efficient analytical activities and making informed management decisions, as well as an applied functional model of the accounting process for the costs to develop products with the ability to provide preliminary, in most cases, automated financial control. Fig.4 demonstrates the developed approach to MA organization at the rocket and space industry enterprises.

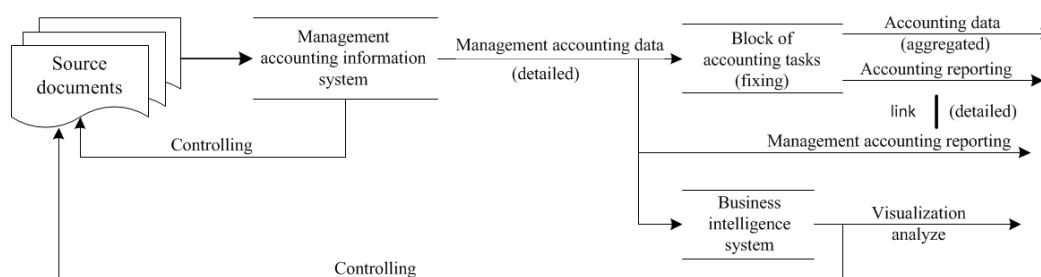


Рис. 4. Предлагаемый подход к организации УУ

Fig. 4. Proposed approach to organizing management accounting

The developed logic of building information systems distributes the entire burden of MA organization among the employees responsible for the primary documents, and the add-on in the form of the proposed software ensures the structuring and storing the data in the database according to the rules allowing to form MA and the related accounting and tax accounting, and not only hampering the work of the system users, but also facilitating it due to preliminary automated controlling. Many potential errors are eliminated at the stages of inputting primary information and linking data in the form of logically completed BTs. The result of the MA information support implementation system at the enterprise, based on the proposed approach, will be a unified database of the structured data concerning the progressing BT, suitable for a comprehensive operational analysis by SQL means.

Realizing this approach is possible when forming an OLAP solution based on a specially designed data warehouse meeting the MA goals. The most effective way of realization seems to be the development of a ROLAP system with storing actual data in the database tables [20]. The database logical structure must be developed to integrate functional systems on the same solution, which is also the most effective way of integrating IS. To form an up-to-date set of data available at any time, it is more expedient to use an incremental update of data changed in the OLTP system [21]. This approach contributes to developing a structured data repository prepared for the management analysis before it enters the accounting system.

To ensure the possibility of measuring MA controlled parameters, it is necessary to introduce analytical markers to the primary documents, selected from the reference books developed for MA purposes, corresponding to the logic of BP primary documents. As a basis for the formation of an OLAP cube for the main external primary financial documents, the most effective is to use the storage architecture with dimensions according to the "snowflake" scheme, in which it is necessary to create

fact tables providing the physical organization of data and organize links of primary documents corresponding to the logic of the fixed BP. It is also rational to use normalized data warehouses in one relational data storage systems (RDSS) for linking with OLTP systems of our own design. Metadata deserves paramount attention in the development of a data warehouse: information about the structure, placement and transformation of data, due to which the effective interaction of various components of the warehouse is ensured.

Management solution is, as a rule, a respond to a comparison of indicators that characterize the process. For MA, the forecast manufacture process values are compared to the actual accumulated data of the EA results. For convenience, efficiency, traceability and the possibility of automated analysis of ongoing processes, it is advisable to build planning systems according to the same principles in the SIS with a fact collection system, based on the same reference information (NRI). The systems should conduct efficient and automated plan/actual analysis. Adhering to the opinion that the cost of products is formed by the processes, it becomes obvious to develop and improve BP to eliminate information gaps, forming a root model (without information gaps and loss) and the basis for BP regulation, this results in increasing labour efficiency, management efficiency, and reducing manufacture costs.

For planning, amenable to operational analysis by means of SQL, it is advisable to build a project management system in the SIS as a central node integrated with all accounting systems, that contribute to linking all work performed at the enterprise with the concept of a project, which should go through all software and form the EA management basis. It is the work from the project work plan that should be the connecting element in all BPs, and its cost attributes should become the basis for the MA system. By linking work with sales objects (accounting objects), it is possible to obtain the opportunity to quickly manage the timing of production, estimate resources, predict the prospects for the activities of departments, as well as evaluate profitability both for individual projects and across the enterprise, which increases efficiency and transparency in the field of management.

The data in MICS in all of its accounting systems should be linked to forming the main information flow; Fig.5 demonstrates its diagram.

Applying certain methods of data structuring, based on the coding of analytical information about the object of control, the SIS prepares data suitable for automated control, increases their connectivity and traceability, which contributes to reducing the time of their analysis, improving the quality and relevance of the solutions generated and the management effectiveness in general.

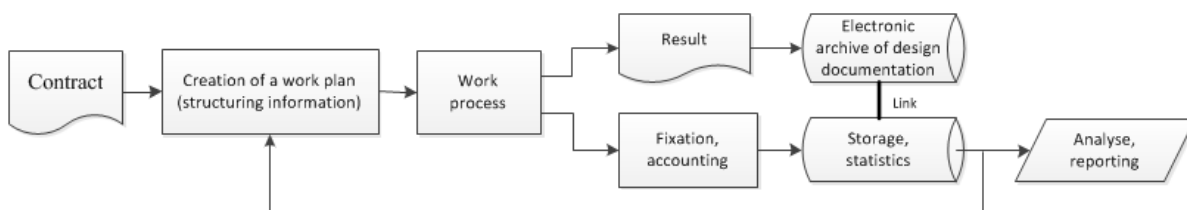


Рис. 5. Схема основного информационного потока в АСУП

Fig. 5. Diagram of the main information flow in the automated control system

Fig. 6 shows a simplified diagram to arrange SIS for the information support system, where each process is organized using the developed software, its implementation leads to automating the main information flows controlled in MA, and thereby, ensures the efficiency of the enterprise management process. Introducing such processes and software organizing the presented information flows in the

SIS makes it possible to conduct an operational plan/actual analysis at any time and generate any detailed reporting that corresponds to official accounting and tax accounting.

To support the process of forming a structured data warehouse when automating the MICS financial and economic part based on the presented method of data arrangement, the main software modules "Purchases" and "Sales" have been developed, in which all primary financial documents accompanying commodity-money relations are entered, registered and taken into account with counterparties, as well as proactive control over the legality of spending money. The main purpose of these modules is to create and maintain SIS by linking the reflections of primary documents to each other in the database tables and marking the resulting lines with analytical features. Documents are linked according to the principle of belonging to each other, where one document is the basis for generating another, or documents are two parties to one financial and economic transaction (FET). Documents are linked both fully and partially in the amount of money that identifies the weight in monetary terms of a particular FET [22].

The actual links of documents are stored in database tables and are supported by a set of rules and restrictions that correspond to the developed logic through user interfaces. The software logic provides the information structuring, the organization and maintenance of data connections in the described way for the entities "Purchase" and "Sale"; it is shown in Fig. 7 and 8 respectively.

Connecting within the framework of the developed method of reflecting the primary documents to purchases and sales, we obtain a lined up detailed MA within the framework of the cash flow before financial transactions on the accounting. The link between purchases and sales is carried out by connecting a contract and a customer with contracts for supplying goods, work, services through an open order in an integrated project management system [22].

Accounting records the same FET with the same analytics with a link to the primary documents. When using the developed method of linking primary financial documents, there is no need to build MA while analyzing receivable and payable on accounting entries, as it is arranged in most economic systems. Actual data are available to analyze them immediately after linking the documents and it can be changed before the documents are posted on accounting.

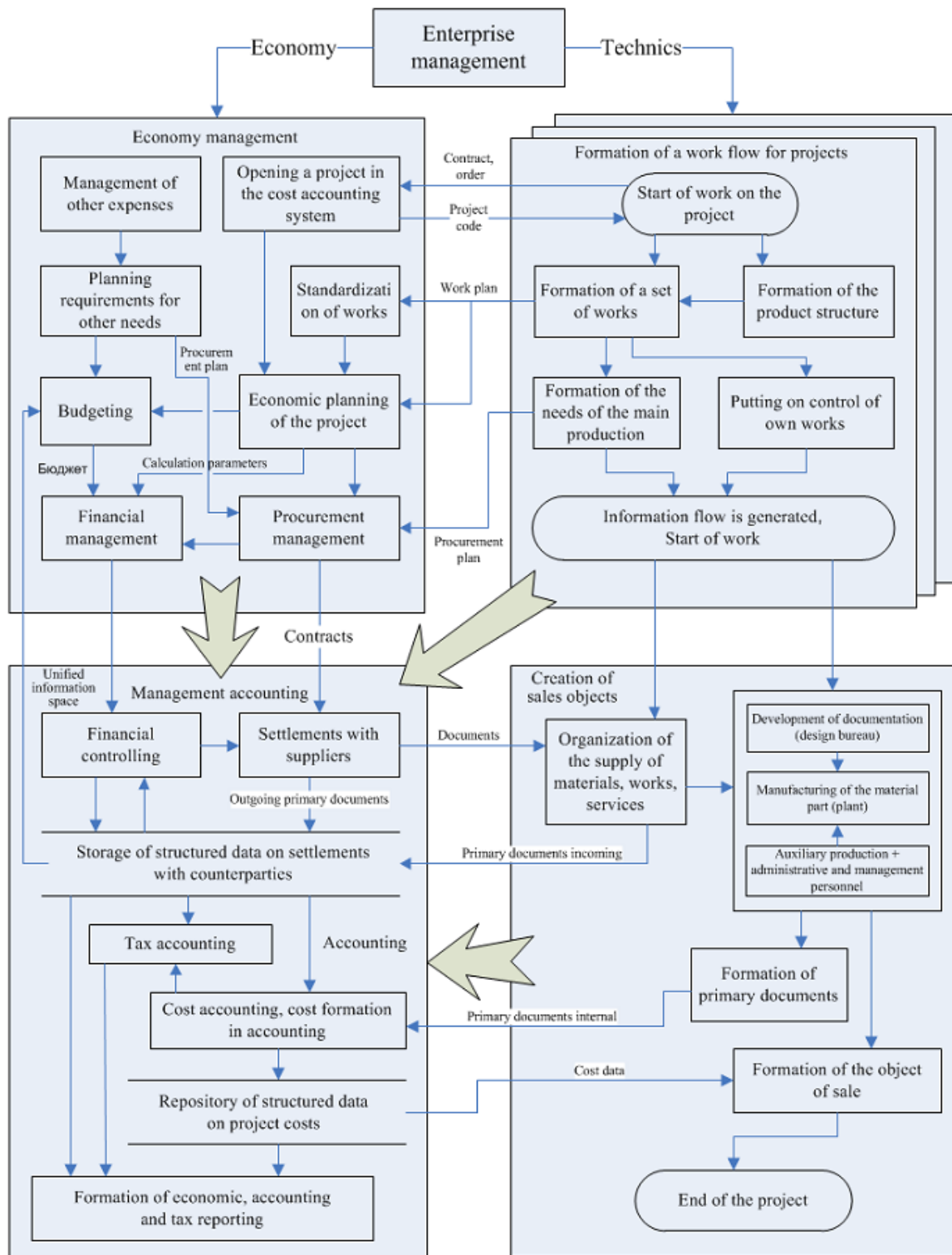


Рис. 6. Схема организации системы ИП процессов управления предприятием

Fig. 6. Organization diagram of the information support system for enterprise management processes

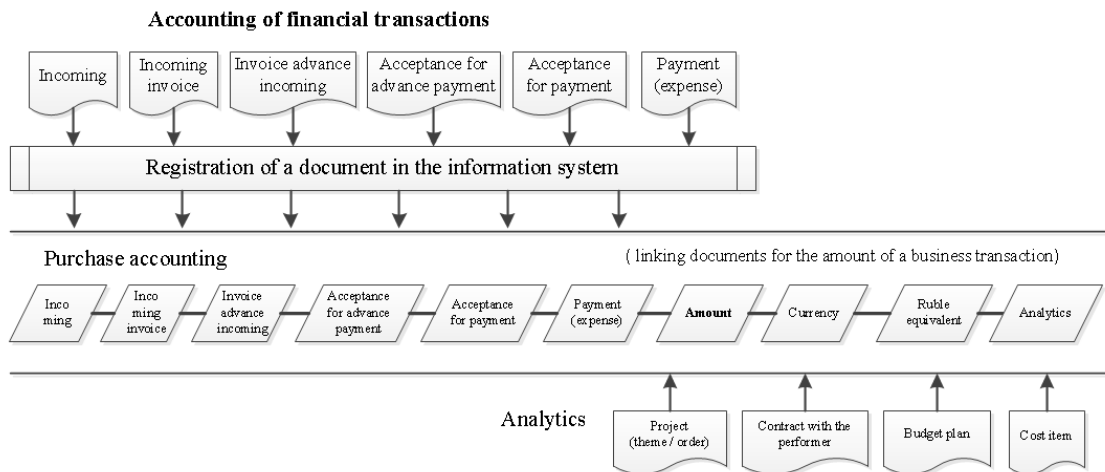


Рис. 7. Связь первичных документов для сущности «Покупка»

Fig. 7. Linking primary documents for the Purchase entity

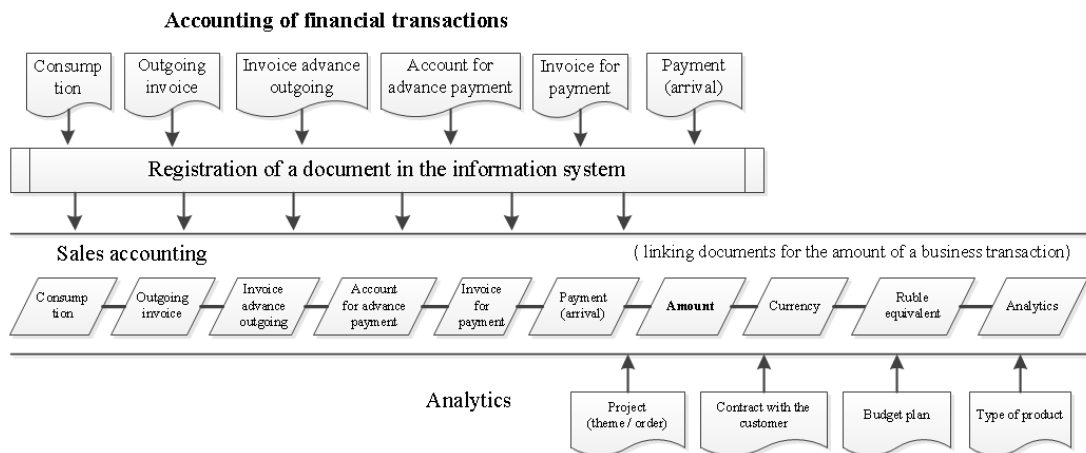


Рис. 8. Связь первичных документов для сущности «Продажа»

Fig. 8. Linking primary documents for the Sale entity

Since the primary documents being the grounds for accounting entries, are interconnected at the database level, then in accounting there is no need to keep a complete set of analytics tools characterizing FET in every entry. These data are easy to find and analyze in a multidimensional array supported in the described way, which is the basis of the OLAP system. Due to this approach, the relevance of data is maintained in one place, where the primary document is born and the information flow is generated, the logic of which is supported by the developed system and user applications.

The developed system links management, accounting and tax accounting, which are based on detailed data on FET with the necessary analytics and fixed links between them, forming a multidimensional array of structured data or OLAP solution. As a result, SIS is formed, containing up-to-date and consistent information about the state of all FETs based at least on one of the listed primary documents.

SIS, formed by the “Sales” and “Purchases” software modules, is a repository of structured data corresponding to primary documents, detailed to logically completed operations and having rigid links to each other in the form of external keys in the database table. Fig. 9 presents an example of organiz-

ing data within a separate process of supplying manufactured products (Sale) in the form of a structured array.

consignment note		invoice		invoice for advance payment		invoice for payment		account for advance payment		payment		analytics	amount in the currency of registration	currency	ruble equivalent	
№	Date	№	Date	№	Date	№	Date	№	Date	№	Date					
								1	15.12.2017			a	1	E	75	registration of an account for advance payment
										2	15.01.2018	a	1	E	75	registration of payment
				3	15.01.2018							a	1	E	75	registration of an invoice for advance payment
				3	15.01.2018			1	15.12.2017	2	15.01.2018	a	1	E	75	link of invoice for advance + payment + invoice
4	10.04.2018											a	3	E	225	registration of a consignment note
		5	15.04.2018									a	3	E	225	registration of an invoice
4	10.04.2018	5	15.04.2018									a	3	E	225	link of a consignment note + invoice
						6	20.04.2018					a	2	E	150	registration of an invoice for payment
						6	20.04.2018			7	25.04.2018	a	2	E	150	registration of payment
										7	25.04.2018	a	2	E	150	link of account + payment
4	10.04.2018	5	15.04.2018	3	15.01.2018			1	15.12.2017	2	15.01.2018	a	1	E	75	link of primary documents
4	10.04.2018	5	15.04.2018			6	20.04.2018			7	25.04.2018	a	2	E	150	link of primary documents

Рис. 9. Пример связи первичных документов для сущности «Продажа» в рамках сквозного процесса поставки произведенной продукции

Fig. 9. An example of the relationship of primary documents for the entity Sale in the framework of the end-to-end delivery process of manufactured products

Proactive control of cash flow is performed in documents of the "Acceptance" type in the "Purchases" module, where all the characteristics of the future payment are automatically checked for the legality: budget plan item, payment purpose, contract balance, state contract identifier (SCI), bank details, accounting policy restrictions and various customizable conditions. Acceptance is an internal document of an enterprise, it acts as an integrator of the process of cash flow and it can be "loaded" with any checks. In its turn, preparing a payment document for budget planning items requires obligatory presence of an agreed registered acceptance, this budget rule is monitored. Software does not allow registering a payment document in the system if it does not meet the budget rules.

The forms for entering financial documents contain all the necessary reference books for MA for marking the data of primary documents with MA attributes for subsequent analytical tasks in the formed multidimensional array of structured data. Fig.10 presents the user interface for working with the financial document data structured and linked in the form of an OLAP solution. This application analyzes the relationship with counterparties, estimates receivables and payables.

Due to this data organization, the budget of the enterprise for a specific date is automatically collected; the budget can be compared with its planned values (Fig. 11).

Software, providing the rules to structure and store the data, consists of two classes. This is a class to maintain the logic of recording and process data about the primary documents and the links between them, and a class to maintain the logic of recording and process data on (VAT) in the documents taken into account, thereby forming tax accounting. The technically developed software maintains up-to-date a multidimensional data array distributed over several tables in the database, each being responsible for the necessary display of the same data on the operations that have taken place for various purposes of accounting and analysis. The set of attributes in various database tables is determined by the stored entity, technical fields to implement the method of data connection and additional fields to organize and maintain the rules laid down in the accounting policy of the enterprise. Additional details in database tables about VAT may vary depending on the selected accounting policy, while the part of the software responsible for calculating the purchase ledger and sales ledger can be modified to comply with the accepted accounting rules at the enterprise. As a result, the database tables can collect and store the current data about the primary financial document data on the document linkage, reflecting BT, thereby forming MA, and related data on VAT, calculated according to the accounting policy rules, forming the tax accounting.

The screenshot displays the ASUP financial OLAP system interface. It features a top menu bar with options like 'Файл', 'Вид', 'Действие', and 'Помощь'. Below the menu is a toolbar with icons for various functions. The main area contains a large data table with columns for 'Предприятие' (Company), 'Примечание' (Note), 'С/З (Сет-факт)' (S/Z (Set-fact)), 'С/З (Сет-факт)' (S/Z (Set-fact)), 'Анализ' (Analysis), 'Анализ на аванс' (Analysis on advance), 'Оплата' (Payment), 'Документ об оплате' (Document on payment), 'Договор' (Contract), 'Заказы' (Orders), 'Характеристики' (Characteristics), and 'Зарегистрировано' (Registered). The table contains numerous rows of data, including dates, amounts, and various codes. A summary section at the bottom shows totals for 'Итого' (Total) and 'Среднее' (Average).

Рис. 10. Форма для работы в финансовой OLAP-системе АСУП

Fig. 10. Form for working in the financial OLAP-system

The screenshot displays the ASUP enterprise budget analysis interface. It features a top menu bar with options like 'Файл', 'Вид', 'Действие', and 'Помощь'. Below the menu is a toolbar with icons for various functions. The main area contains a large data table with columns for 'СБП' (SBP), 'Наименование' (Name), 'Год' (Year), 'I Квартал' (I Quarter), 'II Квартал' (II Quarter), 'III Квартал' (III Quarter), and 'IV Квартал' (IV Quarter). The table contains numerous rows of data, including dates, amounts, and various codes. A summary section at the bottom shows totals for 'Итого' (Total) and 'Среднее' (Average).

Рис. 11. Форма анализа бюджета предприятия в АСУП

Fig. 11. Form of analysis of the enterprise budget in the automated control system

In their turn, accounting entries in dependent accounting areas are developed on the basis of data from the prepared tables of links of primary documents and related tables that consider the VAT distribution. This allows analyzing the activities of the enterprise reflecting the BP financial and economic reflection of in real time, which increases transparency and accuracy in management. An analytical base is created for making timely and well-grounded management decisions, as well as preliminary financial control is carried out for the legality of financial transactions and their characteristics. The possibility of an automated solution of many typical financial and economic operations is formed, this results in saving time resources and increasing mobility and management efficiency. SIS, formed and maintained in this way, is a single data source of contemporary and consistent information for var-

ious types of reporting to various controlling organizations.

Conclusion

The studies demonstrate that the existing approaches to the automation of the control system are mainly in developing autonomous control systems operating in parallel with the control unit, which will certainly lead to data discrepancies and distrust of information. We consider the most effective way to develop MA information support to create a MA database in the form of SIS, where the storage and accounting of the data of the main primary documents is organized in the form of OLAP solution excluding the consolidation and overloading of primary data, while the same structured array is used for purposes of accounting and tax accounting. The proposed approach is realized through a specially designed data warehouse that meets the MA goals. ROLAP system is developed with the contemporary data stored in the database tables. To support the process of forming a structured data warehouse on the basis of the presented method of organizing data, software modules are developed; the software stores registers and considers all primary financial documents accompanying commodity-money relations with counterparties, as well as it performs proactive control of the legality of spending funds. The developed system links management, accounting and tax accounting, which are based on detailed data on the FET with the necessary analytics and fixed links between them, forming a multidimensional array of structured data. This results in developing SIS, that contains contemporary and consistent information about the state of all FETs, an analytical base is created for making timely and well-grounded management decisions and automated financial controlling.

Библиографические ссылки

1. Салихзянова Н. А., Галлямова Д. Х. Роль информационных систем в эффективном управлении современным предприятием // Вестник Казан. технол. ун-та. 2012. № 4. С. 170–172.
2. Волкова В. Н., Голуб Ю. А. Информационная система, к вопросу определения понятия // Прикладная информатика. 2009. № 5(23). С. 112–120.
3. Картамышев А. С., Черныш Б. А. Информационная поддержка управления предприятием в условиях гособоронзаказа. // Инновационные технологии и технические средства специального назначения : тр. XII общерос. науч.-практ. конф. СПб. : Балтийский гос. техн. ун-т «Военмех», 2020. С. 264–270.
4. Бухгалтерский учет, налогообложение, аудит в РФ [Электронный ресурс]. URL: https://www.audit-it.ru/terms/accounting/upravlencheskiy_uchet.html (дата обращения: 21.08.2020).
5. Авдеева Е. А. Автоматизация управленческого учета на сельскохозяйственных предприятиях Оренбургской области // Вестник ОГУ. 2006. № 13(63). С. 38–43.
6. Кияметдинова Н. И. Автоматизация управленческого учета, учет себестоимости при помощи программного продукта «1С: Управление производственным предприятием» // Информационные технологии в науке, управлении, социальной сфере и медицине : сб. науч. тр. II Междунар. конф. Томск : Нац. исслед. Томский политех. ун-т, 2015. С. 259–261.
7. Куджева А. А., Костюкова Е. И. Автоматизация системы управленческого учета в России // Новая наука: теоретический и практический взгляд. 2016. № 117-1. С. 73–76.
8. Никитин В. Автоматизация управленческого учета: как не выбросить деньги на ветер // Финансовый директор. 2013. № 2. С. 26–31.
9. Симонян С. Р., Крамских А. С. Выбор инструмента автоматизации управленческого учета // Россия молодая : сб. материалов VIII Всерос. науч.-практ. конф. молодых ученых с междунар. участием. Кемерово : Кузбасский гос. техн. ун-т им. Т. Ф. Горбачева, 2016. 210 с.

10. Маленкова Л. А., Тынчерова В. Р. Современные информационные технологии как средства автоматизации управленческого учета // Информационные технологии в управлении, обучении, правоохранительной деятельности : сб. материалов IV Междунар. электронной науч. конф. Вологда : Вологодский ин-т права и экономики Федер. службы исполнения наказаний, 2015. С. 68–72.
11. Богатый Д. В. Развитие методики управленческого учета и контроля в коммерческих организациях: автореферат диссертации. Ростов-на-Дону : Ростовский гос. эконом. ун-т, 2014. 287 с.
12. Гарифуллин К. М. Организация хозяйственного учета в условиях информационного общества // Социально-экономические явления и процессы. 2013. № 7(53). С. 29–34.
13. Яргулова А. Управленческий учет: опыт экономически развитых стран. М. : Финансы и статистика, 1991. 237 с.
14. Котова К. Ю., Лукина П. И. Совершенствование процессов информационного обеспечения и автоматизации управленческого учета // Экономические исследования и разработки. 2016. № 5. С. 166–181.
15. TADVISER. Государство. Бизнес. ИТ [Электронный ресурс]. URL: http://www.tadviser.ru/index.php/Статья:CALS_Непрерывная_информационная_поддержка_поставок_и_жизненного_цикла_изделия (дата обращения: 03.02.2020).
16. Кондратьев В. В., Кузнецов М. Н. Показываем бизнес-процессы. М. : Эксмо, 2007. 352 с.
17. Лютов А. Г., Чугунова О. И. Компьютерная система управления качеством на основе CALS-технологий для автоматизированных производств // Вестник УГАТУ. 2011. № 45. С. 27–35.
18. Управление производством. Информационные системы в промышленности [Электронный ресурс]. URL: http://www.up-pro.ru/library/information_systems/production/promyshennost-is.html (дата обращения: 24.09.2020).
19. Доросинский Л. Г., Зверева О. М. Информационные технологии поддержки жизненного цикла изделия. Ульяновск : Зебра, 2016. 243 с.
20. OLTP и OLAP технологии [Электронный ресурс]. URL: https://life-prog.ru/1_759_OLTP-i-OLAP-tehnologii.html (дата обращения: 01.03.2018).
21. Корпоративный менеджмент. Введение в OLAP и многомерные базы данных [Электронный ресурс]. URL: <https://www.cfin.ru/itm/olap/intro.shtml> (дата обращения: 18.09.2020).
22. Картамышев А. С., Способ организации данных при формировании многомерного массива актуальной аналитической информации в автоматизированной системе управления предприятием // Вестник Самарского университета. Аэрокосмическая техника, технологии и машиностроение. 2018. Т. 17, № 1. С. 170–179.

References

1. Salichzyanova N. A., Gallyamova D. H. [The role of information systems in the effective management of a modern enterprise]. *Vestnik Kazanskogo tehnologicheskogo universiteta*. 2012, No. 4, P. 170–172. (In Russ.)
2. Volkova V. N., Golub Y. A. [Information system, to the definition of the concept]. *Prikladnaja informatika*. 2009, No. 5(23), P. 112–120. (In Russ.)
3. Kartamyshev A. S., Chernysh B. A. [Information support for enterprise management in the context of the state defense order]. *Trudy XII obshherossijskoj nauchno-prakticheskoy konferencii "Innovacionnye tehnologii i tehnicheckie sredstva special'nogo naznachenija"*. [Proc. of the XII All-

Russian Scientific and Practical Conference “Innovative Technologies and Special Purpose Equipment”]. St. Petersburg, 2020, P. 264–270. (In Russ.)

4. *Buhgalterskiy uchët, nalogooblozhenie, audit v RF*. [Accounting, taxation, audit in the Russian Federation] (In Russ.). Available at: https://www.audit-it.ru/terms/accounting/upravlencheskiy_uchet.html (accessed: 21.08.2020).

5. Avdeeva E. A. [Automation of management accounting at agricultural enterprises of the Orenburg region]. *Vestnik OGU*. 2006, No. 13(63), P. 38–43. (In Russ.)

6. Kiyametdinova N. I. [Automation of management accounting, cost accounting using the software product “1C: Manufacturing Enterprise Management”]. *Sbornik nauchnykh trudov II Mezhdunarodnoy konferencii “Informacionnye tehnologii v nauke, upravlenii, social’noy sfere i medicine”*. [Proc. of the II International conference “Information technologies in science, management, social sphere and medicine”]. Tomsk, 2015, P. 259–261. (In Russ.)

7. Kudzheva A. A., Kostyukova E. I. [Automation of the management accounting system in Russia]. *Novaya nauka: teoreticheskiy i prakticheskiy vzglyad*. 2016, No. 117-1, P. 73–76. (In Russ.)

8. Nikitin V. [Automation of management accounting: how not to waste money]. *Finansovyy director*. 2013, No. 2, P. 26–31. (In Russ.)

9. Simonyan S. R., Kramskih A. S. [Choosing a management accounting automation tool]. *Sbornik materialov VIII vserossiyskoy, nauchno-prakticheskoy konferencii molodykh uchenykh. S mezhdunarodnym uchastiem “Rossiya molodaya”*. [Collection of materials of the VIII all-Russian scientific and practical conference of young scientists. With international participation “Young Russia”] Kemerovo, 2016, 210 p. (In Russ.)

10. Malenkova L. A., Tyncherova V. R. [Modern information technologies as a means of automating management accounting]. *Informacionnye tehnologii v upravlenii, obuchenii, pravoohranitel’noy deyatel’nosti. Sbornik materialov IV mezhdunarodnoy elektronnoy nauchnoy konferencii* [Information technology in management, training, law enforcement. Collection of materials of the IV international electronic scientific conference]. Vologda, 2015, P. 68–72. (In Russ.)

11. Bogatyy D. V. *Razvitiye metodiki upravlencheskogo ucheta i kontrolya v kommercheskikh organizatsiyah: avtoreferat dissertatsii*. [Development of methods of management accounting and control in commercial organizations: thesis abstract]. Rostov-on-Don, 2014, 287 p.

12. Garifullin K. M. [Organization of business accounting in the information society]. *Social’no-ekonomicheskie javleniya i processy*. 2013, No. 7(53), P. 29–34. (In Russ.)

13. Yargulova A. *Upravlencheskiy uchët: opyt jekonomicheskikh razvitykh stran* [Management accounting: experience of economically developed countries]. Moscow, Finansy i statistika Publ., 1991, 237 p.

14. Kotova K. Y., Lukina P. I. [Improving the processes of information support and automation of management accounting]. *Ekonomicheskie issledovaniya i razrabotki*. 2016, No. 5, P. 166–181. (In Russ.)

15. TADVISER. *Gosudarstvo. Biznes. IT* [State. Business. IT] (in Russ.). Available at: http://www.tadviser.ru/index.php/Статья:CALS_Непрерывная_информационная_поддержка_поставок_и_жизненного_цикла_изделия (accessed: 03.02.2020).

16. Kondratyev V. V., Kuznetsov M. N. *Pokazyvaem biznes-processy* [We show business processes]. Moscow, Jeksmo Publ., 2007, 352 p.

17. Lyutov A. G., Chugunova O. I. [Computerized quality management system based on CALS technology for automated production]. *Vestnik UGATU*. 2011, No. 45, P. 27–35. (In Russ.)

18. *Upravlenie proizvodstvom. Informacionnye sistemy v promyshlennosti* [Production Management. Information systems in industry]. (In Russ.) Available at: http://www.up-pro.ru/library/information_systems/production/promyshennost-is.html (accessed: 24.09.2020).
19. Dorosinskiy L. G., Zvereva O. M. *Informacionnye tehnologii podderzhki zhiznennogo cikla izdelija* [Information technology to support the product life cycle]. Ulyanovsk, Zebra, 2016, 243 p.
20. *OLTP i OLAP tehnologii* [OLTP and OLAP technologies]. (In Russ.) Available at: https://life-prog.ru/1_759_OLTP--i-OLAP-tehnologii.html (accessed 01.03.2018).
21. *Korporativnyi menedzhment. Vvedenie v OLAP i mnogomernye bazy dannyh* [Corporate management. Introduction to OLAP and multidimensional databases]. (In Russ.) Available at: <https://www.cfin.ru/itm/olap/intro.shtml> (accessed: 18.09.2020).
22. Kartamyshev A. S. [A method to organize data in the formation of a multidimensional array of relevant analytical information in an automated enterprise management system] *Vestnik of Samara University. Aerospace and Mechanical Engineering*. 2018. Vol. 17, No. 1. P. 170–179.

© Картамышев А. С., Черныш Б. А., 2021

Картамышев Александр Сергеевич – начальник группы автоматизации задач управления в Обществе; АО «Информационные спутниковые системы» имени академика М. Ф. Решетнева». E-mail: kartam@iss-reshetnev.ru.

Черныш Борис Александрович – аспирант; Сибирский государственный университет науки и технологий имени академика М. Ф. Решетнева. E-mail: borisblack@mail.ru.

Kartamyshev Alexandr Sergeevich – Chief of control process automation group in the Company; JSC Academician M. F. Reshetnev “Information Satellite Systems”. E-mail: kartam@iss-reshetnev.ru.

Chernysh Boris Aleksandrovich – postgraduate student; the Reshetnev University. E-mail: borisblack@mail.ru.

UDC 539.3

Doi: 10.31772/2712-8970-2021-22-2-244-260

For citation: Matveev A. D. The method of fictitious discrete models in the calculation of bodies with an inhomogeneous regular structure. *Siberian Aerospace Journal*. 2021, Vol. 22, No. 2, P. 244–260. Doi: 10.31772/2712-8970-2021-22-2-244-260.

Для цитирования: Матвеев А. Д. Метод фиктивных дискретных моделей в расчетах тел с неоднородной регулярной структурой // Сибирский аэрокосмический журнал. 2021. Т. 22, № 2. С. 244–260. Doi: 10.31772/2712-8970-2021-22-2-244-260.

The method of fictitious discrete models in the calculation of bodies with an inhomogeneous regular structure

A. D. Matveev

Institute of Computational Modeling of SB RAS
50/44, Akademgorodok, Krasnoyarsk, 660036, Russian Federation
E-mail: mtv241@mail.ru

When the strength of elastic composite structures (plates, beams, shells) widely used in aviation, rocket and space technology is calculated with the finite element method (FEM), it is important to know the solution error. To analyze the solution error, it is necessary to use a sequence of approximate solutions constructed according to the FEM using the grinding procedure for basic discrete models (BM), which take into account an inhomogeneous microheterogeneous structure of bodies within the microapproach. Discrete models obtained by grinding BMs have a high dimension, which makes it difficult to use the FEM for them. In addition, there are BMs of composite solids (CSs), for example, BMs of bodies with a microheterogeneous structure, which have such a high dimension that the implementation of the FEM for such BMs is practically impossible due to limited computer resources. To solve these problems, it is proposed to use fictitious discrete models in the calculations of CSs according to the FEM.

In this paper we propose a method of fictitious discrete models (MFDM) for calculating the strength of elastic bodies with an inhomogeneous microheterogeneous regular structure. The MFDM is implemented with the help of the FEM using corrected strength conditions, which take into account the error of approximate solutions. The method is based on the following provision. We believe that BMs of CSs generate solutions that slightly differ from the exact ones. Such BMs always exist for CSs due to the convergence of the FEM. The calculation of CSs according to the MFDM is reduced to the construction and calculation of the strength of fictitious discrete models (FMs), the dimensions of which are smaller than the dimension of the BMs. FMs reflect: the shape, characteristic dimensions, fastening, loading and the type of the inhomogeneous structure of CSs and the distribution of the elastic moduli corresponding to the BM of the CS. The sequence consisting of the FM converges to the BM, i.e., the limiting FM coincides with the BM. The convergence of such a sequence ensures uniform convergence of the FM stresses to the corresponding BM stresses. The implementation of the FEM for FMs with the use of multigrid finite elements leads to a large saving of computer resources, which makes it possible to use the MFDM for strength calculations of bodies with a microheterogeneous regular structure. Calculation of the CS strength according to the MFDM requires $10^3 \div 10^6$ times less computer memory volume than a similar calculation using the BM of the CS, and does not contain the procedure for grinding the BM. The given example of calculating the strength of a beam with an inhomogeneous regular fibrous structure according to the MFDM shows its high efficiency. Applying the adjusted strength conditions allows using approximate solutions with larger errors in CS strength calculations, which leads to improving the efficiency of the MFDM.

Keywords: elasticity, composites, adjusted strength conditions, fictitious discrete models, multigrid finite elements.

Метод фиктивных дискретных моделей в расчетах тел с неоднородной регулярной структурой

А. Д. Матвеев

Институт вычислительного моделирования СО РАН
Российская Федерация, 630036, г. Красноярск, Академгородок, стр. 50/44
E-mail: mtv241@mail.ru

В расчетах на прочность упругих композитных конструкций (пластины, балки, оболочки), которые широко применяются в авиационной и ракетно-космической технике, с помощью метода конечных элементов (МКЭ) важно знать погрешность решения. Для анализа погрешности решения необходимо использовать последовательность приближенных решений, построенных по МКЭ с применением процедуры измельчения для базовых дискретных моделей (БМ), которые учитывают в рамках микроподхода неоднородную, микронеоднородную структуру конструкций (тел). Дискретные модели, полученные путем измельчения БМ, имеют высокую размерность, что затрудняет для них применение МКЭ. Кроме того, существуют БМ композитных тел (КТ), например, БМ тел с микронеоднородной структурой, которые имеют такую высокую размерность, что реализация МКЭ для таких БМ, в силу ограниченности ресурсов ЭВМ, практически невозможна. Для решения данных проблем здесь предлагается в расчетах КТ по МКЭ использовать фиктивные дискретные модели.

В данной работе предлагается метод фиктивных дискретных моделей (МФДМ) для расчета на прочность упругих тел с неоднородной, микронеоднородной регулярной структурой. МФДМ реализуется с помощью МКЭ с применением скорректированных условий прочности, которые учитывают погрешность приближенных решений. В основе метода лежит следующее положение. Считаем, что БМ КТ порождают решения, которые мало отличаются от точных. В силу сходимости МКЭ такие БМ для КТ всегда существуют. Расчет КТ по МФДМ сводится к построению и расчету на прочность фиктивных дискретных моделей (ФМ), размерности которых меньше размерности БМ. ФМ отражают: форму, характерные размеры, крепление, нагружение и вид неоднородной структуры КТ и распределение модулей упругости, отвечающее БМ КТ. Последовательность, состоящая из ФМ, сходится к БМ, т. е. предельная ФМ совпадает с БМ. Сходимость такой последовательности обеспечивает равномерную сходимость напряжений ФМ к соответствующим напряжениям БМ. Реализация МКЭ для ФМ с применением многосеточных конечных элементов приводит к большой экономии ресурсов ЭВМ, что позволяет использовать МФДМ для расчетов на прочность тел с микронеоднородной регулярной структурой. Расчет на прочность КТ по МФДМ требует в $10^3 \div 10^6$ раз меньше объема памяти ЭВМ, чем аналогичный расчет с использованием БМ КТ, и не содержит процедуру измельчения БМ. Приведенный пример расчета на прочность балки с неоднородной регулярной волокнистой структурой по МФДМ показывает его высокую эффективность. Применение скорректированных условий прочности позволяет использовать в расчетах КТ на прочность приближенные решения с большой погрешностью, что приводит к повышению эффективности МФДМ.

Ключевые слова: упругость, композиты, скорректированные условия прочности, фиктивные дискретные модели, многосеточные конечные элементы.

Introduction

Composite structures (plates, beams, shells) especially those with a microheterogeneous fibrous structure are widely used in modern aviation, rocket and space technology. Calculation of the structure strength is one of the most important at the stage of preliminary design, which is a feasibility study of a structure project. As a rule, the static strength calculation of an elastic structure (body) of a certain class (for example, aircraft structures) is carried out according to the safety margins [1–3] and comes down to determining the maximum equivalent stress of the structure. In this case for the body V_0 the specified conditions (in terms of safety margins) have the form $n_1 \leq n_0 \leq n_2$, where n_1 , n_2 are specified; n_0 is the body V_0 safety factor, $n_0 = \sigma_T / \sigma_0$; σ_T is a yield point (ultimate stress) [1]; σ_0 is the maximum equivalent body stress corresponding to the exact solution of the elasticity problem (constructed for the body V_0). For stresses that are determined approximately, the corrected strength conditions are used [4], taking into account the stress error. When analyzing the stress-strain state (SSS) of elastic bodies, the finite element method (FEM) is actively used [5–11]. Basic discrete models (BM) of bodies, which take into account their inhomogeneous, microheterogeneous structure within the micro-approach [12], have a very high dimension.

Let us consider the main difficulties in composite solids (CSs) calculation using the FEM. To analyze the error of the approximate solution, it is necessary to use a sequence of solutions constructed according to the FEM using the grinding procedure (within the microapproach) of composite discrete models. The use of the grinding procedure leads to a sharp increase in the dimensions of discrete models. The multigrid finite element method (MFEM) [13–19] which uses multigrid finite elements (MFEs) [24–29] is effectively used to solve problems of the elasticity theory [20–23]. Since n nested grids ($n \geq 2$) are used instead of one grid when constructing a n -grid finite element (FE), the MFEM can be considered to be a generalization of the FEM, i.e., the FEM is a special case of the MFEM. From here it follows that if the MFEs are used in the calculations of bodies according to the FEM, then in this case, in fact, the MFEM is implemented. Inhomogeneous, microheterogeneous structures in multigrid discrete models are taken into account within the microapproach. MFEs generate discrete models of small dimension. However, for example, BMs of bodies with a microheterogeneous regular structure have such a high dimension that the implementation of the FEM for such BMs with the use of MFEs is difficult due to limited computer resources. To solve this problem, it is proposed to use fictitious discrete models when calculating the strength of CSs according to the FEM. Let us note that the existing approximate approaches and methods for calculating CSs have complex formulations, are laborious and difficult to implement for CSs of complex shapes [30–38].

In this paper, we propose the method of fictitious discrete models (MFDm) for calculating the strength of bodies with an inhomogeneous, microheterogeneous regular structure, which is implemented with the help of the MFEM using the corrected strength conditions. Let us introduce the following definition.

Definition 1. Discrete models constructed for the CS V will be called fictitious models (FM) if these FM have the following properties.

1. Inhomogeneous FM structures differ from the inhomogeneous structure of the CS V BM.
2. FM reflect the shape, characteristic dimensions, fastening, loading and type of the inhomogeneous structure of the CS V , as well as the distribution of elastic moduli corresponding to the CS V BM.
3. The sequence consisting of FM converges to the CS V BM, that is, the limiting FM of the sequence coincides with the CS V BM.

4. The dimensions of the FM are smaller than the dimension of the CS V BM, except for the limiting FM, the dimension of which is equal to the dimension of the CS V BM.

Let us note that properties 3, 4 are important for practice.

Scaled composite discrete models, the dimensions of which are smaller than the dimension of the CS BM, are considered as FMs in this paper. The proposed FMs formed with a scaled regular CS cell have the same characteristic dimensions, shape, fastening, and loading as BMs, but the inhomogeneous FM structures differ from the inhomogeneous BM structure. The considered FMs reflect the form of the BM inhomogeneous structure and the distribution of the elastic moduli corresponding to the BM. The FM sequence that converges to the BM is used in the calculations, i.e., the limiting FM of this sequence coincides with the BM. The convergence of such a sequence (see property 3 in definition 1) ensures the convergence of the FM stresses to the corresponding BM stresses. Calculations show a uniform monotonic convergence of the maximum equivalent stress of the FM to the maximum equivalent stress of the CS BM. The implementation of the MFDM requires $10^3 \div 10^6$ times less computer memory than a similar calculation using the CS BM, and does not require grinding the CS BM. The implementation of the FEM for FMs with the use of MFEs leads to a large saving of computer resources, which makes it possible to use the MFDM for strength calculations of bodies with a micro-heterogeneous regular structure. The given example of calculating a beam with an inhomogeneous regular fibrous structure according to MFDM shows its high efficiency. The use of the corrected strength conditions allows using the approximate solutions with a large error in the CS strength calculations, which leads to an increase in the MFDM efficiency. When calculating a CS of a complex shape according to the MFDM, it is advisable to use FMs with variable characteristic dimensions.

1. The main provisions of the method of fictitious discrete models. The MFDM is applied for CSs that satisfy the following basic provisions.

Provision 1. CSs consist of isotropic homogeneous bodies of different modulus, connections between which are ideal, i.e., the functions of displacements and stresses are continuous on the common boundaries of different-modulus isotropic homogeneous bodies.

Provision 2. Displacements, deformations and stresses of different-modulus isotropic homogeneous bodies correspond to the Cauchy relations and Hooke's law of the three-dimensional linear problem of the elasticity theory [39].

Provision 3. Approximate solutions that correspond to the CS BM differ little from the exact ones. Such approximate solutions will be considered to be exact ones. Let us note that such BMs for CSs always exist due to the convergence of the FEM.

2. The theorem of the method of fictitious discrete models. Corrected strength conditions which take into account the error of approximate solutions are used in the MFDM.

Theorem. Let the strength conditions be given for the safety factor n_0 of the elastic body V_0

$$n_1 \leq n_0 \leq n_2, \quad (1)$$

where n_1, n_2 are given; $n_1 > 1$, $n_0 = \sigma_T / \sigma_0$; σ_T is ultimate stress of the body V_0 ; σ_0 is the maximum equivalent body V_0 stress, which corresponds to the exact solution of the problem of the elasticity theory, constructed for the body V_0 .

Let the safety factor n_b of the body V_0 , corresponding to the approximate solution of the problem of the elasticity theory, satisfy the corrected strength conditions

$$\frac{n_1}{1-\delta_\alpha} \leq n_b \leq \frac{n_2}{1+\delta_\alpha}. \quad (2)$$

Then the safety factor n_0 of the body V_0 , which corresponds to the exact solution of the problem of the elasticity theory, satisfies the given strength conditions (1), where $n_b = \sigma_T / \sigma_b$; σ_b is the maximum equivalent stress of the body V_0 , corresponding to the approximate solution of the problem of the elasticity theory, constructed for the body V_0 , and found with such an error δ_b that

$$|\delta_b| \leq \delta_\alpha < C_\alpha = \frac{n_2 - n_1}{n_1 + n_2}, \quad (3)$$

where δ_α is the upper estimate of the relative error δ_b ; δ_α is given, the error δ_b for the stress σ_b is determined by the formula $\delta_b = (\sigma_0 - \sigma_b) / \sigma_0$.

Let us note that if the body V_0 consists of plastic materials, then σ_T is the yield point. From (3) it follows that if $n_2 - n_1$ is small, then it is necessary to determine σ_b with a small error δ_b . The proof of the theorem is presented in [4].

3. Implementation of the method of fictitious discrete models. For the sake of simplicity, without losing the generality of judgments, we will consider the main procedures for implementing the MFDM using the example of the beam V_0 with an inhomogeneous regular structure with dimensions $H \times L \times H$, where $H = 96h$, $L = 1152h$, h is given, the beam is located in the Cartesian rectangular coordinate system (Fig. 1).

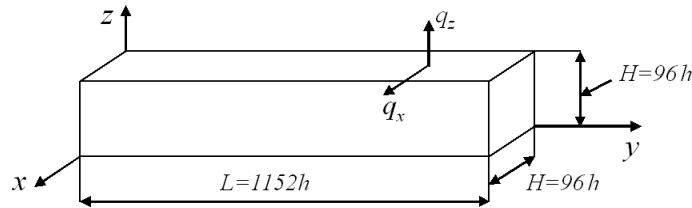


Fig. 1. The dimensions of the beam (body) V_0 (model R_n)

Рис. 1. Размеры балки (тела) V_0 (модели R_n)

The regular cell G_0 of the beam V_0 has a cubic shape with the side $6h$ (Fig. 2). The cell G_0 is located in the local Cartesian rectangular coordinate system $Oxyz$, $i, j, k = 1, \dots, 7$. Fibers with the cross-section $h \times h$ are located along the axis Oy , the cross-sections of the fibers in the plane Oxz are colored (Fig. 2). So, the beam is reinforced with longitudinal continuous fibers. When $y = 0$ the beam is fixed, when $z = H$ it has the loading q_x, q_z . Strength conditions are specified for the beam V_0 (1).

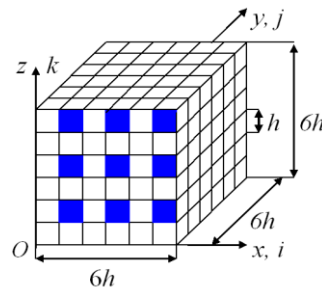


Fig. 2. The regular cell G_0

Рис. 2. Регулярная ячейка G_0

Isotropic homogeneous fibers have the same elastic moduli. It is believed that if the thickness of the fibers is less than 0.5 mm, then these fibers form a microheterogeneous fibrous structure.

3.1. Basic discrete model of the composite body V_0 . The BM R_0 of the CS V_0 , which consists of one-grid finite elements (1gFEs) V_j^h of the 1st order of a cubic shape with the side h (in which a three-dimensional SSS is realized [39]), takes into account the inhomogeneous structure of the CS V_0 within the microapproach and generates a uniform (basic) grid with the step h of the dimension $97 \times 1153 \times 97$ with the total number of nodal unknowns of the FEM equal to $N_0 = 32517504$, the bandwidth of the FEM simultaneous equations (SE) is equal to $b_0 = 28524$. Since the BM R_0 has a high dimension (over 32 million of unknown FEMs) and taking into account that $h/H \ll 1$ ($h/H = h/(96h) = 0,0104 \ll 1$), we believe that the maximum equivalent stress corresponding to the BM R_0 differs little from the exact one, provision 3 MFDM for BM R_0 is performed (see item 1). Fig. 2 shows the basic grid of the regular cell G_0 .

3.2. Scaled composite discrete models. Following the MFDM, (see Fig. 1) we determine the FM sequence for the CS V_0 . We use scaled composite discrete models R_n that form the sequence $\{R_n\}_{n=1}^{16}$ as FMs. The model R_n , $n=1, \dots, 16$, has the same characteristic dimensions, shape, fastening and loading as the BM R_0 (Fig. 1). The discrete model R_n , consisting of 1gFEs of the 1st order of a cubic shape with the side h_n (a three-dimensional SSS is implemented in 1gFE V_e^n), has a uniform grid with the step h_n of the dimension $n_1^{(n)} \times n_2^{(n)} \times n_3^{(n)}$, where

$$n_1^{(n)} = 6n + 1, \quad n_2^{(n)} = 12 \times 6n + 1, \quad n_3^{(n)} = 6n + 1, \quad n = 1, \dots, 16. \quad (4)$$

The steps of the nodal grid of the model R_n along the axes Ox , Oy , Oz respectively, are equal to $h_x^{(n)} = H/(6n)$, $h_y^{(n)} = L/(72n)$, $h_z^{(n)} = H/(6n)$. Since $L = 12H$, then $h_n = h_x^{(n)} = h_y^{(n)} = h_z^{(n)}$. By virtue of (4), we have

$$h_n = \beta_n h, \quad n = 1, \dots, 16, \quad (5)$$

where β_n is the scale factor, $\beta_n = 16/n$, for $n = 1, \dots, 15$ we have $\beta_n > 1$, i.e. $h_n > h$, for $n \rightarrow 16$ we have $\beta_n \rightarrow 1$, $\beta_{16} = 1$, $h_{16} = h$.

According to (4), the model R_n consists of a finite number of bodies G_n of the same shape with dimensions $6h_n \times 6h_n \times 6h_n$, $n = 1, \dots, 16$ (Fig. 3). The CS G_n is located in the local Cartesian rectangular coordinate system $Oxyz$. The body G_n has the same number of fibers (with the cross-section $h_n \times h_n$) and the same mutual arrangement of these fibers as the regular cell G_0 (Fig. 2). In Fig. 3 the fiber sections of the cell G_n in the plane Oxz are coloured, $i, j, k = 1, \dots, 7$. The fibers and the binder of the CSs G_n and G_0 have the same modulus of elasticity.

Let us introduce the following definitions, which are used in the construction of scaled composite discrete models.

Definition 2. We will say that the three-dimensional elastic body G is formed by scaling the elastic three-dimensional body G^0 with the scale factor $p > 0$ if any point $A \in G^0$ corresponds to such a single

point $B \in G$ that $x_B = px_A$, $y_B = py_A$, $z_B = pz_A$, where x_A, y_A, z_A (x_B, y_B, z_B) are the coordinates of the point A (point B) corresponding to the Cartesian rectangular coordinate system $Oxyz$. And vice versa, if any point $B \in G$ corresponds to such a single point $A \in G^0$ that $x_A = x_B / p$, $y_A = y_B / p$, $z_A = z_B / p$. The elastic moduli at the points $A \in G^0$, $B \in G$ are the same.

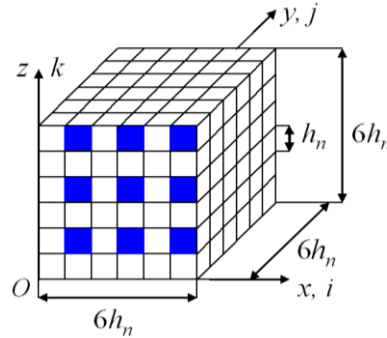


Fig. 3. The regular cell G_n

Рис. 3. Регулярная ячейка G_n

Definition 3. The three-dimensional elastic body G obtained by scaling the given (basic) elastic three-dimensional body G^0 with the given scale factor p will be called a scaled one. The relationship between the scaled body G and the base body G^0 is represented as $G = p G^0$, where p is the scale factor.

So, by virtue of (5), the CS G_n is formed by scaling the regular cell G_0 of the CS V_0 BM with the scale factor β_n (see Definition 2), that is, the body G_n is a scaled regular cell (see Definition 3). The shapes and inhomogeneous structures of the bodies G_n and G_0 are geometrically similar, that is, they differ only in scale (Fig. 2, 3, where $h_n > h$, at $n=1,15$). Then, taking into account (5) and that the fibers and the binder of the CSs G_n and G_0 have the same elastic moduli, the connection between the bodies G_n , G_0 is represented in the form (see definition 3).

$$G_n = \beta_n G_0, \quad (6)$$

where $\beta_n = 16/n$; $n=1, \dots, 16$, at $n \rightarrow 16$ we have $\beta_n \rightarrow 1$, $\beta_{16} = 1$.

Since the inhomogeneous structure is taken into account in the regular cell G_0 , by virtue of (6) and in the CS G_n , the inhomogeneous structure is also taken into account with the help of a 1gFE V_e^n of a cubic shape with the side h_n . The model R_n , which by virtue of (5), (6) is formed using the scaled regular cell G_n , will be called a scaled one. We note that the CS G_n is, in fact, a regular cell of the model R_n . Since the inhomogeneous structure is taken into account in the regular cell G_n , therefore, the inhomogeneous structure is also taken into account in the model R_n . For the model R_n , we note the following properties, which show the main advantages of the MFDM.

1. The dimension of the model R_n at $n \leq 15$ due to (4) is smaller than the dimension of the BM R_0 . Therefore, the implementation of the FEM for the model R_n (at $n \leq 15$) requires less computer resources than for the BM R_0 .

2. When constructing scaled composite discrete models R_n , the procedure of grinding the BM of the CS is not used.

We note that the models R_n , $n = \overline{1, 15}$ are, in fact, fictitious discrete models.

3.3. Convergence of a sequence of scaled discrete models. Let us show that the sequence $\{R_n\}_{n=1}^{16}$ consisting of scaled discrete models R_n converges to BM R_0 at $n \rightarrow 16$. According to (5), (6) at $n = 16$ ($h_{16} = h$, $\beta_{16} = 1$, $G_{16} = G_0$) the discrete models R_{16} , R_0 coincide, that is, $R_{16} = R_0$. Since the model R_{16} , like the BM R_0 , has a high dimension, that is, it has $N_0 = 32517504$ nodal unknown FEMs, and taking into account that $h \ll H$ ($h/H = h/(96h) = 0,0104$), we assume that the maximum equivalent stress σ_{16} of the model R_{16} differs little from the exact stress σ_0 of the CS V_0 . Then we assume $\sigma_0 = \sigma_{16}$, that is, provision 3 of the MFDM for the BM R_0 is satisfied (see item 1). By virtue of (5), (6) at $n \rightarrow 16$ (at $\beta_n \rightarrow 1$) we have $G_n \rightarrow G_0$. Hence, taking into account that CSs G_n , G_0 are regular cells of the models R_n , R_0 , respectively, and that these models have the same shape and characteristic sizes, we obtain

$$R_n \rightarrow R_0 \quad \text{for } n \rightarrow 16. \quad (7)$$

According to (7), for $n \rightarrow 16$ (taking into account that $R_{16} = R_0$) we have $\sigma_n \rightarrow \sigma_{16}$ or (taking into account the equality $\sigma_0 = \sigma_{16}$) $\sigma_n \rightarrow \sigma_0$, where σ_n is the maximum equivalent stress of the discrete model R_n . Let $\delta_\sigma = |\sigma_n - \sigma_{n-1}|/\sigma_n$ be a small value and $|\delta_n| \leq \delta_\alpha$, where δ_n is the relative error for the stress σ_n , that is, $\delta_n = (\sigma_0 - \sigma_n)/\sigma_0$, δ_α is given, $\delta_\alpha < C_\alpha$ (see (3)), $n = 2, 3, \dots$. Then we accept $\sigma_b = \sigma_n$. Let the safety factor n_b (where $n_b = \sigma_T / \sigma_b$, taking into account that $\sigma_b = \sigma_n$, we have $n_b = \sigma_T / \sigma_n$), corresponding to the approximate solution of the elasticity problem, satisfies the adjusted strength conditions (2). Then the safety factor n_0 of the CS V_0 corresponding to the exact solution of the elasticity problem satisfies the given strength conditions (1) (see the theorem in item 2). MFEs are used to reduce the dimension of the model R_n .

4. The results of numerical experiments. Let us consider a model problem of calculating the strength of a cantilever beam V_0 with an inhomogeneous regular fibrous structure with dimensions $96h \times 1152h \times 96h$ (Fig. 1). The regular cell G_0 of the beam is shown in Fig. 2. For the safety factor n_0 of the beam, the strength conditions are specified

$$1,8 \leq n_0 \leq 3,4. \quad (8)$$

For the model problem we have the following initial data:

$$h = 0,2083; \quad \sigma_T = 4,5; \quad E_c = 1, \quad E_v = 10, \quad \nu_c = \nu_v = 0,3, \quad (9)$$

where E_c , E_v (ν_c, ν_v) are Young's moduli (Poisson's ratios) of the binder and fiber, respectively; σ_T is the fiber yield point; loads $q_z = q_x = 0,00075$ act on the surface $z = H$, $0,5L \leq y \leq L$ (Fig. 1).

We use two-grid FEs (2gFEs) in the calculations. We will consider the main provisions of the construction of 2gFEs using the example of the 2gFE $V_d^{(2)}$ with dimensions $6h \times 6h \times 6h$ (Fig. 4), which consist of one regular cell G_0 (Fig. 2). The two-grid FE $V_d^{(2)}$ is located in the local Cartesian rectangu-

lar coordinate system $Oxyz$. When constructing the $2gFE V_d^{(2)}$, we use two nested grids: a uniform fine grid h_d with the step h of the dimension $7 \times 7 \times 7$ and a coarse one H_d with dimensions $2 \times 3 \times 2$. The grid H_d has the step $6h$ along the axes Ox , Oz and the step $3h$ along the axis Oy . Fig. 4 shows the grids h_d and H_d , the nodes of the coarse grid H_d are marked with dots (12 nodes). The fine grid h_d is generated by the basic partition R_d of the $2gFE V_d^{(2)}$, which consists of $1gFE V_j^h$ of the 1st order of a cubic shape with the side h (in which three-dimensional SSS is realized, $j=1, \dots, M$, M is the total number of $1gFE V_j^h$, $M=216$) and takes into account the inhomogeneous structure of the $2gFE V_d^{(2)}$.

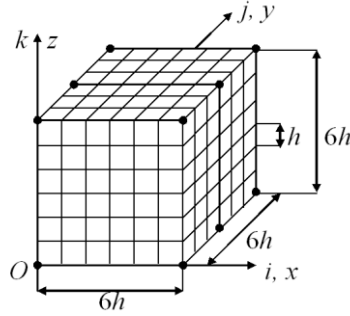


Fig. 4. Fine and coarse grids $2gFE V_d^{(2)}$

Рис. 4. Мелкая и крупная сетки $2сКЭ V_d^{(2)}$

We construct a superelement V_S on the partition R_d using the condensation method [10]. We represent the total potential energy Π_d of the partition R_d of $2gFE V_d^{(2)}$ in the form

$$\Pi_d = \frac{1}{2} \mathbf{q}_S^T [K_S] \mathbf{q}_S - \mathbf{q}_S^T \mathbf{F}_S, \quad (10)$$

where T is the transposition; $[K_S]$ is the stiffness matrix (dimensions 654×654); \mathbf{F}_S , \mathbf{q}_S are the vectors of nodal forces and displacements (of the dimension 654) of the superelement V_S .

We write the basis function $N_{ijk}(x, y, z)$ for the node i, j, k of the coarse grid H_d using Lagrange polynomials in the form $N_{ijk} = L_i(x)L_j(y)L_k(z)$, where

$$L_i(x) = \prod_{\alpha=1, \alpha \neq i}^2 \frac{x - x_\alpha}{x_i - x_\alpha}, \quad L_j(y) = \prod_{\alpha=1, \alpha \neq j}^3 \frac{y - y_\alpha}{y_j - y_\alpha}, \quad L_k(z) = \prod_{\alpha=1, \alpha \neq k}^2 \frac{z - z_\alpha}{z_k - z_\alpha},$$

where x_i, y_j, z_k are the coordinates of the node i, j, k of the grid H_d in the coordinate system $Oxyz$; i, j, k are the coordinates of the integer coordinate system ijk introduced for the nodes of the coarse grid H_d ; $i, k=1, 2$, $j=1, 2, 3$ (fig. 4).

Let us denote: $N_\beta = N_{ijk}$, $u_\beta = u_{ijk}$, $v_\beta = v_{ijk}$, $w_\beta = w_{ijk}$, where u_{ijk} , v_{ijk} , w_{ijk} are the values of displacements u , v , w in the node i, j, k of the grid H_d ; $i, k=1, 2$; $j=1, 2, 3$; $\beta=1, \dots, 12$. Then the approximating functions of displacements $u^{(2)}$, $v^{(2)}$, $w^{(2)}$ of the $2gFE$ can be written in the form

$$u^{(2)} = \sum_{\beta=1}^{12} N_\beta u_\beta, \quad v^{(2)} = \sum_{\beta=1}^{12} N_\beta v_\beta, \quad w^{(2)} = \sum_{\beta=1}^{12} N_\beta w_\beta. \quad (11)$$

Let us denote the vector of nodal displacements of the grid H_d (of dimension 36), that is, the vector of nodal unknowns 2gFE $V_d^{(2)}$ by \mathbf{q}_d . Using (11), the vector \mathbf{q}_s of nodal displacements of the superelement V_s is expressed through the vector \mathbf{q}_d , that is

$$\mathbf{q}_s = [A_s^d] \mathbf{q}_d, \quad (12)$$

where $[A_s^d]$ is the rectangular matrix (of dimension 654×36).

Substituting (12) into (10), from the condition $\partial \Pi_d / \partial \mathbf{q}_d = 0$, we obtain $[K_d] \mathbf{q}_d = \mathbf{F}_d$, where

$$[K_d] = [A_s^d]^T [K_s] [A_s^d], \quad \mathbf{F}_d = [A_s^d]^T \mathbf{F}_s, \quad (13)$$

where $[K_d]$ is the stiffness matrix (of dimension 36×36) and \mathbf{F}_d is the vector of nodal forces (of dimension 36) of 2gFE $V_d^{(2)}$.

The solution built for a coarse grid H_d of 2gFE $V_d^{(2)}$ is projected onto the super element V_s grid using formula (12), and then, according to the condensation method [10], is projected onto the fine grid h_d , which makes it possible to calculate stresses in any 1gFE V_j^h of the basic partition R_d of 2gFE $V_d^{(2)}$.

On the basis of the model R_n , we construct a two-grid discrete model R_n^o , which consists of composite 2gFEs of the type $V_d^{(2)}$ with dimensions $6h_n \times 6h_n \times 6h_n$, $n=1, \dots, 12$. For the two-grid model R_n^o , we determine (according to the 4th theory of strength [1]) the maximum equivalent stress σ_n^o , $n=1, 12$. The calculation results are presented in table 1, where σ_n^o is the maximum equivalent stress of the model R_n^o ; N_n^o and b_n^o are the dimension and the bandwidth of the FEM SE of the model R_n^o , $n=5, \dots, 12$, the relative error δ_n (in percent) is determined by the formula

$$\delta_n(\%) = 100 \% \times |\sigma_n^o - \sigma_{n-1}^o| / \sigma_n^o, \quad n=6, \dots, 12. \quad (14)$$

The analysis of the results shows uniform monotonic convergence of stresses σ_n^o , $n=5, \dots, 12$, and relative errors $\delta_n(\%)$, $n=6, \dots, 12$.

Table 1

Calculation results for models $R_5^o - R_{12}^o$

n	R_n^o	σ_n^o	$\delta_n(\%)$	N_n^o	b_n^o	n	R_n^o	σ_n^o	$\delta_n(\%)$	N_n^o	b_n^o
5	R_5^o	1,476	—	12960	240	9	R_9^o	1,819	4,01	64800	636
6	R_6^o	1,576	6,34	21168	321	10	R_{10}^o	1,888	3,65	87120	765
7	R_7^o	1,665	5,34	32256	414	11	R_{11}^o	1,952	3,28	114048	906
8	R_8^o	1,746	4,64	46656	519	12	R_{12}^o	2,012	2,98	146016	1059

Let us note that the BM R_0 generates the maximum equivalent stress σ_0 of the CSV₀, which differs little from the exact one. The stress σ_0 is considered to be accurate (see provision 3, item 1). According to calculations, $\sigma_{16}^o = 2,140$ where σ_{16}^o is the maximum equivalent stress of the model R_{16}^o . We have $R_{16} = R_0$ (see Section 3.3). The two-grid model R_{16}^o is built on the basis of the model R_{16} using 2gFE $V_d^{(2)}$ (Fig. 4). Since the dimensions of the 1gFE of the BM R_0 are small, the dimensions of the 2gFE model R_{16}^o are also small, so we accept $\sigma_{16}^o = \sigma_0 = 2,140$.

Calculations show that if $\delta_n(\%) \leq 3\%$ (see (14)), then the error of the maximum equivalent stress σ_n^o of the model R_n^o is not more than 10 %. Since the stresses $\sigma_{12}^o = 2,012$ and $\sigma_{11}^o = 1,952$ differ by $\delta_{12}(\%) = 2,98\%$ (see Table 1), that is, we have $\delta_{12}(\%) \leq 3\%$, the stress error σ_{12}^o is not more than 10%. We note that the stress σ_{12}^o differs from the stress σ_0 by 5.98%. We will assume that the upper estimate for the stress error σ_{12}^o is 10%. Then we accept $\delta_\alpha = 0,1$, $\sigma_b = \sigma_{12}^o = 2,012$. Condition (3) is satisfied, that is, we have the inequality $\delta_\alpha = 0,1 < C_\alpha = 0,3$. Substituting $\delta_\alpha = 0,1$, $n_1 = 1,8$, $n_2 = 3,4$ in (2), we obtain the corrected strength conditions for the CS V_0 in the form

$$2 \leq n_b \leq 3, \quad (15)$$

where n_b is the safety factor of the CS V_0 corresponding to the approximate solution of the elasticity problem,

$$n_b = \sigma_T / \sigma_b. \quad (16)$$

Using in (16) $\sigma_T = 4,5$, $\sigma_b = 2,012$, we find the safety factor n_b for the CS V_0 .

$$n_b = \sigma_T / \sigma_b = 4,5 / 2,012 = 2,24. \quad (17)$$

So, the safety factor $n_b = 2,24$ of the CS V_0 (corresponding to the approximate solution of the elasticity problem) satisfies the corrected strength conditions (15). Then, according to the theorem of item 2, the safety factor n_0 of the CS V_0 (corresponding to the exact solution of the elasticity problem) satisfies the given strength conditions (8). We note that the BM R_0 of the CS V_0 has over 32 million nodal unknown FEMs, which makes it difficult to implement FEM using 1gFE of the 1st order of a cubic shape with the side h for constructing the solution for the BM R_0 , which we consider to be accurate (see provision 3, item 1 and item 3.1). In calculating the strength according to the MFDM of the composite beam V_0 (see Fig. 1) we use the model R_{12}^o that has $N_{12}^o = 146016$ nodal unknowns of the FEM and the bandwidth of the FEM SE of which is equal to $b_{12}^o = 1059$ (see Table 1). The discrete model R_{12}^o requires $k_1 = \frac{N_0 \times b_0}{N_{12}^o \times b_{12}^o} = \frac{32517504 \times 28524}{146016 \times 1059} = 5998,34$ times less computer memory, that is, almost 6×10^3 times less than the BM R_0 (see item 3.1), which shows the high efficiency of the MFDM.

5. The application of approximate solutions with a large error in the MFDM. Let us consider the case of calculating a CS for strength according to the MFDM, when it is possible to use elastic approximate solutions with a large error on the example of calculating the CS V_0 (see section 4). Calculations show that if $\delta_n(\%) \leq 5\%$ (see (14)), then the error of the maximum equivalent stress σ_n^o of the model R_n^o is not more than 25%. Since the stresses $\sigma_8^o = 1,746$ and $\sigma_7^o = 1,665$ differ by $\delta_8(\%) = 4,64\%$ (see Table 1), that is, $\delta_8(\%) \leq 5\%$, the stress error σ_8^o is not more than 25 %. In fact, the stress σ_8^o is different from the stress $\sigma_0 = 2,140$ by 18,41 %. We will assume that the upper estimate for the stress error σ_8^o is 25 %. Then we accept $\delta_\alpha = 0,25$, $\sigma_b = \sigma_8^o = 1,746$. Condition (3) is satisfied, that is, we have $\delta_\alpha = 0,25 < C_\alpha = 0,3$. Substituting $\delta_\alpha = 0,25$, $n_1 = 1,8$, $n_2 = 3,4$ in (2), we obtain the following corrected strength conditions for the CS V_0

$$2,4 \leq n_b \leq 2,7. \quad (18)$$

Using $\sigma_T = 4,5$, $\sigma_b = 1,746$ in (16), we find the safety factor n_b for the CS V_0

$$n_b = \sigma_T / \sigma_b = 4,5 / 1,746 = 2,58. \quad (19)$$

The safety factor $n_b = 2,58$ of the CS V_0 (corresponding to the approximate solution of the elasticity problem) satisfies the corrected strength conditions (18). Then the safety factor n_0 of the CS V_0 (corresponding to the exact solution of the elasticity problem) satisfies the given strength conditions (8) (see item 2). In this case, when calculating the strength of the CS V_0 according to the MFDM, we use the model R_8^o that has $N_8^o = 46656$ of unknown FEMs and the bandwidth of the FEM SE of which is equal to $b_8^o = 519$. The model R_8^o requires $k_2 = \frac{N_0 \times b_0}{N_8^o \times b_8^o} = \frac{32517504 \times 28524}{46656 \times 519} = 38304,76$ times less computer memory, that is, almost 38×10^3 times less than the BM R_0 .

So, it has been shown that when calculating the CS V_0 , it is possible to use elastic approximate solutions with a large error. In this case, in the calculations we use the stress σ_8^o of the model R_8^o , the error $\varepsilon_8 = 18,41\%$ of which is greater than the error $\varepsilon_{12} = 5,98\%$ of the stress σ_{12}^o of the model R_{12}^o , which leads to an increase in the efficiency of the MFDM (the coefficient k_2 is 6,38 times greater than the coefficient k_1). This is due to the fact that the dimension and the bandwidth of the FEM SE of the model R_8^o are smaller than the dimension and the bandwidth of the FEM SE of the model R_{12}^o (see Table 1). The following conclusion can be drawn on the basis of the results obtained in the given example. The use of discrete CS models in MFDM, the maximum equivalent stresses of which have a large error, leads to an increase in the MFDM efficiency.

6. Fictitious models with variable characteristic dimensions. When calculating CSs of complex shapes according to the MFDM, it is advisable to use FMs with variable characteristic dimensions. For the sake of simplicity, let us consider the brief essence of such FMs without losing the generality of reasoning, using the example of the beam $V_0^{(1)}$ of a complex shape, that is, with a constant cross-section of a complex shape (such as an I-beam) (Fig. 5). The beam $V_0^{(1)}$ is located in the Cartesian rectangular coordinate system $Oxyz$, the axis Oy is parallel to the beam axis. Let the beam be reinforced with continuous longitudinal fibers with the cross-section $h \times h$, that is, which are parallel to the axis Oy , where $h = L_0 / N$, N is given; L_0 is the length of the beam $V_0^{(1)}$. The BM $R_0^{(1)}$ of the beam $V_0^{(1)}$ consists of the FE V_e of the 1st order of a cubic shape with the side h that takes into account the inhomogeneous structure of the beam and generates an approximate solution that does not differ much from the exact one. We consider such an approximate solution to be exact (see provision 3, item 1). The FM $R_n^{(1)}$ of the beam differs from its BM $R_0^{(1)}$ only by one (variable) characteristic dimension L_n (along the axis Oy) (Fig. 5). The FM $R_n^{(1)}$ has fastening and the same loading pattern as the BM $R_0^{(1)}$ of the beam $V_0^{(1)}$.

We determine the characteristic dimension L_n of the FM $R_n^{(1)}$ by the formula

$$L_n = L_0 n / N = hn, \quad (20)$$

where $n = n_0, \dots, N$; $n_0 > 2$, n_0 is given.

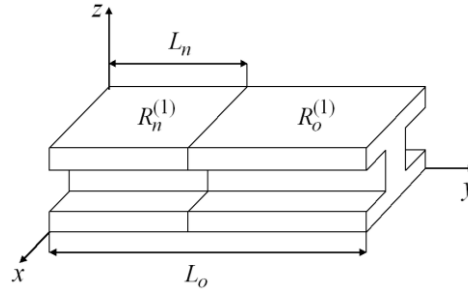


Fig. 5. The beam $V_0^{(1)}$

Рис. 5. Балка $V_0^{(1)}$

The FM $R_n^{(1)}$ has the same inhomogeneous structure as the BM $R_0^{(1)}$, that is, the FM $R_n^{(1)}$ is reinforced with continuous longitudinal fibers with the cross section $h \times h$ and has the same fiber distribution in the cross section as the BM $R_0^{(1)}$ of the beam $V_0^{(1)}$. Inhomogeneous structures of the FM $R_n^{(1)}$ and the BM $R_0^{(1)}$ are taken into account using the FE V_e of the first order of a cubic shape with the side h . From the above, taking into account that according to (20) $L_n \rightarrow L_0$ at $n \rightarrow N$, it follows

$$R_n^{(1)} \rightarrow R_0^{(1)} \quad \text{at } n \rightarrow N. \quad (21)$$

From the fulfillment of (21) we obtain

$$\sigma_n^{(1)} \rightarrow \sigma_0^{(1)} \quad \text{at } n \rightarrow N, \quad (22)$$

where $\sigma_n^{(1)}$ ($\sigma_0^{(1)}$) is the maximum equivalent stress corresponding to the FM $R_n^{(1)}$ (corresponding to the BM $R_0^{(1)}$ of the beam $V_0^{(1)}$).

Since the FM $R_n^{(1)}$ and the BM $R_0^{(1)}$ beams consist of the FE V_e of the 1-st order of a cubic shape with the side h and the cross sections of these models are the same, then the sections of the FM $R_n^{(1)}$ and the BM $R_0^{(1)}$ contain the same number of nodes, which we denote by N_0 . Then the total number of nodes M_0 of the BM $R_0^{(1)}$ is equal to $M_0 = N_0(N+1)$, the total number of nodes M_n of the FM $R_n^{(1)}$ is $M_n = N_0(n+1)$. When $n_0 \leq n < N$ we get that $M_n < M_0$, that is, the dimension of the FM $R_n^{(1)}$ is smaller than the dimension of the BM $R_0^{(1)}$. For $n = N$ we have $M_N = M_0$, that is, the dimensions of the FM $R_N^{(1)}$ and the BM $R_0^{(1)}$ coincide. So, it is shown that when calculating the composite beam $V_0^{(1)}$ (Fig. 5) of a complex shape according to the MFDM, it is advisable to use the FM $R_n^{(1)}$ with the variable characteristic dimension L_n , which leads to saving computer resources.

Conclusion

The method of fictitious discrete models is proposed for calculating the static strength of elastic bodies with an inhomogeneous, microheterogeneous regular structure. The proposed method is re-

duced to constructing and calculating the strength of fictitious discrete models, the dimensions of which are smaller than the dimensions of the basic discrete models of composite solids, and is implemented with the help of the FEM using corrected strength conditions that take into account the error of approximate solutions. The FEM implementation for fictitious discrete models with the use of multigrid finite elements provides a great economy of computer resources, which makes it possible to use the proposed method for calculating the strength of bodies with microheterogeneous regular structure. The implementation of the method of fictitious discrete models requires less computer resources than the implementation of the FEM for basic discrete models. When constructing fictitious discrete models, the grinding procedure for basic models is not used. The calculations show the high efficiency of the proposed method in calculating the strength of bodies with an inhomogeneous regular fibrous structure. The use of the corrected strength conditions makes it possible to use approximate solutions with a large error in the calculations, which leads to an increase in the efficiency of the method of fictitious discrete models.

References

1. Pisarenko G. S., Yakovlev A. P., Matveev V. V. *Spravochnik po soprotivleniyu materialov* [Hand book of resistance materials']. Kiev, Nauk. Dumka Publ., 1975, 704 p.
2. Birger I. A., Shorr B. F., Iosilevich G. B. *Raschet na prochnost' detalej mashin* [Calculation of the strength of machine parts]. Moscow, Mashinostroenie Publ., 1993, 640 p.
3. Moskvichev V. V. *Osnovy konstrukcionnoy prochnosti tekhnicheskikh sistem i inzhenernykh sooruzheniy* [Fundamentals of structural strength of technical systems and engineering structures]. Novosibirsk, Nauka Publ., 2002, 106 p.
4. Matveev A. D. [Calculation of elastic structures using the adjusted terms of strength]. *Izvestiya AltGU*. 2017, No. 4, P. 116–119 (In Russ.). Doi: 10.14258/izvasu (2017)4-21.
5. Zienkiewicz O. C., Taylor R. L., Zhu J. Z. *The finite element method: its basis and fundamentals*. Oxford: Elsevier Butterworth-Heinemann, 2013, 715 p.
6. Golovanov A. I., Tiuleneva O. I., Shigabutdinov A. F. *Metod konechnykh elementov v statike i dinamike tonkostennykh konstruksii* [Finite element method in statics and dynamics of thin-walled structures]. Moscow, Fizmatlit Publ., 2006, 392 p.
7. Bate K., Vilson E. *Chislennyye metody analiza i metod konechnykh elementov* [Numerical analysis methods and finite element method]. Moscow, Stroiizdat Publ., 1982, 448 p.
8. Obratsov I. F., Savel'ev L. M., Khazanov Kh. S. *Metod konechnykh elementov v zadachakh stroitel'noi mekhaniki letatel'nykh apparatov* [Finite element method in problems of aircraft structural mechanics]. Moscow, Vysshaya shkola Publ., 1985, 392 p.
9. Sekulovich M. *Metod konechnykh elementov* [Finite element method]. Moscow, Stroiizdat Publ., 1993, 664 p.
10. Norri D., de Friz Zh. *Vvedenie v metod konechnykh elementov* [Introduction to the finite element method]. Moscow, Mir Publ., 1981, 304 p.
11. Zenkevich O. *Metod konechnykh elementov v tekhnike* [Finite element method in engineering]. Moscow, Mir Publ., 1975, 544 p.
12. Fudzii T., Dzako M. *Mekhanika razrusheniya kompozitsionnykh materialov* [Fracture mechanics of composite materials]. Moscow, Mir Publ., 1982, 232 p.
13. Matveev A. D. [The method of multigrid finite elements in the calculations of three-dimensional homogeneous and composite bodies]. *Uchen. zap. Kazan. un-ta. Seriya: Fiz.-matem. Nauki*. 2016, Vol. 158, Iss. 4, P. 530–543 (In Russ.).

14. Matveev A. D. [Multigrid method for finite elements in the analysis of composite plates and beams]. *Vestnik KrasGAU*. 2016, No. 12, P. 93–100 (In Russ.).
15. Matveev A. D. Multigrid finite element method in stress of three-dimensional elastic bodies of heterogeneous structure. *IOP Conf. Ser.: Mater. Sci. Eng.* 2016, Vol. 158, No. 1, Art. 012067, P. 1–9.
16. Matveev A. D. [Multigrid finite element Method in the calculations of composite plates and beams of irregular shape]. *The Bulletin of KrasGAU*. 2017, No. 11, P. 131–140 (In Russ.).
17. Matveev A. D. [Multigrid finite element Method]. *The Bulletin of KrasGAU*. 2018, No. 2, P. 90–103 (In Russ.).
18. Matveev A. D. [The method of. multigrid finite elements of the composite rotational and bi-curved shell calculations]. *The Bulletin of KrasGAU*. 2018, No. 3, P. 126–137 (In Russ.).
19. Matveev A. D. [Method of. multigrid finite elements to solve physical boundary value problems]. Information technologies and mathematical modeling. Krasnoyarsk, 2017. P. 27–60.
20. Rabotnov Y. N. [Mechanics of a deformed solid]. Moscow, Nauka Publ., 1988, 711 p.
21. Demidov S. P. *Teoriya uprugosti* [Theory of elasticity]. Moscow, Vysshaya shkola Publ., 1979. 432 p.
22. Timoshenko S. P., Dzh. Gud'er. *Teoriya uprugosti* [Theory of elasticity]. Moscow, Nauka Publ., 1979, 560 p.
23. Bezuhov N. I. *Osnovy teorii uprugosti, plastichnosti i polzuchesti* [Fundamentals of the theory of elasticity, plasticity and creep]. Moscow, Vysshaya shkola Publ., 1968, 512 p.
24. Matveev A. D. [Some approaches of designing elastic multigrid finite elements]. *VINITI Proceedings*. 2000, № 2990-B00, P. 30 (In Russ.).
25. Matveev A. D. [Mixed discrete models in the analysis of elastic three-dimensional inhomogeneous bodies of complex shape]. *Vestnik PNIPU. Mekhanika*. 2013, No. 1, P. 182–195 (In Russ.).
26. Matveev A. D. [Multigrid modeling of composites of irregular structure with a small filling ratio]. *J. Appl. Mech. Tech. Phys.* 2004, No. 3, P. 161–171 (In Russ.).
27. Matveev A. D. [The construction of complex multigrid finite element heterogeneous and micro-inhomogeneities in structure]. *Izvestiya AltGU*. 2014. № 1/1, P. 80–83. Doi: 10.14258/izvasu(2014)1.1-18.
28. Matveev A. D. [Method of generating finite elements]. *The Bulletin of KrasGAU*. 2018, No. 6, P. 141–154 (In Russ.).
29. Matveev A. D. [Construction of multigrid finite elements to calculate shells, plates and beams based on generating finite elements]. *PNRPU Mechanics Bulletin*. 2019, No. 3, P. 48–57 (In Russ.). Doi: 10/15593/perm.mech/2019.3.05.
30. Golushko S. K., Nemirovskij Y. V. *Pryamye i obratnye zadachi mekhaniki uprugih kompozitnyh plastin i obolochek vrashcheniya* [Direct and inverse problems of mechanics of elastic composite plates and shells of rotation]. Moscow, Fizmatlit Publ., 2008, 432 p.
31. Nemirovskij Y. V., Reznikov B. S. *Prochnost' elementov konstrukcij iz kompozitnyh materialov* [Strength of structural elements made of composite materials]. Novosibirsk, Nauka Publ., 1984, 164 p.
32. Kravchuk A. S., Majboroda V. P., Urzhumcev Y. S. *Mekhanika polimernyh i kompozicionnyh materialov* [Mechanics of polymer and composite materials]. Moscow, Nauka Publ., 1985, 201 p.
33. Alfutov N. A., Zinov'ev A. A., Popov B. G. *Raschet mnogosloynnyh plastin i obolochek iz kompozicionnyh materialov* [Calculation of multilayer plates and shells made of composite materials]. Moscow, Mashinostroenie Publ., 1984, 264 p.
34. Pobedrya B. E. *Mekhanika kompozicionnyh materialov* [Mechanics of composite materials]. Moscow, MGU Publ., 1984, 336 p.

35. Andreev A. N., Nemirovskij Y. V. *Mnogosloynnye anizotropnye obolochki i plastiny. Izgib, ustojchivost', kolebaniya* [Multilayer anisotropic shells and plates. Bending, stability, vibration]. Novosibirsk, Nauka Publ., 2001, 288 p.
36. Vanin G. A. *Mikromekhanika kompozicionnyh materialov* [Micromechanics of composite materials]. Kiev, Naukova dumka Publ., 1985, 302 p.
37. Vasil'ev V. V. *Mekhanika konstrukcij iz kompozicionnyh materialov* [Mechanics of structures made of composite materials]. Moscow, Mashinostroenie Publ., 1988, 269 p.
38. Guz' A. N., Ignatov I. V., Girchenko A. G. et al. [Mechanics of composite materials and structural elements]. *Prikladnye issledovaniya*. 1983, Vol. 3, 262 p.
39. Samul' V. I. *Osnovy teorii uprugosti i plastichnosti* [Fundamentals of the theory of elasticity and plasticity]. Moscow, Vysshaia shkola Publ., 1982, 264 p.

Библиографические ссылки

1. Писаренко Г. С., Яковлев А. П., Матвеев В. В. Справочник по сопротивлению материалов. Киев : Наук. думка, 1975. 704 с.
2. Биргер И. А., Шорр Б. Ф., Иосилевич Г. Б. Расчет на прочность деталей машин. М. : Машиностроение, 1993. 640 с.
3. Москвичев В. В. Основы конструкционной прочности технических систем и инженерных сооружений. Новосибирск : Наука, 2002. 106 с.
4. Матвеев А. Д. Расчет упругих конструкций с применением скорректированных условий прочности. // Известия АлтГУ. Математика и механика. 2017. № 4. С. 116–119. Doi: 10.14258/izvasu (2017)4-21.
5. Zienkiewicz O. C., Taylor R. L., Zhu J. Z. The finite element method: its basis and fundamentals. Oxford: Elsevier Butterworth-Heinemann, 2013. 715 p.
6. Голованов А. И., Тюленева О. И., Шигабутдинов А. Ф. Метод конечных элементов в статике и динамике тонкостенных конструкций. М. : Физматлит, 2006. 392 с.
7. Бате К., Вилсон Е. Численные методы анализа и метод конечных элементов. М. : Стройиздат, 1982. 448 с.
8. Образцов И. Ф., Савельев Л. М., Хазанов Х. С. Метод конечных элементов в задачах строительной механики летательных аппаратов. М. : Высшая школа, 1985. 392 с.
9. Секулович М. Метод конечных элементов. М. : Стройиздат, 1993. 664 с.
10. Норри Д., Ж. де Фриз. Введение в метод конечных элементов: М. : Мир, 1981. 304 с.
11. Зенкевич О. Метод конечных элементов в технике. М. : Мир, 1975. 542 с.
12. Фудзии Т., Дзако М. Механика разрушения композиционных материалов. М. : Мир, 1982. 232 с.
13. Матвеев А. Д. Метод многосеточных конечных элементов в расчетах трехмерных однородных и композитных тел // Учен. зап. Казан. ун-та. Серия: Физ.-мат. науки. 2016. Т. 158, кн. 4. С. 530–543.
14. Матвеев А. Д. Метод многосеточных конечных элементов в расчетах композитных пластин и балок. // Вестник КрасГАУ. 2016. № 12. С. 93–100.
15. Matveev A. D. Multigrid finite element method in stress of three-dimensional elastic bodies of heterogeneous structure // IOP Conf. Ser.: Mater. Sci. Eng. 2016. Vol. 158, No. 1. Art. 012067. P. 1–9.
16. Матвеев А. Д. Метод многосеточных конечных элементов в расчетах композитных пластин и балок сложной формы. // Вестник КрасГАУ. 2017. № 11. С. 131–140.

17. Матвеев А. Д. Метод многосеточных конечных элементов. // Вестник КрасГАУ. 2018. № 2. С. 90–103.
18. Матвеев А. Д. Метод многосеточных конечных элементов в расчетах композитных оболочек вращения и двоякой кривизны // Вестник КрасГАУ. 2018. № 3. С. 126–137.
19. Матвеев А. Д. Метод многосеточных конечных элементов в решении физических краевых задач // Информационные технологии и математическое моделирование. Красноярск, 2017. С. 27–60.
20. Работнов Ю. Н. Механика деформированного твердого тела. М. : Наука, 1988. 711 с.
21. Демидов С. П. Теория упругости. М. : Высшая школа, 1979. 432 с.
22. Тимошенко С. П., Дж. Гудьер. Теория упругости. М. : Наука, 1979. 560 с.
23. Безухов Н. И. Основы теории упругости, пластичности и ползучести. М. : Высшая школа, 1968. 512 с.
24. Матвеев А. Д. Некоторые подходы проектирования упругих многосеточных конечных элементов // Деп. в ВИНТИ. 2000. № 2990–В00. 30 с.
25. Матвеев А. Д. Смешанные дискретные модели в анализе упругих трехмерных неоднородных тел сложной формы. // Вестник ПНИПУ. Механика. 2013. № 1. С. 182–195.
26. Матвеев А. Д. Многосеточное моделирование композитов нерегулярной структуры с малым коэффициентом заполнения. // Прикладная механика и техническая физика. 2004. № 3. С. 161–171.
27. Матвеев А. Д. Построение сложных многосеточных конечных элементов с неоднородной и микрон неоднородной структурой // Известия АлтГУ. Серия: Математика и механика. 2014. № 1/1. С. 80–83. Doi: 10.14258/izvasu(2014)1.1-18.
28. Матвеев А. Д. Метод образующих конечных элементов // Вестник КрасГАУ. 2018. № 6. С. 141–154.
29. Матвеев А. Д. Построение многосеточных конечных элементов для расчета оболочек, пластин и балок на основе образующих конечных элементов // Вестник ПНИПУ. Механика. 2019. № 3. С. 48–57. Doi: 10/15593/perm.mech/2019.3.05.
30. Голушко С. К., Немировский Ю. В. Прямые и обратные задачи механики упругих композитных пластин и оболочек вращения. М. : Физматлит, 2008. 432 с.
31. Немировский Ю. В., Резников Б. С. Прочность элементов конструкций из композитных материалов. Новосибирск : Наука ; Сибирское отделение, 1984. 164 с.
32. Кравчук А. С., Майборода В. П., Уржумцев Ю. С. Механика полимерных и композиционных материалов. М. : Наука. 1985. 201 с.
33. Алфутов Н. А., Зиновьев А. А., Попов Б. Г. Расчет многослойных пластин и оболочек из композиционных материалов. М. : Машиностроение, 1984. 264 с.
34. Победра Б. Е. Механика композиционных материалов. М. : МГУ, 1984. 336 с.
35. Андреев А. Н., Немировский Ю. В. Многослойные анизотропные оболочки и пластины. Изгиб, устойчивость, колебания. Новосибирск : Наука, 2001. 288 с.
36. Ванин Г. А. Микромеханика композиционных материалов. Киев : Наукова думка, 1985. 302 с.
37. Васильев В. В. Механика конструкций из композиционных материалов. М. : Машиностроение, 1988. 269 с.
38. Механика композитных материалов и элементов конструкций. Т. 3. Прикладные исследования / А. Н. Гузь, И. В. Игнатов, А. Г. Гирченко и др. Киев : Наукова думка, 1983. 262 с.
39. Самуль В. И. Основы теории упругости и пластичности. М. : Высшая школа, 1982. 264 с.

© Matveev A. D., 2021

Матвеев Александр Данилович – кандидат физико-математических наук, доцент, старший научный сотрудник, Институт вычислительного моделирования СО РАН. E-mail: mtv241@mail.ru.

Matveev Alexander Danilovich is a Candidate of Physical and Mathematical Sciences, an associate Professor, a senior researcher of the Institute of computational modeling of SB RAS. E-mail: mtv241@mail.ru.

УДК 621.791.722

Doi: 10.31772/2712-8970-2021-22-2-261-274

Для цитирования: Программная система математического моделирования процесса электронно-лучевой сварки / А. В. Мурыгин, В. С. Тынченко, С. О. Курашкин и др. // Сибирский аэрокосмический журнал. 2021. Т. 22, № 2. С. 261–274. Doi: 10.31772/2712-8970-2021-22-2-261-274.

For citation: Murygin A. V., Tynchenko V. S., Kurashkin S. O., Bocharov A. N., Petrenko V. E. Software system for mathematical simulation of the electronic beam welding process. *Siberian Aerospace Journal*. 2021, Vol. 22, No. 2, P. 261–274. Doi: 10.31772/2712-8970-2021-22-2-261-274.

Программная система математического моделирования процесса электронно-лучевой сварки*

А. В. Мурыгин, В. С. Тынченко **, С. О. Курашкин, А. Н. Бочаров, В. Е. Петренко

Сибирский государственный университет науки и технологий имени академика М. Ф. Решетнева
Российская Федерация, 660037, г. Красноярск, просп. им. газ. «Красноярский рабочий», 31

**E-mail: vadimond@mail.ru

В рамках настоящего исследования предложена программная система моделирования распределения температурного поля в установившемся режиме процесса электронно-лучевой сварки тонкостенных конструкций аэрокосмического назначения. Целью создания такой программной системы является повышение качества управления процессом электронно-лучевой сварки и, соответственно, снижение количества дефектов в сварных соединениях тонкостенных конструкций. Программная система имеет модельную структуру и реализует предложенные ранее авторами модели распределения энергии. В качестве средств реализации программы были выбраны системы управления базами данных MySQL и программирования Embarcadero RAD Studio. Центральным звеном системы выступает база данных, позволяющая хранить и обрабатывать информацию как по математическому моделированию, так и по результатам имитационных и натурных экспериментов. В статье описана структура разработанной программной системы, а также представлены алгоритмы работы ее составных модулей. Система предоставляет пользователю возможность не только проводить моделирование по заданным технологическим параметрам (скорость сварки, ускоряющее напряжение, ток пучка, граничные условия, время моделирования, материал изделия), но и визуализировать результаты и сохранять их в единой базе данных. Применение предложенной системы позволяет не только минимизировать затраты предприятия на отработку технологических параметров установившегося режима для процесса электронно-лучевой сварки, но и создать гибкую информационную базу для сбора экспериментальной информации с целью дальнейшей автоматизации и интеллектуализации технологического процесса создания неразъемных соединений в рамках Индустрии 4.0.

Ключевые слова: электронно-лучевая сварка, моделирование, технологические параметры, программа, оптимизация, распределение энергии.

* Исследование выполнено при финансовой поддержке РФФИ, Правительства Красноярского края и Краевого фонда науки в рамках научного проекта № 20-48-242917 «Модели и методы управления процессом электронно-лучевой сварки тонкостенных конструкций».

The reported study was funded by Russian Foundation for Basic Research, Government of Krasnoyarsk Territory, Krasnoyarsk Regional Fund of Science, to the research project: “Models and methods for controlling the process of electron beam welding of thin-walled structures”, project No. 20-48-242917.

Software system for mathematical simulation of the electronic beam welding process

A. V. Murygin, V. S. Tynchenko*, S. O. Kurashkin, A. N. Bocharov, V. E. Petrenko

Reshetnev Siberian State University of Science and Technology
31, Krasnoyarskii rabochii prospekt, Krasnoyarsk, 660037, Russian Federation
*E-mail: vadimond@mail.ru

Within the framework of this study, a software system for modeling the distribution of the temperature field in the steady-state mode of the electron-beam welding process for thin-walled aerospace structures is proposed. The purpose of creating such a software system is to improve the quality of control of the electron-beam welding process and, accordingly, to reduce the number of defects in welded joints of thin-walled structures. The software system has a model structure and implements the energy distribution models proposed earlier by the authors. The MySQL database management system and the Embarcadero RAD Studio programming system were chosen as the means of implementing the program. The central link of the system is a database that allows you to store and process information both on mathematical modeling and on the results of simulation and field experiments. The article describes the structure of the developed software system, and also presents algorithms for the operation of its constituent modules. The system provides the user with the opportunity not only to carry out simulation according to the specified technological parameters (welding speed, accelerating voltage, beam current, boundary conditions, simulation time, product material), but also to visualize the results and save them in a single database. The use of the proposed system allows not only to minimize the costs of the enterprise for the development of technological parameters of the steady state for the electron-beam welding process, but also to create a flexible information base for collecting experimental information with the aim of further automating and intellectualizing the technological process of creating permanent joints in the framework of Industry 4.0.

Keywords: electron-beam welding, modelling, technological parameters, software, optimisation, normal distribution law.

Introduction

The basis of electron beam welding is the use of thermal energy released during the deceleration of a sharply focused stream of electrons accelerated to high energy levels.

The process of electron beam welding as a whole is considered in sources [1–3], where the authors propose to conduct research on various metals and in various branches of mechanical engineering. The wide possibilities of electron beam welding make it possible to use this technology for the manufacture of various types of products. For example, the authors of [4–6] use the technology of electron beam welding to obtain a channel for heating the blades of the inlet guide vane of gas turbines, and also determine the optimal options for the constructible structure of the welded joint, depending on the amount of allowance for machining.

Studies carried out in [7–9] have shown that during electron beam welding of tungsten single crystals, conditions are provided for epitaxial crystallization of the weld material, as a result of which its parameters correspond to the parameters of the single crystals being welded. After welding the joints using electric spark cutting, the technological sections are separated from the workpiece. Thus, a hollow monohedral tube is obtained, which is further used to produce the cathode of a thermionic converter.

At present, in order to further improve the quality of the technological process of electron-beam welding, many authors have carried out mathematical modeling of this technological process in differ-

ent modes and with different materials. For example, the authors of [10–12] considered the multicriteria optimization of the electron beam welding process using experimental data obtained on the basis of real exact models of the electron beam welding process, which describe the dependence of the geometry of welded joints on stainless steel on the parameters of the electron beam welding mode. In turn, the authors of [13–15] investigated the processes of formation of a melting channel in electron beam welding with full penetration of the material.

Within the framework of this study, a dynamic mathematical model has been proposed that makes it possible to describe the formation of a reverse bead of a welded seam depending on the parameters of the technological process of electron beam welding. The mathematical model of the processes of evaporation, condensation, and diffusion of the AMg-6 alloy in electron beam welding with dynamic positioning of the electron beam is described in [16–18]. The developed model makes it possible to predict the chemical composition of welds in electron beam welding.

The model was verified by comparing it with the results of the analysis of the chemical composition of the penetration zones in the material. The development of electron beam welding technology, the development of new control methods for this technological process gave rise to a wide range of modes of action of an electron beam on the surface of the parts to be welded. In [19–21], a differential heat conduction equation is presented, which is a mathematical model of a whole class of heat conduction phenomena.

The authors of [22–24] developed a mathematical model of scanning electron beam welding, which made it possible to simulate the dynamics of the technological process and obtain a criterion for its optimization.

Mathematical support of the software

The software system proposed in the study allows calculating the distribution of the temperature field for given process parameters, such as:

1. Welding speed.
2. Accelerating voltage and beam current.
3. The considered coordinate area (coordinate limits and grid step).
4. Time of exposure.
5. Product material.

All the above-described parameters stored in the database are used as input data for the model, and the output is vector temperature correspondences depending on coordinates and time. In addition, the data obtained during the simulation, if necessary, can be used to optimize the parameters of the electron beam welding (EBW) process within the framework of the investigated mode. For this, the possibility of both data export and integration into the software system of the module for optimization is provided.

In accordance with fig. 1 point source of heat of constant power q moves with constant speed v rectilinearly from point O_0 in the direction of the x -axis. Since the moment of movement of the source, time t_h has passed and it is at point O . Together with the source of heat, a moving coordinate system move, the origin of which coincides with the location of the heat source, i.e with point O [25].

As the basic formulas for calculating the temperature field [25], expressions are used that describe the actions of an instantaneous point source on the surface of a semi-infinite body (1) and a linear source in an infinite plate (2):

$$T_1(x, y, z, q, v, t) = T_h + \frac{2q}{c\rho\sqrt{(4\pi a)^3}} e^{-\frac{v\tau}{2a}t} \int_0^t e^{-\frac{v^2\tau}{4a} - \frac{x^2+y^2+z^2}{4a\tau}} \frac{d\tau}{\tau^{3/2}}, \quad (1)$$

where x, y, z are the coordinates of the point in question in space; q is the effective power of the electron beam; v is the welding speed; t is the time counted from the moment the source passes through the section in which the point under consideration is located; T_H is the initial temperature of the product; cp is the heat capacity of the material; a is a coefficient of thermal diffusivity; $\tau = t - t'$ is the duration of heat propagation in the moving coordinate system; t is the current moment in time; t' is a certain moment of time after the start of heating, in which the heat source is located at point O' with coordinates $(vt', 0, 0)$ (fig. 1).

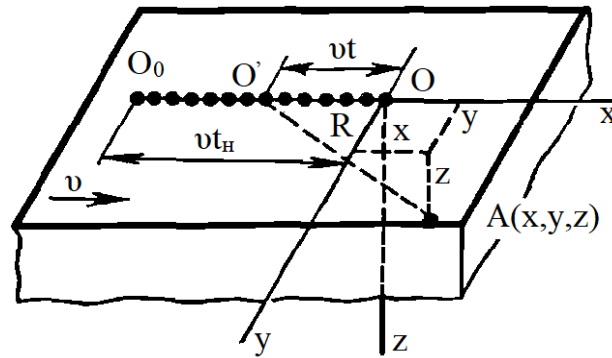


Рис. 1. Схема движения непрерывно действующего точечного источника на поверхности полубесконечного тела мощностью q , перемещающегося со скоростью v

Fig. 1. Scheme of motion of a continuously acting point source on the surface of a semi-infinite body of power q , moving with speed v

In accordance with fig. 2, a linear heat source of power q with a uniform distribution over the thickness of the plate moves at a constant speed v . Boundary planes

$z = 0$ and $z = \delta$ give off heat to the environment, the temperature of which T_H is equal to the initial temperature of the body [25].

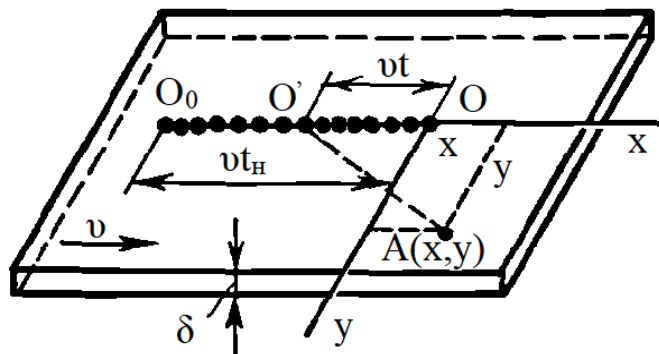


Рис. 2. Схема движения непрерывно действующего линейного источника в бесконечной пластине мощностью q , перемещающегося со скоростью v

Fig. 2. The scheme of motion of a continuously operating linear source in an infinite plate of power q , moving with a speed v

$$T_2(x, y, q, v, t) = T_H + \frac{q}{4\pi\lambda\delta} e^{-\frac{vx}{2a}} \int_0^t e^{-\frac{v^2\tau}{4a} - \frac{2\lambda\tau}{cp\delta} - \frac{x^2+y^2}{4a\tau}} \frac{d\tau}{\tau}, \quad (2)$$

Where δ is the thickness of the product; λ is the coefficient of thermal conductivity; t is the warmth propagation time.

In this paper we apply the model of power, representing a function (3), recorded as follows:

$$Q = I \cdot U \cdot \eta \cdot 0,24, \quad (3)$$

Where U is accelerating voltage; I is a beam current; η is efficiency.

A complex fast-moving source was selected as a combination of two sources - a point and a linear one, equivalent to the real ones, taking place in the literature [25]. The calculation of the value of the functional is performed for an area whose dimensions are comparable to the dimensions of the penetration channel.

These formulae allow, when they are added (superposition of sources) in the process of calculation, to describe the nature of the distribution of thermal energy after exposure to an electron beam.

The algorithm for calculating the model is shown in fig. 3.

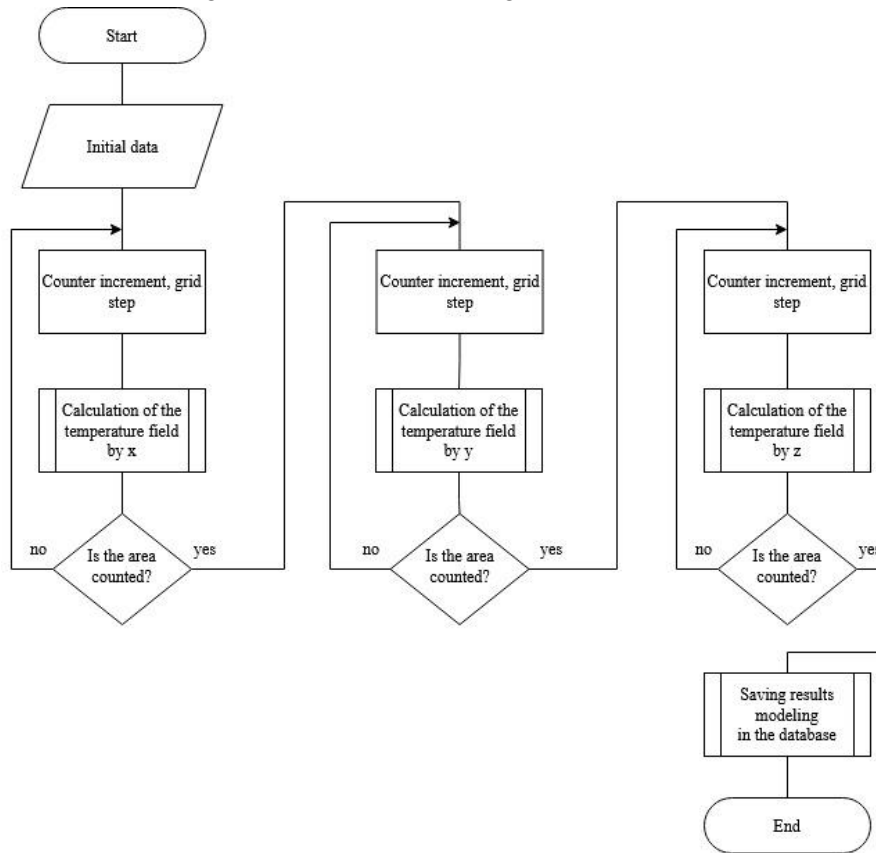


Рис. 3. Алгоритм математического моделирования теплового поля

Fig. 3. Algorithm for mathematical modeling of the thermal field

At the initial stage of the algorithm shown in Fig. 3, the original data is received from the corresponding record in the database. Further, a sequential calculation of the temperature field is carried out along three coordinate axes; the results obtained are recorded in the database and remain available for further analysis and use.

Fig. 4 shows a block diagram of the sub-process for calculating the field in one coordinate. Its cyclic use in all directions makes it possible to obtain a temperature field.

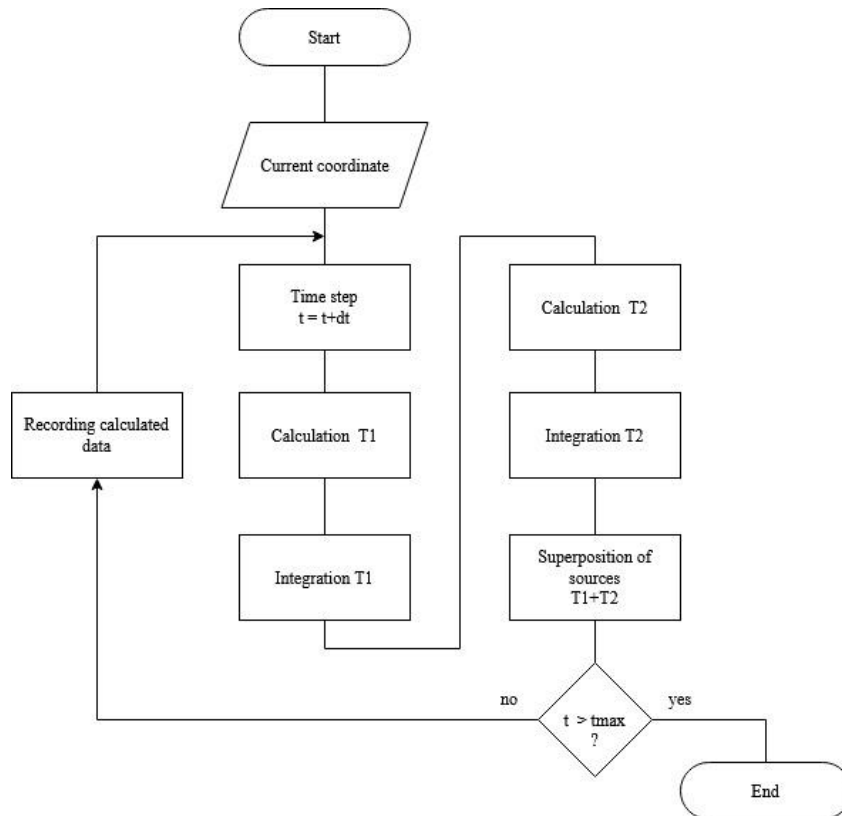


Рис. 4. Алгоритм подпроцесса расчета температурного поля в рамках одной координаты

Fig. 4. Algorithm for the sub-process of calculating the temperature field within one coordinate

Within the software system, a graphical display of simulation results is available, which can be carried out according to the principle of assigning axes and the corresponding codependent value.

This module of the software environment allows the operator to assess the feasibility of certain technological modes, which in turn, greatly facilitates the task of exploratory research in field experiments.

Software design

The software system for mathematical modeling of the electron beam welding process was developed in the C++ language and is a Windows application that can work in the environment of Windows 7/8/10 operating systems. The block diagram of the software system is shown in fig.5.

The software system consists of 6 modules with the following functions:

1. The module of mathematical modeling implements the model of the electron beam welding process.
2. The module for editing the parameters of the model carries out the input and editing of the physical parameters of materials, the parameters of the ELS process and the parameters of the product.
3. The simulation data import module carries out the input of data and simulation graphs implemented in third-party simulation software products, Comsol Multiphysics and Ansys.
4. The module for importing data from a full-scale experiment carries out the input of the results of full-scale experiments carried out on an electron-beam installation, including photographs of thin sections, a description of welding defects, etc.
5. The graphics module provides graphical construction of the results of mathematical modeling of the ELS process.
6. The data viewing module displays and edits the results of simulation and field experiments.

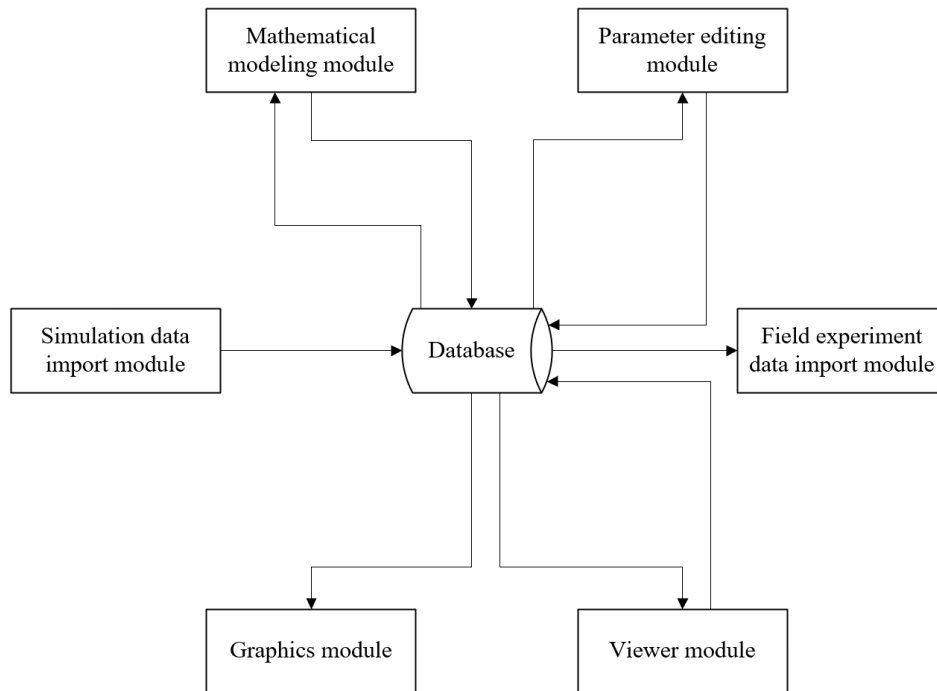


Рис. 5. Структурная схема программной системы математического моделирования процесса ЭЛС

Fig. 5. Block diagram of the software system for mathematical modeling of the EBW process

The block diagram of the software system is shown in Fig.6.

The central object of the system is an experiment, which can be presented as the result of a mathematical model, simulation and field experiments. Work in the software system begins with the creation of an experiment and the determination of its parameters (material properties, parameters of the ELS process, product parameters). You can also work with experiments that are already in the system by editing their parameters.

After saving the parameters of the experiment, it is necessary to select one of the actions: start mathematical modeling of the ELS process, load the data of simulation and full-scale experiment, edit and view the data already obtained. As a result of performing actions, there is a constant interaction with the database.

At the end of all manipulations with experiments and their results, you must log out of the system.

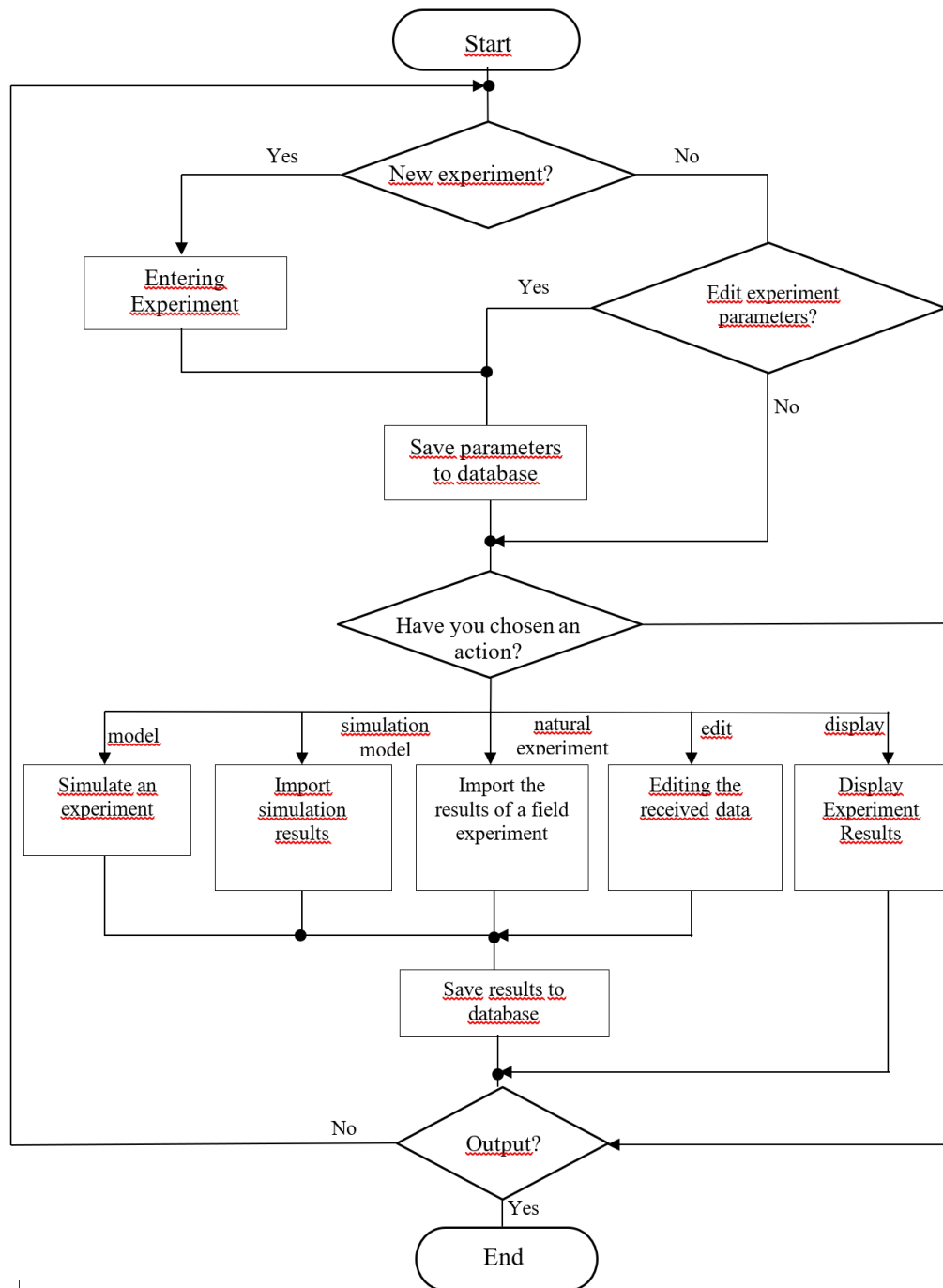


Рис. 6. Блок-схема работы программной системы моделирования ЭЛС

Fig. 6. Block diagram of the EBW simulation software system

Information support of the software system

The central link table is the experiment table. Physical parameters of materials, EBW process parameters, and product parameters are stored in the material table, techprocess and workpiece tables, respectively. These parameters describe the experiment and are used for mathematical modeling of the process. The modeling and data_modeling tables are designed to store the results of mathematical modeling of the ELS process, and the simulation and data_simul tables are designed to store the results of the simulation modeling carried out in third-party software products. The practice table stores the results of field experiments.

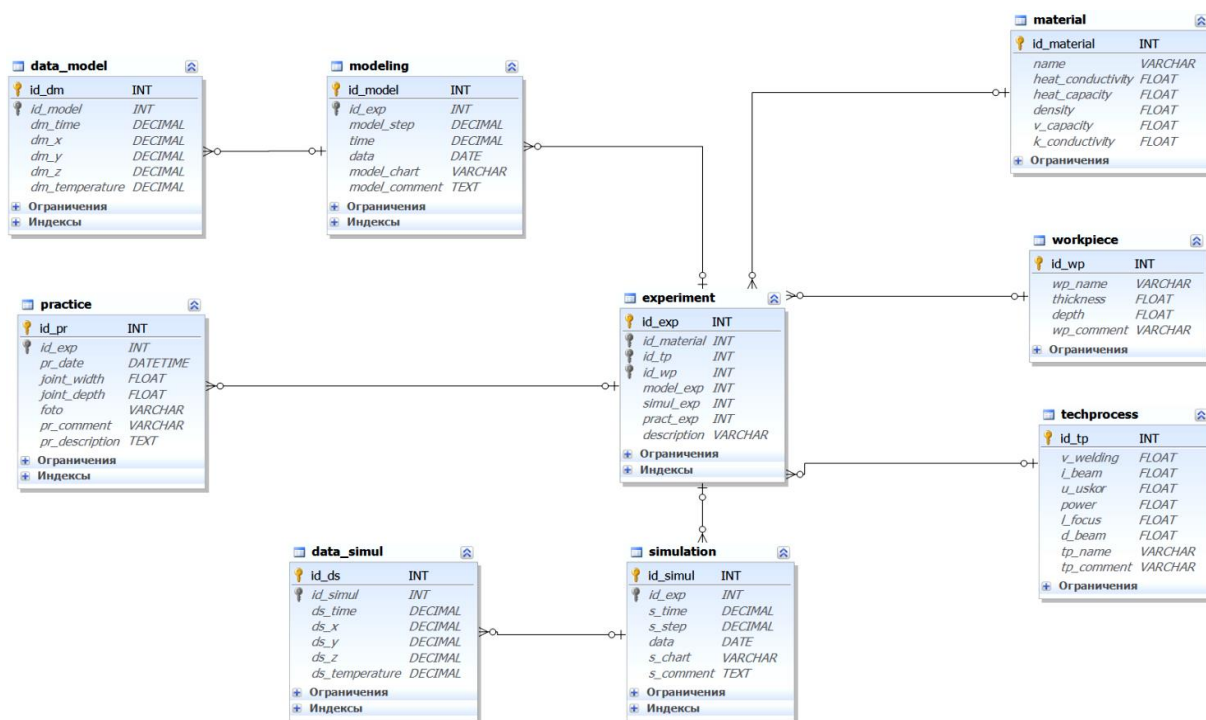


Рис. 7. Структурная схема базы данных программной системы моделирования ЭЛС

Fig. 7. Block diagram of the database of the EBW modeling software system

Description of the software system operation

Fig. 8 shows the basic form of the software system for mathematical modeling of the ELS process.

The main form has four tabs: experiment planning, modeling, simulation, natural experiment. The work of the software system begins with the main tab - experiment planning. This tab is designed to control the modeling process. Here new experiments are created or old ones are displayed, experiment parameters are displayed, and new simulation conditions are set.

This tab is divided into three main blocks: material, process technology and product. In these blocks, the physical parameters of the product material, the parameters of the ELS process and the parameters of the product itself are specified. The specified parameters will then be used to simulate the ELS process.

Each block contains a block of buttons for defining new materials, processes and products. Gray color of the labels indicates that the blocks are in the information display mode. Black color signals the input of experimental conditions. At the bottom of the screen, there is a list of experiments, the parameters of which are displayed above. The block of buttons allows you to create, delete, save and edit experiment conditions. The block "State of the experiment" displays the fullness of the experiment, that is, whether the simulation was carried out, whether the data of the simulation and the full-scale experiment were loaded.

Файл | Помощь

Планирование эксперимента | Моделирование | Имитационное моделирование | Натурный эксперимент

Материал

Добавить

не выбран

Сохранить

Отменить

yt14

Теплопроводность: 13,819996948242

Удельная теплоемкость: 0,712000012397766

Плотность: 4520

Объемная теплоемкость: 0

Коэффициент температуропроводности: 9

Техпроцесс

Добавить

не выбран

Сохранить

Отменить

результатов моделирования

Скорость сварки: 5

Ток Сварки: 140

Ускоряющее напряжение: 20

Энергия: 0

Фокусное расстояние: 140

Диаметр луча: 3

Натурный эксперимент основанный на результатах математического и имитационного моделирования

Изделие

Добавить

не выбрано

Сохранить

Отменить

Имитационный диск из VT14

Толщина изделия: 1,2

Глубина проплавления: 0,7

Диск из титанового сплава (vt14) диаметром 15см

Материал	Техпроцесс	Изделие	Описание эксперимента
Материал1	процесс1	изделие1	
Материал2			
Материал3			

Новый эксперимент | Редактирование параметров | Сохранить | Удалить | Отменить

Рис. 8. Основная форма программной системы математического моделирования ЭЛС

Fig. 8. The main form of the software system for mathematical modeling of EBW

Conclusion

Within the framework of this study, a software system for modeling the distribution of the temperature field in the steady-state mode of the electron-beam welding process for thin-walled aerospace structures is proposed. The software system has a model structure and implements the energy distribution models proposed earlier by the authors. The central link of the system is a database that allows you to store and process information both on mathematical modeling and on the results of simulation and field experiments. The use of the proposed system allows not only to minimize the costs of the enterprise for the development of technological parameters of the steady state for the electron-beam welding process, but also to create a flexible information base for collecting experimental information for the purpose of further automation and intellectualization of the technological process of creating permanent joints within the framework of Industry 4.0.

Библиографические ссылки

1. Yunlian Q., Ju D., Quan H., Liying Z. Electron beam welding, laser beam welding and gas tungsten arc welding of titanium sheet // Materials Science and Engineering A. 2000. Vol. 280, No. 1. P. 177–181.

2. Саломатова Е. С. Электронно-лучевая сварка – от изобретения до наших дней // Вестник Пермского нац. исслед. политехнич. ун-та. Машиностроение, материаловедение. 2013. № 1. С. 74–87.
3. Пермяков Г. Л., Олышанская Т. В., Беленький В. Я., Трушников Д. Н. Моделирование электронно-лучевой сварки для определения параметров сварных соединений разнородных материалов // Вестник Пермского нац. исслед. политехнич. ун-та. Машиностроение, материаловедение. 2013. № 4. С. 48–58.
4. Шаронов Н. И. Применение электронно-лучевой сварки в турбостроении // Науч.-технич. ведомости СПбПУ. Естественные и инженерные науки. 2010. № 3 (106). С. 170–175.
5. Denlinger E. R. Thermo-mechanical modeling of large electron beam builds // Thermo-Mechanical Modeling of Additive Manufacturing. – Butterworth-Heinemann. 2018. Vol. 150, No. 2. P. 167–181.
6. Raj R. A., Anand M. D. Modeling and prediction of mechanical strength in electron beam welded dissimilar metal joints of stainless steel 304 and copper using grey relation analysis // Int. J. Eng. Technol. 2018. Vol. 7, No. 1. P. 198–201.
7. Ластовирия В. Н., Новокрещенов В. В., Родякина Р. В. Использование электронно-лучевой сварки для создания термоэмиссионных преобразователей (ТЭП) из монокристаллов вольфрама // Глобальная ядерная безопасность. 2015. № 3 (16). С. 27–35.
8. Chowdhury S., Yadaiah N., Khan S. M., Ozah R., Das B., Muralidhar M. A perspective review on experimental investigation and numerical modeling of electron beam welding process // Materials Today: Proceedings. 2018. Vol. 5, No. 2. P. 4811–4817.
9. Wang J., Hu R., Chen X., Pang S. Modeling fluid dynamics of vapor plume in transient keyhole during vacuum electron beam welding // Vacuum. 2018. Vol. 157, No. 1. P. 277–290.
10. Младенов Г., Колева Е., Беленький В. Я., Трушников Д. Н. Моделирование и оптимизация электронно-лучевой сварки сталей // Вестник Пермского нац. исслед. политехнич. ун-та. Машиностроение, материаловедение. 2014. Т. 16. № 4. С. 7–21.
11. Kanigalpula P. K. C., Jaypuria S., Pratihari D. K., Jha M. N. Experimental investigations, input-output modeling, and optimization of spiking phenomenon in electron beam welding of ETP copper plates // Measurement. 2018. Vol. 129, No. 1. P. 302–318.
12. Luo M., Hu R., Liu T., Wu B., Pang S. Optimization possibility of beam scanning for electron beam welding: Physics understanding and parameters selection criteria // International Journal of Heat and Mass Transfer. 2018. Vol. 127, No. 1. P. 1313–1326.
13. Беленький В. Я., Трушников Д. Н., Пискунов А. Л., Лялин А. Н. Динамическая модель электронно-лучевой сварки со сквозным проплавлением // Вестник Пермского нац. исслед. политехнич. ун-та. Машиностроение, материаловедение. 2011. Т. 13. № 3 (5). С. 72–84.
14. Das D., Pratihari D. K., Roy G. G. Cooling rate predictions and its correlation with grain characteristics during electron beam welding of stainless steel // The International Journal of Advanced Manufacturing Technology. 2018. Vol. 97, No. 5-8. P. 2241–2254.
15. Tadano S., Hino T., Nakatani Y. A modeling study of stress and strain formation induced during melting process in powder-bed electron beam melting for Ni superalloy // Journal of Materials Processing Technology. 2018. Vol. 257, No. 1. P. 163–169.
16. Саломатова Е. С., Трушников Д. Н., Цаплин А. И. Моделирование процессов испарения при электронно-лучевой сварке с динамическим позиционированием электронного пучка // Известия Тульского гос. ун-та. Технические науки. 2015. № 6-2. С. 124–133.
17. Węglowski M. S., Błacha S., Phillips A. Electron beam welding—Techniques and trends—Review // Vacuum. 2016. Vol. 130, No. 1. P. 72–92.

18. Trushnikov D. N., Belenki'y V. Y., Mladenov G. M., Portnov N. S. Secondary Emission signal for weld formation monitoring and control in electron beam welding (EBW) // *Materialwissenschaft und Werkstofftechnik*. 2012. Vol. 43, No. 10. P. 892–897.
19. Ольшеванская Т. В., Федосеева Е. М., Колева Е. Г. Построение тепловых моделей при электронно-лучевой сварке методом функций Грина // *Вестник Пермского нац. исслед. политехнич. ун-та. Машиностроение, материаловедение*. 2017. Т. 19, № 3. С. 49–74.
20. Трушников Д. Н., Беленький В. Я. Исследование формирования сигнала вторичного тока в плазме при электронно-лучевой сварке с осцилляцией электронного пучка // *Сварочное производство*. 2012. № 11. С. 9–13.
21. Nishimura F., Nakamura H., Takahashi H., Takamoto T. Development of a new investment for high-frequency induction soldering // *Dental materials journal*. 1992. Vol. 11, No. 1. P. 59–69.
22. Wang D., Wang S., Zhang W. Numerical Simulation and Experimental Investigation on Ti70 Titanium Alloy Electron-Beam-Welded Joint // *Transactions of the Indian Institute of Metals*. 2020. Vol. 73, No. 9. P. 2361–2369.
23. Lanin V. L., Sergachev I. I. Induction devices for assembly soldering in electronics // *Surface engineering and applied electrochemistry*. 2012. Vol. 48, No. 4. P. 384–388.
24. Moghaddam M., Mojallali H. Neural network based modeling and predictive position control of traveling wave ultrasonic motor using chaotic genetic algorithm // *International Review on Modelling and Simulations*. 2013. Vol. 6, No. 2. P. 370–379.
25. Коновалов А. В. Теория сварочных процессов. М. : Изд-во МГТУ им. Н. Э. Баумана. 2007. 752 с.
26. MySQL [Электронный ресурс]. URL: <https://www.mysql.com/> (дата обращения 01.05.2021).
27. MySQL для больших данных / Ш. Чаллавала, Дж. Лакхатария, Ч. Мехта, К. Патель. М. : ДМК Пресс, 2018. 226 с.

References

1. Yunlian Q., Ju D., Quan H., Liying Z. Electron beam welding, laser beam welding and tungsten arc welding of titanium sheet. *Materials Science and Engineering A*. 2000. Vol. 280, No. 1. P. 177–181.
2. Salomatova E. S. [Electron beam welding - from invention to the present day]. *Bulletin of the Perm National Research Polytechnic University. Mechanical engineering, materials science*. 2013. No. 1. P. 74–87. (In Russ.)
3. Permyakov G. L., Olshanskaya T. V., Belenkiy V. Ya., Trushnikov D. N. [Simulation of electron beam welding to determine the parameters of welded joints of dissimilar materials]. *Bulletin of the Perm National Research Polytechnic University. Mechanical engineering, materials science*. 2013, No. 4, P. 48–58. (In Russ.)
4. Sharonov N. I. [Application of electron-beam welding in turbine construction]. *Nauchno-tekhnicheskie vedomosti SPbPU. Natural and engineering sciences*. 2010, No. 3 (106), P. 170–175. (In Russ.)
5. Denlinger E. R. Thermo-mechanical modeling of large electron beam builds. *Thermo-Mechanical Modeling of Additive Manufacturing*. – *Butterworth-Heinemann*. 2018, Vol. 150, No. 2, P. 167–181.
6. Raj R. A., Anand M. D. Modeling and prediction of mechanical strength in electron beam welded dissimilar metal joints of stainless steel 304 and copper using grey relation analysis. *Int. J. Eng. Technol*. 2018, Vol. 7, No. 1, P. 198–201.

7. Lastovirya V. N., Novokreshchenov V. V., Rodyakina R. V. [The use of electron beam welding to create thermoemission converters (TEC) from tungsten single crystals]. *Global Nuclear Safety*. 2015, No. 3 (16), P. 27–35. (In Russ.)
8. Chowdhury S., Yadaiah N., Khan S. M., Ozah R., Das B., Muralidhar M. A perspective review on experimental investigation and numerical modeling of electron beam welding process. *Materials Today: Proceedings*. 2018, Vol. 5, No. 2, P. 4811–4817.
9. Wang J., Hu R., Chen X., Pang S. Modeling fluid dynamics of vapor plume in transient keyhole during vacuum electron beam welding. *Vacuum*. 2018, Vol. 157, No. 1, P. 277–290.
10. Mladenov G., Koleva E., Belenky V. Ya., Trushnikov D. N. [Modeling and optimization of electron beam welding of steels]. *Bulletin of the Perm National Research Polytechnic University. Mechanical engineering, materials science*. 2014, Vol. 16, No. 4, P. 7–21. (In Russ.)
11. Kanigalpula P. K. C., Jaypuria S., Pratihari D. K., Jha M. N. Experimental investigations, input-output modeling, and optimization of spiking phenomenon in electron beam welding of ETP copper plates. *Measurement*. 2018, Vol. 129, No. 1, P. 302–318.
12. Luo M., Hu R., Liu T., Wu B., Pang S. Optimization possibility of beam scanning for electron beam welding: Physics understanding and parameters selection criteria. *International Journal of Heat and Mass Transfer*. 2018, Vol. 127, No. 1, P. 1313–1326.
13. Belenky V. Ya., Trushnikov D. N., Piskunov A. L., Lyalin A. N. [Dynamic model of electron beam welding with through penetration]. *Bulletin of the Perm National Research Polytechnic University. Mechanical engineering, materials science*. 2011, Vol. 13, No. 3 (5), P. 72–84. (In Russ.)
14. Das D., Pratihari D. K., Roy G. G. Cooling rate predictions and its correlation with grain characteristics during electron beam welding of stainless steel. *The International Journal of Advanced Manufacturing Technology*. 2018, Vol. 97, No. 5-8, P. 2241–2254.
15. Tadano S., Hino T., Nakatani Y. A modeling study of stress and strain formation induced during melting process in powder-bed electron beam melting for Ni superalloy. *Journal of Materials Processing Technology*. 2018, Vol. 257, No. 1, P. 163–169.
16. Salomatova E. S., Trushnikov D. N., Tsaplin A. I. [Simulation of evaporation processes in electron beam welding with dynamic positioning of the electron beam]. *Izvestiya Tula State University. Technical science*. 2015, No. 6-2, P. 124–133. (In Russ.)
17. Węglowski M. S., Błacha S., Phillips A. Electron beam welding—Techniques and trends—Review. *Vacuum*. 2016, Vol. 130, No. 1, P. 72–92.
18. Trushnikov D. N., Belenkiy V. Ya., Mladenov G. M., Portnov N. S. Secondary Emission signal for weld formation monitoring and control in electron beam welding (EBW). *Materialwissenschaft und Werkstofftechnik*. 2012, Vol. 43, No. 10, P. 892–897.
19. Olshanskaya T. V., Fedoseeva E. M., Koleva E. G. [Construction of thermal models in electron beam welding by the method of Green's functions]. *Bulletin of the Perm National Research Polytechnic University. Mechanical engineering, materials science*. 2017, Vol. 19, No. 3, P. 49–74. (In Russ.)
20. Trushnikov D. N., Belenkiy V. Ya. [Investigation of the formation of a secondary current signal in plasma during electron beam welding with electron beam oscillation]. *Welding production*. 2012, No. 11, P. 9–13. (In Russ.)
21. Nishimura F., Nakamura H., Takahashi H., Takamoto T. Development of a new investment for high-frequency induction soldering. *Dental materials journal*. 1992, Vol. 11, No. 1, P. 59–69.
22. Wang D., Wang S., Zhang W. Numerical Simulation and Experimental Investigation on Ti70 Titanium Alloy Electron-Beam-Welded Joint. *Transactions of the Indian Institute of Metals*. 2020, Vol. 73, No. 9, P. 2361–2369.

23. Lanin V. L., Sergachev I. I. Induction devices for assembly soldering in electronics. *Surface engineering and applied electrochemistry*. 2012, Vol. 48, No. 4, P. 384–388.
24. Moghaddam M., Mojallali H. Neural network based modeling and predictive position control of traveling wave ultrasonic motor using chaotic genetic algorithm. *International Review on Modelling and Simulations*. 2013, Vol. 6, No. 2, P. 370–379.
25. Konovalov A. V. *Teoriya svarochnykh protsessov* [Theory of welding processes]. Moscow, Izd-vo MGTU im. N. E. Bauman Publ., 2007, 752 p.
26. MySQL. Available at: <https://www.mysql.com/> (accessed 01.05.2021).
27. Challawala Sh., Lakhataria J., Mehta Ch., Patel K. *MySQL dlya bol'shikh dannykh* [MySQL for Big Data]. Moscow, DMK Press Publ., 2018, 226 p.

© Мурыгин А. В., Тынченко В. С., Курашкин С. О.,
Бочаров А. Н., Петренко В. Е., 2021

Мурыгин Александр Владимирович – доктор технических наук, заведующий кафедрой информационно-управляющих систем; Сибирский государственный университет науки и технологий имени академика М. Ф. Решетнева. E-mail: avm514@mail.ru.

Тынченко Вадим Сергеевич – кандидат технических наук, доцент кафедры информационно-управляющих систем; Сибирский государственный университет науки и технологий имени академика М. Ф. Решетнева. E-mail: vadimond@mail.ru.

Курашкин Сергей Олегович – аспирант; Сибирский государственный университет науки и технологий имени академика М. Ф. Решетнева. E-mail: scorpion_ser@mail.ru.

Бочаров Алексей Николаевич – кандидат технических наук, доцент кафедры информационно-управляющих систем; Сибирский государственный университет науки и технологий имени академика М. Ф. Решетнева. E-mail: sibalexbo@gmail.com.

Петренко Вячеслав Евгеньевич – аспирант; Сибирский государственный университет науки и технологий имени академика М. Ф. Решетнева. E-mail: dpblra@inbox.ru.

Murygin Aleksandr Vladimirovich – Dr. Sc., Professor, Head of the Information-Control Systems Department; Reshetnev Siberian State University of Science and Technology. E-mail: avm514@mail.ru.

Tynchenko Vadim Sergeevich – Ph. D. in Technical Sciences, Associate Professor, Department of Information-Control Systems; Reshetnev Siberian State University of Science and Technology. E-mail: vadimond@mail.ru.

Kurashkin Sergei Olegovich – post-graduate student, Department of Information-Control Systems; Reshetnev Siberian State University of Science and Technology. E-mail: scorpion_ser@mail.ru.

Bocharov Aleksey Nikolaevich – Ph. D. in Technical Sciences, Associate Professor, Department of Information-Control Systems; Reshetnev Siberian State University of Science and Technology. E-mail: sibalexbo@gmail.com.

Petrenko Vyacheslav Evgenievich – graduate student; Reshetnev Siberian State University of Science and Technology. E-mail: dpblra@inbox.ru.

УДК 681.518.5:004.421.4

Doi: 10.31772/2712-8970-2021-22-2-275-287

Для цитирования: Подкопаев А. В., Подкопаев И. А. Централизованный адаптивный алгоритм процедуры оптимального условного поиска места отказа динамических систем // Сибирский аэрокосмический журнал. 2021. Т. 22,

№ 2. С. 275–287. Doi: 10.31772/2712-8970-2021-22-2-275-287.

For citation: Podkopaev A. V., Podkopaev I. A. Centralized adaptive algorithm for the procedure of optimal conditional search for the place of failure of dynamic systems. *Siberian Aerospace Journal*. 2021, Vol. 22, No. 2, P. 275–287. Doi: 10.31772/2712-8970-2021-22-2-275-287.

Централизованный адаптивный алгоритм процедуры оптимального условного поиска места отказа динамических систем

А. В. Подкопаев^{1*}, И. А. Подкопаев²

¹Военный учебно-научный центр Военно-воздушных сил
«Военно-воздушная академия имени профессора Н. Е. Жуковского и Ю. А. Гагарина»
Российская Федерация, 394064, г. Воронеж, ул. Старых большевиков, 54а

²Государственный летно-испытательный центр имени В. П. Чкалова
Российская Федерация, 141110, Московская область, г. Щелково-10, войсковая часть 27237

*E-mail: aleksanpodkopaev@mail.ru

Современные и перспективные динамические системы комплексов авиационного вооружения Воздушно-космических сил (далее – системы) характеризуются усложнением структуры и повышением требований к надежности и эффективности функционирования. Более того, системы поколения 4++ и 5 достаточно уникальны и (или) малосерийны, а составляющие их элементы в своей основе миниатюрны и дороги, поэтому необходимым условием при выполнении требований контролепригодности к системам и составляющим элементам является максимально возможное сохранение качества исходного базиса при неизбежной новой трактовке дополнительной информации. Дальнейшее внедрение в практику решения задач технической диагностики (ТД) технологий искусственного интеллекта позволяет получать адекватные результаты практически с любой точностью. Достоверность результатов будет определяться исключительно пунктуальностью задания данных и полнотой математического описания систем, процессов и событий рассматриваемой предметной области. Поэтому следует ожидать, что дальнейшее развитие теории и практики ТД будет идти по пути более глубокого изучения физических процессов, происходящих в системах, и более точного математического задания процедур поиска места отказа систем. Целью работы установлена разработка взаимосвязанной совокупности математических и логических блок-схем получения и применения диагностических знаний в программно-математическом обеспечении современных и перспективных бортовых средств контроля технического состояния (ТС) систем. Приоритетным направлением в подобных исследованиях является дифференцированная селекция апробированных методов ТД с выбором соответствующего математического и алгоритмического аппарата прямого вероятностного моделирования систем. Представлена блок-схема и рассмотрен вариант практического приложения разработанного алгоритма последовательного распознавания отказов систем (далее – алгоритм, если из контекста изложения материала ясно, что речь идет именно о разработанном алгоритме). С применением алгоритма отсутствует необходимость в декомпозиции систем, а потенциал многократных повторений результатов случайного процесса смены ТС систем

предопределяет возможность получения больших выборок с высокой точностью программной компиляции.

Ключевые слова: элементарная проверка, диагностический признак (ДП), вероятность класса ТС системы, метод поиска места отказа системы, метод принятия решения, средний риск принятия решения технического диагностирования.

Centralized adaptive algorithm for the procedure of optimal conditional search for the place of failure of dynamic systems

A. V. Podkopaev^{1*}, I. A. Podkopaev²

¹Air Force Military educational and scientific center

“Air Force academy named after professor N. E. Zhukovsky and Y.A. Gagarin”

54a, Starykh bol'shevikov St., Voronezh, 394064, Russian Federation

² State flight test center named after V. P. Chkalov

military unit 27237, Moscow region, Shchelkovo-10, 141110, Russian Federation

*E-mail: aleksanpodkopaev@mail.ru

Modern and promising dynamic systems of aviation weapon systems of the Aerospace Forces (hereinafter for brevity in the text – the system) are characterized by a more complex structure and increased requirements for reliability and efficiency of functioning. Moreover, systems of generation 4 ++ and 5 are quite unique and (or) small-scale, and their constituent elements are basically miniature and expensive, therefore, a prerequisite for fulfilling the requirements for traceability to systems and constituent elements is the maximum possible preservation of the quality of the initial basis with the inevitable new interpretation of additional information. Further introduction of artificial intelligence technologies into the practice of solving problems of technical diagnostics makes it possible to obtain adequate results with almost any accuracy. The reliability of the results will be determined solely by the punctuality of the data assignment and the completeness of the mathematical description of systems, processes and events in the subject area under consideration. Therefore, it should be expected that the further development of the theory and practice of technical diagnostics will follow the path of a deeper study of the physical processes occurring in systems, and a more accurate mathematical specification of procedures for finding the place of failure of systems. The aim of the work is to establish the development of an interconnected set of mathematical and logical block diagrams for obtaining and applying diagnostic knowledge in the software and mathematical support of modern and advanced onboard means of monitoring the technical state of systems. The priority direction in such studies is the differentiated selection of approved methods of technical diagnostics with the choice of the appropriate mathematical and algorithmic apparatus for direct probabilistic modeling of systems. A block diagram is presented and a variant of the practical application of the developed algorithm for sequential recognition of system failures (hereinafter referred to as an algorithm, if it is clear from the context of the presentation of the material that it is the developed algorithm) is considered. By using the algorithm, there is no need for decomposition of systems, and the potential for multiple repetitions of the results of a random process of changing the technical states of systems predetermines the possibility of obtaining large samples with high accuracy of software compilation.

Keywords: elementary check, diagnostic sign, probability of a class of the technical condition of the system, method for finding the place of a system failure, decision method, average risk of making a technical diagnosis decision.

Introduction

Programs of the Ministry of Defense of the Russian Federation aimed at improving the quality of control of TS of weapons and military (special) equipment are used to maintain and restore the serviceable (opera-

ble) state of various types of systems. At the same time, the analysis of the properties of systems of the form [1; 2], the results of scientific research of the theory, methods and means of determining TS systems [3; 4] have shown that the complexity of systems has reached a level at which, in most cases, an individual human expert or a group of experts is not able to fully and accurately process the amount of information about inhomogeneous processes occurring during the operation, damage and system failures. Consequently, the further development of TD as a necessary component of the control process of TS systems seems to expand the base of theoretical foundations and their practical applications, focused on the partial or complete transfer of analytical functions of an expert from a human operator to a machine.

An important role in this is assigned to the improvement of algorithms that provide maximum automation of optimal operations to find the place of failure of systems.

Algorithms for probabilistic modelling of problems of combinational and sequential recognition of system failures are developed in great detail and are considered in special literature, for example [5; 6]. We also note a useful overview of current results in the subject area. So, in articles [7; 8] algorithms for identifying defects and assessing their impact on the safety of systems operation using the rules of inference and formal conceptual analysis are proposed; in [9], the algorithms for TD of the compressors of aircraft gas turbine engines were developed using parameters that are highly sensitive to changes in the vehicle of the controlled object; in the work [10], original algorithms for individual and group diagnostics of the functioning of information-measuring complexes for electricity metering are presented; publication [11] argues the possibilities of applying the achievements of neural network technologies in the algorithms of TD of digital systems.

Taking into account the actualization of the vehicle control strategy based on the state and the mixed vehicle control strategy, as well as the processes of increasing the readiness coefficient of military systems, [2] as the most natural, practically feasible form that meets modern requirements, we will determine the feasibility of further improving the failure recognition procedure the development of an algorithm that has the properties of centralization and adaptation. The block "decision making" of such an algorithm is considered as the central one, which provides the functions of the regulator when the proposed algorithm is applied for its intended purpose. The adaptation property reflects the fact that the formation of branches of such an algorithm is carried out on the basis of possible structures of systems, and the connections between the branches of the procedure for conditional search for the place of failure of systems are implemented on the basis of an optimal combination of all algorithmic blocks.

Presentation of the initial data and the main result

In the implementation of the structure and content of the algorithm, the apparatus of the theory of pattern recognition is used and the tools of direct probabilistic (imitation) modelling are used, in which the algorithm reproduces, imitates real human actions that are randomly dependent from the type of a priori information and the structure of the system.

Based on the classical formulations of the problem of optimal search for the place of failure of systems [12], the synthesized algorithm is presented in the form of a block diagram of operators, separate of which represent a fairly large group of elementary arithmetic and logical operations, as shown in fig. 1.

The developed algorithm operates on the basis of the initial data systematized in operator 2.

The system under study, which belongs to the class of dynamical systems, is represented in the so-called system theory by the "input - state - output" model [12–14].

$$E = (T, X, Y, Z, A, F), \quad (1)$$

where T is a set of points in time t ; X is a set of input signals of the system x ; Y is the set of output signals of the system y ; Z is the set of state variables of the system z ; A – operator of outputs, describing the mechanism of the formation of the output signal as a reaction of the

system to internal and external disturbances; F – is the transition operator, reflecting the change in the state of the system under the influence of internal and external disturbances.

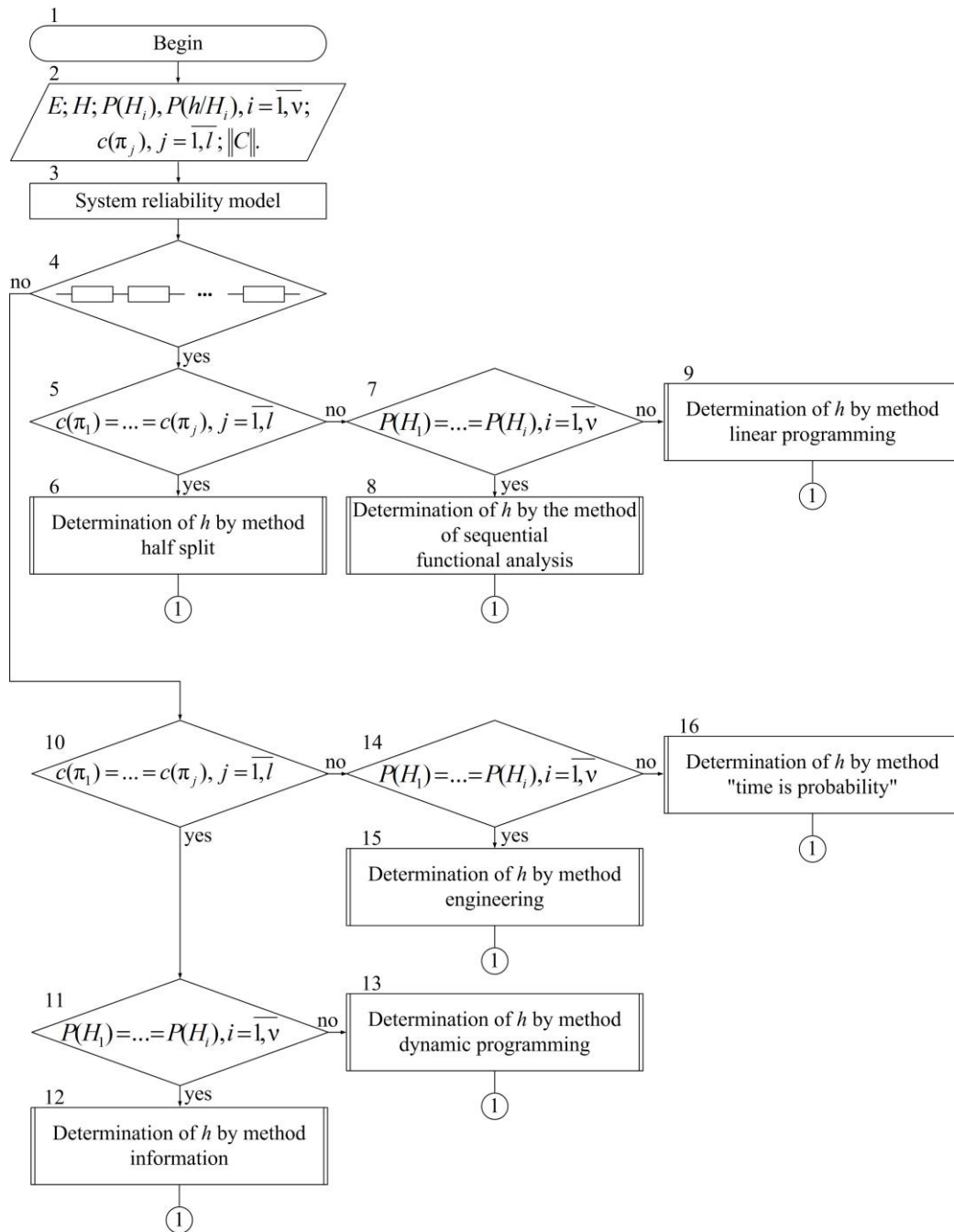


Рис. 1. Блок-схема оптимального условного алгоритма поиска места отказа динамических систем (Начало)

Fig. 1. Block diagram of the optimal conditional algorithm for finding the place of failure of dynamic systems (Beginning)

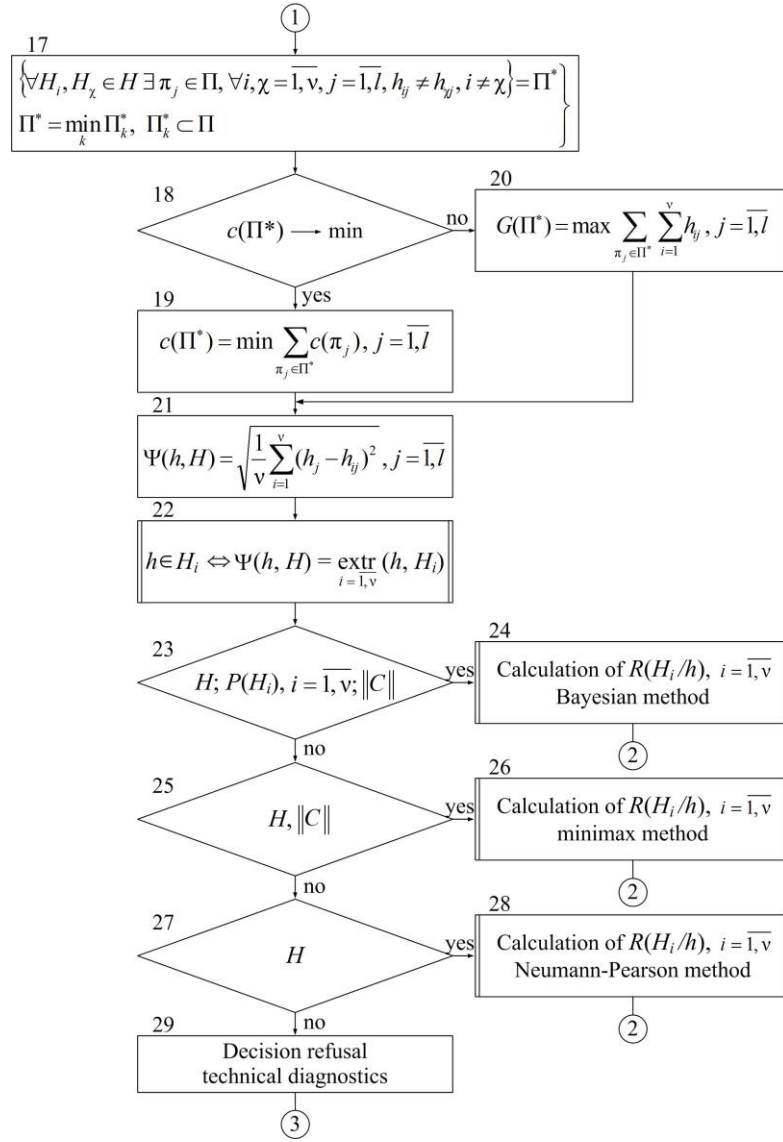


Рис. 1. Продолжение (начало на с. 277)

Fig. 1. Continued (beginning on p. 277)

To organize the recognition of failures, it is necessary to use a pre-formed DS reference dictionary, the number of descriptions in which should be equal to a given number v of the determined i -th classes of the TS of the system, $i = \overline{1, v}$. The DS system dictionary, formed in a form convenient for further actions, is presented in the form of vectors

$$H_i = (h_{i1}, h_{i2}, \dots, h_{ij}, \dots, h_{il}), i = \overline{1, v}, \quad (2)$$

whose components are the supporting j -th (out of the total number l) DS h_{i1}, \dots, h_{il} of any type describing properties of the system of this class TS H_i , $i = \overline{1, v}$.

It is known that the j -th DS h_{ij} , $j = \overline{1, l}$ means a possible outcome of an elementary check in the i -th class of TS of the system and shows what the outcome of an elementary check should be if the state of the system belongs to the i -th class of TS [12]. Therefore, to denote an elementary check, the symbol π is used with the index $j - \pi_j$, $j = \overline{1, l}$, of the same name for the number of DSs, and for brevity, an elementary check is herein-after called simply a check.

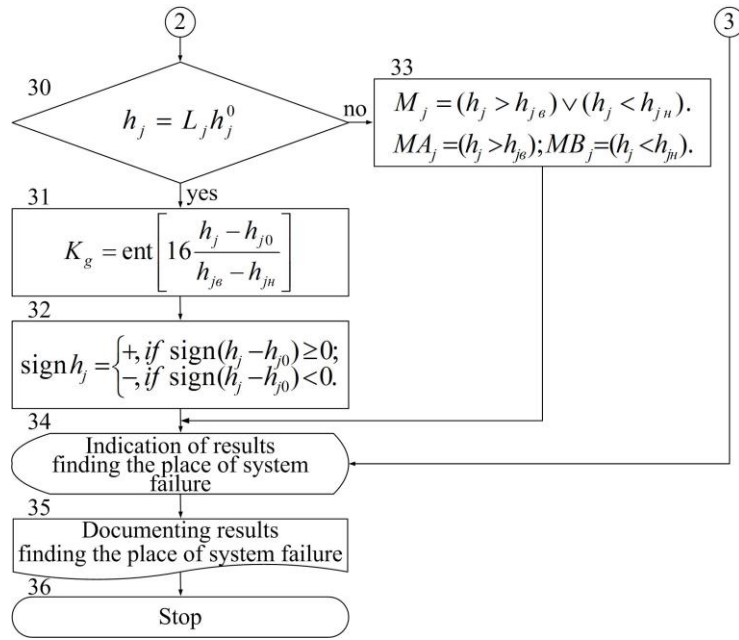


Рис. 1. Окончание (начало на с. 277)

Fig. 1. End (beginning on p. 277)

It should be noted here that the descriptions of classes formed at the stage of preliminary study of the properties of systems do not remain unchanged. They are usually refined according to the results of recognition of newly created or modernized systems, which determines the open architecture of the algorithm.

The set of specified classes, obtained at the end of the learning process, forms an array of the alphabet of classes of the TS system in a mathematical formulation, similar to formula (2), but representing it in a form that excludes programming errors

$$H = \begin{vmatrix} h_{11} & h_{12} & \dots & h_{1j} & \dots & h_{1l} \\ h_{21} & h_{22} & \dots & h_{2j} & \dots & h_{2l} \\ \dots & \dots & \dots & \dots & \dots & \dots \\ h_{i1} & h_{i2} & \dots & h_{ij} & \dots & h_{il} \\ \dots & \dots & \dots & \dots & \dots & \dots \\ h_{\chi 1} & h_{\chi 2} & \dots & h_{\chi j} & \dots & h_{\chi l} \\ \dots & \dots & \dots & \dots & \dots & \dots \\ h_{v1} & h_{v2} & \dots & h_{vj} & \dots & h_{vl} \end{vmatrix}. \quad (3)$$

The alphabet of classes (3) assumes the existence of a maximum number of separate classes corresponding to inoperable states of the system. It is also assumed that the recognition of failures is performed on the set of the indicated DSs and that their number is sufficient for the correct classification of all inoperable states of the system.

By their nature, all states of systems are random events caused by the randomness of failures of individual elements and other random factors. Under these conditions, generally speaking, it is necessary to consider the TD problem in a probabilistic formulation, and its solution within the framework of the application of probabilistic decision-making methods, assuming the presence of information specifying:

- the probabilities of the i -th classes of the TS of the system $P(H_i)$, $i = \overline{1, v}$;

- the probabilities of the appearance of images of the system h when the system is in the i -th classes of the TS $P(h/H_i)$; $i = \overline{1, v}$;
- the prices of the j -th checks $c(\pi_j)$, $j = \overline{1, l}$.

In addition, in the structure of the initial data generated in operator 2, it is mandatory to provide for the presence of a payment matrix that assigns average losses in case of correct and erroneous decisions of technical diagnostics obtained at the stage of training the system

$$\|C\| = \begin{bmatrix} c_{11} & c_{12} & \dots & c_{1v} \\ \dots & \dots & \dots & \dots \\ \dots & \dots & \dots & \dots \\ c_{v1} & c_{v2} & \dots & c_{vv} \end{bmatrix}. \quad (4)$$

On the main diagonal of the payoff matrix (4), there are losses with correct decisions, on the right side of the main diagonal are losses associated with errors of the 1st kind, on the left are losses associated with errors of the 2nd kind [15].

Upon completion of the process of entering the initial data, using operator 3, an analysis of the interaction of elements with each other in the spatio-temporal organization of the system that determines the types, nature of connections and relationships between elements is performed. Operator 3 is typical for identifying a sequential model of system reliability or other structure of connecting elements and is intended to determine the conditions for the applicability of one of the known methods for finding the place of system failure. To structure the system, frames can be used – constructions for describing a certain system, that has certain properties and stores all information about the properties and relationships of the system [4].

In general, such an analysis is an intermediate stage in solving the TD problem on a computing machine.

Next, a group of operators 4-16 functions, designed to reproduce the failure recognition method and determine the system image, which, by analogy with the DS dictionary (2), is represented in the form of vectors

$$h = (h_1, h_2, \dots, h_j, \dots, h_l). \quad (5)$$

where h_1, \dots, h_l are features of any kind obtained as a result of performing checks π_j , $j = \overline{1, l}$.

Obviously, features h_{ij} , $i = \overline{1, v}$, $j = \overline{1, l}$ from the DS dictionary of system (2) and features h_j , $j = \overline{1, l}$ from the image of system (5) assume comparable units and an identical form that allows their comparison.

Logical operator 4 provides a branching of the general procedure for recognizing failure depending on the identification of the structure of the system.

When sequentially connecting elements in the system, operator 5 checks the condition of equality of prices of the checks performed. When the condition $c(\pi_1) = c(\pi_2) = \dots = c(\pi_j)$ is satisfied, the set of checks $P = \{\pi_1, \pi_2, \dots, \pi_j\}$, $j = \overline{1, l}$ is obtained, and the final image formation of the system h of the form (5) is carried out using the program of the half-partition method [6] introduced by operator 6. Here we note that the conditions for the applicability of the half-partition method are not limited by the requirements for the equality of the probabilities of the classes of TS of the system $P(H_i)$, $i = \overline{1, v}$.

If the condition $c(\pi_1) = c(\pi_2) = \dots = c(\pi_j)$, $j = \overline{1, l}$ is not satisfied, then operator 7, regardless of the previous cycle checks the equality of the probabilities of the classes of the TS of the system, $P(H_1) = P(H_2) = \dots = P(H_i)$, $i = \overline{1, v}$ and connects operator 8, which implements the program of the method of sequential functional analysis [5]. Failure to meet the conditions $c(\pi_1) = c(\pi_2) = \dots = c(\pi_j)$, $j = \overline{1, l}$ and $P(H_1) = P(H_2) = \dots = P(H_i)$, $i = \overline{1, v}$, means the choice of a failure recognition program by the linear programming method [12] contained in statement 9. With a mixed structure of connecting elements in the system, control from operator 4 is trans-

ferred directly to operator 10, which, when the prices of the performed checks, $c(\pi_1) = c(\pi_2) = \dots = c(\pi_j)$, $j = \overline{1, l}$, are equal, requests operator 11. If probabilities of classes of TS of the system, $P(H_1) = P(H_2) = \dots = P(H_i)$, $i = \overline{1, v}$, obtaining a set of checks $P = \{ \pi_1, \pi_2, \dots, \pi_j \}$, $j = \overline{1, l}$, and the final formation of the image of the system h of the form (5) is carried out using the information method program [6].

The lack of conditions for the applicability of the information method leads to the need to include in the operation of the algorithm operator 13, synthesizing the method of dynamic programming of recognition of failures [6].

If the condition $c(\pi_1) = c(\pi_2) = \dots = c(\pi_j)$, $j = \overline{1, l}$ does not hold for a mixed structure of the connection of elements in the system, then operator 14 checks the equality of the probabilities of the classes of the TS of the system, $P(H_1) = P(H_2) = \dots = P(H_i)$, $i = \overline{1, v}$, and connects operator 15, which implements the program of the "engineering" method of finding the place of failure of the system [5]. If the prices of checks are not equal, $c(\pi_1) \neq c(\pi_2) = \dots \neq c(\pi_j)$, $j = \overline{1, l}$, and the probabilities of the classes of the TS of the system are not the same, $P(H_1) \neq P(H_2) \neq \dots \neq P(H_i)$, $i = \overline{1, v}$, then to establish the set of checks $P = \{ \pi_1, \pi_2, \dots, \pi_j \}$, $j = \overline{1, l}$ and to determine the image of the system h of the form (5), the "time - probability" method [5] is selected, contained in operator 16.

Thus, the operation of the group of operators 4–16 is carried out under the conditions of an active experiment, which dictates the need to form certain optimality requirements for specific control conditions of the TS systems.

The requirements for optimization of the set of checks are presented on the basis of the condition of pairwise distinguishability of the TS of the system, supplemented by restrictions on finding the optimal subset $\Pi_k^* \subset \Pi$, such that the formulations [12] presented in operator 17 are resolved.

Operator condition 17 defines a given number of checks required to determine the i -th TS of the system and requires that in the required subset P^* there is at least one check π_j , such that any two dictionaries $DS H_i$ и H_χ , $\forall i, \chi = \overline{1, v}$, $i \neq \chi$, were pairwise distinguishable by the results of this check and so that this subset was the minimum of all possible ones.

In the general case, several subsets P^* , can be found that satisfy the condition of operator 17. For the final choice of one of these subsets, operators 18–20 additional specific optimization requirements are formulated.

Optimization requirements are expressed in minimizing the total costs associated with performing checks π_j , included in the desired optimal subset P^* (operator 19) or in maximizing the reliability of recognition of failures when performing checks π_j , included in the sought optimal subset P^* (operator 20). When requesting a minimum of total costs associated with performing checks included in the desired subset P^* , operator 18 transfers control to operator 19, and, if necessary, to ensure maximum reliability of failure recognition, to operator.

Operator 21 in each case makes a classifying solution to the problem of recognizing failures by calculating the index $\Psi(h, H)$ of similarity (measure of proximity) between the vector (5) and each of the classes (2) of the alphabet (3). The use of the proximity measure $\Psi(h, H)$ in the algorithms for recognizing failures is due to the type of DS used to find the place of failure of systems; therefore, the options for calculating the similarity indicator $\Psi(h, H)$ for a large number of states are extremely diverse. By decomposing and generalizing the working dependencies proposed in the considered section of the developed algorithm, the arithmetic operations of the operator 21 are reduced to a single scheme for calculating the root-mean-square distance between the image components of the system (5) and the DS dictionary (2).

The decision rule of the problem of classifying the search for the place of failure of the system is presented in the operator 22. The minimization or maximization of the decision rule of the operator 22 is determined by the specification of the types of DS given by the type of system with previously known design features (1).

After optimizing the solution to the problem of finding the place of failure of the system, operators 23–29 are included in the process of functioning of the developed algorithm, designed to make a final conclusion based on the results of the process of technical diagnostics of the system using an assessment of the average risk of decision-making $R(H_i/h)$, $i = \overline{1, v}$. Operators 23–29 implement the Bayesian decision-making strategy for technical diagnostics with its required modifications depending on the availability of the initial data and the applied criteria for developing the final decision. Without violating the generality of reasoning, we note the potential of probabilistic decision-making methods when processing, including data of deterministic and logical DS, assuming the values of such DS to be probabilistic, with the probability of occurrence of unity.

Operator 23 checks the conditions for the direct statement of the Bayesian method. When defining the image of the system (5) at the previous stages of the functioning of the algorithm, the stability of the description of the alphabet of classes of the TS of the system (3), the given probabilities of the classes of the TS of the system $P(H_i)$, $i = \overline{1, v}$ and the probabilities of the appearance of images when the system is in the i -th classes of TS $P(h/H_i)$, $i = \overline{1, v}$, the invariability of the payment matrix (4), the operator 24 calculates the average risk of making a decision of technical diagnostics $R(H_i/h)$, $i = \overline{1, v}$ by direct application of Bayes' theorem [12; 16].

The value of the average risk of making a decision of technical diagnostics $R(H_i/h)$, $i = \overline{1, v}$ is an indicator by which the final decision is made about the belonging of the recognized state of the system to one of the classes of inoperable states.

In the absence of information about the probabilities of the classes of the TS of the system $P(H_i)$, $i = \overline{1, v}$ control is transferred to the operator 25, who checks the conditions for the applicability of the minimax method. With the known alphabet of classes of the TS of the system of the form (3) and the pay-out matrix of the form (4), the operator 25 connects the operator 26, which contains the apparatus of the minimax method. The average risk of making a decision $R(H_i/h)$, $i = \overline{1, v}$ is calculated in this case according to the modified rules of the specified method [6; 15].

Operator 27 is intended for inclusion in the decision-making process of technical diagnostics of the tools of the Neumann – Pearson method. If there is only information about the alphabet of classes of TS of a system of the form (3), the average risk of making a decision $R(H_i/h)$, $i = \overline{1, v}$ is calculated in operator 28 according to the criteria of the Neumann - Pearson method [15].

Otherwise, the decision on the diagnosis is not made and control is transferred to the operator 29, which performs the process of refusal to make the decision of technical diagnosis.

In order to exclude operator 29 from the structure of the optimal conditional algorithm for finding the place of failure of systems, further improvement of diagnostic knowledge is assumed in the following areas:

- justification and acceptance of assumptions about the neglect of losses associated with correct solutions of the TD problem, incomparably small in relation to the losses associated with errors of the I-st and II-nd kind;
- estimation of the probability distribution densities for all classes of recognizable states of systems;
- introduction into consideration of the so-called threshold value of the likelihood coefficient, which is the ratio of the conditional distribution densities of DS values in the classes of inoperable states systems.

In the developed algorithm, operator 29 is a dead-end test for finding a defect. Information about the absence of a solution related to the most probable place of system failure is transmitted to operator 34.

Depending on the requirements, the output of the results of solving the TD problem involves the branching of the developed algorithm by the operator 30 on the line of quantitative or qualitative assessment of the control results.

The structure of the developed algorithm also assumes the presence of a set of control and processing blocks located in a certain sequence, indication (registration) of control results in the appropriate units of measurement of the j -th DS or in the form of logical conditions for the assessment "Defect".

When specifying the requirements for the quantitative (measuring) presentation of the failure recognition results, the assessment of the results of technical diagnostics is expressed by the operator 30 in the form of the number L_j , showing the quantitative value of the j -th DS and the unit of measurement of the j -th DS – h_j^0 .

A quantitative approach to recognizing failures involves determining the deviation of the measured value of the j -th DS h_j from the nominal h_{j0} in the gradations of the tolerance and scrap fields. The value of the gradation in most modern control systems is chosen equal to 12.5% of the half of the tolerance [4]. The measured DS value is considered positive when the tolerance band is exceeded and negative if the measured DS value is less than the tolerance band. Further, the operator 30 includes in the work operator 31, which determines the estimate of the defect of the j -th DS. In operator 31, based on the known maximum permissible upper $h_{jв}$ and lower $h_{jн}$ values of the j -th DS, respectively, by rounding to the nearest number from below (ent), the gradation number K_g , corresponding to the DS value is determined.

The sign of the deviation of the measured value of DS from the nominal value is determined using an obvious formula, resolved by operator 32.

When specifying the requirements for a qualitative (tolerance) presentation of the results of searching for the place of system failure, operator 30 transfers control to operator 33.

In case of qualitative recognition of failures, the evaluation of the type "Defect" (D), or "Defect above" (DA), "Defect below" (DB) of technical diagnostics results is carried out by operator 33 by trivial comparison of the measured value of the j -th DS h_j with the maximum permissible upper $h_{jв}$ and lower $h_{jн}$ values.

Data of a quantitative or qualitative assessment of the results of solving the TD problem are submitted to operators 34 and 35, intended, respectively, for displaying and documenting diagnostic information.

Development of recommendations for the practical application of solutions

A variant of the practical application of the developed algorithm is possible in the structure of information diagnostic systems related to the typology of artificial intelligence systems [4]. The inclusion of the algorithm in the mechanism for obtaining solutions (solver) of the information diagnostic system eliminates the need to operate with rules - rather voluminous constructions for expressing connections, dependencies between facts and their combinations. Automatic connection of knowledge procedures that allow performing calculations or transformations of functions and making decisions in a certain situation is performed by the algorithm depending on the data of operator 2. Very laborious, especially with large systems, the process of enumerating possible options is eliminated. Consequently, the mechanism for obtaining solutions of the artificial intelligence system containing the obtained algorithm is assumed to be maximally optimized.

In the structure of concepts formed in the form of abstracted systems that have definitions, structures and constituent elements, the initial data indicated above are mandatory, which imposes significant requirements on the amount of permanent memory and the speed of the calculator processor. However, this drawback is less significant in comparison with the advantages of the proposed approach. Moreover, the resources of the information diagnostic system are freed up by the absence in its structure of complex models for representing the knowledge base and the rules involved in the derivation - the so-called production models and semantic networks [4].

Conclusion

The resulting set of prescriptions determines the optimal sequence of actions of performers and means necessary and sufficient to recognize failures with minimal costs and (or) maximum reliability of control of TS systems. The operations of recognizing unworkable states of the system are defined as multi-step actions to transform the input information about the DS into the output one, which is a conclusion about which class of TS the system image belongs to.

Thus, using the proposed algorithm, there is no the need for combination and unconditional checks of system elements and at the same time predetermines the possibility of research, primarily of elements with low reliability.

Библиографические ссылки

1. Комплексы авиационного вооружения / под ред. В. А. Конуркина. М. : ВВИА им. Н. Е. Жуковского, 2005. 947 с.
2. Эксплуатация комплексов авиационного вооружения / под ред. А. И. Буравлева. М. : ВВИА им. Н. Е. Жуковского, 2006. 287 с.
3. Александровская Л. Н., Афанасьев А. П., Лисов А. А. Современные методы обеспечения безотказности сложных технических систем. М. : Логос, 2001. 206 с.
4. Робототехнические системы подготовки и контроля комплексов авиационного вооружения / под ред. В. Д. Закутаева. М. : ВУНЦ ВВС ВВА им. Н. Е. Жуковского и Ю. А. Гагарина, 2011. 360 с.
5. Системы контроля и метрологическое обеспечение авиационного вооружения / под ред. В. В. Сергушина. М. : ВВИА им. Н. Е. Жуковского, 1992. 372 с.
6. Контроль и управление техническим состоянием комплексов авиационного вооружения / под ред. О. А. Лапсакова. М. : ВВИА им. Н. Е. Жуковского, 1994. 312 с.
7. Морозова Т. Ю., Бекаревич А. А., Будадин О. Н. Новый подход к идентификации дефектов материалов изделий // Контроль. Диагностика. 2014. № 8. С. 42–48.
8. Kastner J., Heinzl C., Plank B. et al. New X-ray computed tomography methods for research and industry // Materials VII Intern. Scientific Conf. on Industrial Computed Tomography. Leuven, Belgium, 2017. P. 1–10.
9. Посадов В. В. (мл.), Посадов В. В., Ремизов А. Е. Алгоритмы диагностики аэродинамических и аэроупругих колебаний компрессора авиационного газотурбинного двигателя // Контроль. Диагностика. 2016. № 3. С. 34–38.
10. Солдатов А. А., Евдокимов Ю. К. Построение многофункциональной автоматизированной системы и алгоритмов контроля и диагностики режимов работы систем учета электроэнергии электросетевых подстанций // Приборы и системы. Управление, контроль, диагностика. 2017. № 3. С. 1–10.
11. Асылбеков Н. С., Кыдыралиева Г. Ж., Оморов Т. Т. Идентификация неисправных элементов цифровой системы на основе анализа нейронной сети // Приборы и системы. Управление, контроль, диагностика. 2017. № 7. С. 50–53.
12. Дмитриев А. К., Мальцев П. А. Основы теории построения и контроля сложных систем. Л. : Энергоатомиздат, 1988. 192 с.
13. Вунш Г. Теория систем. М. : Советское радио, 1978. 288 с.
14. Директор С., Рорер Р. Введение в теорию систем. М. : Мир, 1974. 464 с.
15. Горелик А. Л., Скрипкин В. А. Методы распознавания. М. : Высшая школа, 1984. 208 с.
16. Корн Г., Корн Т. Справочник по математике для научных работников и инженеров. М. : Наука, 1984. 832 с.

References

1. *Kompleksy aviatsionnogo vooruzheniya* [Aircraft weapon systems]. Ed. by V. A. Konurkin. Moscow, AFIA named after professor N. E. Zhukovsky Publ., 2005, 947 p.
2. *Ekspluatatsiya kompleksov aviatsionnogo vooruzheniya* [Exploitation of aircraft weapons systems]. Ed. by A. I. Buravlev. Moscow, AFIA named after professor N. E. Zhukovsky Publ., 2006, 287 p.
3. Alexandrovskaya L. N., Afanasyev A. P., Lisov A. A. *Sovremennyye metody obespecheniya bezotkaznosti slozhnykh tekhnicheskikh sistem* [Modern methods for ensuring the reliability of complex technical systems]. Moscow, Logos Publ., 2001, 206 p.
4. *Robototekhnicheskiye sistemy podgotovki i kontrolya kompleksov aviatsionnogo vooruzheniya* [Robotic systems for the preparation and control of aircraft weapons systems]. Ed. by V. D. Zakutaev. Moscow, AF-MESC AFA named after professor N. E. Zhukovsky and Yu. A. Gagarin Publ., 2011, 360 p.
5. *Sistemy kontrolya i metrologicheskoye obespecheniye aviatsionnogo vooruzheniya* [Control systems and metrological support of aviation weapons]. Ed. by V. V. Sergushin. Moscow, AFIA named after professor N. E. Zhukovsky Publ., 1992, 372 p.
6. *Kontrol' i upravleniye tekhnicheskim sostoyaniyem kompleksov aviatsionnogo vooruzheniya* [Monitoring and control of the technical condition of aircraft weapons systems]. Ed. by O. A. Lapsakov. Moscow, AFIA named after professor N. E. Zhukovsky Publ., 1994, 312 p.
7. Morozova T. Yu., Bekarevich A. A., Budadin O. N. [The new approach to identifying defects in product materials]. *Kontrol'. Diagnostika*. 2014, No. 8, P. 42–48 (In Russ.).
8. Kastner J., Heinzl C., Plank B. et al. [New X-ray computed tomography methods for research and industry]. *Materialy VII Mezhdunar. nauch. konf. po promyshlennoy komp'yuternoy tomografii* [Materials VII Intern. Scientific Conf. on Industrial Computed Tomography]. Leuven, 2017. P. 1–10.
9. Posadov V. V. (jr.), Posadov V. V., Remizov A. E. [Algorithms of aerodynamic and aeroelastic vibrations diagnostics in compressor of gas turbine engine]. *Kontrol'. Diagnostika*. 2016, No. 3, P. 34–38 (In Russ.).
10. Soldatov A. A., Evdokimov Yu. K. [Construction of a multifunctional automated system and control algorithms and diagnostics of the operating modes of electricity metering systems of power grid substations]. *Pribory i sistemy. Upravleniye, kontrol', diagnostika*. 2017, No. 3, P. 1–10 (In Russ.).
11. Asylbekov N. S., Kydyralieva G. Zn., Omorov T. T. [Faulty elements identification of digital system on the basis of the analysis neural network]. *Pribory i sistemy. Upravleniye, kontrol', diagnostika*. 2017, No. 7, P. 50–53 (In Russ.).
12. Dmitriev A. K., Maltsev P. A. *Osnovy teorii postroyeniya i kontrolya slozhnykh sistem* [Fundamentals of the theory of construction and control of complex systems]. Leningrad, Energoatomizdat Publ., 1988, 192 p.
13. Vunsh G. *Teoriya sistem* [System theory]. Moscow, Sovetskoe radio Publ., 1978, 288 p.
14. Director S., Rourer D. *Vvedeniye v teoriyu sistem* [Introduction to systems theory]. Moscow, Mir Publ., 1974, 464 p.
15. Gorelik A. L., Skripkin V. A. *Metody raspoznavaniya* [Recognition methods]. Moscow, Vysshaya shkola Publ., 1984, 208 p.
16. Korn G., Korn T. *Spravochnik po matematike dlya nauchnykh rabotnikov i inzhenerov* [Mathematical handbook for scientists and engineers]. Moscow, Nauka Publ., 1984, 832 p.

© Подкопаев А. В., Подкопаев И. А., 2021

Подкопаев Александр Владимирович – кандидат технических наук, доцент, профессор кафедры эксплуатации комплексов авиационного вооружения (и прицельных систем); Военный учебно-научный центр Военно-воздушных

сил «Военно-воздушная академия имени профессора Н. Е. Жуковского и Ю. А. Гагарина» (г. Воронеж). E-mail: aleksanpodkopaev@mail.ru.

Подкопаев Илья Александрович – инженер-испытатель; Государственный лётно-испытательный центр имени В. П. Чкалова. E-mail: ilya.podkopaev.96@bk.ru.

Podkopaev Aleksandr Vladimirovich – Cand. Sc., associate professor, professor of the department operation of aircraft weapon systems (and sighting systems); Air Force Military educational and scientific center “Air Force academy named after professor N. E. Zhukovsky and Y. A. Gagarin” (Voronezh). E-mail: aleksanpodkopaev@mail.ru.

Podkopaev Илья Александрович – engineer and tester; State flight test center named after V. P. Chkalov. E-mail: ilya.podkopaev.96@bk.ru.

UDC 519.65, 629.783

Doi: 10.31772/2712-8970-2021-22-2-288-300

For citation: Pustoshilov A. S., Tsarev S. P., Ushakov Yu. Yu., Ovchinnikova E. V. Anomalies in IGS ephemeris and clock products and their influence on the solution of navigation problems. *Siberian Aerospace Journal*. 2021, Vol. 22, No. 2, P. 288–300. Doi: 10.31772/2712-8970-2021-22-2-288-300.

Для цитирования: Аномалии эфемеридных и временных продуктов IGS и их влияние на решение навигационных задач / А. С. Пустошилов, С. П. Царев, Ю. Ю. Ушаков, Е. В. Овчинникова // Сибирский аэрокосмический журнал. 2021. Т. 22, № 2. С. 288–300. Doi: 10.31772/2712-8970-2021-22-2-288-300.

Anomalies in IGS ephemeris and clock products and their influence on the solution of navigation problems

A. S. Pustoshilov^{1**}, S. P. Tsarev¹, Yu. Yu. Ushakov¹, E. V. Ovchinnikova²

¹Siberian Federal University

79, Svobodny Av., Krasnoyarsk, 660041, Russian Federation

²Reshetnev Siberian State University of Science and Technology

31, Krasnoyarskii rabochii prospekt, Krasnoyarsk, 660037, Russian Federation

**E-mail: alphasoft@inbox.ru

The subject of research of this paper is anomalies in the final products of the International GNSS Service (IGS), namely in the orbits and clock drifts of navigation satellites (NSs). The purpose of research is to determine the influence of such anomalies on the accuracy of solving the precise point positioning (PPP) problem. The method of approximation by polynomials of high degrees previously proposed by the authors is used as a method for detecting and distinguishing anomalies in the orbits of navigation satellites. The methodology recommended by the IGS is used in solving the PPP problem. The proposed method for detecting and distinguishing anomalies in orbits is applied to the analysis of anomalies in the orbits of GPS navigation satellites. The examples of anomalies that can be detected using the proposed method are demonstrated. The brief statistical analysis and comparison of the frequencies of anomalies occurrence in the orbits of GPS navigation satellites published by various IGS analytical centers from 2010 to 2018 are presented. It is shown that orbital anomalies occurring at the boundaries of daily intervals are, as a rule, correlated with anomalies in clock drifts and have a partially mutually compensating effect on the solution of navigation problems. Experiments showed that when solving the PPP problem, anomalies significantly increase the root-mean-square deviation (RMSD) of the solution residual. Two options for solving the problem with anomalous orbits are considered: the exclusion of satellites with anomalous boundaries of daily intervals from the solution and the "correction" of the anomaly in the orbit. The most natural method of correcting orbits (changing the orbit in order to remove large anomalies) at the boundaries of the daily segments of the published final orbits was tested. The exclusion of satellites with anomalies in the orbit turned out to be the most effective from the point of view of PPP problems, since attempts to "correct" the orbit more often led not to a decrease in the RMSD of the pseudorange residuals, but to its increase, which is associated with correlated anomalies in the navigation satellite clock drift. According to the research results, we can conclude: before solving the PPP problems, it is necessary to study the orbits and the navigation satellites clocks drifts for the presence of anomalies by the proposed methods and, if possible, to exclude such satellites from the data used to solve the PPP problem. Our proposed methods for detecting and accounting for anomalies in the orbits and clocks of navigation satellites, in addition to obvious applications to solving ground navigation problems, are also applicable to monitoring the quality of the space and ground segments of the GLONASS and GPS systems.

Key words: IGS, GPS, satellite orbits, satellite clocks, PPP.

Аномалии эфемеридных и временных продуктов IGS и их влияние на решение навигационных задач*

А. С. Пустошилов^{1**}, С. П. Царев¹, Ю. Ю. Ушаков¹, Е. В. Овчинникова²

¹Сибирский федеральный университет

Российская Федерация, 660041, г. Красноярск, просп. Свободный, 79

²Сибирский государственный университет науки и технологий имени академика М. Ф. Решетнева

Российская Федерация, 660037, г. Красноярск, просп. им. газ. «Красноярский рабочий», 31

**E-mail: alphasoft@inbox.ru

Предметом исследования в данной работе являются аномалии в финальных продуктах Международной службы ГНСС (IGS), а именно в орбитах и уходах часов навигационных спутников (НКА). Цель исследования: определить влияние таких аномалий на точность решения задачи высокоточного позиционирования (PPP). В качестве метода для обнаружения и различения аномалий в орбитах навигационных спутников используется описанный ранее авторами метод аппроксимации полиномами высоких степеней. При решении задачи PPP используется методология, рекомендованная IGS. Предложенный метод обнаружения и различения аномалий в орбитах применен к анализу аномалий в орбитах навигационных спутников GPS. Продемонстрированы примеры аномалий, которые можно обнаружить, используя предложенный метод. Приводится краткий статистический анализ и сравнение частот появления аномалий в орбитах навигационных спутников GPS с 2010 по 2018 гг., опубликованные различными аналитическими центрами IGS. Показывается, что аномалии в орбитах, встречающиеся на стыках суточных интервалов, как правило, коррелированы с аномалиями в уходах часов и имеют частично взаимно компенсирующий эффект на решение навигационных задач. Эксперименты показали, что при решении задачи PPP аномалии существенно увеличивают среднеквадратичное отклонение (СКО) невязки решения. Рассмотрены два варианта решения проблемы с аномальными орбитами: исключение из решения спутников с аномальными стыками суточных интервалов и «исправление» аномалии в орбите. Опробована наиболее естественная методика исправления орбит (изменения орбиты с целью удаления больших аномалий) на стыках суточных отрезков публикуемых финальных орбит. Наиболее эффективным с точки зрения задач PPP оказалось исключение спутников с аномалиями в орбите, так как попытки «исправить» орбиту чаще приводили не к уменьшению СКО невязок псевдодальностей, а к его увеличению, что связано с коррелированными аномалиями в уходе часов навигационного спутника. По результатам исследования можно сделать вывод: перед решением задач PPP необходимо исследовать предложенными методами орбиты и ухода часов навигационных спутников на присутствие в них аномалий и по возможности исключать такие спутники из данных для решения задачи PPP. Предлагаемые нами методы обнаружения и учета аномалий орбит и часов навигационных спутников, кроме очевидных приложений к решению наземных навигационных задач, применимы и для мониторинга качества работы космического и наземного сегментов систем ГЛОНАСС и GPS.

Ключевые слова: IGS, GPS, орбиты спутников, часы спутников, PPP.

* This work is supported by the Krasnoyarsk Mathematical Center and financed by the Ministry of Science and Higher Education of the Russian Federation in the framework of the establishment and development of regional Centers for Mathematics Research and Education (Agreement No. 075-02-2020-1534/1).

Работа поддержана Красноярским математическим центром, финансируемым Минобрнауки РФ в рамках мероприятий по созданию и развитию региональных НОМЦ (Соглашение 075-02-2020-1534/1).

Introduction

The problem of precise point positioning (PPP) is of great importance in geodesy and is one of the ways to use global navigation satellite systems (GNSSs). To solve this problem, phase and code measurements from a navigation receiver as well as updated information about the orbits and clocks of navigation satellites are used. The analytical centers of the International GNSS Service (IGS) [1]: IAC GLONASS [2], CODE [3], ESA [4] and others are a source of information about the updated (final) orbits and clocks (frequency-time corrections to the satellite time scale). Information about the orbits is transmitted in the SP3 format for each daily time interval in the form of time series of data with a time step of 15 min [5], information about the satellite clock is transmitted in the CLK format with a time step of 30 s or 5 min [6]. The method for detecting anomalies in orbits used by us was previously described in detail in [7; 8] and allows detecting small (centimeter) anomalies in the orbits of navigation satellites. Also, in [7] it is noted that at the boundaries of daily intervals there are often discontinuities ("jumps") in orbits. It is not difficult to detect anomalies in clock drifts: it is enough to remove linear and quadratic (for large time intervals) trends using the least squares method (OLS).

We made attempts to "correct" the detected orbit anomalies, that is, to correct the orbit so that a new orbit would not have a discontinuity at the boundary of the day and would be close to the published final orbits. However, such a correction did not always lead to an increase in the positioning precision or worsened it. This is due to the presence of similar anomalies in the time information (the NS clock drift).

Orbit anomaly detection method

The technique for anomalies searching in SP3 data (standard text format for ephemeris IGS products, available in daily intervals with a step of 15 min in time) consists in searching for orbital discontinuities (time series jumps) at the boundary of two daily intervals by approximating each of the satellite coordinates for this two-day interval by a high degree polynomial. Next, the approximation residual is calculated. As it is shown in [7; 8], from the obtained residual it is easy to determine the type of anomaly ("jump" or "ejection", as well as the satellite maneuver or the period of entering the shadow). The approximation method we used is based on the application of a precomputable set of discrete orthogonal Chebyshev – Khan polynomials [8]. Such polynomials are calculated in timestamps of the analyzed series up to the chosen degree r (in our case, $r = 100$), after which the polynomial of the best RMS approximation is easily calculated. The main problem is calculating Chebyshev-Khan polynomials. The standard formulas of the theory of orthogonal discrete polynomials are not suitable due to the accumulation of large errors for high degrees and with a large number of points (in our case, 192 points). Stable algorithms for computing Chebyshev – Khan polynomials are described in [8]. In this work, we used a software package [9] adapted to the problem of approximating orbits. The method of polynomial approximation is much simpler than the approach considered earlier in [10; 11], which provided for high-precision modeling of the motion of the NS by solving the equations of motion using a lot of additional data.

For the precise positioning problems we are solving, not the orbital anomaly along each individual coordinate is important, but the value of its projection onto the sighting axis between the satellite and the receiver. To simplify the analysis, the center of mass of the Earth was used as the coordinates of the receiver, i.e., the value of the anomaly was calculated along the radius vector of the NS - the center of the Earth.

Anomalies detected in IGS final orbits

The issue of anomalies in the orbits of navigation satellites is discussed in [7; 8; 10; 11]. The work [7] shows the detected anomalies in the orbits of GLONASS satellites; the same anomalies are observed in the orbits of GPS satellites. The examples of the detected "jumps" in the final orbits of satellites G03 and G08 at

the boundary of the day (more precisely, their effect on the approximation residuals) according to the IAC PNT analytical center are shown in Fig. 1 and 2.

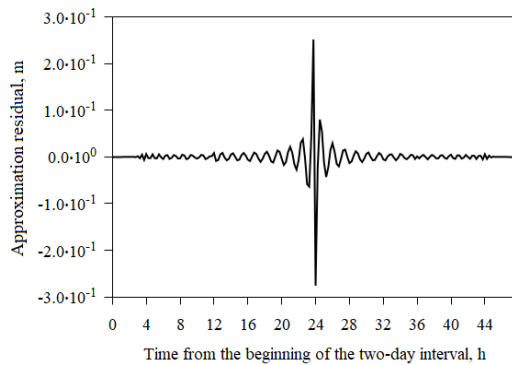


Fig. 1. Approximation residual of the G03 satellite Y coordinate by the 100th degree polynomial at the day boundary 21–22 November 2014 by the IAC PNT

Рис. 1. Невязка аппроксимации полиномом степени 100 координаты Y спутника G03 на стыке суток 21–22 ноября 2014 г. ИАЦ КВНО

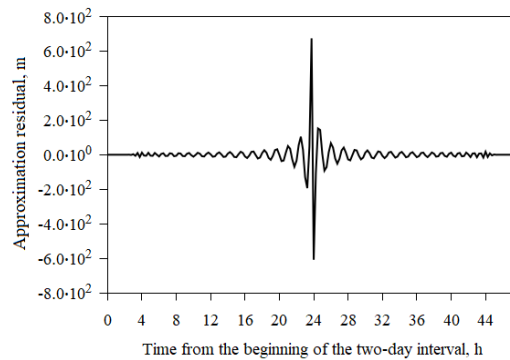


Fig. 2. Approximation residual of the G08 satellite Y coordinate by the 100th degree polynomial at the day boundary 5–6 April 2018 by the IAC PNT

Рис. 2. Невязка аппроксимации полиномом степени 100 координаты Y спутника G08 на стыке суток 5–6 апреля 2018 г. ИАЦ КВНО

According to the recommendations given in [7], we determine the size of the "jump" at each boundary of the day. For the approximation residual shown in Fig. 1, the magnitude of the "jump" is about 70 cm, for the approximation residual in Fig. 2 the magnitude of the "jump" is about 1.8 km. Large "jumps" in the final orbits of analytical centers are not very common (on average 1 "jump" per year for each satellite), while small "jumps" are common.

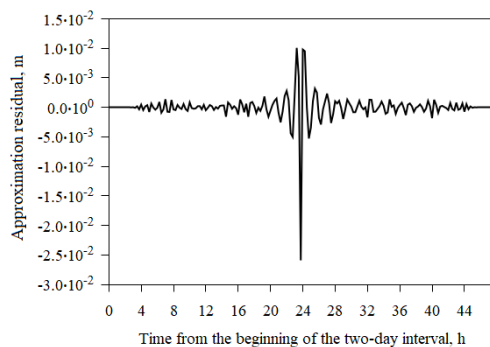


Fig. 3. Approximation residual of the G04 satellite Y coordinate by the 100th degree polynomial at the day boundary («ejection») 22–23 May 2016 by the IAC PNT

Рис. 3. Невязка аппроксимации полиномом степени 100 координаты Y спутника G04 на стыке суток («выброс») 22–23 мая 2016 г. ИАЦ КВНО

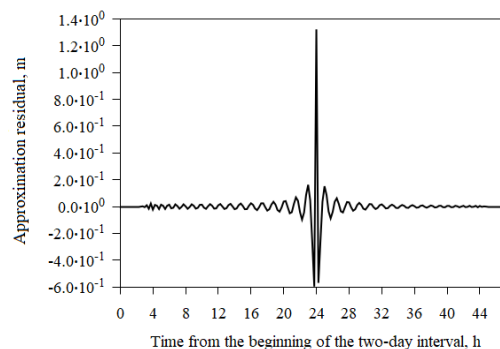


Fig. 4. Approximation residual of the G01 satellite Y coordinate by the 100th degree polynomial at the day boundary («ejection») 7–8 November 2016 by the IAC PNT

Рис. 4. Невязка аппроксимации полиномом степени 100 координаты Y спутника G01 на стыке суток («выброс») 7–8 ноября 2016 г. ИАЦ КВНО

In addition to "jumps", "ejections" were also observed in the final orbits of the GPS satellites.

Figures 3 and 4 show "ejections" in the final orbits of GPS satellites G01 and G04, respectively (to be more exact, the effect of "ejections" on the approximation residuals).

The magnitude of the "ejection" in the orbit of the G04 satellite (Fig. 3) determined from the approximation residual is approximately 3.5 cm. In the orbit of the G01 satellite (Fig. 4) the magnitude of the "ejection" is approximately 1.8 m.

The next anomaly that this technique can detect is the behavior of the final orbit of the navigation satellite when performing a maneuver. It is possible to confirm the presence of the GPS satellite's maneuver using NANU messages (Notice Advisory to Navstar Users) [12; 13]. The satellite G15, according to NANU reports, performed one of the maneuvers on August 20, 2013. Let us consider the approximation residual of X coordinate of this satellite's final orbit by the 100th degree polynomial for August 20–21, 2013 (Fig. 5).

According to NANU, the satellite maneuver began at 13:01 GPS Time and ended at 19:42 GPS Time. From the timing diagram of the residual in Fig. 3 it can be seen that in the middle of this section there is a peak in the residual of the satellite orbit approximation. We note the difference in the shape (stretching along the time axis) of the residual anomalies for Fig. 3-5.

On the basis of the residuals of the approximation results it is possible to determine the areas of entering the shadow, the time diagram of the residual for such a situation is shown in Fig. 6. To confirm entering the shadow, the SOE angle (Sun - Object - Earth) which corresponded to the presence of shadow parts of the orbit in this time interval was determined.

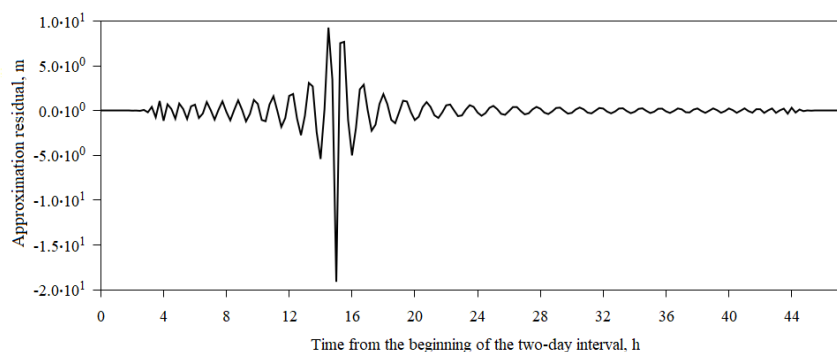


Fig. 5. Approximation residual of the G15 satellite X coordinate by the 100th degree polynomial at the day boundary 20–21 August 2013 by the IAC PNT

Рис. 5. Невязка аппроксимации полиномом степени 100 «маневра» координата X спутника G15 на стыке суток 20–21 августа 2013 г. ИАЦ КВНО

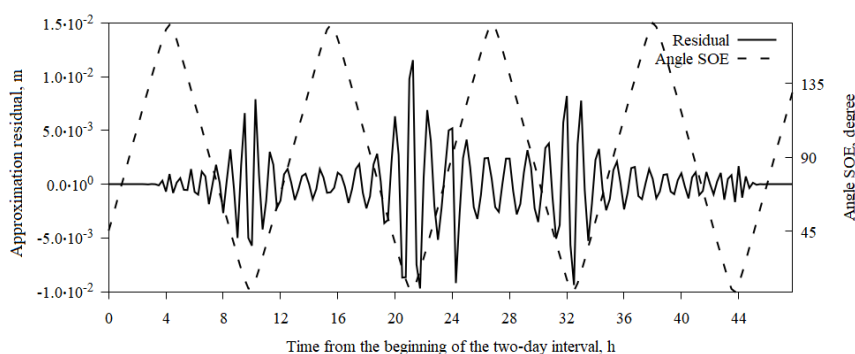


Fig. 6. The time diagrams of the approximation residual for the satellite R03 for the time interval 30–31 May 2013

Рис. 6. Временные диаграммы невязки аппроксимации для спутника R03 для временного интервала 30–31 мая 2013 г.

In the future, when accumulating statistics of anomalies at various analytical centers, we will consider the maximum of the residual modulus (for each satellite, the maximum value of three coordinates is taken).

Anomaly statistics in final GPS orbits

In [7], statistics of anomalies in the final orbits of various analytical centers for GLONASS satellites is given. This section shows anomaly statistics for GPS satellites from 2010 to 2018.

We divide the found maxima of the residual modulus (in all three coordinates) into 2 groups: less than 10 and more than 10 cm.

For the group where the value is less than 10 cm, we construct a two-dimensional distribution, where we choose the satellite to which the maximum of the residual modulus belongs at each two-day interval (the interval starts at the beginning of each day) as one of the measurements, and the value of this maximum residual modulus with a step of 1 cm - as the second measurement. The accumulation of the number of anomalies is performed over the entire time interval (from 2010 to 2018), for each analytical center graphs are plotted separately. Two-dimensional histograms for each analytical center are shown: in fig. 7 for CODE, in fig. 8 for ESA, in fig. 9 for IAC PNT, in fig. 10 for IGS. To the right of the histogram there is the legend of the number of anomalies from 2010 to 2018.

For the group of less than 10 cm, it can be noted that the final orbits of different analytical centers have a different number of anomalies exceeding 1 cm. The CODE Analytical Center has no more than 120 anomalies per satellite in the range from 1 to 2 cm. The ESA Analytical Center has on average from 1500 to 1800 anomalies in the range from 1 to 2 cm for each satellite. The analytical center of the IAC PNT has an average of 1000 to 1400 anomalies in the range from 1 to 2 cm for each satellite. The IGS analytical center has an average of 400 to 900 anomalies ranging from 1 to 2 cm per satellite. In this regard one can see the relationship in the number of anomalies per satellite between the CODE and IGS analytical centers.

There are significantly fewer situations when the maximum of the residual modulus exceeds the threshold of 10 cm; for such situations, we also construct a two-dimensional distribution. We choose a satellite as one of the measurements, and the beginning of the annual interval (with a step of 1 year) as the second measurement. For each year, the number of anomalies with a maximum residual modulus of more than 10 cm is accumulated at all two-day intervals of approximation, for each analytical center separately. The resulting distributions are shown in Fig. 11 for CODE, 12 - ESA, 13 - IAC PNT, 14 - IGS. The legend of the number of events is shown to the right of the histogram.

The most significant anomalies of a massive nature (for almost all NSs) were observed at the IAC PNT analytical center in 2014 and 2016. For different analytical centers, it can be noted that there were years when, for certain satellites, the maximum number of anomalies per year was reached for a given center. Moreover, such situations are not always interconnected at different centers. This is partly explained, among other things, by gaps in the SP3 data published by each center (when the center did not lay out orbits that were unreliable from its point of view): the day with large anomalies for one center could have simply been thrown out by another center and are not present thereby in the statistics in Fig. 11-14. Availability (availability on IGS servers) of SP3 data for the CODE analytical center is 97%, for ESA - 90%, for IAC PNT - 93%, and for IGS - 95%. On average, for all analytical centers, the maximum number of anomalies exceeding 10 cm is no more than 20.

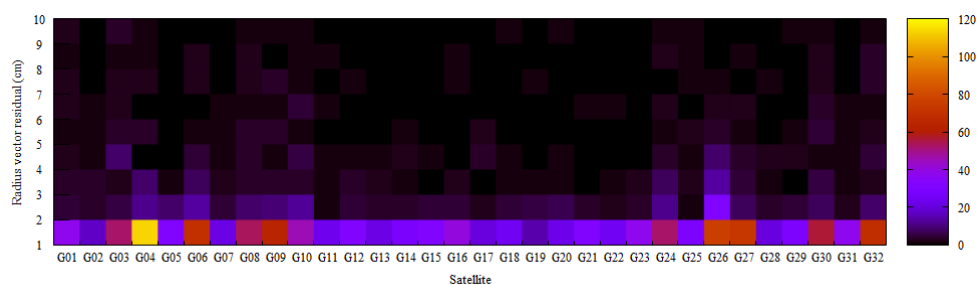


Fig. 7. Distribution of the number of anomalies of less than 10 cm over the observation interval from 2010 to 2018 for the CODE analytical center

Рис. 7. Распределение количества аномалий менее 10 см за интервал наблюдения с 2010 по 2018 гг. для аналитического центра CODE

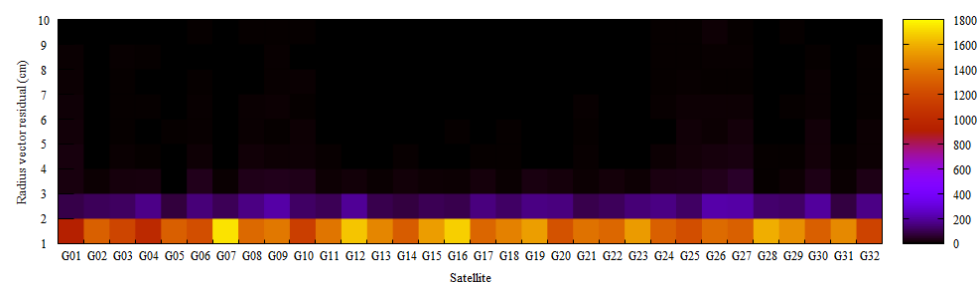


Fig. 8. Distribution of the number of anomalies of less than 10 cm over the observation interval from 2010 to 2018 for the ESA analytical center

Рис. 8. Распределение количества аномалии менее 10 см за интервал наблюдения с 2010 по 2018 гг. для аналитического центра ESA

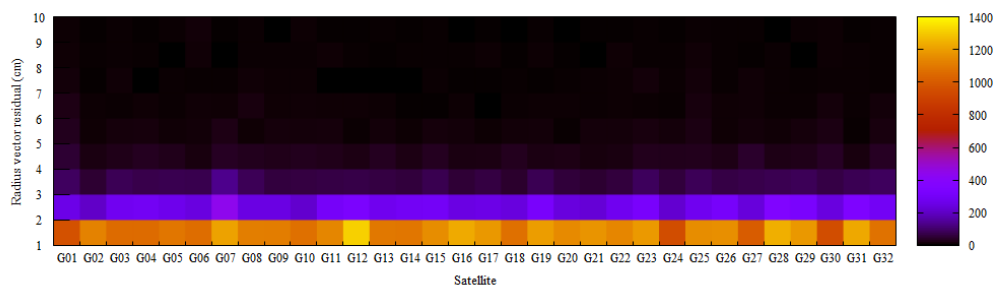


Fig. 9. Distribution of the number of anomalies of less than 10 cm over the observation interval from 2010 to 2018 for the IAC PNT analytical center

Рис. 9. Распределение количества аномалии менее 10 см за интервал наблюдения с 2010 по 2018 гг. для аналитического центра ИАЦ

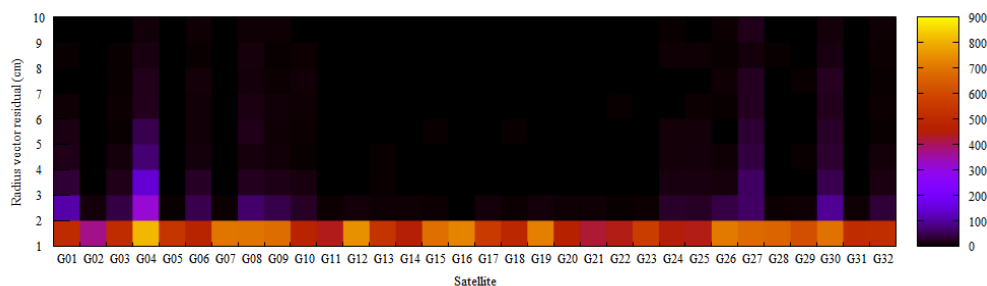


Fig. 10. Distribution of the number of anomalies of less than 10 cm over the observation interval from 2010 to 2018 for the IGS analytical center

Рис. 10. Распределение количества аномалии менее 10 см за интервал наблюдения с 2010 по 2018 гг. для аналитического центра IGS

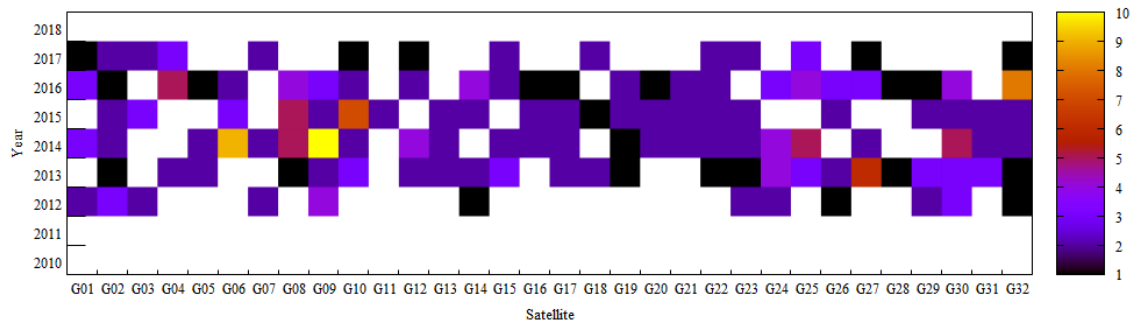


Fig. 11. Distribution of anomalies over 10 cm by year for the CODE analytical center

Рис. 11. Распределение аномалий более 10 см по годам для аналитического центра CODE

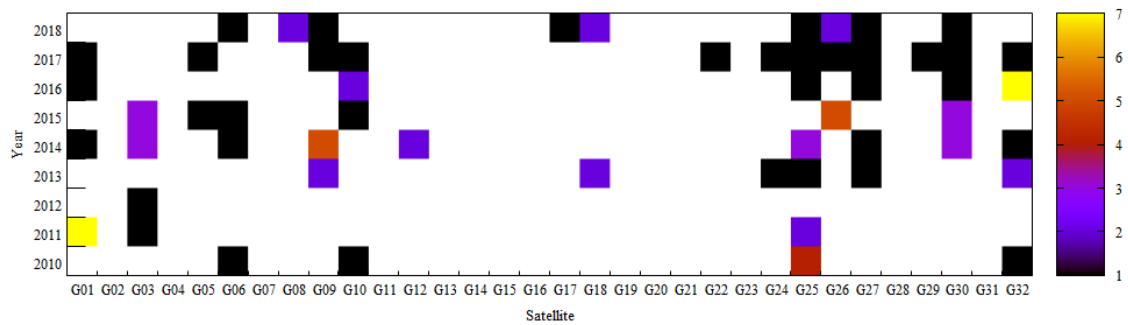


Fig. 12. Distribution of anomalies over 10 cm by year for the ESA analytical center

Рис. 12. Распределение аномалий более 10 см по годам для аналитического центра ESA

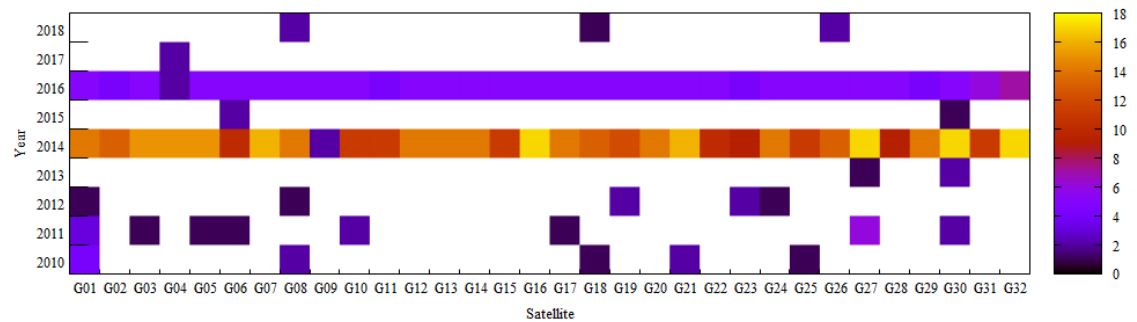


Fig. 13. Distribution of anomalies over 10 cm by years for the IAC PNT analytical center

Рис. 13. Распределение аномалий более 10 см по годам для аналитического центра ИАЦ

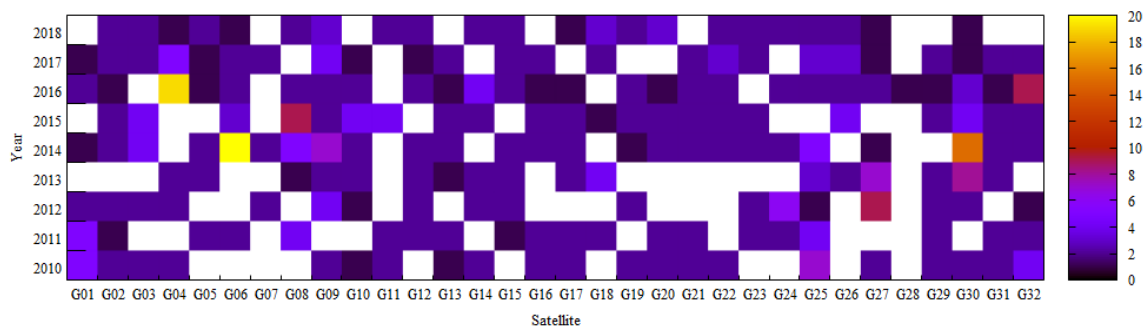


Fig. 14. Distribution of anomalies over 10 cm by year for the IGS analytical center

Рис. 14. Распределение аномалий более 10 см по годам для аналитического центра IGS

The position of the maximum of the residual modulus in the approximation window was analyzed. Most often, the maximum occurred at the boundaries of daily intervals, however, for GPS satellites there were situations when the anomaly did not occur at the boundary of daily intervals, which was almost always associated with the maneuvers of GPS satellites.

As it can be seen from the histograms, all analytical centers have both large (more than 10 cm) and small (less than 10 cm) anomalies in the final orbits, which, nevertheless, are proposed to be used in high-precision positioning problems.

Anomalies detected in GPS satellites clock drifts

For two-day intervals at the end of the day, for which anomalies in the maximum of the residual modulus exceeding several cm were observed (for different analytical centers, different minimum deviations were chosen), the clock drifts with the removal of the linear (and quadratic for large time intervals) trend were investigated.

For the period from 2010 to 2018 statistics of discontinuities whose magnitude in the radius vector exceeded 5 cm was accumulated. For GPS satellites in the data of the CODE analytical center there were 42 such situations. In the data of the IGS analytical center there were 275 of them, while situations were excluded when the discontinuity in the radius vector exceeded 10 cm. At the boundaries of the day with a discontinuity in the orbit, the satellite clock drifts were approximated by a linear function and the approximation residual was calculated. Further, a joint analysis of the residuals of the orbit approximation and the clock drift of this NS was carried out. As it turned out, when solving the PPP problem, these residuals (data discontinuities), as a rule, cancel each other out. A typical example of compensation for discontinuities at the boundary of the day in orbit and clock drift is shown in Fig. 15, 16.

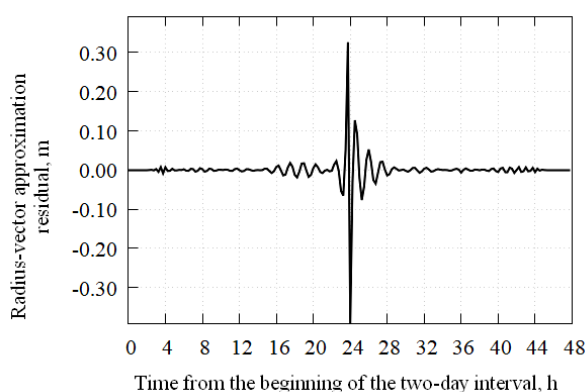


Fig. 15. Radius-vector distance approximation residual by the 100th degree polynomial of the G30 satellite at the day boundary 30 November 2010 – 01 December 2010 by the CODE

Рис. 15. Невязка аппроксимации расстояния по радиус-вектору полиномом степени 100 орбиты спутника G30 на стыке суток 30 ноября – 1 декабря 2015 г., центр CODE

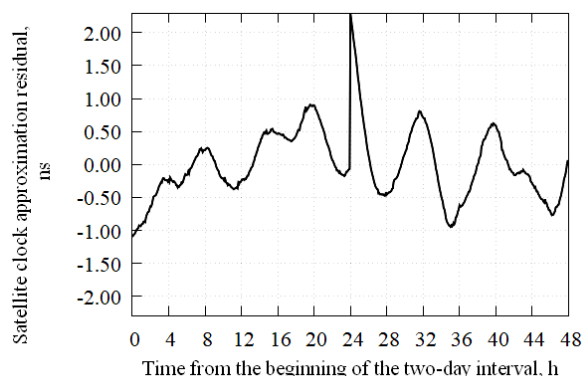


Fig. 16. Clock drift approximation residual of the G30 satellite by the 1st degree polynomial at the day boundary 30 November 2010 – 01 December 2010 by the CODE

Рис. 16. Невязка аппроксимации ухода часов спутника G30 полиномом степени 1 на стыке суток 30 ноября – 1 декабря 2015 г., центр CODE

In fig. 13 the discontinuity in the orbit along the radius vector is about 60 cm; in solving PPP problems it is partially compensated for by a time gap (about 2 ns).

Influence of anomalies in IGS products on solving the PPP problem

The problem of high-precision positioning (PPP) is to find the coordinates of the station with centimetric accuracy and its clock drift from direct measurements of the phase and pseudo-range from the NS signals. To solve this problem, it is necessary to use high-precision ephemeris and a posteriori estimates of the NS clock drift, which we take from the final SP3 and RINEX Clock files of the IGS service, as well as other processing centers. Besides, according to [14], to achieve adequate accuracy it is necessary to take into account the following effects:

- relativistic clock correction [15];
- signal delay in the troposphere (when performing this work, the model from [15] is used, the formula (9.12), while the parameters D_{hz} , D_{wz} , G_N , G_E are modeled using a piecewise linear function, the values of the functions at the nodes are estimated together with the coordinates and station clock drift);
- displacement of the phase center of the NS and station antennas, as well as the variation of the phase center depending on the angle at which the signal is transmitted and received with respect to the nadir and zenith, respectively (these corrections are transmitted in ANTEX files by the IGS service);
- correction for the rotation of the signal phase when turning the NS relative to the receiver;
- displacement of the ground measuring point due to deformations of the earth's crust caused by tides in the solid body of the Earth, uneven rotation of the Earth, as well as the pressure of oceanic water moving under the action of the tidal forces of the Moon and the Sun [15].

The initial data in the PPP problem are pseudo-range and phase measurements according to NS signals. The estimated parameters are station coordinates, receiver clock drift, tropospheric signal delay model parameters, and phase ambiguity. A measurement data model is a system of conditional equations linking measured and estimated quantities. The system is solved by linearization according to the specified parameters; the linear system is solved by the least squares method.

In this work we used measurement data from IGS stations [1]: KOKV, MGUE, MAD2, and HRAO. For such stations, the days were chosen when the satellite with an anomaly in orbit was in the radio visibility zone of the station at the boundary of the day (anomalies were determined by polynomial approximation). Two series of experiments were carried out in which parameters such as the pseudo-range residual between the measured non-ionospheric combination and the one modeled in the PPP problem as well as the coordinates of the observation station were estimated.

In the first series of experiments, the PPP problem was solved at two-day intervals with an anomaly in the orbit of a satellite at the boundary of these intervals. In the experiments the influence of the anomaly in the satellite's orbit on the residuals between the measured non-ionospheric phase pseudorange and its model value was estimated first of all. In the residuals, anomalous "jumps" were observed, both for the satellite with an anomaly in its orbit and for other satellites. At the next stage of this series of experiments we excluded satellites with an anomaly in the orbit from the solution of the PPP problem. After that, the residuals of the pseudorange were analyzed again. As a result, the anomalies in the pseudo-ranges near the boundary of the day decreased their value or completely disappeared. At the third stage of this series of experiments, instead of excluding the satellite with an anomaly in its orbit, we tried to "correct" this anomaly by forming a new orbit using the satellite motion model described in the IERS Conventions [15], matching it with the published final orbits on a two-day interval. The analysis of the pseudo-range residuals showed that orbits corrected in such a way not only do not reduce the magnitude of the "jump" or "ejection" of the residuals, but often lead to their increase. This situation is a consequence of the fact that satellite clock drifts also contain anomalies, and these anomalies often compensate for anomalies in orbits, therefore, an approach related to correcting only anomalies in orbits cannot be applied.

The second series of experiments was devoted to assessing the quality of the PPP problem solution on a relatively small interval, which is located at the boundary of the day with the anomaly. In the experiments an

interval of 2 hours before and after the boundary of the day (Fig. 17) was considered, during which the PPP problem was solved.

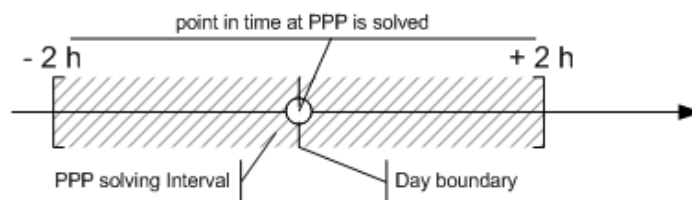


Fig. 17. Timing diagram of solving the PPP problem in the second series of experiments

Рис. 17. Временная диаграмма решения задачи PPP во второй серии экспериментов

Thus, the PPP problem was solved in three versions: a) satellites with an anomaly in orbit were included in the solution; b) satellites with an anomaly were excluded from the solution; c) for satellites with an anomaly the orbit was corrected. The station coordinates obtained by averaging three solutions of the PPP problem were taken as the reference coordinates over a two-day interval: at the beginning, in the middle, and at the end. As a result, it was revealed that in most cases excluding a satellite with an anomaly in its orbit from the PPP solution reduces the error in determining the coordinates. Attempts to "correct" the satellite's orbit with an anomaly in it only increase the error in determining the coordinates.

The Euclidean norm of the distance between three averaged coordinates and three coordinates determined in solving the PPP problem was also determined to assess the quality of solving the PPP problem in this series of experiments. Their statistics for all stations at all solution intervals are shown in the table.

**Euclidean distance norm distribution statistics
between averaged and determined coordinates**

	Without anomalous satellites	With anomalous satellites	Orbit correction was carried out for anomalous satellites
Maximum	151 cm	115 cm	28088 cm
Mean	37 cm	36 cm	2682 cm
RMSD	26 cm	21 cm	3407 cm

As it can be seen from the table, the solution without satellites with orbital anomaly is on average 1 cm worse than the solution with the anomalous satellite, while the solution with the corrected orbit is on average 2682 cm worse.

Conclusion

In the ephemeris and clock products of GNSS analytical centers there are often significant anomalies at the boundaries of the day, which negatively affects the accuracy of solving navigation problems. We proposed and tested on a 9-year time interval a simple technique for finding discontinuities and other anomalies in the final orbits published by the IGS analytical centers. The above analysis of the anomalies showed that there is a mutual compensation of discontinuities in the orbit and the drift of the satellite clock when solving PPP problems. Attempts to "correct" the orbits in order to remove discontinuities at the boundary of the day do not make sense without a corresponding correction of the NS clock drift, which is not possible at this stage.

References

1. IGS Products. Available at: <http://www.igs.org/products> (accessed 10.01.2021).
2. GLONASS information and analysis center for positioning, navigation and timing. Available at: <https://www.glonass-iac.ru/> (accessed 10.01.2021).
3. Center for Orbit Determination in Europe (CODE). Available at: http://www.aiub.unibe.ch/research/code__analysis_center/index_eng.html (accessed: 10.01.2021).
4. The European Space Agency (ESA). Available at: <https://www.esa.int> (accessed: 10.01.2021).
5. SP3-c format description. Available at: <ftp://igs.org/pub/data/format/sp3c.txt> (accessed: 10.01.2021).
6. CLK format description. Available at: ftp://igs.org/pub/data/format/rinex_clock304.txt (accessed: 10.01.2021).
7. Pustoshilov A. S. [Method for detection of small anomalies in final orbits of GLONASS navigation satellites]. *Uspehi sovremennoy radioelektroniki*. 2019, No. 12, P. 142–147. Available at: <http://www.radiotec.ru/article/24375#english> (accessed: 10.01.2021).
8. Tsarev S. P., Kytmanov A. A. Discrete orthogonal polynomials as a tool for detection of small anomalies of time series: a case study of GPS final orbits. arXiv preprint arXiv:2004.00414. 2020. Available at: <https://arxiv.org/abs/2004.00414> (accessed: 10.01.2021).
9. High degree least squares polynomial fitting using discrete orthogonal polynomials. Available at: <https://github.com/sptsarev/high-deg-polynomial-fitting> (accessed: 01.09.2020).
10. Griffiths J., Ray J. R. On the precision and accuracy of IGS orbits. *Journal of Geodesy*. 2009, Vol. 83, No. 3-4, P. 277–287.
11. Ray J. Precision, accuracy, and consistency of GNSS products. *Encyclopedia of geodesy*. Springer, Cham. 2016, P. 1–5.
12. Interface Control Document ICD-GPS-240. Available at: https://navcen.uscg.gov/pdf/gps/ICD_GPS_240C.pdf (accessed: 10.01.2021).
13. Kouba J., Héroux P. Precise point positioning using IGS orbit and clock products. *GPS solutions*. 2001, Vol. 5, No. 2, P. 12–28.
14. Kouba J. A Guide to Using International GNSS Service (IGS) products. Available at: https://kb.igs.org/hc/en-us/article_attachments/203088448/UsingIGSProductsVer21_cor.pdf (accessed: 19.01.2021).
15. Pent G., Luzum B. IERS conventions 2010. *IERS Technical Note*. 2010, No. 36.

Библиографические ссылки

1. Продукты IGS. [Электронный ресурс]. URL: <http://www.igs.org/products> (дата обращения: 10.01.2021).
2. Официальный сайт ИАЦ КВНО [Электронный ресурс]. URL: <https://www.glonass-iac.ru/> (дата обращения: 10.01.2021).
3. Официальный сайт CODE [Электронный ресурс]. URL: http://www.aiub.unibe.ch/research/code__analysis_center/index_eng.html (дата обращения: 10.01.2021).
4. Официальный сайт ESA [Электронный ресурс]. URL: Режим доступа: <https://www.esa.int> (дата обращения: 10.01.2021).
5. Описание формата SP3-c [Электронный ресурс]. URL: Режим доступа: <ftp://igs.org/pub/data/format/sp3c.txt> (дата обращения: 10.01.2021).
6. Описание формата CLK [Электронный ресурс]. URL: ftp://igs.org/pub/data/format/rinex_clock304.txt (дата обращения: 10.01.2021).

7. Пустошилов А. С. Метод обнаружения малых аномалий в финальных орбитах навигационных спутников ГЛОНАСС // Успехи современной радиоэлектроники. 2019. № 12. С. 142–147. <https://doi.org/10.18127/j20700784-201912-22>.
8. Tsarev S. P., Kytmanov A. A. Discrete orthogonal polynomials as a tool for detection of small anomalies of time series: a case study of GPS final orbits // arXiv preprint arXiv:2004.00414. 2020. [Электронный ресурс]. URL: <https://arxiv.org/abs/2004.00414> (дата обращения: 10.01.2021).
9. Программа аппроксимации дискретными ортогональными полиномами высоких степеней [Электронный ресурс]. URL: <https://github.com/sptsarev/high-deg-polynomial-fitting> (дата обращения: 01.09.2020).
10. Griffiths J., Ray J. R. On the precision and accuracy of IGS orbits // Journal of Geodesy. 2009. Vol. 83, No. 3-4. P. 277–287.
11. Ray J. Precision, accuracy, and consistency of GNSS products // Encyclopedia of geodesy. Springer, Cham. 2016. P. 1–5.
12. Interface Control Document ICD-GPS-240 [Электронный ресурс]. URL: https://navcen.uscg.gov/pdf/gps/ICD_GPS_240C.pdf (дата обращения: 10.01.2021).
13. Kouba J., Héroux P. Precise point positioning using IGS orbit and clock products // GPS solutions. 2001. Vol. 5, No. 2. P. 12–28.
14. Kouba J. A Guide to Using International GNSS Service (IGS) products [Электронный ресурс]. URL: https://kb.igs.org/hc/en-us/article_attachments/203088448/UsingIGSProductsVer21_cor.pdf (дата обращения 19.01.2021).
15. Pent G., Luzum B. IERS conventions 2010 // IERS Technical Note. 2010. No. 36.

© Pustoshilov A. S., Tsarev S. P., Ushakov Yu. Yu., Ovchinnikova E. V. 2020

Pustoshilov Alexander Sergeevich is a senior lecturer; Institute of Engineering Physics and Radioelectronics, Siberian Federal University. E-mail: alphasoft@inbox.ru.

Ushakov Yuriy Yurievich is a Candidate of Physical and Mathematical Sciences, associate professor; Institute of Space and Information Technologies, Siberian Federal University. E-mail: yuron@akadem.ru.

Tsarev Sergey Petrovich is a Doctor of Physical and Mathematical Sciences; professor of the Institute of Space and Information Technologies, Siberian Federal University. E-mail: sptsarev@mail.ru.

Ovchinnikova Elena Vladimirovna is a Candidate of Physical and Mathematical Sciences, associate professor; Institute of Informatics and Telecommunications, Department of Applied Mathematics, Reshetnev Siberian State University of Science and Technology. E-mail: ovchinnikova_ev@sibsau.ru.

Пустошилов Александр Сергеевич – старший преподаватель; Институт инженерной физики и радиоэлектроники, Сибирский федеральный университет. E-mail: alphasoft@inbox.ru.

Ушаков Юрий Юрьевич – кандидат физико-математических наук, доцент; Институт космических и информационных технологий, Сибирский федеральный университет. E-mail: yuron@akadem.ru.

Царев Сергей Петрович – доктор физико-математических наук, профессор; Институт космических и информационных технологий, Сибирский федеральный университет. E-mail: sptsarev@mail.ru.

Овчинникова Елена Владимировна – кандидат физико-математических наук, доцент; Институт информатики и телекоммуникаций, кафедра прикладной математики, Сибирский государственный университет науки и технологий имени академика М. Ф. Решетнева. E-mail: ovchinnikova_ev@sibsau.ru.

UDC 628.7.036.54 – 662.61

Doi: 10.31772/2712-8970-2021-22-2-302-315

For citation: Astakhov S. A., Biryukov V. I., Sizov G. A. A technique for determining the acoustic characteristics of combustion chambers of a solid propellant rocket engine. *Siberian Aerospace Journal*. 2021, Vol. 22, No. 2, P. 302–315. Doi: 10.31772/2712-8970-2021-22-2-302-315.

Для цитирования: Астахов С. А., Бирюков В. И., Сизов Г. А. Методика определения акустических характеристик камер сгорания ракетного двигателя твердого топлива // Сибирский аэрокосмический журнал. 2021. Т. 22, № 2. С. 302–315. Doi: 10.31772/2712-8970-2021-22-2-302-315.

A technique for determining the acoustic characteristics of combustion chambers of a solid propellant rocket engine

S. A. Astakhov^{1*}, V. I. Biryukov², G. A. Sizov^{1,2}

¹Federal Treasury Enterprise “State Treasury Research and Testing Range of Aviation Systems”

Belozersky settlement, Moscow region, 140250, Russian Federation

²Moscow Aviation Institute (National Research University)

4, Volokolamskoe highway, A-80, GSP-3, Moscow, 125993, Russian Federation

*E-mail: aviatrix@mail.ru

Many developers of new high-thrust solid-propellant rocket engines are faced with the problem of acoustic instability of combustion. The phenomenon of resonant combustion of solid fuel is associated with a number of specific features. The cavities of the combustion chambers of such engines have complex geometric shapes. The gas channel is long enough. Its length usually exceeds five or more calibers. The thickness of the flame front is measured in micrometers and the combustion zone is localized over the open fuel surface. The flame front often turns out to be capable of amplifying pressure perturbations at the frequency of one of the acoustic eigenmodes if the wave antinode falls on a thin combustion zone. The oscillatory process can be regular or sporadic. Resonances of the longitudinal acoustic mode are most often observed. However, there were cases of simultaneous oscillation of two modes. In some cases, during the operation of the engine, the amplitude of the resulting oscillations began to decrease and the combustion process became almost quasi-stationary. Self-oscillatory processes in the combustion chambers of solid propellants have a threshold sensitivity to pressure overshoots. The vibration amplitudes can be several tens of percent, sometimes reaching the nominal working pressure in the chamber. The amplitude-frequency characteristics of the oscillations are sensitive to the composition of the fuel, responding to changes in the chemical composition, as well as to the mechanical properties of the fuel. The regions of unstable regimes are definitely related to the geometry of the gas cavity. Together with pressure fluctuations, the combustion process is influenced by gas-dynamic factors, significant non-uniformity of the gas flow parameters along the length of the channel, its turbulence, and other factors. When designing solid-propellant rocket engines, it is necessary to estimate the frequencies of the natural acoustic resonances of the combustion chambers.

The article discusses a technique for determining the frequencies of natural resonances of the first and second tone of the longitudinal mode of acoustic vibrations in the combustion chambers of solid propellant rocket engines. The gas path of the combustion chamber is divided into homogeneous sections, for which the solutions of the wave equation are presented. To determine the natural frequencies and distribution of vibrational pressures and velocities, the method of “stitching” acoustic fields at the boundaries of the cavities was used.

Keywords: acoustic vibrations, longitudinal mode, frequency, damping decrement, wavenumber, quality factor.

Методика определения акустических характеристик камер сгорания ракетного двигателя твердого топлива

С. А. Астахов^{1*}, В. И. Бирюков², Г. А. Сизов^{1,2}

¹Федеральное казенное предприятие «Государственный казенный научно-испытательный полигон авиационных систем»

Российская Федерация, 140250, Московская обл., п. Белозерский

²Московский авиационный институт (национальный исследовательский университет)
Российская Федерация, 125993, г. Москва, А-80, ГСП-3, Волоколамское шоссе, 4

*E-mail: aviatex@mail.ru

С проблемой акустической неустойчивости горения сталкиваются многие разработчики новых ракетных двигателей твердого топлива больших тяг. Явление резонансного горения твердого топлива сопряжено с рядом специфических особенностей. Полости камер сгорания таких двигателей имеют сложные геометрические формы. Газовый канал выполняется достаточно протяженным. Его длина обычно превышает пять и более калибров. Толщина фронта пламени измеряется микрометрами и зона горения локализуется по открытой поверхности топлива. Фронт пламени зачастую оказывается способным усиливать возмущения давления на частоте одной из собственных акустических мод, если пучность волны приходится на тонкую зону горения. Колебательный процесс может быть регулярным или спорадическим. Чаще всего наблюдаются резонансы продольной акустической моды. Однако встречались случаи колебания одновременно двух мод. В некоторых случаях в процессе работы двигателя амплитуда возникших колебаний начинала уменьшаться и процесс горения становился почти квазистационарным. Автоколебательные процессы в камерах сгорания РДТТ имеют пороговую чувствительность к забросам давления. Амплитуды колебаний могут составлять несколько десятков процентов, порой достигая номинального рабочего давления в камере. Амплитудно-частотные характеристики колебаний чувствительны к составу топлива, откликаясь на изменения химического состава, а также и на механические свойства топлива.

Области неустойчивых режимов определенно связаны с геометрией газовой полости. Вместе с колебаниями давления на процесс горения влияют газодинамические факторы, существенная неравномерность параметров газового потока по длине канала, его турбулентность и другие факторы. При проектировании РДТТ необходима оценка частот собственных акустических резонансов камер сгорания.

В статье рассматривается методика определения частот собственных резонансов первого и второго тона продольной моды акустических колебаний в камерах сгорания ракетных двигателей твердого топлива. Газовый тракт камеры сгорания разбивается на однородные участки, для которых представлены решения волнового уравнения. Для определения собственных частот и распределения колебательных давлений и скоростей использован метод «сшивания» акустических полей на границах полостей.

Ключевые слова: акустические колебания, продольная мода, частота, декремент затухания, волновое число, добротность.

Introduction

The problem of acoustic instability of combustion in solid-propellant rocket engines is no less urgent in comparison with high-thrust liquid-propellant rocket engines [1–4]. As a rule, the acoustic cavity has a complex geometric shape. The combustion zone is located in close proximity to the interface between the phases – a solid charge and a gas path. The thickness of the combustion zone of the mixed composition at a pressure

of up to 4 MPa and a gas temperature of the order of (2500–3000) K is approximately 70–90 microns. A thin combustion zone often turns out to be capable of amplifying the pressure disturbances of the acoustic mode for which the maximum wave falls on the combustion surface. The effect of acoustic pressure fluctuations on the combustion process, in accordance with the Rayleigh criterion, causes fluctuations in the combustion rate [2–12]. The presence of this feedback leads to an increase in pressure fluctuations in a thin zone of chemical reactions with high temperature gradients, fuel vapor concentration, and high rates of energy and mass transfer. In addition, the possible thermodynamic heating of the gas during its compression should be noted. In some cases, fluctuations in acoustic velocity can also play an important role. When solid fuels are burned, turbulent pulsations are present in the channels of the checker – combustion noises. They are due to different excitation mechanisms and have a different physical nature. Sound noise is usually associated with gas-dynamic reasons of the same nature as in turbulent gas flows. In combustion chambers, regular pressure fluctuations with a frequency close to the natural (acoustic) frequency of the gas column oscillations [7–12] can increase, and more often stabilize at a certain level due to acoustic losses. The acoustic instability of combustion is an autowave process with feedback through the action of sound waves on combustion. The parameters of the wave process: frequency, amplitude and form of oscillations are determined by the properties of the solid-propellant rocket engine charge as a dynamic system. Sound noise in the chamber cavity can also be considered as a self-oscillatory process [6], in which the energy source is heat release during combustion, and feedback arises due to the effect of sound waves on combustion, while persistent pulsations of a stochastic nature arise [11], which have a wide frequency band and random phases. However, the frequency response of the acoustic cavity often has frequency selectivity characterized by a high Q factor with respect to the longitudinal mode [2–4].

Most theoretical works analyze the effect of small perturbations on the stability of combustion. However, given the complex nonlinear mechanism of solid fuel transformation into the gas phase (heating, pyrolysis, sublimation, etc.), the combustion process and its interaction with gas-dynamic phenomena in the acoustic path of solid-propellant rocket engines are often characterized by “hard” excitation of self-oscillations. Otherwise, the dynamic system can become unstable when the amplitude of the disturbances increases above a certain threshold limit. Disturbances with an amplitude below the threshold attenuate. Rigid excitation of oscillations is characteristic of nonlinear dynamic systems. The development of nonlinear theories is greatly complicated by mathematical difficulties. Linear theories can be quite useful for understanding instability and, in some cases, for nonlinear applications.

An assessment of the stability of combustion in solid-propellant rocket engines can be carried out on the basis of determining the balance of acoustic energy in the combustion chamber, taking into account the influx of acoustic energy (due to the interaction of acoustic vibrations with the combustion process) and losses of acoustic energy during the period of vibrations. The diagnostic indicator of the margin of linear stability of the combustion process is the coefficient (decrement) of damping of oscillations [2; 7–12]. The attenuation coefficient has a certain physical meaning:

$$\delta_v = \frac{E_2 - E_1}{2E_{\text{CYM}}}, \quad (1)$$

where E_2 is the inflow of acoustic energy generated by the oscillating system during the vibration period; E_1 is a part of the energy dissipated by the oscillatory system during the vibration period; E_{CYM} – acoustic energy stored by the system during the vibration period.

The influx of acoustic energy from the combustion process depends – at certain phase ($0 \div \pi/2$) the relationship between pressure fluctuations and combustion rate – from the amplitude of pressure fluctuations, increasing in proportion to the square of the latter. To determine the flow of acoustic energy in combustion chambers, experimental methods have been developed using a T-shaped chamber [3–4]. Losses of acoustic energy in the gas volume of the combustion chamber are essential in the presence of condensed particles in the combustion products. Calculation of losses at the boundaries of a combustion chamber with a complex configuration in the case of solid fuel engines is associated with great difficulties. These losses can be approximately determined by carrying out experiments on models of combustion chambers without gas flow. It follows from the foregoing that the acoustic properties of the combustion chamber: the frequency of natural vibrations, the distribution of the vibration amplitude – can amplify the vibrations or damp them, and thereby affect the stability of combustion in the engine. It should be noted that the properties of the combustion chamber of solid-propellant rocket engines as an oscillatory system differ from the properties of systems considered in acoustics. The differences are due to the fact that a high-speed gas flow is superimposed on the vibrations in the combustion chambers, the specific configuration of the nozzle affects, there are distributions of the parameters of the working process, etc. But despite these important differences, the forms and frequencies of natural vibrations do not change significantly [2; 7–12], which makes it possible to carry out calculations and experiments to determine the properties of the combustion chamber as an oscillatory system in the acoustic approximation, that is, without taking into account complicating factors.

As a result of theoretical and experimental studies of the acoustic instability of combustion, a certain level of knowledge of physical processes has now been achieved, which makes it possible to predict the influence of changes in design and operating factors on the instability regions. Solid-propellant rocket engines are characterized by acoustic vibrations of the longitudinal mode due to the large ratio of the charge length to the cavity diameter ($L/D \geq 5$), and transverse modes are much less common.

Natural vibration frequencies and acoustic pressure fields in the combustion chambers of solid-propellant rocket engines

Acoustic waves propagating in the paths of various systems often have a wavelength comparable to the dimensions of the channels. In this case, it is advisable to consider the solution of the wave equation in the form of standing waves. Standing waves are formed as a result of the interaction of direct waves and waves reflected from the “hard” walls. Consider a superposition of two waves F moving towards each other with constant phase velocities. For this, we represent the solution of the wave equation as a sum of particular solutions of the form [7]

$$\frac{\partial^2 F(x)}{\partial x^2} = -k^2 F(x); \quad \frac{\partial^2 F(t)}{\partial t^2} = -k^2 c_0^2 F(t) = -\omega^2 F(t), \quad (2)$$

where $\omega^2 = k^2 c_0^2$.

System (2) is equivalent to equations describing elastic vibrations of a material point. The solutions to these equations represent harmonic vibrations with their own phase shift:

$$F(x) = A \cos(kx + \varphi_x); \quad F(t) = B \cos(\omega t + \varphi_t). \quad (3)$$

The solution to the wave equation is written as a product

$$\psi = F(x)F(t) = C \cos(kx + \varphi_x) \cos(\omega t + \varphi_t). \quad (4)$$

Here $C = A B$.

The function $F(x)$ describes the distribution of the vibration amplitude, constant in time, and the function $F(t)$ shows that all points of the wave move synchronously. Oscillation does not propagate, displacements of all points reach their maximum or minimum values at the same times. The resulting particular solution is called a standing wave or natural vibration. To describe wave motion in an unlimited volume requires an infinite number of solutions with a continuous spectrum of frequency ω and $k = \omega / c_0$. Here c_0 is the speed of sound and k is the wave number. The general solution has the form of a Fourier integral. In the case of the implementation of a standing wave in a finite path with rigid walls, both the general solution and each particular solution are found, satisfying the boundary conditions

$$\xi_v(x, t) = 0; \quad \frac{\partial \xi_v(x, t)}{\partial x} = 0.$$

Each particular solution must satisfy the wave equation and describe the possible oscillation of the system

$$\psi_v(x, t) = A_v \cos(k_v x + \varphi_{vx}) \cos(k_v c_0 t + \varphi_{vt}), \quad (5)$$

where $\psi_v(x, t)$ – velocity potential; $\omega_v = k_v c_0$ – circular vibration frequency.

If the potential function at the boundaries of the tract is equal to zero, then for any moment of time the following should be fulfilled:

$$A_v \cos \varphi_{vx} \cos(\omega_v t + \varphi_{vt}) = A_v \cos(\omega_v t + \varphi_{vt}) \cos(k_v l + \varphi_{vx}) = 0, \quad (6)$$

$$\varphi_{vx} = \frac{v\pi}{2}, \quad k_v l = v\pi, \quad v = 1, 2, \dots \quad (7)$$

Each particular solution can be represented by the expression

$$\psi_v(x, t) = \psi_v(x) \cos(\omega_v t + \varphi_{vt}), \quad (8)$$

where

$$\psi_v(x) = A_v \sin \frac{v\pi x}{l}, \quad \omega_v = k_v c_0 = \frac{v\pi c_0}{l}. \quad (9)$$

The function $\psi_v(x)$ describes the natural vibrations of the system in the absence of external forces and damping, and the frequencies ω_v are the natural angular frequencies.

A more general solution can be obtained by adding all the natural vibrations of the system with the corresponding amplitudes:

$$\psi_v(x, t) = \sum \psi_v(x) \cos(\omega_v t + \varphi_{vt}) = \sum A_v \sin \frac{v\pi x}{l} \cos(\omega_v t + \varphi_{vt}), \quad v = 1, 2, \dots \quad (10)$$

Consider a particular case of plane wave propagation in a moving stream and find relations for velocity fluctuations and pressure perturbations. We represent the general solution of the equation in the form of two waves moving in the opposite direction:

$$\psi = A e^{i\omega t - ik_1 x} + B e^{i\omega t - ik_2 x}, \quad (11)$$

where

$$k_1 = \frac{\omega}{c_0 + v_0}; \omega = k_1(c_0 + v_0); k_2 = \frac{\omega}{c_0 - v_0}; \omega = -k_2(c_0 - v_0). \quad (12)$$

Velocity fluctuation

$$v'_x = -\frac{\partial \Psi}{\partial x} = ik_1 A e^{-k_1 x + i\omega t} + ik_2 B e^{-k_2 x + i\omega t}. \quad (13)$$

Pressure perturbations are related to the velocity potential by the equation

$$\delta p \frac{c_0^2}{\gamma} = \frac{p'}{\rho_0} = \frac{\partial \Psi}{\partial t} + v_0 \frac{\partial \Psi}{\partial x}.$$

Let us differentiate this expression with respect to time t and coordinate x

$$p' = \rho_0 \left(i\omega A e^{-k_1 x + i\omega t} + i\omega B e^{-k_2 x + i\omega t} - v_0 ik_1 A e^{-k_1 x + i\omega t} - v_0 ik_2 B e^{-k_2 x + i\omega t} \right).$$

Next, we introduce new coefficients, then the expression for the pressure perturbation will be somewhat simplified

$$p' = C e^{i\omega t - ik_1 x} + D e^{i\omega t - ik_2 x}, \quad (14)$$

where the coefficients are:

$$C = (i\omega - v_0 ik_1) \rho_0 A = \frac{i\rho_0 c_0 \omega}{c_0 + v_0} A; \quad D = (i\omega - v_0 ik_2) \rho_0 B = \frac{i\rho_0 c_0 \omega}{c_0 - v_0} B.$$

Taking into account the form of these coefficients, the expression for the velocity perturbation will look as follows:

$$v'_x = \frac{C}{\rho_0 c_0} e^{+i\omega t - ik_1 x} - \frac{D}{\rho_0 c_0} e^{+i\omega t - ik_2 x}. \quad (15)$$

Let us express the mechanical resistance of the medium in the form of the ratio of pressure perturbations to velocity fluctuation. For a wave traveling downstream, this ratio is

$$\frac{p'_+}{v'_{x+}} = \rho_0 c_0,$$

and against the stream

$$\frac{p'_-}{v'_{x-}} = -\rho_0 c_0.$$

Magnitude

$$z_c = \rho_0 c_0 \quad (16)$$

is the wave impedance of the medium. Thus, the sound pressure is equal to the propagation velocity of a plane wave multiplied by the magnitude of the wave resistance and has a positive sign if the wave propagates in the positive direction of the coordinate axis. When the wave propagates in the opposite negative direction, the particle velocity is negative, and the sound pressure is positive. Wave resistance characterizes the environment and is constant for it. The dispersion relation for the perturbation in the form of a plane entropy wave is defined as follows [7–8]:

$$\omega - k_s v_0 = 0 \rightarrow v_0 = \frac{\omega}{k_s}, \quad \text{from here} \quad \delta S = \delta S_H e^{i\omega t - ik_s x}. \quad (17)$$

Entropy waves propagate without dispersion, while plane vortex waves do not exist.

Let us consider plane standing waves in a cylindrical combustion chamber closed on one side. Let us take the solution of the wave equation in the form $\psi = (A \cos kx + B \sin kx) e^{-i\omega t}$. Then at $x = 0$

$$v'_x = \frac{\partial \psi}{\partial x_{x=0}} = (-Ak \sin kx + Bk \cos kx)e^{i\omega t} = 0. \quad (18)$$

Identity (18) is fulfilled at $B = 0$, from which it follows that standing vibrations are excited and they are the same in phase at all points simultaneously

$$\psi = A \cos(kx)e^{i\omega t}; \quad \frac{\partial \psi}{\partial x} = (-Ak \sin kx)e^{i\omega t}. \quad (19)$$

At $x = l$, the vibrational pressure is assumed to be zero ($\psi = 0$), then $\cos(kl) = 0$; from this we obtain $kl = m\pi/2$, and m are odd.

Thus, for a pipe closed at one end and open at the other

$$\psi = A \cos\left(\frac{m\pi}{2l}x\right)e^{i\omega t}; \quad v'_x = \frac{\partial \psi}{\partial x} = \frac{m\pi}{2l} \left(Ak \sin \frac{m\pi}{2l}x\right)e^{i\omega t}, \quad (20)$$

where $m = 1, 3, 5, \dots$

In the case of a pipe closed on both sides, i.e., at $x = 0$ and $x = l$, from expression (20) it follows $B = 0$ and $\sin(kl) = 0$, whence $m\pi = kl$; $m = 0, 1, 2, \dots$

$$\psi = A \cos\left(\frac{m\pi}{2l}x\right)e^{i\omega t}. \quad (21)$$

The gas cavity of the combustion chambers of solid-propellant rocket engines has a more complex configuration. Fig. 1 shows a gas cavity that is formed if the charge is tightly bound with the chamber and combustion occurs along the inner surface of the charge channel and chamber ends.

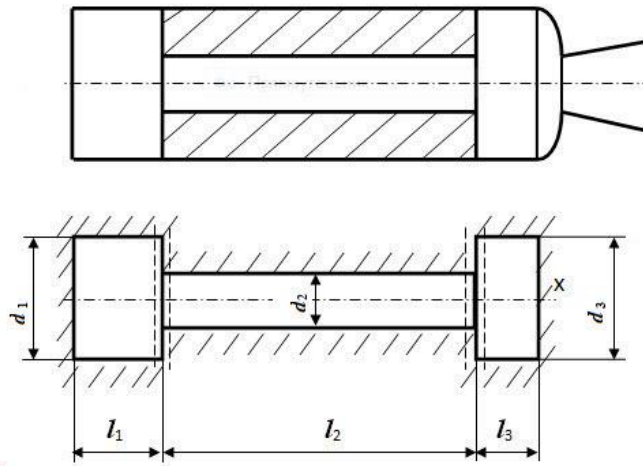


Fig. 1. Diagram of the gas cavity of the chamber:
 a – constructive; b – calculated

Рис. 1. Схема газовой полости камеры:
 a – конструктивная; b – расчетная

The propagation of vibrations in such a complex cavity is accompanied by diffraction phenomena. Considering that most of the sound wave approaching the nozzle is reflected from it into the chamber (due to the presence of a converging part of the nozzle and a change in the acoustic resistance of the medium ρc) to simplify the considered oscillatory system, we replace the nozzle with a rigid wall. We divide a complex gas cavity into three cylindrical cavities, each of which has a constant cross-sectional area. For each component

of a complex cavity, we represent the solution of the wave equation. Further, for the natural frequencies and the distribution of vibrational pressures and velocities, we use the method of “stitching” acoustic fields at the boundaries of the cavities [13], taking into account the continuity of the medium during the transition of a sound wave from one cavity to another. For example, the conditions for the continuity of the medium during the transition from the first cavity to the second are determined by the equality of sound pressures (or velocity potentials) at $x = l_1$

$$\psi_1(l_1) = \psi_2(l_1) \quad (22)$$

and the equality of the volume velocities

$$S_1 \left(\frac{\partial \psi}{\partial x} \right)_1 = S_2 \left(\frac{\partial \psi}{\partial x} \right)_2, \quad (23)$$

where S_1 and S_2 – are the cross-sectional areas of the first and second cavities.

The solution of the wave equation for a complex three-stage cavity should be written in the form of a series, taking into account the fact that there is a standing wave in the cavity and diffraction reflections of vibrations during the transition from cavity to cavity (at $x = l_1$ and $x = l_2$), i.e., for each cavity taking into account zero boundary conditions for vibrational velocities at $x = 0$ and $x = l_1 + l_2 + l_3$. If to simplify the problem we neglect the diffraction of acoustic waves at the joints of the cavities, then the solution of equation (21) for standing waves in each cavity can be written in the form

$$\psi_i = A_i [k(x - \alpha_i)] e^{i\omega t}, \quad (24)$$

i – is the number of the cavity, α_i – is the parameter that determines the conditions for the phase transition from cavity to cavity; A_i - vibration amplitude.

For the first cavity

$$\psi_1 = A_1 [k(x - \alpha_1)] e^{i\omega t}. \quad (25)$$

From the zero boundary condition for the vibrational velocity $v = 0$ at $x = 0$ it follows that $\alpha_1 = 0$. Hence

$$\psi_1 = A_1 \cos(kx) e^{i\omega t}, \quad (26)$$

And for the second cavity

$$\psi_2 = A_2 \cos[k(x - \alpha_2)] e^{i\omega t}. \quad (27)$$

Similarly for the third cavity

$$\psi_3 = A_3 \cos[k(x - \alpha_3)] e^{i\omega t}. \quad (28)$$

However, from the zero boundary condition for the vibrational velocity

$$v' = \frac{\partial \psi_3}{\partial x} = 0 \text{ при } x = l_1 + l_2 + l_3 \text{ следует, что } \alpha_3 = l_1 + l_2 + l_3.$$

The unknown wavenumber k and the parameter α_2 can be determined by substituting expressions (26) and (27) into conditions (22) and (23), which characterize the continuity of the medium at $x = l_1$. Eliminating the coefficients A_1 and A_2 from the system of equations, we obtain the relationship of the unknown parameters

$$\operatorname{tg} k l_1 = \frac{S_2}{S_1} \operatorname{tg} [k(l_1 - \alpha_2)]. \quad (29)$$

The conditions for “matching” acoustic fields at $x = l_1 + l_2$ are fulfilled similarly to conditions (22) and (23):

$$\psi_2(l_1 + l_2) = \psi_3(l_1 + l_2); S_2 \left(\frac{\partial \psi}{\partial x} \right)_2 = S_3 \left(\frac{\partial \psi}{\partial x} \right)_3. \quad (30)$$

Eliminating the amplitude coefficients A_2 and A_3 , we obtain the second equation for determining the unknowns k and the parameter α_2

$$\frac{S_3}{S_2} \operatorname{tg} kl_3 + \operatorname{tg} [k(l_1 + l_2 - \alpha_3)] = 0. \quad (31)$$

Solving algebraic equations (31) and (33) together, we obtain the transcendental algebraic equation

$$\operatorname{tg} kl_2 + \frac{S_1}{S_2} \operatorname{tg} kl_1 + \frac{S_3}{S_2} \operatorname{tg} kl_3 - \frac{S_1 S_3}{S_2^2} \operatorname{tg} kl_1 \cdot \operatorname{tg} kl_2 \cdot \operatorname{tg} kl_3 = 0. \quad (32)$$

Dependence (32) includes the geometrical dimensions of the gas cavity and the unknown wave number k .

The distribution of the amplitude of pressure fluctuations (in relative values) along the length of the combustion chamber can be determined by the following formulas:

for the first cavity:

$$\delta p_1 = \frac{p'_1}{p_0} = \cos kx; \quad (33)$$

for the second cavity:

$$\delta p_2 = \frac{p'_2}{p_0} = \frac{\cos kl_1}{\cos [k(l_1 - \alpha_2)]} \cos [k(x - \alpha_2)], \quad (34)$$

where α_2 is calculated from equation (30)

$$\alpha_2 = \frac{kl_1 - \operatorname{arctg} \left[\frac{S_1}{S_2} \operatorname{tg} kl_1 \right]}{k}. \quad (35)$$

For the third cavity:

$$\delta p_3 = \frac{p'_3}{p_0} = \frac{\cos kl_1 \cdot \cos [k(l_1 + l_2 - \alpha_2)]}{\cos kl_3 \cdot \cos [k(l_1 - \alpha_2)]} \cos [k(x - \alpha_3)]. \quad (36)$$

Here p_0 – is pressure amplitude at $x = 0$.

Fig. 2 shows the graph $p/p_0 = f(x)$ according to the calculated data.

According to the described algorithm, approximate calculated dependences can be obtained for other configurations of the gas cavity of the combustion chambers. Comparing the calculated data found by approximate formulas with the experimental data obtained on an acoustic installation, one can find out the accuracy of the calculations. The tasks of the experimental work include the determination of the natural resonances of the acoustic longitudinal mode and the estimation of the vibrational energy losses.

Description of the test unit

The test unit consists of a model chamber, an electrodynamic emitter, a sound generator that sets the excitation frequency, an amplifier, and receiving and recording equipment.

The model chamber is split and consists of several sections. Charge dummies can be inserted inside the chamber. The geometric dimensions of the acoustic cavity are shown in Fig. 2.

Sound heads of the 10 GRAD-5 type are used as a source of small vibrations. The frequency range of these heads ranges from 90 to 12,000 Hz. The sound heads are powered from the UM-50A type amplifier. A sound generator of the GZ-18 type is used as a master oscillator. Receiving and recording equipment includes a pressure sensor and a computer. The sensing part of the detector is a hollow piezoceramic ball with a diameter of 7 mm and a wall thickness of 0.25 mm. The dimensions of the detector's sensitive element are

chosen so that they are an order of magnitude smaller than the measured wavelengths, in order to avoid distortion of the sound field.

The method of procedure

In operation with the help of an electrodynamic emitter, vibrations of a certain frequency in a given range are excited. To obtain the acoustic characteristics of the chamber at different moments of engine operation, experiments are carried out with several charge mock-ups having different sizes (imitating the burnout of the charge). For each version of the gas cavity, by tuning the sound generator, the amplitude-frequency characteristic is taken within the limits of the first two resonances of the longitudinal vibration mode. The frequency response is used to determine the natural frequencies of the camera. At the same frequencies, the distribution of the amplitude of the oscillatory pressure for the longitudinal mode of oscillation is recorded using a sensor moved along the axis of the chamber.

Sequence of calculations and processing of experimental data

I. Calculation of the acoustic characteristics of a model combustion chamber:

– the lowest values of the wave number k are determined by the formula (32) (using auxiliary tables) and the natural frequencies of longitudinal vibrations are calculated according to the formula

$$f = \frac{kc_0}{2\pi}.$$

When calculating the vibration frequency on an acoustic model installation, the speed of sound in air is taken, and for a natural combustion chamber, the speed of sound should be calculated in combustion products;

– the amplitude of pressure fluctuations in relative values is calculated (attributed to the pressure amplitude p_0 at $x = 0$) according to formulas (33)–(36), (Fig. 2);

– approximate determination of acoustic energy losses in the combustion chamber. The loss of acoustic energy per unit time, dE/dt is proportional to the energy density E . Denoting the coefficient of proportionality through 2δ , we have $dE/dt = 2\delta E$, whence integrating we find

$$E = E_0 \exp(-2\delta t),$$

where E_0 – is energy density at the moment $t = 0$.

The pressure amplitude due to losses in the oscillatory system decreases exponentially

$$p' = p_0 e^{-\delta t}.$$

The magnitude $\delta = \frac{dE}{2Edt}$ is the attenuation coefficient for the longitudinal mode and characterizes the

acoustic energy loss per unit time. Approximately the damping coefficient δ can be determined, having the amplitude-frequency characteristic of the oscillatory system, by the value of the quality factor Q [2; 6]. It should be noted that Q is a characteristic of a linear system with lumped parameters, but conditionally Q can be used as a characteristic of nonlinear systems with distributed parameters. The value of Q represents the ratio of the time-average available energy to the amount of energy loss over the period of oscillation [2; 6–8; 14–15], therefore

$Q = \frac{\pi}{\delta \cdot T}$, or $Q = \frac{\omega}{2\delta}$, here $T = \frac{2\pi}{\omega}$ is the period of fluctuations. The quality factor of the oscillating system, having an amplitude-frequency characteristic, can be determined from the width of the curve (Fig. 3) ($f_1 - f_2$) at a level equal to $\frac{\sqrt{2}}{2} p_{\max}$, according to the formula $Q = \frac{f^x}{f_2 - f_1}$.

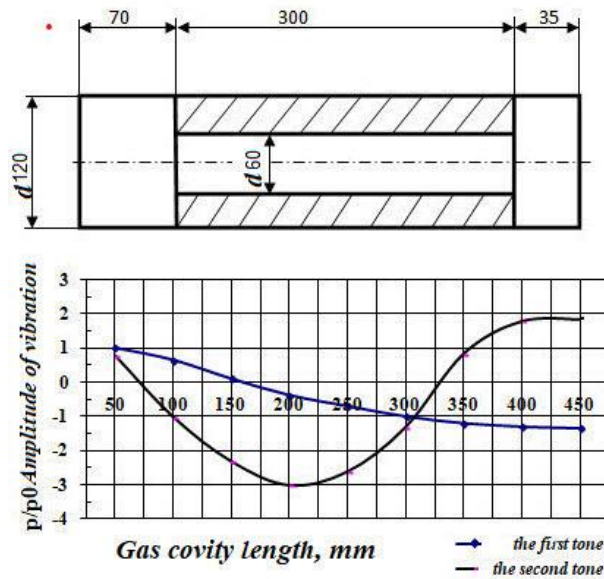


Fig. 2. Distribution of vibrational pressure in the gas cavity of the chamber (according to calculated data):
1 – the first tone of the longitudinal mode; 2 – the second tone of the longitudinal mode

Рис. 2. Распределение колебательного давления в газовой полости камеры (по расчетным данным):
1 – первый тон продольной моды; 2 – второй тон продольной моды

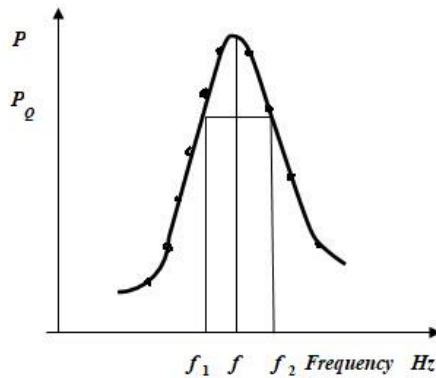


Fig. 3. Determination of the quality factor Q by the amplitude-frequency characteristic of the oscillating system

Рис. 3. Определение добротности Q по амплитудно-частотной характеристике колебательной системы

From the above expressions for Q we obtain $\delta = \pi(f_2 - f_1)$.

If the combustion chamber is filled with gas with such characteristics that the ratio is fulfilled

$$\frac{(RT)_k k_k}{(RT)_{\text{mod}} k_{\text{mod}}} \cong 1,$$

then in model experiments the vibration frequencies and loss characteristics will be simulated which are close to those occurring in the combustion chamber of a running engine (counting losses with flow through the nozzle small).

II. Construction of acoustic characteristics of a model combustion chamber based on experimental data.

1. Graphs of the amplitude-frequency characteristics of the combustion chamber are constructed.
2. A graph of the natural frequency of vibrations of the combustion chamber is constructed as a function of the ratio of the diameter of the charge channel to the diameter of the combustion chamber.
3. Graphs $p/p_0 = f(x)$ are plotted for the first and second tones of the longitudinal mode.
4. A graph of the attenuation coefficient is plotted as a function of the ratio of the diameter of the charge channel to the diameter of the combustion chamber.

Conclusion

A method of computational and experimental approximate determination of the acoustic characteristics of the combustion chambers of solid-propellant rocket engines has been developed, without taking into account the effect of solid propellant combustion. Taking into account the high costs of creating a T-shaped experimental solid propellant rocket engine combustion chamber and the significant difficulties in conducting such experimental studies, the proposed algorithm makes it possible to determine the frequencies of natural acoustic resonances in the cavities of solid-propellant rocket engines, in particular for the longitudinal mode, less costly in time and money, and to predict their coefficients (decrements) damping.

References

1. Zel'dovich Ya. B., Barenblatt G. I., Librovich V. B., Mixviladze G. M. *Teoriya nestacionarnogo gorenija poroxa* [Theory of non-stationary combustion of gunpowder]. Moscow, Nauka Publ., 1980, 478 p.
2. Abugov D. I., Bobylev V. M. *Teoriya i raschet raketny'x dvigateley tverdogo topliva*. [Theory and calculation of solid-propellant rocket engines]. Moscow, Mashinostroenie Publ., 1987, 272 p.
3. Kouts F. L., Xarton M. D. [Analysis of the stability of the working process in the design of RDTT]. *Voprosy` raketnoy texniki*. 1969, No. 7, P. 11–28 (In Russ.).
4. Barrer M., Nado L., Lyujner I. [Studies of the instability of combustion of RDTT fuels]. *Voprosy` raketnoy texniki*. 1973, No. 7, P. 10–28 (In Russ.).
5. Bloxincev D. I. *Akustika neodnorodnoj dvizhushheysya sredy`* [Acoustics of an inhomogeneous moving medium]. Moscow, Nauka Publ., 1966, 205 p.
6. Doroshenko V. E., Furletov V. I. [On the effect of sound on a turbulent flame]. *Fizika gorenija i vzry`va*. 1969, No. 1, P. 114–121 (In Russ.).
7. Biryukov V. I., Mosolov S. V. *Akustika gazovy`x traktov zhidkostny`x raketny`x dvigateley*. [Acoustics of gas paths of liquid rocket engines]. Moscow, MAI Publ., 2013, 164 p.
8. Biryukov V. I., Mosolov S. V. *Dinamika gazovy`x traktov zhidkostny`x raketny`x dvigateley*. [Dynamics of gas paths of liquid rocket engines]. Moscow, MAI Publ., 2016, 168 p.
9. Biryukov V. I., Nazarov V. P., Tsarapkin R. A. The Algorithm for Estimating Reserves of the Working Process Stability in Combustion Chambers of Liquid-Propellant Rocket Engines. *Siberian Journal of Shience and Technology*. 2017, Vol. 18, No. 3, P. 558–566 (In Russ.).
10. Biryukov V. I., Tsarapkin R. A. Damping Decrements in the Combustion Chambers of Liquid-Propellant Rocket Engines. *Russian Engineering Research*. 2019, Vol. 39, No.1, P. 6–12.
11. Biryukov V. I., Ivanov V. N., Tsarapkin R. A. Method for Predicting the Stability Limit to Acoustic Oscillations in Liquid – Propellant Rocket Engine Combustion Chambers Based on Combustion Noise. *Fizika Gorenija i Vzryva*. 2021, Vol. 57, No. 1, P. 80–89.
12. Czarapkin R. A., Biryukov V. I. [Experimental determination of the attenuation constants in the combustion chambers of liquid rocket engines]. *Vestnik mashinostroeniya*. 2018, No. 10, P. 21–27 (In Russ.).

13. Osipov A. A. [Propagation of three-dimensional acoustic perturbations in channels of variable cross-sectional area at frequencies close to the cut-off frequency]. *Izvestiya AN SSSR. Seriya Mexanika zhidkosti i gaza*. 1980, No. 6, P. 149–159 (In Russ.).
14. Rudenko A. N. [Experimental study of the frequency characteristics of nozzles with respect to longitudinal and transverse vibrations]. *Akusticheskiy zhurnal*. 1979, Vol. 20, No. 6, P. 897–906 (In Russ.).
15. Sukhinin S. V., Akhmadeev V. F. Self Oscillations in the Gas Cavity of a Solid Rocket Motor. *Fizika Goreniya i Vzryva Combustion*. 2001, Vol. 37, No. 1, P. 42–52.

Библиографические ссылки

1. Теория нестационарного горения пороха / Я. Б. Зельдович, Г. И. Баренблатт, В. Б. Либрович, Г. М. Михвильдзе. М. : Наука, 1980. 478 с.
2. Абугов Д. И., Бобылев В. М. Теория и расчет ракетных двигателей твердого топлива : учебник для машиностроительных вузов. М. : Машиностроение, 1987. 272 с.
3. Коутс Ф. Л., Хартон М. Д. Анализ устойчивости рабочего процесса при проектировании РДТТ // Вопросы ракетной техники. 1969. № 7. С. 11–28.
4. Баррер М., Надо Л., Люйнер И. Исследования неустойчивости горения топлив РДТТ // Вопросы ракетной техники. 1973. № 7. С. 10–28.
5. Блохинцев Д. И. Акустика неоднородной движущейся среды. М. : Наука, 1966. 205 с.
6. Дорошенко В. Е., Фурлетов В. И. О воздействии звука на турбулентное пламя // Физика горения и взрыва. 1969. № 1. С. 114–121.
7. Бирюков В. И., Мосолов С. В. Акустика газовых трактов жидкостных ракетных двигателей. М. : Изд-во МАИ, 2013. 164 с.
8. Бирюков В. И., Мосолов С. В. Динамика газовых трактов жидкостных ракетных двигателей. М. : Изд-во МАИ, 2016. 168 с.
9. Biryukov V. I., Nazarov V. P., Tsarapkin R. A. The Algorithm for Estimating Reserves of the Working Process Stability in Combustion Chambers of Liquid-Propellant Rocket Engines // Сибирский журнал науки и технологий. 2017. Vol. 18, No. 3. P. 558–566.
10. Biryukov V. I., Tsarapkin R. A. Damping Decrements in the Combustion Chambers of Liquid-Propellant Rocket Engines // Russian Engineering Research. 2019. Vol. 39, No. 1. P. 6–12.
11. Biryukov V. I., Ivanov V. N., Tsarapkin R. A. Method for Predicting the Stability Limit to Acoustic Oscillations in Liquid – Propellant Rocket Engine Combustion Chambers Based on Combustion Noise // Fizika Goreniya i Vzryva. 2021. Vol. 57, No. 1. P. 80–89.
12. Царапкин Р. А., Бирюков В. И. Экспериментальное определение декрементов затухания в камерах сгорания жидкостных ракетных двигателей // Вестник машиностроения. 2018. № 10. С. 21–27.
13. Осипов А. А. Распространение трехмерных акустических возмущений в каналах переменной площади поперечного сечения при частотах, близких к частоте отсечки // Известия АН СССР. Серия Механика жидкости и газа. 1980. № 6. С. 149–159.
14. Руденко А. Н. Экспериментальное исследование частотных характеристик сопел по отношению к продольным и поперечным колебаниям // Акустический журнал. 1979. Т. 20, № 6. С. 897–906.
15. Sukhinin S. V., Akhmadeev V. F. Self Oscillations in the Gas Cavity of a Solid Rocket Motor // Fizika Goreniya i Vzryva Combustion. 2001. Vol. 37, No. 1. P. 42–52.

Astakhov Sergei Anatolievich – Cand. Sc., director; Federal Treasury Enterprise “State Treasury Research and Testing Range of Aviation Systems”. E-mail: saastahov@yandex.ru.

Biryukov Vasiliy Ivanovich –Dr. Sc., professor; Moscow Aviation Institute (National Research University). E-mail: aviatex@mail.ru.

Sizov Georgiy Alekseyevich – postgraduate student; Moscow Aviation Institute (National Research University). E-mail: georgisiz1994@gmail.com.

Астахов Сергей Анатольевич – кандидат технических наук, директор; федеральное казенное предприятие «Государственный казенный научно-испытательный полигон авиационных систем». E-mail: saastahov@yandex.ru.

Бирюков Василий Иванович – доктор технических наук, профессор; Московский авиационный институт (национальный исследовательский университет). E-mail: aviatex@mail.ru.

Сизов Георгий Алексеевич – аспирант, Московский авиационный институт (национальный исследовательский университет). E-mail: georgisiz1994@gmail.com.

УДК 629.7.036.54

Doi: 10.31772/2712-8970-2021-22-2-316-327

Для цитирования: Проектирование системы охлаждения многоразового жидкостного ракетного двигателя на трёхкомпонентном топливе В. А. Беляков, Д. О. Василевский, А. А. Ермашкевич и др. // Сибирский аэрокосмический журнал. 2021. Т. 22, № 2. С. 316–327. Doi: 10.31772/2712-8970-2021-22-2-316-327.

For citation: Belyakov V. A., Vasilevsky D. O., Ermashkevich A. A., Kolomentsev A. I., Farizanov I. R. Design of the cooling system of a reusable liquid rocket engine with three-component fuel. *Siberian Aerospace Journal*. 2021, Vol. 22, No. 2, P. 316–327. Doi: 10.31772/2712-8970-2021-22-2-316-327.

Проектирование системы охлаждения многоразового жидкостного ракетного двигателя на трёхкомпонентном топливе

В. А. Беляков², Д. О. Василевский^{1, 2*}, А. А. Ермашкевич²,
А. И. Коломенцев², И. Р. Фаризанов³

¹Федеральное казенное предприятие «Научно-испытательный центр
ракетно-космической промышленности»

Российская Федерация, 141320, Московская область, г. Пересвет, ул. Бабушкина, 9

²Московский авиационный институт (национальный исследовательский университет)

Российская Федерация, 125993, г. Москва, А-80, ГСП-3, Волоколамское шоссе, 4

³АО «Уральский завод гражданской авиации»

Российская Федерация, 123308, г. Москва, просп. Маршала Жукова, 1, стр. 1

*E-mail: zudwa_dwesi_dwa@rambler.ru

В настоящее время в области двигателестроения весьма перспективной задачей является разработка трехкомпонентных двигательных установок (ДУ). Особый интерес представляют жидкостные ракетные двигатели (ЖРД), работающие на начальном участке выведения ракеты-носителя (РН) на паре топлива жидкий кислород + керосин и на высотных участках выведения с использованием криогенного топлива (жидкий кислород + жидкий водород).

ЖРД, использующие трехкомпонентное топливо, имеют высокий уровень давлений в камере сгорания (КС) (до 30 МПа) и температур (до 4000 К). В связи с этим возникают вопросы, связанные с надежным охлаждением таких двигателей, а также обеспечение минимальных гидравлических потерь жидкости в тракте охлаждения в целях дальнейшего использования хладагента в качестве рабочего тела для привода турбины бустерного турбонасосного агрегата (БТНА).

Объектом исследования является двухрежимный однокамерный трехкомпонентный ЖРД, выполненный по закрытой схеме с дожиганием генераторного газа. Окислитель – жидкий кислород, горючее – керосин марки РГ-1 и жидкий водород. Охлаждение камеры – комбинированное, состоит из регенеративного проточного и внутреннего. Тракт регенеративного охлаждения образован с помощью продольных фрезерованных ребер. В качестве охладителя двигателя используется сверхкритический водород. Внутреннее охлаждение включает в себя танталовое покрытие, нанесенное на огневую стенку камеры в районе критического сечения.

В данной статье исследуются проблемы организации системы охлаждения (СО) и реализация эффективного теплосъема с огневой стенки трехкомпонентного ЖРД. На основании существующих систем охлаждения ЖРД в работе предложены оптимальные схемные решения и мероприятия, позволяющие снять тепловую нагрузку в наиболее напряженных местах.

Разработана математическая модель для расчета СО трехкомпонентного ЖРД. Приведены результаты проектного расчета охлаждения по нескольким расчетным методикам.

Ключевые слова: ЖРД на трёхкомпонентном топливе, теплозащита корпуса двигателя, математическая модель ЖРД, теплообмен трехкомпонентных продуктов сгорания (ПС), система охлаждения.

Engeneering of a cooling system for a reusable liquid-propellant rocket engine opereiting on tripropellant fuel

V. A. Belyakov², D. O. Vasilevsky^{1,2*}, A. A. Ermashkevich²,
A. I. Kolomentsev², I. R. Farizanov³

¹Federal State Enterprise “Research and Testing Center of the Rocket and Space Industry”

9, Babushkina St., Peresvet, 141320, Russian Federation

²Moscow Aviation Institute (National research university)

4, Volokolamskoe Higway, A-80, GSP-3, Moscow, 125993, Russian Federation

³AO “Ural Civil Aviation Plant”

1, p. 1, Marshal Zhukov Av., Moscow, 123308, Russian Federation

*E-mail: zudwa_dwesti_dwa@rambler.ru

Currently, in the field of engine building, development of three-component propulsion systems (PS) is a very promising task. Liquid-propellant rocket engines (LPRE) operating at the initial stage of launching a launch vehicle (LV) on liquid oxygen + kerosene fuel and at high-altitude launch sites using cryogenic fuel (liquid oxygen + liquid hydrogen) are in particular interest.

LPRE that use three-component fuel have a high pressure level in a combustion chamber (CC) (up to 30 MPa) and temperatures (up to 4000 K). In this regard, arise questions related to reliable cooling of such engines, as well as ensuring minimal hydraulic fluid losses in a cooling passage in order to further use refrigerant as a working fluid for driving the turbine of a booster turbo pump unit (BTP).

The object of research is a two-mode single-chamber three-component liquid-propellant rocket engine, made in a closed circuit with generator gas afterburning. Oxidizing agent is liquid oxygen, fuel is RG-1 kerosene and liquid hydrogen. Cooling of the chamber is combined: it consists of regenerative and internal. Regenerative cooling passage is formed by longitudinal integral-machined fins. Hipercritical hydrogen is used as an engine coolant. Internal cooling includes a tantalum coating applied to a fire wall of the chamber in a critical section.

The article examines the problems of organizing cooling system (CS) and implementation of effective heat removal from a firing wall of a three-component rocket engine. Basing on existing liquid-propellant engine cooling systems, optimal circuit solutions and measures to remove thermal load in the most stressed places are proposed.

A mathematical model has been developed for calculating a CS of a three-component LPRE. The results of the design calculation of cooling using several calculation methods are presented.

Keywords: LPRE on three-component fuel, thermal protection of an engine body, mathematical model of LPRE, heat and mass transfer of three-component combustion products.

Introduction

During engeneering of LPRE, special attention is paid to the development of engine cooling system. Existing liquid-propellant rocket engines that use high-boiling-point fuel as a cooler of CC are limited by boiling point of coolant medium in the jacket passage. Intensification of heat transfer in cooling jacket entails large hydraulic losses of fluid in the passage, this is especially typical for LPRE.

To achieve the highest efficiency and effectiveness of LPRE, it is proposed to use an additional fuel component as propellant. Operation of such liquid-propellant engine is possible when using a pair of fuel liquid oxygen + hydrocarbon fuel in the first section of the launch vehicle, in the second section - liquid oxygen + liquid hydrogen. It should be noted that during the entire flight, the engine is cooled with super-critical hy-

drogen supplied to the cooling jacket by a separate pump of a turbo pump unit. This measure for organizing a cooling jacket of a three-component LPRE makes it possible to avoid burnout of the walls of CC during engine operation due to efficient heat removal of supercritical hydrogen, and also to reduce the excess pressure of a hydrocarbon pump in the first section of a launch vehicle.

However, at certain Km (ratio of fuel components in CC) and Pk (pressure in CC), the amount of liquid hydrogen supplied to the cooling jacket is not enough to ensure reliable engine cooling. Therefore, the authors of the work considered the use of a heat-protective coating of a fire wall of the chamber in the critical section made of tantalum.

Cooling system of rocket engine on three-component fuel

LPRE running on three-component fuel due to high pressure in the CC has a complex and intense cooling system.

Cooling system is as a set of inlet and outlet coolant manifolds, a cooling passage that provides reliable and sufficient cooling due to optimal geometric parameters of a cooling flow passage (ribs, thicknesses of inner and outer walls, etc.), a system of inlet and outlet openings, a system multi-circuit bypass.

Gas dynamic profile of the engine, shown in fig. 1, was divided into 1200 design sections. As the initial data for cooling system design, the parameters obtained as a result of energy coupling of the engine were taken, as follows: mass flow rate, temperature and pressure at the inlet to cooling passage.

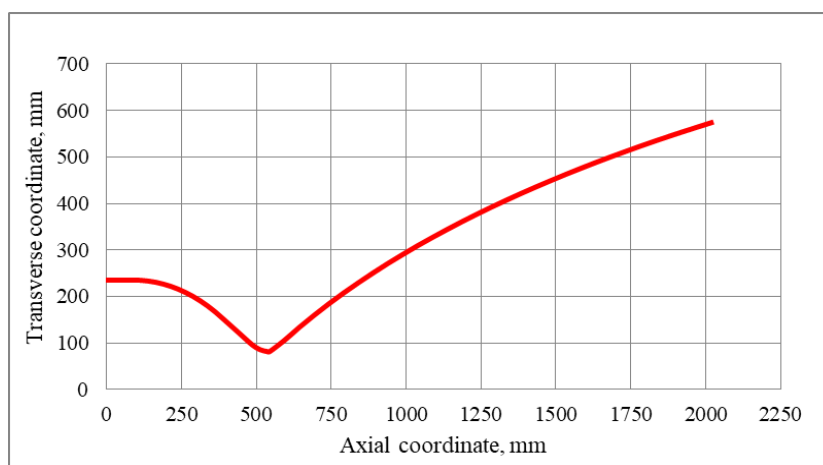


Рис. 1. Газодинамический профиль двигателя, работающего на трёхкомпонентном топливе

Fig. 1. The gas-dynamic profile of the engine operating on tripropellant fuel

The cooling scheme [1] of LPRE operating on tripropellant fuel is shown in Fig. 2.

Cooling system of a three-component LPRE consists of 3 sections with a different number of longitudinal integral-machined fins and 3 coolant manifolds (one input and two output); in each underwater manifold [2] a number of openings are provided for supplying and removing refrigerant from cooling system channels. The inner wall of the regenerative-flowing part of the engine has a thickness of 0.8 mm along the entire length of the engine and consists entirely of copper alloy BrKh-0.8, the outer wall is made of stainless steel 12X18H10T. The thickness of load-bearing wall is chosen according to the strength conditions and is 3 mm.

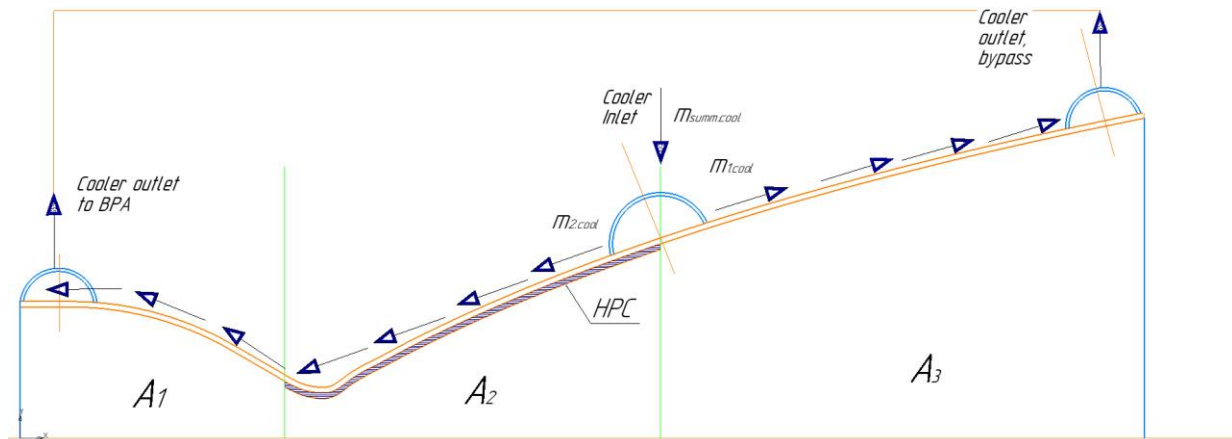


Рис. 2. Схема охлаждения трехкомпонентного ЖРД

Fig. 2. The cooling system of three-component LPRE

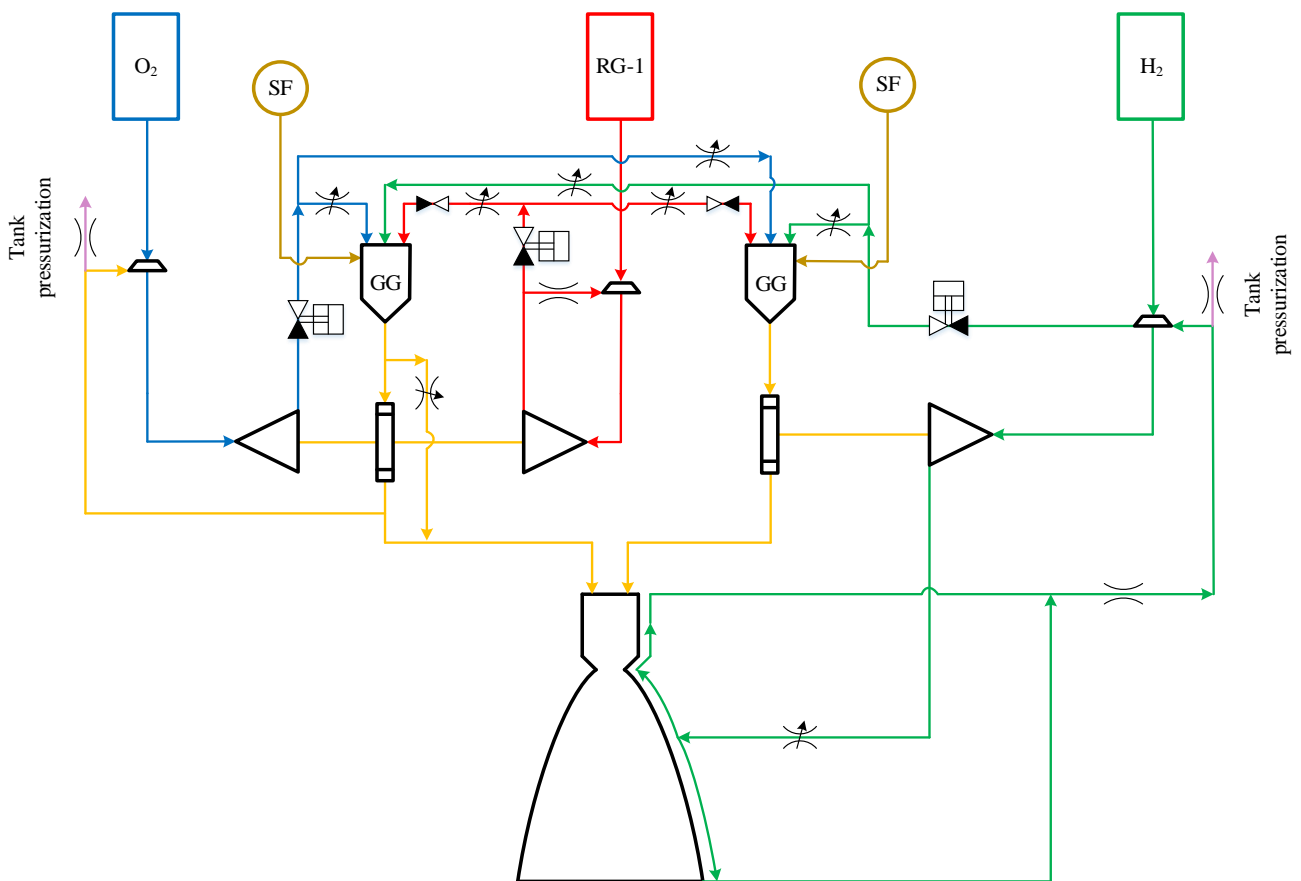


Рис. 3. Предлагаемая ПГС для ЖРД, работающего на трёхкомпонентном топливе

Fig. 3. The proposed PHS for rocket engine operating on tripropellant fuel

In the A_2 segment, a tantalum (Ta) heat-shielding coating [3] (TSP) 0.6 mm thick is applied to the inner fire wall. This coating has a high melting point (3290 K) and good adhesion (cohesion) to the surface of a fire wall.

Cooling system of LPRE works as follows.

Cumulative coolant-flow rate, equal to 9.6 kg/s, is supplied to the inlet manifold, located in the axial longitudinal coordinate of 1150 mm, through two rows of holes located in each channel, enters the cooling passage circuit. Pressure and temperature of the cooler at the inlet to the inlet manifold is 58.58 MPa and 43 K. Cooling passage consists of 2 separate circuits, independent of each other, into which different refrigerant flows enter.

The A_3 segment (corresponding to the second circuit of the two-circuit cooling system) for cooling the nozzle exit receives the coolant flow m_{1cool} equal to 1.6 kg/s, coolant-flow moves in direct flow to the outlet manifold and then through the bypass pipeline to the turbine drive of the booster turbopump assembly of fuel of liquid hydrogen, and then goes to the gas generator (GG) (see Fig. 3).

The A_1 and A_2 segments (corresponding to the first circuit of two-circuit cooling system) receive the cooler flow m_{2cool} equal to 8.0 kg/s; coolant-flow moves in reverse flow, cools the supersonic, subsonic and cylindrical parts of a nozzle, as well as choking section. Further, coolant-flow is directed to the outlet coolant manifold and to pipeline, where it is mixed with a flow rate from A_3 segment, and moves along the bypass pipeline to drive turbine drive of the booster turbopump assembly of fuel with subsequent supply to GG.

Calculation of cooling of a three-component LPRE according to V M Ievlev and D R Bartz methods

Cooling was calculated using the Rocket Propulsion Analysis (RPA) analytical program. The RPA program is a multi-platform analytical tool for conceptual and preliminary design of chemical rocket engines of various concepts (air-jet engines (AJE), LPRE, low-thrust liquid-propellant rocket engines (LTLPRE), low-thrust gas rocket engines (LTGRE), hydrojet engines (HE)), solid propellant rocket engines (SPRE), combined rocket engines (CRE) and others).

The RPA program has its own calculation module for determining the preliminary appearance of cooling passage structure at early stages of design and analyzing cooling and thermal state of LPRE. The mathematical model used in the RPA program includes standard heat and mass transfer models (compliance with the heat balance, direction of heat flow, internal or external heat supply, heat removal, thermal conductivity of single-layer and multilayer walls, internal "blocking" of heat flow by blowing into the wall or boundary layer (influence on near-wall flows by active injection of a gas or liquid with a low temperature), entrainment of material with heat blocking, etc.), thermal protection and cooling (internal film cooling (barrier, film), the use of various heat-protective coatings, external radiation, regenerative-flow or autonomous), heat engineering calculation formulas for the selected design and developed surface of cooling passage (longitudinal and helical (spiral) fins, corrugations, slotted channels, tubes, etc.), heat exchange criterial Nusselt ratios (Nu) for various refrigerants and fluid dynamic one-dimensional and two-dimensional models describing the movement of gases and liquids in the gas passage of the GDS and the annular ducting of cooling passage.

For thermal protection and cooling of walls from the influence of high-enthalpy media in LPRE with different types of Laval nozzles (profiled, conical, spherical, with a central body, pear-shaped, etc.), the most widespread use of regenerative-flow or automatic cooling systems with various heat transfer surfaces in order to intensify heat transfer and remove additional heat removal (for cryogenic heat carriers and refrigerants). Therefore, the process of cooling LPRE is a heat and mass exchange [4] of hot gas (fuel combustion products) and refrigerant by means of thermal conductivity, as well as forced and free convection, taking into account regenerative heat exchange.

An interesting and rare direction in calculation of cooling system and heat exchange in a steam channel of a short linear heat pipe, which is geometrically similar to a Laval nozzle, is practiced by Rudetransservice LLC, located in Veliky Novgorod [5].

In the software package (PC) RPA [6], cooling system is designed. The program allows evaluating the value of heat flux density in a stationary supply, the preliminary design of cooling system, engine cooling according to the method of V.M. Ievlev standardized in the domestic engine-structure and the foreign meth-

od of D R Bartz. Moreover, domestic technique of V M Ievlev is used as the main engineering calculation technique, which is in good agreement with experimental data [7; 8]. After the calculation, convergence of both methods was assessed.

The semiempirical method of V M Ievlev is based on the model of heat transfer of pulses and energy, as well as on an integral approximate solution of the boundary layer using empirical laws of friction and heat transfer, taking into account variability of thermal and physical properties of high-temperature media in the integral approximate solution of the boundary layer and in the flow core. A more detailed description of the technique is given in [9; 10].

The method of convective heat transfer in axially symmetric Laval nozzles by D R Bartz takes into account thickness of the integral approximate solution of the boundary layer, surface friction and heat flux density. The method is based on the integral solution of the equations of momentum and energy for a thin axial symmetric boundary layer with recalculation of the thermophysical and thermodynamic parameters of the "reference nozzle" to a calculated investigated nozzle, and the technique contains a coherent and accessible software algorithm for fast use in electronic computing machine (computer) - International Business Machines 7090 (IBM 7090). A more detailed description of D R Bartz's technique is given in [11; 12].

In Fig. 4–7 when calculating cooling by two methods, the following designations are accepted: $T_{c.g.c.}$ - temperature of a heat-shielding coating on gas side; $T_{w.g.}$ - wall temperature from the side of gas or coating; $T_{w.cool}$ - wall temperature from the side of cooling liquid; P_{cool} - cooler pressure; T_{cool} - cooler temperature.

Calculation of cooling of a three-component rocket engine according to V M Ievlev method

In accordance with the selected cooling system, the calculation of cooling was carried out by Ievlev's method. The thermal state (TS) of the camera body is shown in Fig. 4. Hydraulic losses and calculated heating of the cooler are shown in Fig. 5.

When calculating by Ievlev's method, a complete and high-quality picture of the TS of the camera body, the temperature state of the walls and TZP was obtained.

Calculation of cooling of a three-component rocket engine according to D R Bartz method

In accordance with the selected cooling system, the cooling calculation was carried out by Bartz method. The TS of the camera body is shown in Fig. 6. Hydraulic losses of a cooler [13; 14] and the calculated heating of a cooler is shown in Fig. 7.

When calculating by Bartz method, incomplete agreement with Ievlev method was obtained.

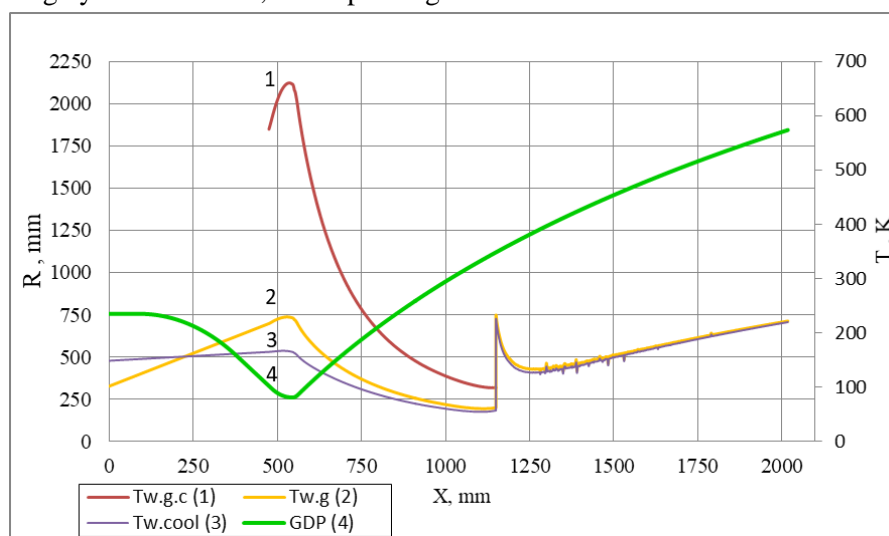


Рис. 4. ТС ЖРД, работающего на трёхкомпонентном топливе

Fig. 4. TS of an LPRE running on tripropellant fuel

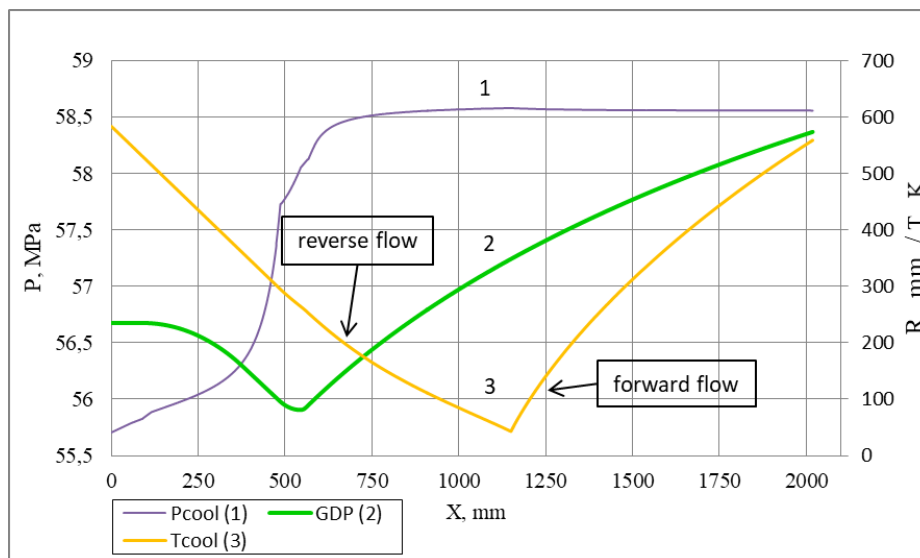


Рис. 5. Гидравлические потери и подогрев охладителя в разных контурах ТО ЖРД

Fig. 5. Hydraulic losses and heating of the cooler at different contours of CJ LPRE

Comparison of the residuals of cooling calculations according to the methods of D.R.Bartz and V.M. Ievliv

As a result of calculating the cooling of a three-component liquid-propellant engine according to the methods of Bartz and Ievliv, an analysis of obtained parameters was carried out using residual formula for the deviation of calculation methods. Fig. 8 and 9 show deviations of the calculation results obtained by Ievlev and Bartz method.

Deviations in the calculations according to Bartz method from Ievlev method according to the TS of the body are no more than 40% in modulus, the error in calculating the heating of the cooler is no more than 36% in modulus, while the error in calculating hydraulic losses is small (less than 1%). Oscillatory nature of wall temperatures on gas and liquid side in the range from 1250 up to 1815 mm is associated with convergence of the calculation results by Ievlev method with a large number of calculated points.

Therefore, we can conclude that estimation of hydraulic losses, with a small deviation in accuracy, is correct to carry out and evaluate by both methods. TS of the chamber body and heating of the coolant can be more accurately assessed by Ievlev method as an accessible engineering technique that correlates well with experimental data in the literature and the test results of firing units of liquid-propellant rocket engines, GG, nuclear rocket engines (NRE), ignition devices, burners, steam and gas generators, evaporators ejectors and gas-dynamic pipes (GDP) [15] and other high-temperature power plants with atomization, chemical transformation and combustion of fuel with a high temperature in a combustion chamber (more than 900 K) [16].

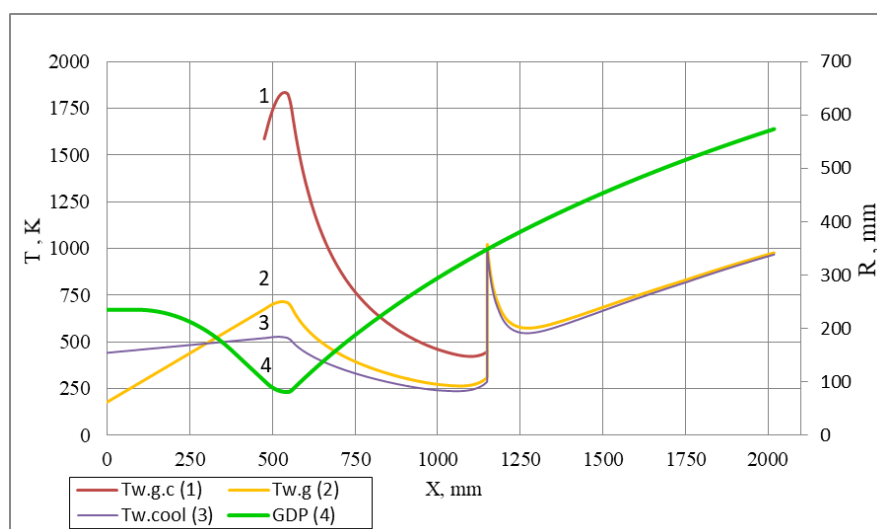


Рис. 6. ТС ЖРД, работающего на трёхкомпонентном топливе

Fig. 6. TS of an LPRE running on tripropellant fuel

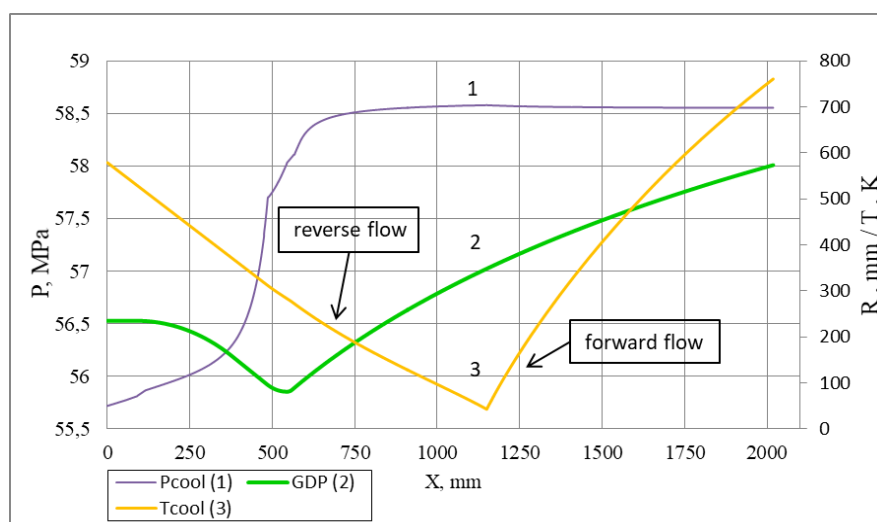


Рис. 7. Гидравлические потери и подогрев охладителя в разных контурах ТО ЖРД

Fig. 7. Hydraulic losses and heating of the cooler at different contours of CJ LPRE

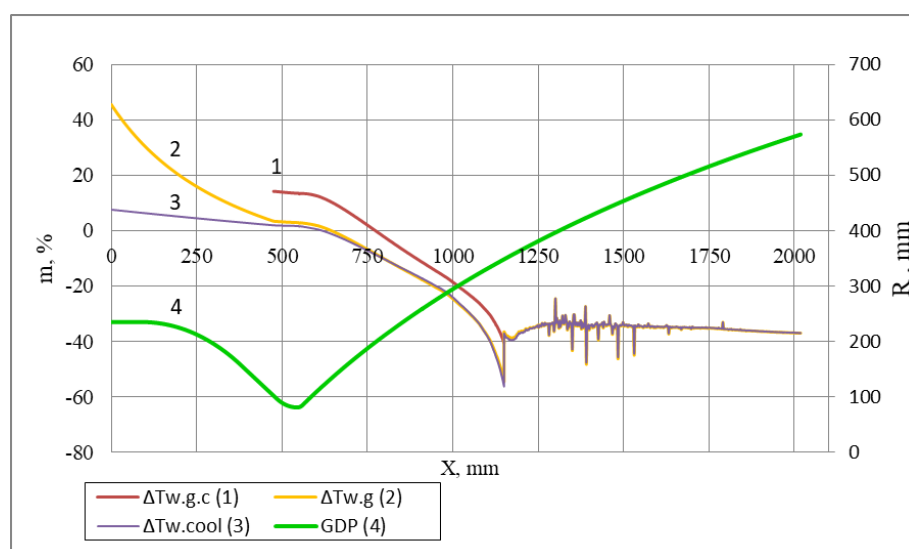


Рис. 8. Невязка теплового состояния ЖРД, работающего на трёхкомпонентном топливе

Fig.8. The discrepancy of the thermal state of LPRE operating on tripropellant fuel

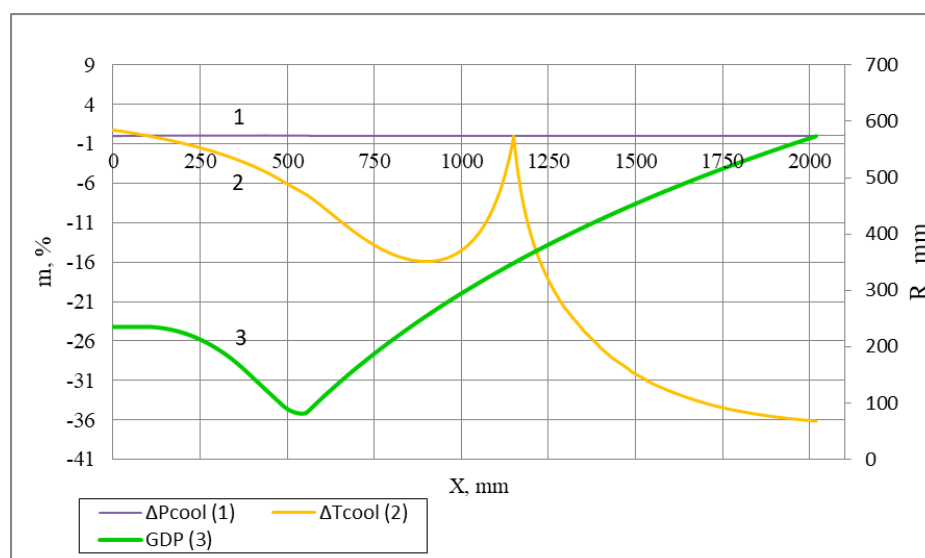


Рис. 9. Невязка гидравлических потерь и подогрева охладителя в разных контурах ТО ЖРД, работающего на трёхкомпонентном топливе

Fig. 9. Residual hydraulic losses and heating of refrigerant in different circuits of CJ LPRE operating on tripropellant fuel

Conclusion

The calculation of cooling system of a three-component rocket engine was carried out. Bartz and Ievlev methods for calculating cooling are considered. Based on the calculation results, the errors of two methods were obtained. According to the hull TS, the error was no more than 40% in modulus, the error in calculating heating of cooler was no more than 36% in modulus, the error in calculating hydraulic losses was less than 1%. Based on the convergence of the experimental and calculated data, the Ievlev method was chosen as the main technique. As a result of the calculation, the temperature and pressure of the refrigerant at the outlet from the primary circuit is 583.6 K and 55.73 MPa, from the second circuit - 558.85 K and 58.55 MPa. The maximum design temperature of the fire wall is 745.7 K, which is lower than the melting temperature of the

BRKh-08 material. The highest temperature of the tantalum coating is below the melting point of the coating material and is 2122.48 K.

As a result of calculations, it was revealed that, with the given parameters, when using precisely a two-circuit regenerative flow-through cooling system with thermal-protective coating applied to the fire wall in the A2 segment, full efficiency of the engine is obtained. Due to these measures, the TS of the chamber housing and coating is at a moderate and permissible level, therefore, the engine has reliable cooling.

References

1. Gakhun G. G., Alekseev I. G., Berezanskaya E. L. et al. *Atlas konstruksiy ZHRD* [ATLAS of LPRE design, Part 1]. Moscow, MAI Publ., 1969, 286 p.
2. Berezinsky R. A., Sokolov S. A., Gudkova S. R. et al. *Modelirovanie rabochih processov i konstruksiya elementov kamerj ZHRD* [Modeling of working processes and construction of elements of the LPRE chamber]. Voronezh, VGTU Publ., 2002, 169 p.
3. Dobrovolsky M. V. *Zhidkostnye raketnye dvigateli, Osnovy proektirovaniya* [Liquid rocket engines, Fundamentals of design]. Moscow, Bauman Moscow state technical University Publ., 2016, 461 p.
4. Shevchenko Yu. N., Kishkin A. A., Tanasiyenko F. V. et al. [Calculation of complex heat transfer in the liquid circuit of the spacecraft thermal control system based on real topology and thermal properties]. *Siberian journal of science and technology*. 2019, Vol. 20, No. 3, P. 375–382 (In Russ.). Doi: 10.31772 / 2587-6066-2019-20-3-375-382.
5. Seryakov A.V. [Investigation of flows in the steam channel of short linear heat pipes]. *Siberian journal of science and technology*. 2017, Vol. 18, No. 3, P. 592–603. (In Russ.)
6. Ponomarenko A. RPA: Tool for Rocket Propulsion Analysis. Available at: <http://propulsion-analysis.com> (accessed: 10.10.2020).
7. Ievlev V. M. *Turbulenthoye dvizheniye vysokotemperaturnykh sploshnykh sred* [Turbulent motion of high-temperature continuous media]. Moscow, Nauka Publ., 1975, 255 p.
8. Ponomarenko A. RPA: Tool for Rocket Propulsion Analysis, Thermal Analysis of Thrust Chambers. Available at: http://propulsion-analysis.com/downloads/2/docs/RPA_ThermalAnalysis.pdf (accessed: 10.10.2020).
9. Kudryavtsev V. M., Vasiliev A. P. et al. *Osnovy teorii i rascheta zhidkostnykh raketnykh dvigatelej* [Fundamentals of the theory and calculation of liquid rocket engines]. Moscow, Higher school Publ., 1975, 656 p.
10. Salakhutdinov G. M. *Razvitie metodov teplozashity v zhidkosntnykh raketykh dvigatelyah* [Development of methods of thermal protection in liquid rocket engines]. Moscow, Nauka Publ., 1984, 256 p.
11. Elliot D. G., Bartz, D. R., Silver S. Culcation of turbulent boundary-layer growth and heat transfer in axi-symmetric nozzles. *Tech. Rep. JPL*. 1963, No. 32-387, 45 p.
12. Dewey M. S. A comparison of experimental heat-transfer coefficients in a nozzle with analytical predictions from Bartz's methods for various combustion chamber pressures in a solid propellant rocket motor. A thesis submitted to the Graduate Faculty of North Carolina State University Raleigh in partial fulfillment of the requirements for the Degree DEPARTMENT OF Master of Science: Department of mechanical and aerospace engineering. Raleigh, 1970. 99 p.
13. Hobler T. *Teploperedacha i teploobmenniki* [Heat transfer and heat exchangers]. Leningrad, Goskhimizdat Publ., 1961, 821 p.
14. Shevchenko Yu. N., Kishkin A. A., Tanasiyenko F. V. et al. [Determining thermal resistances in the model of the liquid circuit of the spacecraft thermal control system]. *Siberian journal of science and technology*. 2019, Vol. 20, No. 3, P. 366–374. (In Russ.) Doi: 10.31772 / 2587-6066-2019-20-3-366-374.

15. Zimin A. Yu. *Razrabotka stenda ognevyh ispytaniy zhidkostnogo raketnogo dvigatelya na toplive zhidkij kislorod I zhidkiy vodorod tyagoy 100 kN . Diplom specialista*. [Development of a stand for fire tests of a liquid rocket engine powered by liquid oxygen and liquid hydrogen with 100kn thrust. Diploma of a specialist]. Moscow, MAI Publ., 2017, 106 p.

16. Lebedinsky E. V. et al. *Rabochie processy v zhidkostnom raketnom dvigatele i ih modelirovanie* [Working processes in a liquid rocket engine and their modeling]. Moscow, Mashinostroenie Publ., 2008, 512 p.

Библиографические ссылки

1. Атлас конструкций ЖРД. Ч. 1 / Г. Г. Гахун, И. Г. Алексеев, Е. Л. Березанская и др. М. : МАИ, 1969. 286 с.

2. Моделирование рабочих процессов и конструкция элементов камеры ЖРД / Р. А. Бережинский, С.А. Соколов, С. Р. Гудкова и др. Воронеж : ВГТУ, 2002. 169 с.

3. Добровольский М. В. Жидкостные ракетные двигатели, Основы проектирования. М. : МГТУ им. Н. Э. Баумана, 2016. 461 с.

4. Расчет комплексной теплопередачи в жидкостном контуре системы терморегулирования космического аппарата по реальной топологии и теплофизическим свойствам / Ю. Н. Шевченко, А. А. Кишкин, Ф. В. Танасиенко и др. // Сибирский журнал науки и технологий. 2019. Т. 20, № 3. С. 375–382. Doi: 10.31772/2587-6066-2019-20-3-375-382.

5. Серяков А. В. Исследование течений в паровом канале коротких линейных тепловых труб // Сибирский журнал науки и технологий. 2017. Т. 18, № 3. С. 592–603.

6. Ponomarenko A. RPA: Tool for Rocket Propulsion Analysis [Электронный ресурс]. URL: <http://propulsion-analysis.com> (дата обращения: 10.10.2020).

7. Иевлев В. М. Турбулентное движение высокотемпературных сплошных сред. М. : Наука, 1975. 255 с.

8. Ponomarenko A. RPA: Tool for Rocket Propulsion Analysis, Thermal Analysis of Thrust Chambers [Электронный ресурс]. URL: http://propulsion-analysis.com/downloads/2/docs/RPA_ThermalAnalysis.pdf (дата обращения: 10.10.2020).

9. Основы теории и расчёта жидкостных ракетных двигателей / В. М. Кудрявцев, А. П. Васильев и др. М. : Высш. шк., 1975. 656 с.

10. Салахутдинов Г. М. Развитие методов теплозащиты в жидкостных ракетных двигателях. М. : Наука, 1984. 256 с.

11. Elliot D. G., Bartz D. R., Silver S. Culculation of turbulent boundary-layer growth and heat transfer in axi-symmetric nozzles // Tech. Rep. JPL. 1963. No. 32-387. 45 p.

12. Dewey M. S. A comparison of experimental heat-transfer coefficients in a nozzle with analytical predictions from Bartz's methods for various combustion chamber pressures in a solid propellant rocket motor // A thesis submitted to the Graduate Faculty of North Carolina State University Raleigh in partial fulfillment of the requirements for the Degree DEPARTMENT OF Master of Science: Department of mechanical and aerospace engineering. Releigh, 1970. 99 p.

13. Хоблер Т. Теплопередача и теплообменники. Л. : Госхимиздат, 1961. 821 с.

14. Определяющие тепловые сопротивления в модели жидкостного контура системы терморегулирования космического аппарата / Ю. Н. Шевченко, А. А. Кишкин, Ф. В. Танасиенко и др. // Сибирский журнал науки и технологий. 2019. Т. 20, № 3. С. 366–374. Doi: 10.31772/2587-6066-2019-20-3-366-374.

15. Зимин А. Ю. Разработка стенда огневых испытаний жидкостного ракетного двигателя на топливе жидкий кислород и жидкий водород тягой 100 кН : диплом специалиста. М. : МАИ, 2017. 106 с.

16. Рабочие процессы в жидкостном ракетном двигателе и их моделирование / Е. В. Лебединский и др. М. : Машиностроение, 2008. 512 с.

© Беляков В. А., Василевский Д. О., Ермашкевич А. А.,
Коломенцев А. И., Фаризанов И. Р., 2021

Беляков Владислав Альбертович – аспирант, инженер кафедры 202 «Ракетные двигатели»; Московский авиационный институт (национальный исследовательский университет). E-mail: titflavii@rambler.ru.

Василевский Дмитрий Олегович – аспирант, инженер кафедры 202 «Ракетные двигатели», Московский авиационный институт (национальный исследовательский университет); инженер 1 категории, Федеральное казенное предприятие «Научно-испытательный центр ракетно-космической промышленности». E-mail: zudwa_dwesti_dwa@rambler.ru.

Ермашкевич Алексей Александрович – аспирант кафедры 202 «Ракетные двигатели»; Московский авиационный институт (национальный исследовательский университет). E-mail: alex.ermashkevich@yandex.ru.

Коломенцев Александр Иванович – кандидат технических наук, профессор, профессор кафедры 202 «Ракетные двигатели», Московский авиационный институт (Национальный исследовательский университет). E-mail: a.i.kolomentsev@yandex.ru.

Фаризанов Ильнур Равиатович – инженер-конструктор 1 категории; АО «Уральский завод гражданской авиации». E-mail: chelsea.physic@gmail.com.

Belyakov Vladislav Albertovich – post-graduate student, engineer of the Department 202 “Rocket Engines”, Moscow aviation Institute (National Research University). E-mail: titflavii@rambler.ru.

Vasilevsky Dmitry Olegovich – post-graduate student, engineer of the Department 202 “Rocket Engines”, Moscow aviation Institute (National Research University); engineer of the 1st category, Federal state enterprise “Research and testing center of the rocket and space industry”. E-mail: zudwa_dwesti_dwa@rambler.ru.

Ermashkevich Alexey Aleksadrovich – post-graduate student of the Department 202 “Rocket Engines”, Moscow aviation Institute (National Research University). E-mail: alex.ermashkevich@yandex.ru.

Kolomentsev Alexander Ivanovich – Cand. Sc., Professor, Professor of Department 202 “Rocket Engines”; Moscow aviation Institute (National Research University). E-mail: a.i.kolomentsev@yandex.ru.

Farizanov Ilnur Ravinatovich – design engineer 1 categories, JSC “Ural works of civil aviation”. E-mail: chelsea.physic@gmail.com.

УДК 629.7.062

Doi: 10.31772/2712-8970-2021-22-2-328-338

Для цитирования: Оптимизация расположения мест крепления приборной панели космического аппарата на основе модального анализа / В. В. Кольга, А. И. Лыкум, М. Е. Марчук, Г. Ю. Филиппсон // Сибирский аэрокосмический журнал. 2021. Т. 22, № 2. С. 328–338. Doi: 10.31772/2712-8970-2021-22-2-328-338.

For citation: Kolga V. V., Lykum A. I., Marchuk M. E., Filipson G. U. Optimization the position of the spacecraft instrument panel mounting points based on modal analysis. *Siberian Aerospace Journal*. 2021, Vol. 22, No. 2, P. 328–338. Doi: 10.31772/2712-8970-2021-22-2-328-338.

Оптимизация расположения мест крепления приборной панели космического аппарата на основе модального анализа

В. В. Кольга*, А. И. Лыкум, М. Е. Марчук, Г. Ю. Филиппсон

Сибирский государственный университет науки и технологий имени академика М. Ф. Решетнева
Российская Федерация, 660037, г. Красноярск, просп. им. газ. «Красноярский рабочий», 31

*E-mail: kolgavv@yandex.ru

В работе представлена оптимизация расположения интерфейсных точек приборной панели космического аппарата (КА) с помощью модального анализа, а также проведен квазистатический расчет исследуемой панели, подтверждающий эффективность предложенных изменений конструкции панели. Приборная панель представляет собой трехслойную сотовую конструкцию, состоящую из двух алюминиевых пластин и сотового заполнителя. Сотовые панели обладают рядом достоинств: небольшая масса конструкции, высокая жесткость, удельная прочность. С помощью конечно-элементного моделирования определен диапазон собственных частот и форм колебаний приборной панели, что позволило определить оптимальное расположение точек крепления панели к корпусу КА для увеличения нижней границы диапазона собственных частот и повышения её несущей способности.

Ключевые слова: приборная панель, оптимизация, форма, собственная частота, интерфейсные точки.

Optimization of the position of spacecraft instrument panel fixing points based on modal analysis

V. V. Kolga*, A. I. Lykum, M. E. Marchuk, G. U. Filipson

Reshetnev Siberian State University of Science and Technology
31, Krasnoyarskii rabochii prospekt, Krasnoyarsk, 660037, Russian Federation

*E-mail: kolgavv@yandex.ru

The paper presents optimization of the location of interface points of the spacecraft instrument panel using modal analysis, as well as a quasi-static calculation of the panel under study, confirming effectiveness of proposed changes in the panel design. The instrument panel is a three-layer honeycomb structure consisting of two aluminum plates and a honeycomb filler. Cellular panels have a number of advantages: a small weight of the structure, high rigidity, specific strength. Using finite element modeling, the range of natural frequencies and vibration patterns of the instrument panel was determined, which made it possible to determine optimal location of

the panel fixing points to the spacecraft body to increase the lower limit of natural frequency range and increase its carrying capacity.

Keywords: instrument panel, optimization, mode, natural frequencies, interface points.

Introduction

Engineering of modern spacecraft (SC) is characterized by a high density of placement of instruments on panels to reduce the size of the spacecraft.

Determination of fixing points of instruments on the panel and fixing points of the on-board panel to spacecraft power elements affects the range of natural frequencies of the spacecraft and its individual elements.

To fulfill the requirements for ensuring spacecraft carrying capacity, its parameters for comparing characteristics with an allowable range, determined by technical task requirements, are required.

In the process of engineering rocket and space technology, in general, and spacecraft, in particular, one of the stages in the analysis of bearing capacity of a structure is to simulate its natural frequencies and the frequencies of its individual elements, for example, instrument panel, in order to ensure the requirements for values of the lower limit of investigated frequency range [1–6].

Research objective

Let us consider an instrument panel, which is part of the Ka-band antenna as a power element, for installing responder equipment on it. The design is a three-layer honeycomb package, consisting of two load-bearing elements in a form of aluminum plates, between which cells of hexagonal aluminum foil are located (Fig. 1). The total panel thickness is 22 mm.

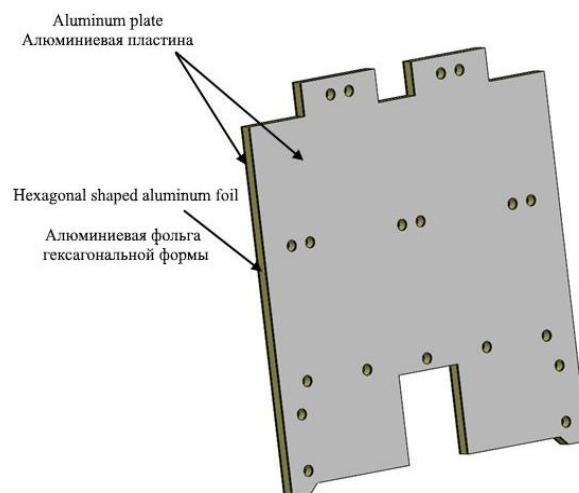


Рис. 1. Модель приборной панели космического аппарата

Fig. 1. Spacecraft instrument panel model

The panel experiences main loads during its transportation and in the spacecraft launching section. Based on the requirements of strength standards for similar devices, when engineering, it is necessary to ensure a minimum natural frequency of at least 150 Hz.

In many cases, the conclusion about bearing capacity of honeycomb structures is accepted as a result of processing the results of field tests, which are quite expensive and intensive. Therefore, assessment of design

parameters based on the results of numerical modeling simulating the conditions of full-scale tests is an urgent task to reduce the cost of engineering process [7].

To carry out a parametric analysis of spacecraft instrument panel, we identified the following tasks:

- to form a finite element model of instrument panel;
- to carry out its modal analysis and compare the range of natural frequencies with the permissible lower value;
- to assess bearing capacity of instrument panel from the action of quasi-static loads;
- to study the influence of location of the panel fixing points on changing natural frequency range of the panel and increasing its bearing capacity.

The finite element discretization of instrument panel surface is shown in Fig. 2.

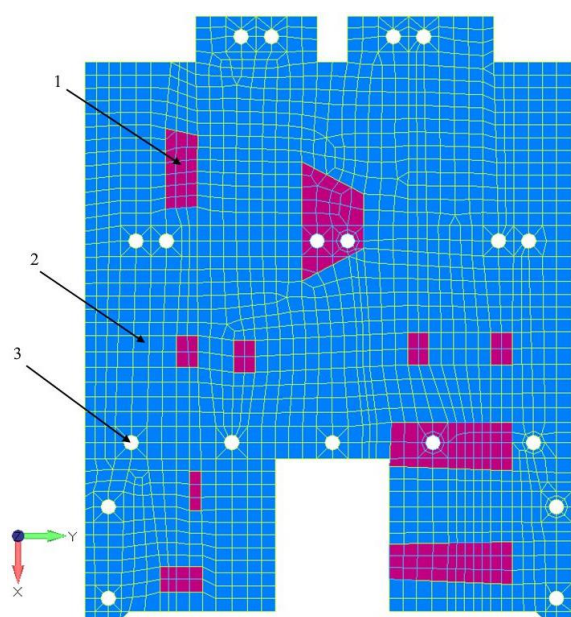


Рис. 2. Конечно-элементная дискретизация приборной панели КА:
1 – расположение приборов; 2 – точки крепления приборной панели –
интерфейсные точки; 3 – приборная панель

Fig. 2. Creating a finite element instrument panel model:
1 – device location; 2 – instrument panel fixing points-interface points;
3 – instrument panel

Table 1a and 1b show the physical and mechanical characteristics of the materials used in instrument panel.

Table 1a

Physical and mechanical properties of an aluminum plate

Material grade	Modulus of elasticity, GPa	Tensile strength, MPa	Yield stress, MPa
Aluminum plate B95	74	520	440

Table 1b

Physical and mechanical properties of honeycomb filler

Material	Tensile strength, MPa			Shear modulus of elasticity, MPa		Volume weight, kg / m ³
	When compressed	When shifting		Parallel to adhesive strips	Perpendicular to adhesive strips	
		Parallel to adhesive strips	Perpendicular to adhesive strips			
Aluminum honeycomb filler 5056-2.6-23p	1.177	0.981	0.588	147.1	78.5	40.0

As ultimate loads, we took the mass forces from weight of the panel with instruments at overload $n = 20g$, applied alternately in the direction of three coordinate axes, in accordance with regulations of requirements for such structures.

Parametric analysis of the panel structure allows solving the problem of determining stress-strain state in its main structural elements, efforts and deformations in characteristic systems, analysis of the natural shapes and frequencies of the panel as a whole and its individual parts in particular.

Design model of instrument panel

When compiling the calculation model, we made the following assumptions:

- all materials of structural elements are considered to be solid and homogeneous;
- metal alloys are assumed to be isotropic and linearly elastic materials;
- deformations at points of the structure are considered small (geometrically linear system) and rigidity of the structure does not change during loading;
- thickness and dimensions of the parts correspond to nominal value (a safety factor has been introduced for deviations from the nominal dimensions).

In the finite element model (FEM), the real object is replaced by a discrete model, which is a collection of systems and associated finite elements with specified properties.

FEM of the instrument panel, developed taking into account accepted assumptions, is shown in Fig. 2. The properties of FEM materials are specified in accordance with the Table 1a and 1b. Rigid termination at nineteen interface points was taken as boundary conditions (Fig. 2).

Finished FEM for calculating the panel was generated using FEMAP software package [8–10]. Fixing of devices at interface points was implemented using a rigid connection - the Rigid element, the mass of the devices was distributed among the panel elements. The instrument panel is composed of finite elements of laminate type (Fig. 2).

For analytical calculation of natural frequencies, let us consider classical equations of plates vibrations [11; 12]. If damping is neglected, differential equation of motion of free vibrations of a system with n degrees of freedom is described by the equation [11; 12]:

$$[M]\{\ddot{u}\} + [K]\{u\} = 0, \quad (1)$$

where $[K]$ are $[M]$ are stiffness and mass matrices; $\{\ddot{u}\}$ and $\{u\}$ are vectors of accelerations and displacements in FEM elements.

Equation (1) has a real periodic solution of the form

$$\{u\} = \{u_0\} \cos \omega t. \quad (2)$$

When fulfilling conditions

$$([K] - \omega^2 [M])\{u_0\} = 0. \quad (3)$$

The problem of calculating eigenmodes and frequencies of oscillations is reduced to the problem of eigenvalues ω_k and vectors $\{u_0\}_k$, that vanish the determinant

$$\det[K] - \omega^2 [M] = 0. \quad (4)$$

A similar problem for a multilayer plate made of composite materials and rectangular orthotropic plates has already been solved earlier [13; 14]. Deformation process is prescribed by equations of the nonlinear theory of plates, the resulting system of equations is solved using the Galerkin method. The resulting formula allows to determine displacements, deformations and stresses at given points in the structure. In addition, a formula was derived to determine the natural frequencies of a plate.

Let us use the analytical formulas derived in [13; 14], to calculate the natural frequencies of the plate.

To verify the results obtained using analytical formulas, let us solve the problem of modal analysis of an inhomogeneous isotropic plate using the finite element method. Let us determine natural frequencies of the structure using the MSC Nastran package [8; 10]. The values of natural frequencies found using the finite element method are compared with the values obtained analytically. The maximum relative error between these displacements does not exceed 5%, which confirms the correctness of our adopted finite element model of the instrument plate.

The results of the modal analysis of finite element model of the plate are given in Table 2. The first value of the natural vibration frequency was 76.13 Hz.

Table 2

Source panel modal analysis results

Tone number	Frequency, Hz	Effective mass, %					
		X	Y	Z	RX	RY	RZ
1	76.13	—	—	15.29	—	6.16	—
2	173.00	—	—	5.10	—	2.03	—
3	189.10	—	—	9.53	—	7.36	—
5	276.34	—	—	2.12	—	—	—
6	282.97	—	—	6.98	—	3.82	—
7	291.93	—	—	1.04	—	—	—
8	297.15	—	—	24.67	—	16.26	—
9	336.53	9.79	10.18	—	10.06	4.26	8.61
Total		9.79	10.18	68.71	10.82	43.40	8.61

Strength calculation from quasi-static loading

To check bearing capacity of the panel, we calculated stress-strain state of the structure from mass forces at overload $n = 20g$ applied in the direction of three coordinate axes. Below are the results of a quasi-static calculation, which reflect the maximum stresses in the instrument panel and its safety margin (Tables 3 and 4).

In this case, the safety margin for finishing material was determined by the formula (5):

$$\eta = \frac{[\sigma]}{\sigma_{\text{ЭKB}}}, \quad (5)$$

where $[\sigma]$ is allowable stress.

The safety margin for honeycomb filler was determined by the formula (6):

$$\eta = \left(\frac{\sqrt{\tau_l \cdot \tau_w}}{\frac{kms_1}{\sqrt{\tau_{xz} \cdot \tau_{yz}}}} - 1 \right) \cdot 100 \%, \quad (6)$$

where τ_{xz} , τ_{yz} are calculated shear stresses in a plane parallel to the adhesive strips and a plane perpendicular to the adhesive strips, respectively, Pa; τ_l , τ_w – shear strength in the plane parallel to adhesive strips and the plane perpendicular to adhesive stripes, respectively, Pa [15].

Table 3

Results of the quasi-static calculation of finishing material before the panel modification

Material	σ	η
Aluminum plate	216	1.65

Table 4

Results of quasi-static calculation of honeycomb filler before panel modification

Material	τ_{yz}	τ_{xz}	η
Aluminum honeycomb filler	0.29	0.18	2.63

Note. η – coefficient of safety; σ – normal voltage; τ – shear stresses.

Stress distribution over the instrument panel surface is shown in Fig. 3.

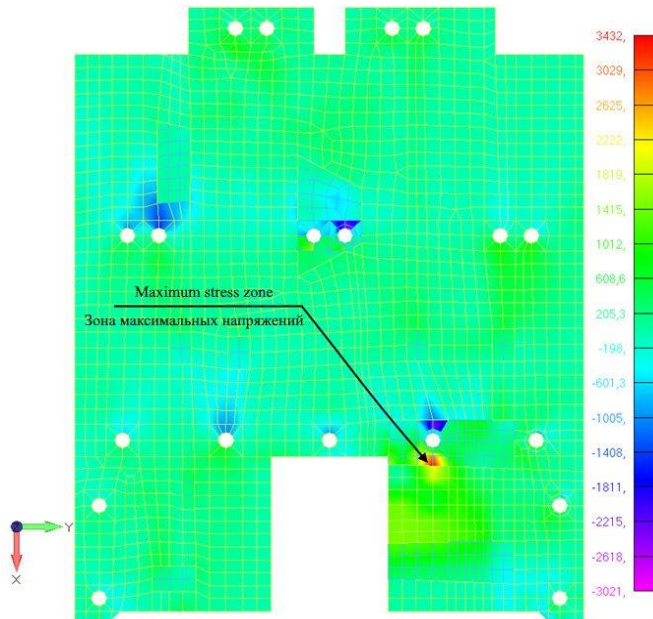


Рис. 3. Зона максимальных напряжений до модификации расположения точек крепления панели

Fig. 3. Maximum stress zone before modifying the location of the panel fixing points

The calculation results showed an admissible margin of safety, which confirms provision of load-bearing capacity of the panel during its operation.

Instrument panel design changes

Since the minimum value of natural vibration frequency of the panel with base position of the brackets does not meet necessary requirements for frequencies and, therefore, the limiting values of linear displacements, it was decided to change the initial configuration of the panel by adjusting the location of the interface

fixing points. Analysis of vibration modes of the panel (Fig. 4) by zones with maximum linear deviations allowed us to determine the places of correction of the interface points. By changing the location of the points for fixing the panel to the spacecraft body (Fig. 5), we managed to achieve an increase in the natural vibration frequency of the entire structure.

Table 5 shows the values of the parameters of the modal analysis of the panel with changed points of the location of the mounting brackets. The minimum natural vibration frequency of the modified instrument panel was 212.96 Hz.

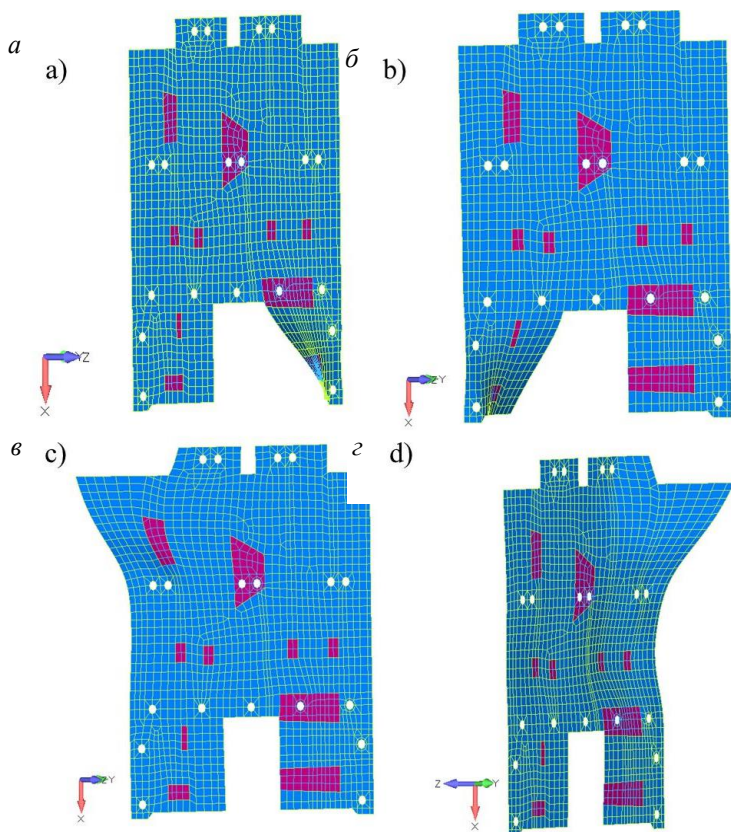


Рис. 4. Основные формы колебаний панели до модификации:
а – первая; б – вторая; в – третья; г – пятая

Fig. 4. Basic panel forms of oscillation before modification:
a – first; b – second; c – third; d – fifth

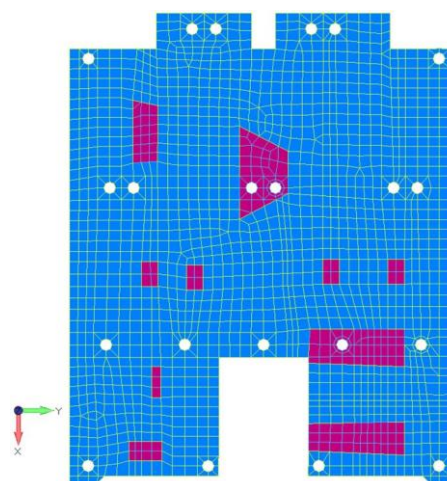


Рис. 5. Измененная конфигурация приборной панели

Fig. 5. Modified dashboard configuration

Fig. 6 shows the first mode of vibration of a modified panel with changed interface points for mounting the brackets.

Table 5

Modal analysis results of the modified panel

Tone number	Frequency, Hz	Effective mass, %					
		X	Y	Z	RX	RY	RZ
1	212.96	—	—	18.21	—	7.43	—
2	238.35	—	—	12.58	—	9.62	—
3	282.14	—	—	19.43	—	11.19	—
5	313.60	—	—	8.85	—	6.08	—

6	322.80	—	—	8.63	—	3.73	—
7	373.70	—	—	2.73	—	1.23	—
8	399.98	—	—	3.44	—	1.68	—
9	421.65	—	—	1.44	—	—	—
10	448.78	7.73	17.01	—	16.81	3.37	14.31
Total		7.73	17.01	75.72	17.66	45.22	14.31

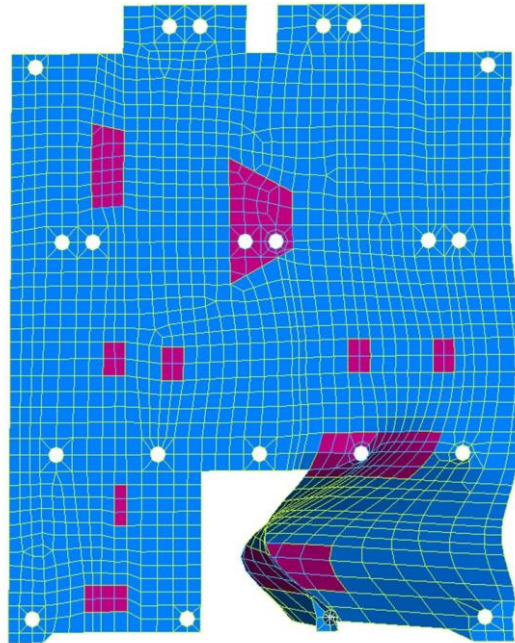


Рис. 6. Первая форма колебаний модифицированной панели

Fig. 6. The first form of oscillation of the modified panel

Calculation of the strength of a modified panel against quasi-static loading

Conducted quasi-static calculation of the instrument panel design (Tables 6, 7) confirms presence of required margin of safety for its safe operation, which is confirmed by stress distribution pattern (Fig. 7).

Table 6

Results of quasi-static calculation of finishing material after panel modification

Material	σ	η
Aluminum plate	65	5.44

Table 7

Results of quasi-static calculation of honeycomb filler after panel modification

Material	τ_{yz}	τ_{xz}	η
Aluminum plate	0.05	0.16	6.65

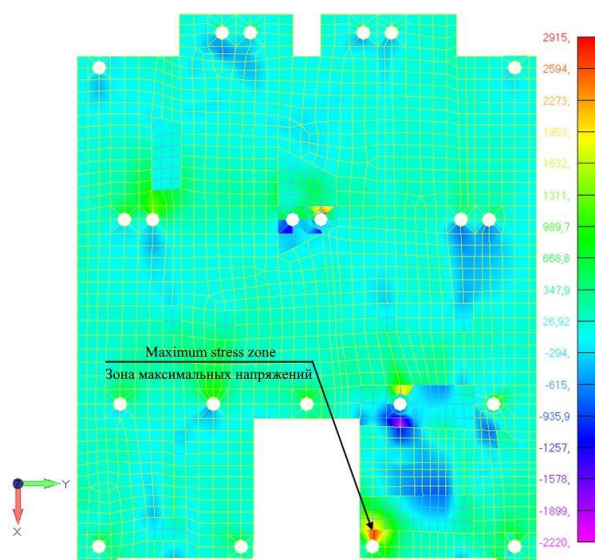


Рис. 7. Зона максимальных напряжений после модификации расположения креплений панели

Fig. 7. Maximum stress zone after modification of the panel mounting configuration

Conclusion

Our modal analysis made it possible to modify the spacecraft instrument panel and bring it in line with the requirements for natural vibration frequencies. With the help of rational redistribution of the interface points, it was possible to achieve an increase in the lower limit of natural vibration frequencies to 212, 96 Hz without increasing the mass of the structure. Quasi-static analysis confirmed the presence of a sufficient margin of safety for instrument panel and possibility of placing additional instruments on it by increasing the safety margin after changing locations of attach points of the panel to a spacecraft body. The proposed approach to modal analysis of structural elements can be used in engineering calculations for spacecraft design.

References

1. Daneev A. V., Rusanov M. V., Sizykh V. N. [Conceptual schemes of dynamics and computer modeling of spatial motion of large structures] *Sovremennyye tekhnologii. Sistemnyy analiz. Modelirovaniye*, 2016, No. 4, P. 17–25 (In Russ.).
2. Kolga V. V., Yarkov I. S., Yarkova E. A. Development of the heat panel of the small space apparatus for navigation support. *Siberian journal of science and technology*. 2020, Vol. 21, No. 3, 382–388. DOI: 10.31772/2587-6066-2020-21-3-382-388.
3. Testoyedov N. A., Kolga V. V., Semenova L. A. *Proyektirovaniye i konstruirovaniye bal-listicheskikh raket i raket nositeley* [Design and construction of ballistic missiles and launch vehicles]. Krasnoyarsk, 2014, 308 p.
4. Zamyatin D. A., Kolga V. V. [Construction of anisogrid power structure of the spacecraft adapter] *Materialy XXII Mezhdunar. nauch. konf. "Reshetnevskie chteniya"* [Materials XXII Intern. Scientific. Conf "Reshetnev reading"]. Krasnoyarsk, 2019, P. 26–28 (In Russ.).
5. Vasiliev V. V., Barynin V. A., Rasin A. F., Petrokovskii S. A., Khalimanovich V. I. Anisogrid composite lattice structures – development and space applications. *Composites and Nanostructures*. 2009, Vol. 3, P. 38–50.

6. Lopatin A. V., Morozov E. V., Shatov A. V. Axial deformability of the composite lattice cylindrical shell under compressive loading: Application to a load-carrying spacecraft tubular body. *Composite Structures*. 2016, Vol. 146, P. 201–206.
7. Gaidachuk V. E., Kirichenko V. V., Kondratyev A. V. [Conceptual approach to the formation of physical and mechanical characteristics of sandwich structures of composite structures of rocket and space technology] *Otkrytyye informatsionnyye i komp'yuternyye integrirovannyye tekhnologii*. 2014, P. 27–36 (In Russ.).
8. Rychkov S. P. *Modelirovaniye konstruksiy v srede Femap with NX Nastran* [Modeling of structures in the Femap with NX Nastran environment]. Moscow, DMK Press Publ., 2013, 784 p.
9. Shimkovich D. G. Femap & Nastran. *Inzhenernyy analiz metodom konechnykh elemen-tov* [Femap & Nastran. Engineering analysis by the finite element method]. Moscow, DMK Press Publ., 2012, 702 p.
10. MSC Nastran. User's guide: MSC. – Siemens Product Lifecycle Management Software Corporation; 2014. P. 886. Available at: https://docs.plm.automation.siemens.com/data_services/resources/nxnastran/10/help/en_US/tdocExt/pdf/User.pdf.
11. Timoshenko S. P. *Kolebaniya v inzhenernom dele* [Oscillations in engineering]. Moscow, NAUKA, 1957, 444 p. (In Russ.).
12. Biderman V. L. *Teoriya mekhanicheskikh kolebaniy* [Theory of mechanical vibrations]. Moscow, Vysshaya shkola Publ., 1980, 408 p.
13. Lopatin A. V., Morozov E. V. Fundamental frequency of an orthotropic rectangular plate with an internal centre point support. *Composite Structures*. 2011, Vol. 93, P. 2487–2495.
14. Lopatin A. V., Morozov E. V. Fundamental frequency of an orthotropic rectangular plate with an internal centre point support. *Composite Structures*. 2011, Vol. 93, P. 2487–2495.
15. Malmeyster A. K., Tamuzh V. P., Teters G. A. *Soprotivleniye polimernykh i kompozitnykh materialov* [Resistance of polymer and composite materials]. Riga, Zinatne Publ., 1980, 572 p.

Библиографические ссылки

1. Данеев А. В., Русанов М. В., Сизых В. Н. Концептуальные схемы динамики и компьютерного моделирования пространственного движения больших конструкций // *Современные технологии. Системный анализ. Моделирование*, 2016. № 4. С. 17–25.
2. Kolga V. V., Yarkov I. S., Yarkova E. A. Development of the heat panel of the small space apparatus for navigation support // *Сибирский журнал науки и технологий*. 2020, Vol. 21, No. 3, 382–388. Doi: 10.31772/2587-6066-2020-21-3-382-388.
3. Тестоедов Н. А., Кольга В. В., Семенова Л. А. Проектирование и конструирование баллистических ракет и ракет-носителей / СибГАУ. Красноярск, 2014. 308 с.
4. Замятин Д. А., Кольга В. В. Построение анизогридной силовой конструкции адаптера космического аппарата // *Решетневские чтения : материалы XXII Междунар. науч.-практ. конф.* / СибГУ им. М. Ф. Решетнева. Красноярск, 2019. Ч. 1. С. 26–28.
5. Anisogrid composite lattice structures – development and space applications / V. V. Vasiliev, V. A. Barynin, A. F. Rasin et al. // *Composites and Nanostructures*. 2009. Vol. 3. P. 38–50.
6. Lopatin A. V., Morozov E. V., Shatov A. V. Axial deformability of the composite lattice cylindrical shell under compressive loading // Application to a load-carrying spacecraft tubular body. *Composite Structures*. 2016. Vol. 146. P. 201–206.
7. Гайдачук В. Е., Кириченко В. В., Кондратьев А. В. Концептуальный подход к формированию физико-механических характеристик сэндвичевых структур композитных конструкций ракетно-космической техники // *Открытые информационные и компьютерные интегрированные технологии*. Харьков, 2014. С. 27–36.

8. Рычков С. П. Моделирование конструкций в среде Femap with NX Nastran. М. : ДМК Пресс, 2013. 784 с.
9. Шимкович Д. Г. Femap & Nastran. Инженерный анализ методом конечных элементов. М. : ДМК Пресс, 2012. 702 с.
10. MSC Nastran. User's guide: MSC. Siemens Product Lifecycle Management Software Corporation [Электронный ресурс]. URL: https://docs.plm.automation.siemens.com/data_services/resources/nxnastran/10/help/en_US/tdocExt/pdf/User.pdf свободный (дата обращения: 21.11.2020).
11. Тимошенко С. П. Колебания в инженерном деле. М. : Наука, 1957. 444 с.
12. Бидерман В. Л. Теория механических колебаний. М. : Высшая школа, 1980. 408 с.
13. Lopatin A. V., Morozov E. V. Fundamental frequency of the CCCF composite sandwich plate // Composite Structures. 2010. Vol. 92. P. 2747–2757.
14. Lopatin A. V., Morozov E. V. Fundamental frequency of an orthotropic rectangular plate with an internal centre point support // Composite Structures. 2011. Vol. 93. P. 2487–2495.
15. Малмейстер А. К., Тамуж В. П., Тетерс Г. А. Сопротивление полимерных и композитных материалов. Рига : Зинатне, 1980. 572 с.

© Кольга В. В., Лыкум А. И., Марчук М. Е., Филипсон Г. Ю., 2021

Кольга Вадим Валентинович – доктор педагогических наук, кандидат технических наук, профессор, профессор кафедры летательных аппаратов; Сибирский государственный университет науки и технологий имени академика М. Ф. Решетнева. E-mail: kolgavv@yandex.ru.

Лыкум Андрей Игоревич – студент пятого курса; Сибирский государственный университет науки и технологий имени академика М. Ф. Решетнева. E-mail: rob4i@mail.ru.

Марчук Максим Евгеньевич – студент пятого курса; Сибирский государственный университет науки и технологий имени академика М. Ф. Решетнева. E-mail: mmarchuk98@mail.ru.

Филипсон Глеб Юрьевич – студент пятого курса; Сибирский государственный университет науки и технологий имени академика М. Ф. Решетнева. E-mail: gortsev2014@gmail.com.

Kolga Vadim Valentinovich – Doctor of Pedagogics, Candidate of Technical Sciences, professor, Professor of Department of Aircraft; Reshetnev Siberian State University of Science and Technology. E-mail: kolgavv@yandex.ru.

Lykum Andrey Igorevich – fifth-year student; Reshetnev Siberian State University of Science and Technology. E-mail: rob4i@mail.ru.

Marchuk Maxim Evgenevich – fifth-year student; Reshetnev Siberian State University of Science and Technology. E-mail: mmarchuk98@mail.ru.

Filipson Gleb Yurevich – fifth-year student; Reshetnev Siberian State University of Science and Technology. E-mail: gortsev2014@gmail.com.

УДК 629.7.036.620

Doi: 10.31772/2712-8970-2021-22-2-339-354

Для цитирования: Особенности испытаний жидкостных ракетных двигателей малой тяги / В. П. Назаров, В. Ю. Пиунов, В. Г. Яцуненко, Д. А. Савчин // Сибирский аэрокосмический журнал. 2021. Т. 22, № 2. С. 339–354. Doi: 10.31772/2712-8970-2021-22-2-339-354.

For citation: Nazarov V. P., Piunov V. Yu., Yatsunenko V. G., Savchin D. A. Characteristics of low thrust liquid-propellant rocket engines testing process. *Siberian Aerospace Journal*. 2021, Vol. 22, No. 2, P. 339–354. Doi: 10.31772/2712-8970-2021-22-2-339-354.

Особенности испытаний жидкостных ракетных двигателей малой тяги*

В. П. Назаров^{1**}, В. Ю. Пиунов², В. Г. Яцуненко¹, Д. А. Савчин¹

¹Сибирский государственный университет науки и технологий имени академика М. Ф. Решетнева
Российская Федерация, 660037, г. Красноярск, просп. им. газ. «Красноярский рабочий», 31

²АО «Конструкторское бюро химического машиностроения имени А. М. Исаева»
Российская Федерация, Московская область, г. Королев, ул. Богомолова, 12

**E-mail: nazarov@sibsau.ru

Жидкостные ракетные двигатели малой тяги (ЖРДМТ) являются основными двигателями, применяемыми в системах управления космических летательных аппаратов (КЛА). Они могут работать как в непрерывном, так и в импульсном режимах, при этом работа в импульсном режиме является одной из наиболее характерных особенностей. Достоверное заключение о надежности созданных двигателей возможно только на основе испытаний их опытных образцов в реальных либо в значительной степени приближенных к реальным условиям.

При создании ЖРДМТ для КЛА различного назначения в процессе конструкторской (опытной) отработки большое внимание уделяется вопросам методологии стендовых испытаний, техническому оснащению стендов, имитирующих воздействие физических условий космического пространства, а также применению диагностических методов и аппаратуры для проведения различных физических исследований и измерений.

Эффективность наземной (стендовой) отработки обеспечивается имитацией условий натурных испытаний и учетом влияния всех эксплуатационных факторов, воздействующих на достоверность оценки показателей надежности при конструкторской отработке в наземных условиях. Особое место в вопросах достижения эффективности испытаний занимают требования по обеспечению точности и достоверности результатов испытаний. Значительный объем испытаний при отработке ЖРДМТ следует проводить в условиях требуемого вакуума на стендах, оборудованных барокамерами с вакуумными системами.

Для повышения эффективности имитации высотных условий предложено использовать барокамеру с трубчатым экраном, в который подается жидкий азот с необходимым расходом. Импульсные режимы работы ЖРДМТ инициируют в трубопроводах неустановившиеся (низкочастотные) процессы движения

* Работа выполнена в соответствии с соглашением о стратегическом партнерстве и сотрудничестве от 29.04.2019 г. № 03-260 между АО «Конструкторское бюро химического машиностроения имени А. М. Исаева» и Федеральным государственным бюджетным образовательным учреждением высшего образования «Сибирский государственный университет науки и технологий имени академика М. Ф. Решетнева».

The work was carried out in accordance with the agreement on strategic partnership and cooperation dated 29.04.2019 No. 03-260 between the Isaev Chemical engineering Design Bureau and the Reshetnev Siberian State University of Science and Technology.

компонентов топлива. Рассмотрены методы обеспечения динамического подобия характеристик систем питания двигателя компонентами топлива на стенде и в двигательной установке, в том числе соответствие гидравлических, инерционных и волновых характеристик питающих магистралей.

Ключевые слова: жидкостные ракетные двигатели малой тяги, стендовые испытания, имитация высотных условий.

Characteristics of low thrust liquid-propellant rocket engines testing process

V. P. Nazarov^{1*}, V. Yu. Piunov², V. G. Yatsunenko¹, D. A. Savchin¹

¹Reshetnev Siberian State University of Science and Technology
31, Krasnoyarskii rabochii prospekt, Krasnoyarsk, 660037, Russian Federation

²Isaev Chemical engineering Design Bureau
12, Bogomolova St., Koroljov, Moscow region, 141070, Russian Federation

*E-mail: nazarov@sibsau.ru

Low thrust liquid-propellant rocket engines (LTLPRE) are the main type of rocket engines for control systems of space aircrafts. The thrusters are able to work either in continuous or impulse regime, which is one of their main characteristics. The suggestion about engines` reliability should come from the results of tests which create real or greatly approximated to the real conditions.

The development process of thrusters takes into a great account the problems of bench testing methodic, technical equipment of test benches for creating the closest possible to space conditions and the use of diagnostic methods and instruments for various types of physical research and dimensions.

The ground test effectiveness depends on the level of real conditions imitation and the level of attention to all operational factors that influence the credibility of reliability parameter estimation during the development. One of the most important questions in terms of testing effectiveness is the question of testing result accuracy and credibility. The testing process of thrusters mainly goes under the requested conditions of vacuum, created in pressure chambers.

To increase the effectiveness of space conditions imitation the paper suggests using the pressure chamber, equipped with the tube shield with the circulating liquid nitrogen under required mass flow rate. The impulse working regime creates instability of propellant moving in pipelines. The paper considers the methods of providing dynamically similar characteristics of supply systems in propulsion systems as well as conformity of hydraulic, inert and wave characteristics of supply pipelines.

Keywords: liquid-propellant rocket engines of low thrust, bench tests, space condition imitation.

Introduction

Low thrust liquid-propellant rocket engines (LTLPRE) are currently the main executive device in the control system of a spacecraft. They serve for orientation, stabilization and correction of the aircraft in space, and are also used in propulsion systems for orientation, stabilization and start-up in the upper stages, carrying out spacecraft launch into specified orbits [1].

The purpose of liquid propellant engines and conditions of their operation impose a number of specific requirements, in particular, the following:

– multimodality due to continuous operation (duration up to $\tau_b > 103$ s) and in various pulse modes with a minimum turn-on time of 0.03 s or less and with various pauses from 0.03 s to several days;

- a large resource in terms of accumulated operation time – up to 50,000 s and more;
- a large resource in terms of the total number of inclusions – up to 106;
- a possibility of any combination of switching times and pauses (negotiated in most cases);

Terminologically, in GOST 22396-77 “low-thrust liquid-propellant rocket engines” are defined as executive devices of a spacecraft control system with thrust from 0.01 to 1,600 N. Liquid-propellant rocket engines of low-thrust can be united by at least one common element (power frame, panel, fuel supply system, thermal insulation, etc.) [2–4].

The development of low-thrust rocket engines for domestic spacecrafts is carried out by the Design Bureau of Chemical Engineering named after A. M. Isaev (DBHimmash), the Scientific Research Institute of Mechanical Engineering (SRIMash), the Turaev Engineering Design Bureau “Soyuz” (TEDB “Soyuz”) [5–7].

DBHimmash created 11 types of engines with thrust from 6 to 2250 N on two-component self-igniting fuel and 8 types on single-component fuel with thrust from 5 to 50 N.

These engines have found wide application in spacecraft for various purposes: ‘Soyuz-TM’, ‘Ekran’, ‘Prognoz’, ‘Spektr’, ‘Relikt’, ‘Coupon’, ‘Globus’, ‘Phobos’ and a number of others, as well as in the stages of reentry vehicles disengagement. They are designed for precise orientation, stabilization and correction of spacecraft orbit, for docking and undocking maneuvers with other vehicles. Motors are characterized by stability, efficiency, high-speed operation, reusable start-ups, start-ups duration from centisecond to hundreds and thousands of seconds.

Two-component low-thrust engines DST-25, DST-100, DST-100A, DST-200 and DMT-600, created at DBHimmash operate on the fuel components traditional for the enterprise – nitrogen tetroxide and asymmetric dimethylhydrazine. Reliability of operation and high performance are ensured by the use of a niobium alloy combustion chamber with a protective coating, radiation and internal film cooling.

The DMT-600 engine, which has an ablative cooling combustion chamber in combination with internal cooling, showed high energy and mass characteristics not only on traditional fuel, but also on monomethylhydrazine used in foreign practice [8].

Currently, the requirements for spacecraft, for their propulsion systems of control and for liquid propellant rocket engines are increasing, first of all, in terms of active shelf life up to 15–20 years, reliability and efficiency. The requirement to optimize the cost of development and manufacture comes to the fore, which can become a determining factor when choosing one or another engine [9; 10].

Despite the experience gained in the study of ongoing processes and the design of low thrust liquid-propellant rocket engines, a valid conclusion about the reliability of the created engines is only possible on the basis of their prototypes testing in real or substantially approximated to real conditions. Testing is a critical part of the program to create a highly efficient and reliable product.

Thus, live fire testing should be considered as a reasonably required stage of design and research work, which finishes with the creation of prototypes.

Basic requirements for testing LTLPRE

When creating liquid propellant rocket engines for spacecraft of various purposes, in the process of design (experimental) much attention is paid to bench tests approach, technical equipment of a bench simulating physical conditions effect of outer space, as well as the use of diagnostic methods and equipment for various physical research and measurements. In reliability assurance programs (RAP) of low-thrust engines, tests are the most important part, requiring significant financial, material and physical costs [2; 11].

As the number of tests of liquid-propellant rocket engines in full-scale operating conditions (flight tests) is very limited, and in most cases is generally excluded due to their high cost, the ultimate efficiency of their ground development should be achieved.

The efficiency of ground (bench) testing is ensured by simulating conditions of full-scale tests taking into account the influence of all operational factors affecting the accuracy of reliability indicators assessment during design testing in ground conditions. Requirements for ensuring the accuracy and reliability of test results occupy a special place in achieving test efficiency.

Certain requirements are imposed on benches for live fire tests of liquid propellant rocket engines, the main of which are as follows:

- achieving the degree of compliance with altitude conditions (rerefied environment);
- creation of the identity or dynamic similarity of characteristics of the liquid-propellant rocket engine power systems with fuel components, including correspondence of inert, wave and hydraulic characteristics of the supply lines;
- ensuring compliance with the laws of change of inlet pressures into the engine, pressures in the combustion chamber;
- ensuring the temperature values of the fuel components (both negative and positive) within the specified limits.

Most LTLPRE operate at very low ambient pressures, therefore, a significant amount of testing during their development should be carried out on benches equipped with vacuum systems. When determining the thrust and specific impulse characteristics in the vacuum chamber (with the engine installed in it for testing), the specified pressure value is provided for the uninterrupted flow of gas from the nozzle.

The dynamic processes that occur in the fuel lines for supplying fuel components depend on many factors determined by the properties of fuel components, pneumatic hydraulic circuit and the cyclogram of the LTLPRE. Therefore, to accurately determine engine characteristics during the tests it is necessary to ensure that the dynamic processes occurring in the bench lines are consistent with the processes occurring in the fuel supply lines in propulsion systems (PS) with LTLPRE.

There is no simple solution to this problem via identity design of the system supplying fuel components to the LTLPRE at the bench and in PS for a number of reasons:

- the need to ensure a high degree of safety during bench tests, which requires sufficient removal of fuel supply tanks from the vacuum chamber;
- the possibility of implementing various test programs at the bench, which is associated with the installation of additional fittings (valves, throttle devices and measuring instruments) in the fuel lines;
- design features of the bench.

It should be noted that at present, to meet the stated requirements, there are practically no standard measuring instruments that allow measuring instantaneous values of thrust and consumption of fuel components with the required accuracy. Therefore, when testing LTLPRE it is necessary to develop and use special measuring instruments and measurement techniques [2; 12].

Thus, the bench for LTLPRE live fire tests must have a system that ensures altitude conditions during the engine operation, a system for supplying fuel components to the engine with parameters that ensure the required test conditions, and a device for measuring thrust in pulsed and continuous modes.

When testing a liquid-propellant rocket engine, pulsed modes of its operation lead to excitation of oscillations in the test bench systems, which generally contribute to obtaining unreliable estimates of engine characteristics based on the test results. Wave phenomena in hydraulic lines lead to a difference between the required and actual nature and pressures values of the fuel components at the inlet of the components to the engine. Oscillations of the traction measuring device elements distort the estimates of the current thrust values and the nature of its change over time.

Elimination of oscillatory processes influence in bench systems on the results of live fire tests of LTLPRE in pulsed modes is an important condition for organizing these tests.

The parameters of high-altitude operating conditions of liquid propellant rocket engines are usually in the

pressure range 10^{-2} - 10^{-5} Pa and depend on the spacecraft orbit in which they are installed. This has a significant impact on the processes taking place in the combustion chamber. For example, it has been experimentally proven that for N2O4 + UDMH fuel with a certain mixture formation system, the ignition delay value when the ambient pressure drops from 0.1 MPa to values close to zero increases from 0.001 to 0.01 s. LTLPRE have design pressures in the outlet section of the nozzle p_a corresponding to high-altitude operating conditions. In the operation modes of the nozzle with overexpansion, when the ambient pressure p_h exceeds the design pressure at the outlet of the nozzle p_a and the degree of off-design reaches a certain limiting value, the supersonic flow is detached from the walls of the nozzle of the engine chamber, and oblique shock waves are formed in the nozzle. In this case, it is not possible to evaluate the actual (reduced to operating conditions) parameters of the tested engine [13].

The nature of the dynamic processes in the lines for supplying fuel components has a significant effect on the engine parameters, which is especially important for LTLPRE, since operation in pulsed modes that cause dynamic processes is one of the features of such engines. Pulse modes are accompanied by a change in the flow rates and pressures of the fuel components over time. Sharp changes in flow rate causes pressure waves, the magnitude of which largely depends on the geometry and elastic properties of the bench hydraulic systems pipelines. The dynamic processes occurring in the fuel lines also depend on other factors determined by the properties of the fuel components, the pneumatic hydraulic circuit and the cyclogram of the liquid-propellant rocket engine. When the frequency of pulsation of the fuel component coincides with the frequency of free oscillations of the component in the fuel pipelines, resonance is inevitable, which leads to a significant increase in the amplitude of pressure fluctuations, causing intense pressure pulsations in the combustion chamber of the LTLPRE. Therefore, to accurately determine the engine characteristics during the tests, it is necessary to ensure that the dynamic processes occurring in the bench lines are consistent with the processes that occur in the supply fuel lines in the propulsion system with LTLPRE [14; 15].

The evacuation system of the bench must create such a pressure in the pressure chamber so that during the entire time of LTLPRE operation uninterrupted outflow of gas from its nozzle is ensured, while in the study of the LTLPRE start-up characteristics - the pressure must correspond to altitude conditions (Fig. 1). As an alternative to the above requirements, it is possible to create test benches without maintaining the required pressure level in the pressure chamber. However, this approach significantly reduces the number and duration of LTLPRE start-ups, and determining the engine compliance with the given parameters is carried out indirectly, based on the pressures inside and outside the nozzle [16; 17].

In the interval $(0, t_1)$, the pressure in the pressure chamber is in a state that is created by working vacuum pumps. At time t_1 the engine is started.

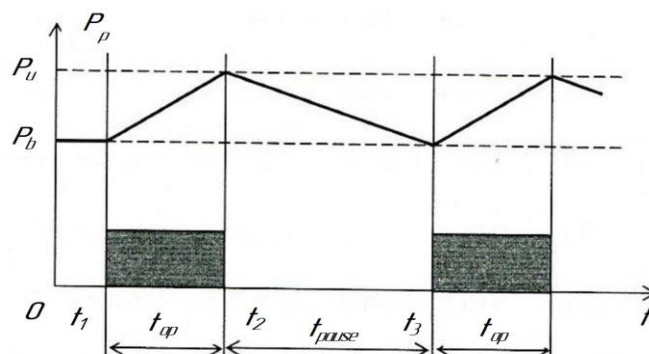


Рис. 1. Принципиальная схема изменения давления в барокамере:
 $t_{\text{раб}}$ – время работы двигателя; $t_{\text{паузы}}$ – время паузы между включениями;
 $P_{\text{в}}, P_{\text{н}}$ – верхнее и нижнее допустимые значения
 давления в барокамере соответственно

Fig. 1. The principal scheme of pressure changing inside a pressure chamber:
 T_w – engine working period; t_{pause} – time between working cycles;
 P_u, P_l – upper and lower limiting pressure values respectfully

In the interval (t_1, t_2) with the engine running, combustion products enter the pressure chamber with mass flow rate $\dot{m}_\Sigma(t)$. The mass of combustion products entering the pressure chamber during engine operation is

$$M_\Sigma = \int_{t_2}^{t_1} \dot{m}_\Sigma(t) dt. \quad (1)$$

Also, in the interval (t_1, t_2) , the vacuum pumps of the test bench are switched on at full capacity, which continue to operate in this mode and in the interval (t_2, t_3) . The mass of the gas mixture removed from the pressure chamber by the vacuum system in periods from t_1 , before t_3 , is considered by the expression:

$$M_{\text{выб}} = \rho_{\text{гв}} \int_{t_1}^{t_3} Q(t) dt, \quad (2)$$

where $\rho_{\text{гв}}$ – density of the gas mixture under normal conditions; $Q(t)$ – volumetric capacity of the vacuum system, reduced to normal conditions..

Thus, the interval (t_1, t_2) is characterized by the fact that during this period a part of the gas mixture in amount of $M_{\text{выб}}^{1-2}$ is carried away from the pressure chamber by the vacuum system, and the remaining part of the gas mixture is determined by the formula

$$M_{\text{бap}}^{1-2} = M_\Sigma - M_{\text{выб}}^{1-2} = \int_{t_1}^{t_2} [m_\Sigma(t) - \rho_{\text{гв}} Q(t)] dt. \quad (3)$$

The value of the mass must satisfy the condition of not exceeding the upper permissible limit P_u when filling the internal volume $V_{\text{бар}}$ of the pressure chamber.

Taking, with some assumptions, the gas mixture in the form of a mixture of ideal gases, we write down the expression for calculating the optimal value of the pressure chamber volume:

$$V_{\text{бap}} = \frac{M_{\text{бap}}^{1-2} R_{\text{гв}} T_{\text{бap}}}{P_{\text{г}}} = \frac{R_{\text{гв}} T_{\text{бap}}}{P_{\text{г}}} \int_{t_1}^{t_2} [m_\Sigma(t) - \rho_{\text{гв}} Q(t)] dt, \quad (4)$$

where $R_{\text{гв}}$ is the gas constant; $T_{\text{бap}}$ is the temperature of the gas mixture.

In the interval (t_2, t_3) , the gas mixture $M_{\text{выб}}^{1-2}$ remaining at time t_2 is evacuated from the pressure chamber by vacuum pumps. By the time t_3 , a pressure value equal to the lower permissible limit P_l should be reached. The average value of the vacuum pumps capacity for the interval (t_2, t_3) can be calculated as

$$Q_\Sigma^* \geq \frac{M_{\text{бap}}^{1-2}}{\rho_{\text{гв}} (t_3 - t_2)}. \quad (5)$$

A significant drawback of formula (4) is the accepted assumption that the functional dependences $m_\Sigma(t)$ and $Q(t)$ are known, while in practice this is not always the case, since these dependences can only be obtained by carrying out a series of tests of the corresponding LTLPRE [18].

With a sufficient degree of reliability, it is possible to estimate the optimal volume of the pressure chamber from the known statistical values of the parameters that affect the volume. These parameters are: the average values of the total consumption of fuel components m_Σ^* and the productivity of the vacuum system $Q_{\text{гв}}^*$ in the range of permissible pressures in the pressure chamber from P_u to P_l .

Taking the test time of the engine under k start-ups according to the cyclogram (Fig. 1), $k\tau_{\text{BK}} = k(t_{\text{раб}} + t_{\text{паузы}})$, the average values of the masses for k start-ups will be as follows:

$$M_{\Sigma}^* = m_{\Sigma}^* k t_{\text{раб}}; M_{\text{выбp}}^* = \rho_{\text{Hy}} Q_{\text{cp}}^* k t_{\text{раб}}; M_{\text{бap}}^* = \rho_{\text{Hy}} Q_{\text{cp}}^* k t_{\text{паузы}}.$$

For the values of masses of combustion products entering the pressure chamber when the engine is started and removed from the pressure chamber during the period t_{work} , we obtain:

$$M_{\text{бap}}^* = M_{\Sigma}^* - M_{\text{выбp}}^* = k t_{\text{раб}} (m_{\Sigma}^* - \rho_{\text{Hy}} Q_{\text{cp}}^*). \quad (6)$$

Then the final expression for estimating the internal volume of the pressure chamber of the test bench according to statistical data is

$$V_{\text{бap}}^* \geq \frac{M_{\text{бap}}^* R_{\text{nc}} T_{\text{бap}}}{P_{\text{B}}} = \frac{R_{\text{nc}} T_{\text{бap}} k t_{\text{раб}}}{P_{\text{B}}} (m_{\Sigma}^* - \rho_{\text{Hy}} Q_{\text{cp}}^*). \quad (7)$$

Thus, the obtained dependence, when organizing the process of fire tests of LTLPRE allows:

- to evaluate the required internal volume of the pressure chamber $V_{\text{бap}}^*$ for the values of P_{B} , τ_{BK} , k , m_{Σ}^* specified by the test program, and the accepted productivity of the vacuum system of the bench Q_{cp}^* ;
- to determine the permissible number of engine starts k under known values of other quantities included in the formula (7), with the provision of the requirement $P_{\text{бap}} \leq P_{\text{B}}$;
- to evaluate the required performance of the bench vacuum system Q_{cp}^* at the accepted value $V_{\text{бap}}^*$, ensuring the execution of the test program, which sets the values of P_{B} , τ_{BK} , k , m_{Σ}^* ;
- to evaluate the possibility of testing a specific LTLPRE with the provision of the condition $P_{\text{бap}} \leq P_{\text{B}}$ at the given program P_{B} , τ_{BK} , k , m_{Σ}^* on a test bench with indicators $V_{\text{бap}}^*$ и Q_{cp}^* .

Based on the analysis of expression (7), it follows that for small numerical values of P_{B} , the quantity $V_{\text{бap}}^*$ can take on such relatively large values that it will require a significant decrease in the number of k inclusions while maintaining the pressure in the pressure chamber within the specified limits.

To improve the efficiency of simulating altitude conditions, it is proposed to use a pressure chamber with a tube shield, into which liquid nitrogen is supplied at the required flow rate (Fig. 2).

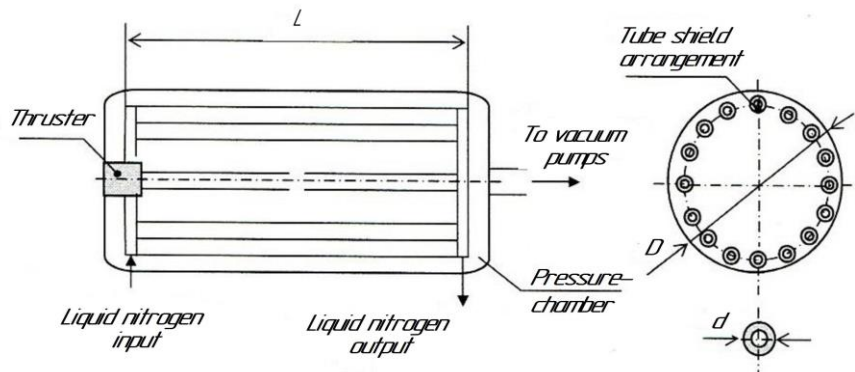


Рис. 2. Схема расположения трубчатого экрана в барокамере

Fig. 2. The scheme of tube shield arrangement inside a pressure chamber

The shield cooled by liquid nitrogen ensures the deposition on it of the combustion products of the fuel components formed during the operation of the tested LTLPRE, which significantly increases the time for

maintaining a given pressure (vacuum) in the pressure chamber at the nozzle output of the combustion chamber during engine operation. In this case, the calculated (without separation of the flow from the nozzle wall) mode is maintained not only by the volume of the pressure chamber, but also by the deposition of the combustion products of the fuel components on the cooled shields. With the length of the tube shield L , the outer diameter d and n of the pipelines that make up the shield, it is possible to obtain the relationship between the engine operation time, the total consumption of fuel components and the geometric dimensions of the tube shield:

$$t_{\text{раб}} = \pi \rho_{\text{ТБП}} \delta n L \frac{d}{k m_{\Sigma}^*}, \quad (8)$$

where δ , $\rho_{\text{ТБП}}$ are the layer thickness and density of combustion products deposited on the shield, respectively.

According to the experience gained while conducting live fire tests of LTLPRE under vacuum conditions at the test facility of one of the rocket and space industry enterprises, the thickness of combustion products deposition on the tube shield with the practical preservation of the deposition efficiency is $\delta = 0,8 \dots 1,0$ mm. The combustion products deposited on the tube shields have a structure similar to the snow cover, with the density $(0,4 \dots 0,6) \cdot 103 \text{ кг/м}^3$ [14; 18].

Taking into account statistical values, the approximate formula for calculating the maximum possible live fire operating time of the engine between two successive shield defrosting processes has the form

$$t_{\Sigma} = K_1 n L \frac{d}{m_{\Sigma}^*}, \quad (9)$$

where $K_1 = 1,0 \dots 1,9$ – empirical factor.

Taking into account $nd \approx 0,8 \pi D$ according to fig. 2 we obtain

$$t_{\Sigma} = K_2 \frac{V_{\text{оап}}}{m_{\Sigma}^* \cdot D}, \quad (10)$$

where $K_2 = 3,2 \dots 6,1$ – coefficient; D – inner diameter of the pressure chamber.

Dynamic equation of fuel components supply lines

Pulse modes of LTLPRE operation initiate unsteady (low-frequency) processes of movement of fuel components in pipelines. Optimization of LTLPRE live fire tests requires solving the problem of dynamic similarity of the engine supply systems characteristics with fuel components on the bench and in the propulsion system, including the correspondence of the hydraulic, inert and wave characteristics of the supply lines [14; 15; 18].

The conditions for hydrodynamic processes similarity arising during unsteady motion of an incompressible fluid can be described using the well-known differential equations of unsteady motion and fluid continuity (Navier – Stokes equations) [19].

To study the unsteady motion of a viscous incompressible fluid in the bench pipelines, we use the following scale or basic values: T – time characteristic of the process; L – linear dimension; $C_{\text{уп}}^*$ are the velocity and pressure known at a selected point of the liquid medium at a given time, respectively.

Analysis of the known Navier – Stokes equations, reduced to dimensionless form, shows that for the similarity of two or more hydrodynamic processes, the same coefficients Sh , Eu , Fr , Re must be the same (idem). Thus, the hydrodynamic similarity of the fuel components lines in the propulsion system and at the bench will be achieved by matching the coefficients:

$$\text{Sh} = \frac{L}{CT} = \text{idem}, \quad \text{Eu} = \frac{p^*}{\rho C^2} = \text{idem}, \quad \text{Fr} = \frac{C^2}{gL} = \text{idem}, \quad \text{Re} = \frac{CL}{\nu} = \text{idem},$$

also the congruence of Mach numbers $M = C / a$, dimensionless wave resistance $\alpha = \rho Ca / p^*$ and relative friction losses $\Delta p / p^*$ (where ρ, ν are the density and kinematic viscosity of the fluid, respectively; a is the reduced sound speed in system "pipeline-liquid") [20].

Inertia is one of the elements with which hydraulic systems models are formed. Assuming for the analysis of the inertial characteristics of the pipeline that its section (Fig. 3) is filled with an inviscid incompressible fluid, we can write the dynamic equation of the pipeline supplying the fuel component to the LTLPRE as follows:

$$j \frac{d\dot{m}}{dt} + \zeta \frac{\rho c^2}{2} = p_{\text{BX}} - p_{\text{ВЫХ}} + p_m, \quad (11)$$

where j is the coefficient of inertial losses; l – length; F – the flow area of the pipeline section; \dot{m} – second liquid consumption; $p_{\text{BX}}, p_{\text{ВЫХ}}$ – pressure at the inlet and outlet of the pipeline section, respectively; p_m is the pressure of the mass forces of the liquid column on F area; ζ – coefficient of hydraulic resistance [20; 21].

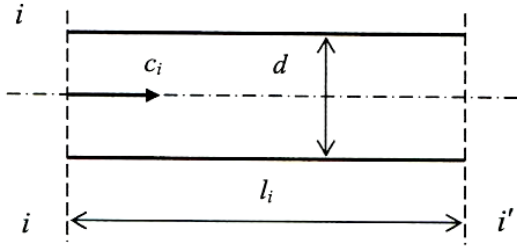


Рис. 3. Гидравлическая схема участка трубопровода

Fig. 3. The hydraulic scheme of pipeline area

To determine the requirements for bench pipelines for fuel components supply in LTLPRE with pulsed operation with frequency f , let us consider the question of the natural frequency of fluid oscillations in the pipeline f_0 . Free vibrations, and first of all the frequencies of free vibrations (natural frequencies), are the determining factors when considering the dynamic characteristics of bench lines. With a frequency ratio $f_0 \approx f$ in the bench fuel lines, resonance is inevitable, and processes that significantly affect the operation of the tested LTLPRE

will be initiated. This will lead to unreliable estimates of engine parameters based on test results.

The frequency of liquid natural vibrations depends on the capacitive time constant, considering the medium compressibility and the inert one, which takes into account inertia. According to the methods described in the works of B.F.Glikman, D.N.Popov, the natural frequency is determined:

$$\omega_0 = \sqrt{2 / (\tau_c \tau_{\text{и}})}, \quad (12)$$

where $\tau_c = pL(\rho Ca_2)$ – capacitive time constant; $\tau_{\text{и}} = \rho cL / p = \dot{m}L / pF$ – inertial time constant.

For thin-walled cylindrical pipes the sound speed in terms of the walls elasticity

$$a_t = \frac{a_{\infty t}}{\sqrt{1 + \chi \frac{E_{\text{ж}}}{E_{\text{тр}}}}}, \quad (13)$$

where $a_{\infty t}$ is the sound speed in an unlimited volume of liquid, with regard to the current temperature T ; $a_{\infty t} = a_{\infty} + \beta_t(T - T_0)$; a_{∞} – the sound speed in an unlimited volume of liquid at a temperature T_0 ; β_t – temperature coefficient; $E_{\text{ж}}, E_{\text{тр}}$ – the elastic moduli of the fluid and the material of the pipe walls, respectively; $\chi = D / \delta$ – dimensionless parameter of the pipe, D and δ – diameter and thickness of the pipe walls, respectively [15;20; 22].

Having performed the substitution and taking into account that $f = \omega / 2\pi$, we obtain the dependence of the natural frequency on the pipeline parameters and liquid characteristics (fuel component):

$$f_o = \frac{a_{\infty l} \sqrt{2}}{2\pi l \sqrt{1 + \frac{D}{\delta} \frac{E_{\text{ж}}}{E_{\text{TP}}}}} \quad (14)$$

Resonant frequencies have the following meanings:

$$f_o = \frac{1 + 2n}{4\pi l} \sqrt{\frac{E_{\text{ж}}}{\rho_{\text{ж}}}}, \quad (15)$$

where $n = 0, 1, 2, \dots$; $c_M = \sqrt{E_{\text{ж}} / \rho_{\text{ж}}}$ – the speed of disturbances propagation in the line (sound speed); l is the line length.

The problems of low-frequency dynamics (up to ≈ 20 Hz), including the problems associated with the study of fluid movement in bench hydraulic lines, can be described with a sufficient degree of accuracy by simple dependencies if the pipeline is considered as a system with lumped parameters. The compressibility of the fluid and deformation of the pipe walls have little effect on the unsteady hydrodynamic process if

$$T \gg l \sqrt{\frac{\rho_{\text{ж}}}{E_{\text{ж}}}} = \frac{l}{c_M},$$

where T is the time characteristic of this process.

In this case, the length of the hydraulic line f_{max} should be significantly less than the wavelength λ_{np} of the highest process frequency f_{max} taken into account in the calculations.

Taking the speed of longitudinal waves propagation equals to the speed of sound in the liquid a and the wavelength $\lambda_{\text{np}} = a / f_{\text{max}}$, we write

$$l_{\text{max}} \leq \frac{a}{f_{\text{max}}^n}. \quad (16)$$

When assessing the dynamic characteristics of LTLPRE under pulsed modes, the arising in a thrust device (TD) inertial forces can introduce significant errors in evaluating parameters that determine the dynamic characteristics. The error in measuring these parameters increases when the frequency of the pulsed mode of the tested LTLPRE is in the range of the natural frequency of TD due to the resonance effect. Therefore, when creating TD, it is necessary to ensure a significant excess of natural frequency $f_{0_{\text{thy}}}$ over the pulse mode frequency $f_{0_{\text{thy}}}$.

It is worth noting that the solution to the problem of reducing the error, arising from the dynamics of pulsed modes of LTLPRE operation, is possible by including in the test bench calibration devices that correct the inertial forces in real time. This method significantly increases testing material costs and also reduces the reliability of the test bench [14; 18].

Performance optimization of bench lines

Proceeding from the main requirement that determines LTLPRE live fire bench tests organization is obtaining reliable information about the engine performance under operating conditions; the main criteria for bench lines performance optimization are formulated as:

- propellant components flows in bench lines and spacecraft lines should be similar;
- oscillatory processes arising as a result of operating pulse modes of the tested LTLPRE should not cause additional errors in the assessment of its performance [16; 19; 21].

The hydrodynamic similarity of the fuel components lines in the spacecraft and on the bench is achieved by the correspondence in the equations of fluid motion with the coefficients of the same name Sh, Eu, Fg, and Re, as well as by the congruencies of Mach numbers, dimensionless wave drag α and relative friction losses, $\Delta p / p^*$ then, for a given fuel components consumption \dot{m} c, taking into account $\dot{m} = c p F$, we obtain:

$$\text{Sh} = \frac{l F \rho}{\dot{m} t} = \text{idem}; \text{Fu} = \frac{p F^2 \rho}{(\dot{m})^2} = \text{idem};$$

$$\text{Fr} = \frac{(\dot{m})^2}{(j + g) F^2 l \rho^2} = \text{idem}; \text{Re} = \frac{\dot{m} l}{\nu F} = \text{idem}.$$

As the tests must be carried out in full-scale conditions, the equations for the spacecraft and the bench are true:

$$t_{\text{CT}} = t_{\text{KA}}; \quad \dot{m}_{\text{CT}}; \quad \rho_{\text{CT}} = \rho_{\text{KA}}; \quad \nu_{\text{CT}} = \nu_{\text{KA}}.$$

After some transformations, with respect to the presented equations, we obtain the following conditions for the similarity of the bench and spacecraft lines:

$$\text{Eu} \cdot \text{Fr} = \frac{P}{(j + g) l} = \text{idem} \text{ или } \frac{P_{\text{CT}}}{(j_{\text{CT}} + g) l_{\text{CT}}} = \frac{P_{\text{KA}}}{(j_{\text{KA}} + g) l_{\text{KA}}} = \text{idem};$$

$$\text{Re} = \frac{l}{F} = \text{idem} \text{ или } \frac{l_{\text{CT}}}{F_{\text{CT}}} = \frac{l_{\text{KA}}}{F_{\text{KA}}}.$$

The last expression can be represented in terms of the diameters of the main lines of the stand D_{CT} and spacecraft D_{KA} in the form

$$l_{\text{CT}} / D_{\text{CT}}^2 = l_{\text{KA}} / D_{\text{KA}}^2.$$

The dependence of the natural frequency of liquid oscillations in the pipeline on the characteristics of the fuel component and the pipeline is expressed by the formulas

$$f_0 = \frac{a_{\infty} \sqrt{2}}{2\pi l \sqrt{1 + \frac{D}{\delta} \frac{E_{\text{ж}}}{E_{\text{тр}}}}} \quad \text{или} \quad l = \frac{a_{\infty}}{\pi f_0 \sqrt{2 + \frac{2D}{\delta} \frac{E_{\text{ж}}}{E_{\text{тр}}}}}. \quad (17)$$

To exclude the resonance phenomenon, which causes negative (in terms of similarity) non-stationary processes, the natural frequency of the lines should differ significantly from the frequency of forced oscillations excited by the pulsed operating mode of the tested LTLPRE. The following dependence of the frequency f_0 and the maximum frequency of forced oscillations $f_{\text{ДВ max}}$ can be taken with respect to the safety factor $f_0 \geq n f_{\text{ДВ max}}$:

Taking the value of the coefficient $n = 10$ and considering that the value a_{∞} significantly exceeds the value β_t , i.e. $a_{\infty} \gg \beta_t (T - T_0)$, the formula can be transformed:

$$l_{\text{CT max}} = \frac{0,1a}{\pi f_{\text{ДВ max}} \sqrt{2 + \frac{2D}{\delta} \frac{E_{\text{ж}}}{E_{\text{тр}}}}}, \quad (18)$$

where $l_{\text{CT max}}$ – the maximum value of the bench pipeline length.

In the obtained expression, the known values are: frequency $f_{\text{ДВ max}}$, determined by the test program for a specific LTLPRE, values a and $E_{\text{ж}}$ - characteristics of the corresponding fuel component. Also known are the elasticity moduli for stainless steels of 12X18H10T type. The unknown variables are D and δ .

Taking into account the dependence $\lambda_{\min \text{ пр}} = a / f_{\max}$, where a is the sound speed in a liquid, we write

$$l_{\text{ст}} \leq 0,1a / f_{\text{дв max}} \quad \text{или} \quad l_{\text{ст max}} = 0,1a / f_{\text{дв max}}.$$

Thus, the bench line length must have its natural frequency at least 10 times higher than the maximum frequency of the LTLPRE pulsed operation during testing.

Then the design criteria for bench pipelines will be determined by the following expressions:

$$l_{\text{ст}} / D_{\text{ст}}^2 = l_{\text{КА}} / D_{\text{КА}}^2; \quad l_{\text{ст max}} = \frac{0,1a}{\pi f_{\text{дв max}} \sqrt{2 + \frac{2D}{\delta} \frac{E_{\text{ж}}}{E_{\text{тр}}}}}; \quad l_{\text{ст max}} = 0,1 / f_{\text{дв max}}.$$

Most often, when designing bench pipelines the available material resources are taken into account - a range of pipes with parameters D_{ϕ} and δ_{ϕ} .

If the assortment of pipes with the parameters D_{ϕ} and δ_{ϕ} is known, then taking this into account the design calculation procedure for pipelines will be as follows:

– according to similarity conditions, the length of the pipeline is determined

$$l_{\text{ст тр}} = D_{\phi}^2 \frac{l_{\text{КА}}}{D_{\text{КА}}^2};$$

– the maximum length of the pipeline is determined according to the value a , known for a particular fuel component

$$l_{\text{ст max}} = 0,1a / f_{\text{дв max}};$$

– the maximum permissible length of the pipeline is calculated according to the known values

$$l_{\text{ст max}} = \frac{0,1a}{\pi f_{\text{дв max}} \sqrt{2 + \frac{2D}{\delta} \frac{E_{\text{ж}}}{E_{\text{тр}}}}};$$

– the design value of the pipeline maximum length is selected and, according to the data obtained, the process stability condition is checked

$$l_{\text{ст nh}} < l_{\text{ст доп}}.$$

When testing LTLPRE, fuel consumption can be measured applying a bellows primary converter with an inductive bellows displacement meter while recording displacement on the oscillogram. The accuracy of the flow measurement depends mainly on the accuracy of the bellows movement measurement. The relative error is 4 %. At very low flow rates, the thrust and fuel consumption are determined as the average value over a series of pulses [14; 18].

The test control is fully automated, so that LTPRE start-up occurs without the observer's intervention at the moment when the pendulum passes the stable equilibrium position.

Conclusion

As a result of theoretical, computational and analytical studies based on practical experience in LTLPRE bench testing, a method for assessing the frequency characteristics of the bench hydraulic lines for testing LTLPRE has been developed. A mathematical model of a complex technical system for simulating high-altitude conditions of LTLPRE operation during the live fire tests in a wide range of pulsed modes has been presented.

Библиографические ссылки

1. Гришин С. Д., Захаров Ю. А., Оделевский В. К. Проектирование космических аппаратов с двигателями малой тяги. М. : Машиностроение, 2003. 236 с.
2. Разработка основных систем стенда огневых испытаний жидкостных ракетных двигателей малой тяги / М. В. Краев, Г. Г. Крушенко, Л. Н. Кайчук, В. Г. Яцуненко Препринт № 1. Красноярск : ИВМ СО РАН, 2008. 47 с.
3. Воробьев А. Г., Воробьев С. С. Метод расчета теплового состояния камеры при установившемся импульсном режиме работы жидкостного ракетного двигателя малой тяги // Вестник СибГАУ. 2016. Том 17, № 4. С. 945–955.
4. Лебединский Е. В. Рабочие процессы в жидкостном ракетном двигателе и их моделирование. М. : Машиностроение, 2008. 512 с.
5. НИИМаш [Электронный ресурс]. URL: <http://niimashspace.ru/index.php/produce/rkt/31-propulsion> (дата обращения: 10.11.2020).
6. Новости космонавтики [Электронный ресурс]. URL: <http://novosti-kosmonavtiki.ru/forum/forum9/topic11175/> (дата обращения 12.08.2020).
7. Продукция Тураевского МКБ «Союз» [Электронный ресурс]. URL: <http://www.tmkb-soyuz.ru/31> дата обращения: 15.09.2020).
8. Продукция ФГУП КБ ХМ имени А. М. Исаева [Электронный ресурс]. URL: <http://www.kbhmisaeva.ru/main.phpid=31> / (дата обращения: 21.08.2020).
9. Двигатели 1944-2000: авиационные, ракетные, морские, наземные / под ред. И. Г. Шустова. М. : МАКС-Конверсалт, 2000. 406 с.
10. Бирюков В. И., Назаров В. П., Царапкин Р. А. Алгоритм оценки запасов устойчивости рабочего процесса в камерах сгорания жидкостных ракетных двигателей // Сибирский журнал науки и технологий. 2017. Том 18, № 3. С. 558–566.
11. AMBR Engine for Science Missions [Электронный ресурс]. URL: nts.nasa.gov/archive/nasa/casi.nts.nasa.../20090001339.pdf (дата обращения: 05.09.2020).
12. Шибанов А. А., Пикалов В. П., Сайдов С. С. Методы физического моделирования высокочастотной неустойчивости рабочего процесса в жидкостных ракетных двигателях. М. : Машиностроение ; Полет, 2013. 512 с.
13. Краев М. В., Яцуненко В. Г. Измерения параметров при огневых испытаниях жидкостных ракетных двигателей малой тяги // Вестник СибГАУ. 2004. № 5. С. 167–172.
14. Яцуненко В. Г., Назаров В. П., Коломенцев А. И. Стендовые испытания жидкостных ракетных двигателей : учеб. пособие / Сиб. гос. аэрокосмич. ун-т ; Моск. авиац. ин-т. Красноярск, 2016. 248 с.
15. Гликман Б. Ф. Нестационарные течения в пневмогидравлических цепях. М. : Машиностроение, 1979. 125 с.
16. Бирюков В. И., Мосолов С. В. Динамика газовых трактов жидкостных ракетных двигателей. М. : Изд-во МАИ, 2016. 168 с.
17. Experimental Demonstration of the Vacuum Specific Impulse of a Hybrid Rocket Engine / J. Lestrade, O. Verberne, G. Khimeche и др. // 50th AIAA/ASME/SAE/ASEE Joint Propulsion Conference, Cleveland, 2014.
18. Яцуненко В. Г. Оптимизация процесса конструкторской отработки ЖРД малой тяги при огневых испытаниях : дис. ... канд. техн. наук / Сиб. гос. аэрокосмич. ун-т. Красноярск, 2006. 124 с.
19. Панчурин К. А. Решение уравнений Навье – Стокса в частном случае нестационарного ламинарного течения в трубах // Труды Лен. ин-та водн. транспорта, 1963. Вып. 45. С. 49–51.

20. Файзулаев Д. Ф., Наврузов К., Фаттаев Ф. Н. Пульсирующее течение вязкой несжимаемой жидкости в круглой трубе с разветвлением // ДАН УзССР, 1981. № 10. С. 20–22.
21. Попов Д. Н. Об особенностях нестационарных потоков в трубах // Изв. вузов. Машиностроение. 1970. № 7. С. 78–82.
22. Jeong Soo Kim, Jeong Park, Sungcho Kim. Test and Performance Evaluation of Small Liquid-monopropellant Rocket Engines. 42nd Joint Propulsion Conference & Exhibit, Sacramento, 2006.

References

1. Grishin S. D., Zakharov Yu. A., Odelevskiy V. K. *Proektirovanie kosmicheskikh apparatov s dvigatelyami maloy tyagi* [Design of aircrafts with liquid propellant rocket engines of low thrust]. Moscow, Mashinostroenie Publ., 2003, 236 p.
2. Kraev M. V., Krushenko G. G., Kaychuk L. N., Yatsunenko V. G. *Razrabotka osnovnykh sistem stenda ognevyykh ispytaniy zhidkostnykh raketnykh dvigateley maloy tyagi* [Design of main systems of thruster test facility]. Krasnoyarsk, IVM SO RAN Publ., 2008, 47 p.
3. Vorob'ev A. G., Vorob'ev S. S. [Methods of thruster chamber heat state calculation in a steady impulse regime]. *Vestnik SibGAU*. 2016, Vol. 17, No. 4, P. 945–955. (In Russ.)
4. Lebedinskiy E. V. *Rabochie protsessy v zhidkostnom raketnom dvigatele i ikh modelirovanie pod red. A. S. Koroteeva* [Working processes in liquid propellant rocket engines and their modelling edited by A. S. Koroteev]. Moscow, Mashinostroenie Publ., 2008, 512 p.
5. *NIIMash* [Research Institute of Mechanical Engineering]. (In Russ.) Available at: <http://niimashspace.ru/index.php/produce/rkt/31-propulsion> (accessed: 10.11.2020).
6. *Novosti kosmonavтики* [Space news]. (In Russ.) Available at: <http://novosti-kosmonavтики.ru/forum/forum9/topic11175/> (accessed: 12.08.2020).
7. *Produktsiya Turaevskogo MKB "Soyuz"* [The products of the Turaev MKB Soyuz]. (In Russ.) Available at: <http://www.tmkb-soyuz.ru/> (accessed: 15.09.2020).
8. *Produktsiya FGUP KB KhM imeni A. M. Isaeva* [Products of the Federal State Unitary Enterprise Isayev Design Bureau] (In Russ.). Available at: <http://www.kbhmisaeва.ru/main.php?id=31> (accessed: 21.08.2020).
9. Shustov I. G. *Dvigateli 1944–2000: aviatsionnye, raketnye, morskije, nazemnye* [Engines 1944–2000: aircraft, rocket, naval, land-based engines]. Moscow, AKS-Konversalt Publ., 2000, 406 p.
10. Biryukov V. I., Nazarov V. P., Tsarapkin R. A. [Estimating algorithm of working process stability reserve in liquid-propellant rocket engines chambers]. *Sibirskiy zhurnal nauki i tekhnologii*. 2017, Vol. 18, No. 3, P. 558–566. (In Russ.)
11. AMBR Engine for Science Missions [NASA in space propulsion technology (ISPT) program]. Available at: nts.nasa.gov/archive/nasa/casi.nts.nasa.../20090001339.pdf (accessed: 05.09.2020).
12. Shibanov A. A., Pikalov V. P., Saydov S. S. *Metody fizicheskogo modelirovaniya vysokochastotnoy neustoychivosti rabochego protsessa v zhidkostnykh raketnykh dvigatelyakh pod red. d-ra tekhn. nauk K. P. Denisova*. [Methods of physical modelling of high-frequency instability in working processes of liquid-propellant rocket engines]. Moscow, Mashinostroenie Publ., Polet Publ, 2013, 512 p.
13. Kraev M. V., Yatsunenko V. G. [Measurements during firing tests of low thrust liquid propellant rocket engines]. *Vestnik SibGAU*. 2004, Vol. 5, P. 167–172. (In Russ.)
14. Yatsunenko V. G., Nazarov V. P., Kolomentsev A. I. *Stendovye ispytaniya zhidkostnykh raketnykh dvigateley* [Bench testing of liquid propellant rocket engines]. Krasnoyarsk, Siberian St. Aerospace Univ. Publ., Moscow Aviation Inst. Publ., 2016, 248 p.
15. Glikman B. F. *Nestatsionarnye techeniya v pnevmogidravlicheskikh tsepyakh* [Non-stationary flows in hydraulic and pneumatic circuits]. Moscow, Mashinostroenie Publ., 1979, 125 p.

16. Biryukov V. I., Mosolov S. V. *Dinamika gazovykh traktov zhidkostnykh raketnykh dvigateley* [Dynamics of gas paths of liquid-propellant rocket engines]. Moscow, Moscow Aviation Inst. Publ., 2016, 168 p.
17. Lestrade J., Verberne O., Khimeche G. et. al. Experimental Demonstration of the Vacuum Specific Impulse of a Hybrid Rocket Engine. *50th AIAA/ASME/SAE/ASEE Joint Propulsion Conference*, Cleveland, 2014.
18. Yatsunenko V. G. *Optimizatsiya protsessa konstruktorskoй otrabotki ZhRD maloy tyagi pri ognevykh ispytaniyakh* [Optimisation of the design process for liquid-propellant low thrust rocket engines firing tests]. Krasnoyarsk, Siberian St. Aerospace Univ., 2006, 124 p.
19. Panchurin K. A. [Solution of the Navier-Stokes equations for the particular case of non-stationary laminar flow in pipes]. *Trudy Leningradskogo Instituta vodnogo transporta*. 1963, Vol. 45, P. 49–51. (In Russ.)
20. Fayzulaev D. F., Navruzov K., Fattaev F. N. [Pulsating flow of a viscous incompressible fluid in a circular branch pipe] *DAN Uzbek SSR*. 1981, No. 10, P. 20–22. (In Russ.)
21. Popov D. N. [Features of non-stationary flows in pipes]. *Izvestiya Vysshikh Uchebnykh Zavedenii, Mashinostroenie*. 1970, No. 7, P. 78–82. (In Russ.)
22. Jeong Soo Kim, Jeong Park, Sungcho Kim. Test and Performance Evaluation of Small Liquid-monopropellant Rocket Engines. *42nd Joint Propulsion Conference & Exhibit*. Sacramento, 2006.

© Назаров В. П., Пиунов В. Ю., Яцуненко В. Г., Савчин Д. А., 2021

Назаров Владимир Павлович – кандидат технических наук, профессор, заведующий кафедрой двигателей летательных аппаратов; Сибирский государственный университет науки технологий имени академика М. Ф. Решетнева. E-mail: nazarov@sibsau.ru.

Пиунов Валерий Юрьевич – кандидат технических наук; заместитель генерального директора; Конструкторское бюро химического машиностроения имени А. М. Исаева – филиал ФГУП ГКНПЦ имени М. В. Хруничева. E-mail: piunovdm@gmail.com.

Яцуненко Владимир Григорьевич – кандидат технических наук, профессор кафедры двигателей летательных аппаратов; Сибирский государственный университет науки технологий имени академика М. Ф. Решетнева. E-mail: vyatsunenko@mail.ru.

Савчин Дмитрий Александрович – аспирант; Сибирский государственный университет науки технологий имени академика М. Ф. Решетнева. E-mail: savchin.dim@yandex.ru.

Nazarov Vladimir Pavlovich – Cand. Sc., Professor, Head of the Department of Aircraft Engines; Reshetnev Siberian State University of Science and Technology. E-mail: nazarov@sibsau.ru.

Piunov Valery Yuryevich – Cand. Sc.; Deputy General Director; Isaev Chemical engineering Design Bureau. E-mail: piunovdm@gmail.com.

Yatsunenko Vladimir Grigorievich – Cand. Sc., Professor of the Department of Aircraft Engines; Reshetnev Siberian State University of Science and Technology. E-mail: vyatsunenko@mail.ru.

Savchin Dmitry Aleksandrovich – Post-graduate student; Reshetnev Siberian State University of Science and Technology. E-mail: savchin.dim@yandex.ru.

УДК 621.11; 620.97

Doi: 10.31772/2712-8970-2021-22-2-356-370

Для цитирования: Конверсионное использование моделей рабочих процессов турбоустановок ракетных двигателей в приложении к локальной энергетике / В. А. Аброськин, В. А. Чернорот, А. А. Кишкин и др. // Сибирский аэрокосмический журнал. 2021. Т. 22, № 2. С. 356–370. Doi: 10.31772/2712-8970-2021-22-2-356-370.

For citation: Abroskin V. A., Chernorot V. A., Kishkin A. A., Delkov A. V., Zhuravlev V. Yu. Conversion use of models of working processes of rocket engine turbine installations in the application to local power engineering. *Siberian Aerospace Journal*. 2021, Vol. 22, No. 2, P. 356–370. Doi: 10.31772/2712-8970-2021-22-2-356-370.

Конверсионное использование моделей рабочих процессов турбоустановок ракетных двигателей в приложении к локальной энергетике

В. А. Аброськин¹, В. А. Чернорот¹, А. А. Кишкин^{2*}, А. В. Делков², В. Ю. Журавлев²

¹ООО ИТЦ «СОЮЗ-ЭНЕРГО»

Российская Федерация, 662971, г. Железногорск Красноярского края, ул. Ленина, 39а

²Сибирский государственный университет науки и технологий имени академика М. Ф. Решетнева

Российская Федерация, 660037, г. Красноярск, просп. им. газ. «Красноярский рабочий», 31

*E-mail: spsp99@mail.ru

В настоящей работе рассмотрена концепция использования методов расчета и проектирования энергетических установок ракетных двигателей для конверсионного моделирования локальной энергетики арктических и северных районов Красноярского края с очевидным обобщением на соседние административные формирования со сходными климатическими и структурно логистическими условиями. Предложенная структура содержит блоки электрогенерации, привязанные как к промышленным отходам деревообработки, так и к природным и промышленным тепловым хвостам, идентифицируемым как источники низкопотенциального тепла, а также в качестве источника предложены современные реакторные установки малой мощности блочного необслуживаемого исполнения. Объединяющим элементом энергоустановок является турбогенератор, спроектированный с учетом использования нетрадиционного, часто бросового и природного низкопотенциального тепла.

Ключевые слова: турбины реактивные, центробежные и центростремительные, энергетические технологии, низкопотенциальное тепло, геотермальное тепло, тепловые сбросы, атомные станции малой мощности.

Conversion use of models of working processes of rocket engine turbine installations in the application to local power engineering

V. A. Abroskin¹, V. A. Chernorot¹, A. A. Kishkin^{2*}, A. V. Delkov², V. Yu. Zhuravlev²

¹ООО ИТЦ «СОЮЗ-ЭНЕРГО»

39a, Lenin St., Zheleznogorsk, 662971, Russian Federation

²Reshetnev Siberian State University of Science and Technology

31, Krasnoyarskii rabochii prospekt, Krasnoyarsk, 660037, Russian Federation

*E-mail: spsp99@mail.ru

In this paper, we consider the concept of using methods for calculating and designing rocket engine power plants for conversion modeling of local energy in the Arctic and northern regions of the Krasnoyarsk Territory, with an obvious generalization to neighboring administrative formations with similar climatic and structural and logistical conditions. The proposed structure contains power generation units linked to both industrial woodworking waste and natural and industrial thermal tails, identified as sources of low-potential heat, as well as modern low-power reactor plants of block maintenance-free design. The unifying element of power plants is a turbo generator, designed with the use of unconventional, often waste and natural low-grade heat.

Keywords: jet turbines, centrifugal and centripetal, energy technologies, low-grade heat, geothermal heat, thermal discharges, low-power nuclear power plants.

Introduction

The experience gathered in calculating the parameters of gas turbine installations of rocket engines makes it possible to apply digital models to technologies for utilizing low-grade heat to create low-power installation.

In the global formulation of the problems of small-scale power generation using fuels from non-conventional sources, renewable and wind energy [1; 2], the authors are considering the aspects of improving characteristics [3] owing to the detailed study of working processes in power equipment using unconventional rare cycles [4]. In the Russian Federation, the problems of small distributed generation are set and determined with a large coverage.

According to the report of Yevgeny Afanasyev (the head of the Regional Ministry of Industry, Energy and Housing and Communal services) at the 10th International Forum "Arctic: Present and Future", held in St. Petersburg, the power system of the Arctic zone of the Krasnoyarsk Territory includes two hydroelectric power plants - Ust-Khantayskaya and Kureyskaya, three gas CHP plants (combined heat and power plants) providing electricity to the Norilsk industrial region, as well as more than 60 diesel power plants and 48 boiler houses in power-insulated villages. The main problems of the power system of the northern regions are significant equipment deterioration, high cost of fuel delivery, as well as restrictions on the supply of fuel, which is caused by a short period of deliveries of goods to the Northern Territories. The significant share of funds is allocated from the regional budget to subsidize energy generation costs.

The measures taken in the field of energy supply are insufficient for developing the northern regions and creating infrastructure that would create decent social living conditions for the local population and the development of commercial farms.

In order to increase the efficiency of energy supply, in the territory of the Tura settlement of the Evenkia Area, the utilization of waste heat has been introduced at three diesel power plants receiving heat energy in the form of hot water. In Russia as a whole and in the Krasnoyarsk Territory, there are modern energy technologies that can significantly reduce operating cost [5–8].

ООО ИТЦ "Сoyuz-Eнерго" in cooperation with Reshetnev Siberian State University of Science and Technology have developed a unique technology for converting low-grade thermal energy (warm water, warm air and exhaust hot gases, etc.) in the organic Rankine cycle into electricity. This technology is based on the use of an organic low-boiling actuation fluid (freon) in the cycle, in combination with both the typical power range of turbines and the experimental design of a centrifugal jet turbine, which, unlike typical designs, allows working in the area of saturated (condensable) steam without disturbing the operation of the nozzle diaphragm and the turbine, as well as structurally combining part of the function of the circulating supercharger [9; 10] and the turbine, which provides some decrease in energy losses by reducing the mechanical losses of the rotor and increasing the overall efficiency of a turbine [11]. A high-speed permanent magnet generator is used as an electric generator.

Mathematical modeling and engineering calculations were carried out by the OOO ITC "Soyuz-Energo" and the Department of Refrigerating and Cryogenic Engineering of Reshetnev Siberian State University of Science and Technology.

Mathematical modeling

The schematic block diagram of the heat recovery unit based on a steam turbine unit (STU) is shown in Fig. 1.

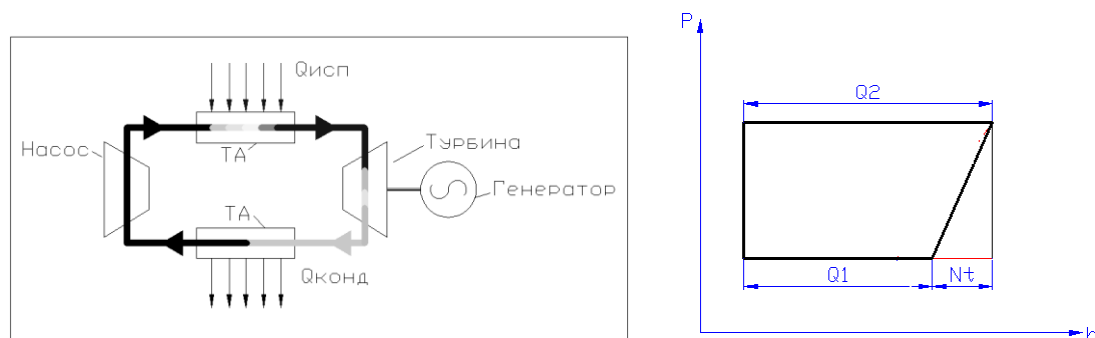


Рис. 1. Структурная схема установки и цикл работы:
ТА – теплообменный аппарат; Q_2 – теплота, подведенная в испарителе;
 Q_1 – теплота, отведенная в конденсаторе; N_t – мощность турбины

Fig. 1. Block diagram of the installation and its operation cycle
ТА – heat-exchange apparatus; Q_2 – heat supplied to the evaporator;
 Q_1 – heat rejected in the condenser; N_t – turbine power

The mathematical model of a steam turbine plant (STP) based on organic actuation fluids (OAF) is based on four basic equations, which, in various interpretations, form the basis of technical hydromechanics and consider the flow of compressible fluids with heat exchange. The equations below are presented for a one-dimensional flow in two forms - differential and integral:

– motion equation (Eulerian equation):

$$\rho \frac{d\bar{W}}{dt} = \rho \bar{F} - \text{grad}(p); \quad (1)$$

– mechanical energy equation (Bernoulli equation):

$$\frac{\rho W^2}{2} + p = \text{const}; \quad (2)$$

where ρ – density; W – speed; t – time; F – strength; p – pressure;

– equation of continuity in notation of calculus:

$$\frac{d\rho}{dt} + \rho \text{div}(\bar{W}) = 0; \quad (3)$$

– equation of continuity in integral form:

$$\rho S W = \text{const}, \quad (4)$$

where S is the passage area of the channel;

– energy-conservation equation in thermodynamic parameters in notation of calculus:

$$\rho \frac{du}{dt} = -p \operatorname{div} \bar{W} + \mu D - \operatorname{div} \bar{q} + \rho \frac{dq}{dt}; \quad (5)$$

– energy-conservation equation in thermodynamic parameters in integral form (First law of thermodynamics):

$$\Delta U = A + \Delta Q, \quad (6)$$

where μD – work of viscosity forces; u , U – internal energy; q , Q – heat flow;

– equation of state (in general form) (see Fig. 1):

$$f(p, \rho, T) = 0. \quad (7)$$

The four equations contain four independent physical quantities: p , ρ , q , T . Thus, the system is closed. These equations are universal and can be applied to the description of any processes in turbine installations of thermal power systems. The system of these equations can be specified for different levels in accordance with the accepted hierarchy of the model:

– the level of final volumes. It considers a geometric volume that is so small that differential equations can be applied;

– the level of system elements. It considers a specific element (component of a complex system) – heat exchanger, pump, capillary tube. Accordingly, the equations are integral. At this level, the equations called component equations of an element are obtained,;

– system level. It considers the system as a whole and integral equations. In the literature, these equations are called topological equations of the system.

The calculation procedure is shown in the operation cycle diagram (Fig. 2). The differential pressure (1) sets the height of the cycle in the diagram, the heat flux (6) sets the width of the cycle. The cycle is balanced in terms of flow and temperature. The system of equations is solved numerically by iterating the flow rate on the balance of the energy equation. The result of solving the system of equations determines the position of the cycle in the diagram with reference to the properties of the actuation fluid (2), (4), (6), (7).

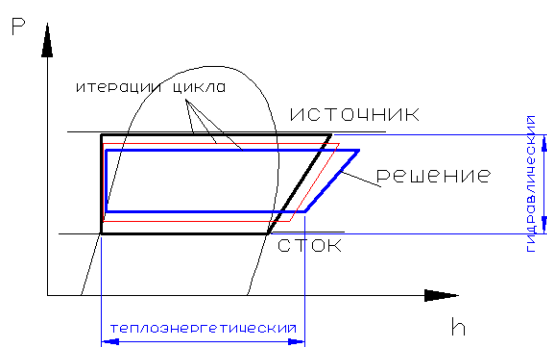


Рис. 2. Определение параметров цикла по системе уравнений

Fig. 2. Determination of the cycle parameters using the system of equations

The surface of the actuation fluid state was developed to take into account the changing properties of the actuation fluid. Mathematical state surface (Fig. 3) of an organic actuation fluid in the coordinates of pressure p , specific volume v ($v = 1/\rho$) and temperature T allows calculating the cycles of power plants by numerical methods, taking into account the continuous change in properties. In addition, using the surface, it is

possible to obtain basic parameters of a body (enthalpy, entropy, heat capacity, speed of sound, etc.) using differential equations of thermodynamics.

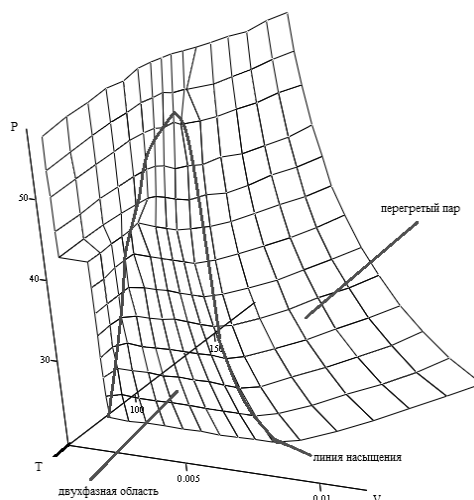


Рис. 3. Поверхность состояния фреона R22

Fig. 3. The state surface of R22 freon

The calculated characteristic for the adiabatic power of the turbine accords well with the theoretical results. As the pump head increases, the pressure differential in the system increases as well, and therefore the temperature differential rises (Fig. 4). The specific work of the turbine and the mass flow rate increase.

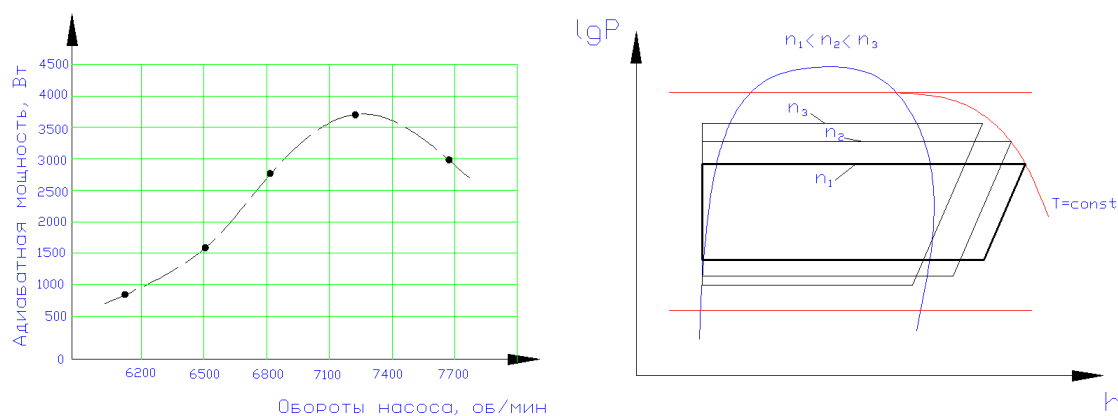


Рис. 4. Реакция ПТУ ОПТ на изменение оборотов насоса

Fig. 4. Reaction of the steam turbine unit on the change of pump speed

The results of numerical experiments presented above, along with the reflection of the adequacy of the mathematical model to theoretical information about the operation of the STP, allow us to formulate the following: due to the ambiguity of the influence (including the mutual influence) of the control parameters on the operation of the STP, the OAF design and operation optimization of similar steam turbine plants is a complex problem that involves consideration of the wide range of possible system states. One of the effective ways to solve this problem is the development of algorithms and methods for its solution based on a mathematical model with conducting numerical research.

An installation test bench was designed to verify the model (Fig. 5). To estimate the power of the turbine, the parameters of the amount of energy imparted to water are required, which is estimated by means of the data on the pressure and temperature of the water at the inlet and outlet of the pump. The main element of the laboratory setup is a steam turbine.

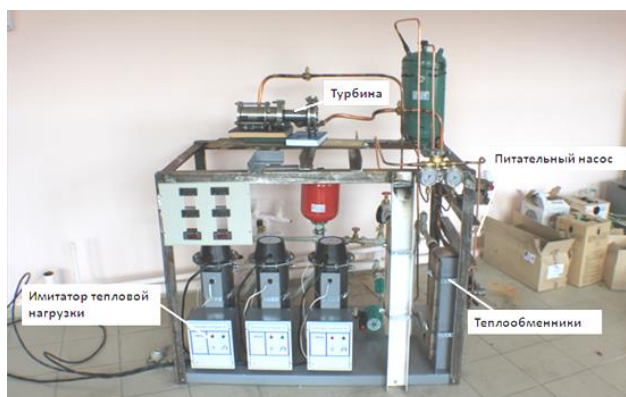


Рис. 5. Испытательный стенд ПТУ на ОПТ

Fig. 5. The test bench of a steam turbine unit

Proposed solutions

The analysis of the results of operation of the experimental turbine generator "Thermoel", the design study and calculations show that the turbine generator can provide electricity generation from units to several thousand kW, providing the efficiency factor of 20 to 40% at a coolant (water, gas) temperature of 20 ° C and above.

Currently, two modular turbine generators are being developed for the research bench for melting metal radioactive waste at one of the enterprises of the Rosatom group company [12]. Three-dimensional models of electric generators with the capacity of 100 kW on a single frame and 1 MW in a 20-foot container are shown in Fig. 6.



Рис. 6. Турбогенераторы мощностью 100 и 1000 кВт

Fig. 6. 100 kW and 1000 kW turbo generators

We propose to consider the following technical solutions for the creation or modernization of the available local energy systems:

- heat recovery with the generation of additional electricity from existing diesel power plants;
- local production for the fabrication of domestic fuel oil and pyrocoal from local wood for sanitary cleaning of forests and wood processing waste;
- mini CHP plants on local wood waste (sawdust, shavings, wood chips, branches of trees and shrubs);

- use of heat from geothermal waters to generate electricity;
- use of atomic energy from low-power nuclear power plants to generate electricity and hot water.

Diesel power plants are used most of all to generate electricity in the Northern regions. During the operation of these stations, large amount of waste heat (so-called thermal tails) is emitted into the atmosphere. Thermal tails are generated from combustion exhaust gases, the cooling system of the internal combustion engine and the oil cooling system. For 1 MW of generated electricity, 1–2 MW of heat is generated.

Recently, cogeneration plants have been used for the recovery of thermal tails, providing a combined process – generating electricity and heat in the form of hot water. The unit for waste gas heat recovery and hot water production is shown in Fig. 7.



Рис. 7. Установка утилизации тепла отходящих газов

Fig. 7. Waste gas heat recovery unit

One of the promising and cost-effective technical solutions is the creation of an integrated energy centre with combined generation of electricity, hot water and electricity from the heat of hot water. For this, it is necessary to add the “Thermoel” turbine generator module to the cogeneration unit.

With the diesel generator capacity of 1 MW, one can obtain additional 0.5 MW of electricity and 0.5 MW of heat the form of hot water.

At the annual electricity generation of $500 \text{ kW} \cdot 8,000 \text{ hours} = 4,000,000 \text{ kW} \cdot \text{h}$ per year, the revenue from the sale of electricity at the cost of $1 \text{ kW} \cdot \text{h}$ of electricity of 10 rubles will be $4 \text{ million kW} \cdot \text{h} \cdot 10 = 40$ million rubles. The payback time is estimated to be 1.1 years. The diagram of the “Thermoel” turbogenerator with the use of thermal tails is shown in Fig. 8.

The northernmost point of wood processing is the town called Lesosibirsk, where wood processing enterprises are located along the river Yenisei for 40 km. Over the years of the activity, the large amount of sawmill waste has been accumulated.

Wood is one of the primary fuel sources. The calorific value of wood is 4600 kcal / kg with the bulk density of 550–600 kg / m³. The calorific value of wood briquettes is 7800 kcal / kg with the bulk density of 600 kg / m³. The calorific value of diesel fuel is on average 10,000 kcal / kg with the bulk density of 800 kg / m³. The analysis of the characteristics of various types of wood briquettes and diesel fuel shows that wood briquettes can fully replace diesel fuel.

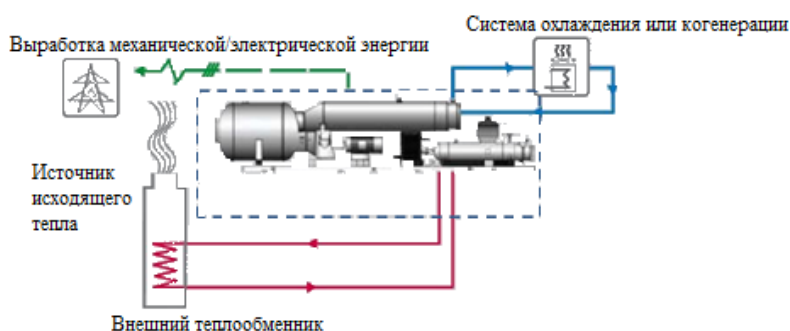


Рис. 8. Схема утилизации тепловых хвостов

Fig. 8. Thermal tails recovery scheme

In the last decade, Russian scientists, designers and equipment manufacturers have developed a technology for the rapid pyrolysis of wood waste to produce domestic fuel oil and pyrolytic coal. Modular complexes are manufactured on the basis of the developed technology.

A three-dimensional model of the complex of a rapid pyrolysis plant is shown in Fig. 9.

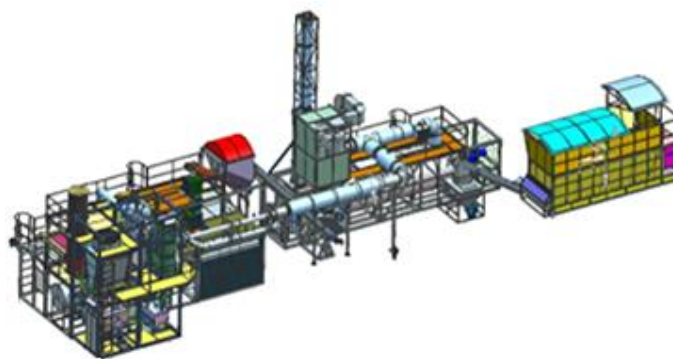


Рис. 9. Общий вид установки быстрого пиролиза с габаритными размерами 31,5×7×9,1 [м]

Fig. 9. General view of the rapid pyrolysis plant with the overall dimensions 31,5×7×9,1 [m]

Plant specifications:

- productivity, kg / h – 500, dry;
- power consumption, kW * h - 25;
- operating mode – continuous;
- maximum temperature in the reactor, °C – 650;
- maximum temperature in the furnace, °C – 1000.

Yield of pyrolysis products:

- gas, kg / h – 130;
- carbon, kg / h – 100;
- bio-oil, kg / h – 270.

Domestic fuel oil (bio-oil) can be used in boiler houses in remote northern regions, as well as carbon (pyrolytic coal) can be used as a solid fuel with injection of carbon powder into a furnace.

With further distillation of bio-oil, one can obtain:

- phenol-formaldehyde adhesive for the production of plywood and glued wood;
- woody acetic acid – antiseptic and fertilizer for soil treatment.

Currently, Russia manufactures and sells boiler houses with the capacity from 100 kW to 50 MW, operating on wood waste. When using the boiler houses with the turbo generators "Thermoel" it is possible to create an efficient energy system for generating heat in the form of hot water and electricity, as well as to avoid kilometer-long heaps of wood waste in Lesosibirsk.

Fig. 10 shows a three-dimensional model of a modular boiler house with the power of 1-3 MW.

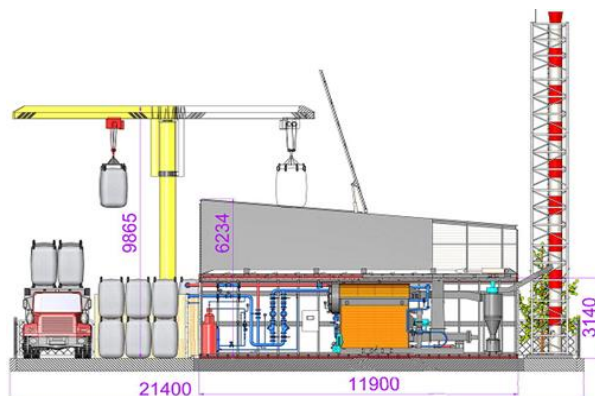


Рис. 10. Модульно-двухблочная котельная ООО «СОЮЗ»
тепловой мощностью от 1 до 3 МВт с многотопливными котлами
(щепа, пеллеты, брикеты, уголь)

Fig. 10. Modular-2-block boiler house of ООО SOYUZ
with the thermal power of 1 to 3 MW with multi-fuel boilers
(wood chips, pellets, briquettes, coal)

One of the inexhaustible sources of energy is geothermal heat, released as a result of nuclear processes inside our planet.

It is known that there is an amount of water inside the Earth that exceeds its amount on the surface, and due to water heat exchange, heat is released into the atmosphere [9].

The Krasnoyarsk Territory is partially located on the territory of the West Siberian Plain. The geological studies of prospecting for oil deposits, as well as hydrological studies on a vast territory back in the 50s of the last century show that at the depth of several hundred to several thousand meters, there is a hot water source with the volume exceeding the Mediterranean Sea.

Near Biysk, Semipalatinsk or Kustanai, the water temperature reaches only + 5 ... + 10 degrees Celsius, further north, at the latitude of Pavlodar, Petropavlovsk, Tomsk, where the depth is already 500-600 m, the thermometer in the borehole shows +25 degrees Celsius (Fig. 11).

Even hotter water (+75 degrees Celsius) was found at the depth of 1.5 km near Tyumen. And where it is necessary to drill boreholes to the depth of 2.5-3 km, fountains of boiling water sometimes break to the height of up to 50 m. The temperature of one of these artificial geysers (in Kolpashevo) reaches +125 degrees Celsius.

Russia has experience in using geothermal heat to generate electricity. In 1965, the Institute "Thermophysics" of the Siberian Branch of the USSR Academy of Sciences built a freon geothermal power plant with the power of 1 MW at a geothermal water temperature of 80 ° C in the Sredneparatunskoye field. As a unit for generating electricity, a blade turbine was used, the efficiency of which was no more than 7%, the rest of the heat of hot water was used for heat supply [13; 14].



Рис. 11. Геотермальное теплое море

Fig. 11. Geothermal warm sea

Using the centrifugal turbine of the Thermoel model, it is possible to create local power and heat supply systems with high energy efficiency in places where thermal waters are available, without damaging the environment. To search for geothermal horizons with the relatively high temperature of 40–70 °C, it is necessary to carry out engineering-geological and hydrological surveys. A schematic diagram of the use of geothermal waters for electricity generation is shown in Fig. 12.

According to the experience of building geothermal power plants in Europe, the cost of capital investments is 3,000 dollars for 1 kW of generated electricity.

To provide a reliable autonomous system of heat and power supply for small settlements and low-power industries, it is worth considering the possibility of building small nuclear power plants (SNPPs) up to 400 MW. The developments on the creation of SNPPs were carried out 50 years ago. However, they did not end with a specific implementation.

At present, power sources have been developed on the basis of the 35 MW KLT-40S reactor system (RS), the 6 MW ABV-6E RS, and the 50 MW RITM 200 RS [15–17].

The floating power unit with the KLT-40S RS has been built and put into operation, the other two projects have not been implemented yet.

The main advantages of the SNPPs are the following: the ability to create the required power of the SNPP depending on the requirements of consumers; short construction period; environmentally friendly form of energy; long service life (more than 35–40 years).

The three-dimensional model of a floating SNPP and SNPP with the RITM 200 RS is shown in Fig. 13.

The scheme of the modular design of the SNPP with two Master reactors with a thermal power of 30 MW each is shown in Fig. 14.



Рис. 12. Принципиальная схема использования геотермальных вод для производства электроэнергии

Fig. 12. Schematic diagram of using geothermal water for electricity generation



Рис. 13. Модель плавучей АСММ

Fig. 13. Model of the floating SNPP

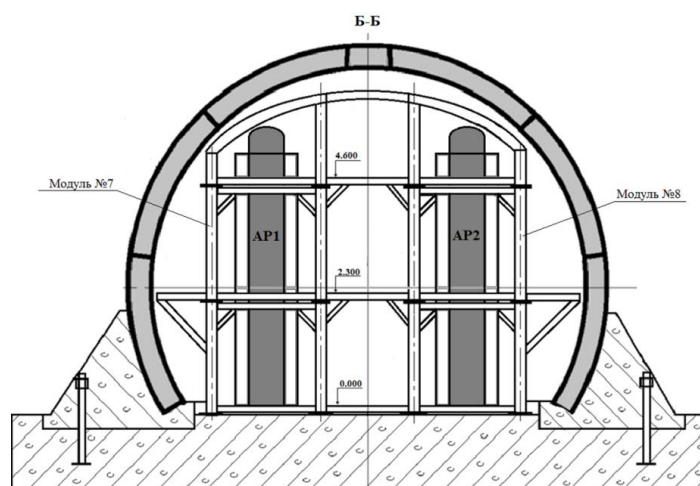


Рис. 14. Схема модульной конструкции АСММ

Fig. 14. Diagram of the modular design of the SNPP

Conclusion

The accumulated experience of mathematical modeling of heat and mass transfer and heat power processes in the flow path of aircraft engines allows using the results for individual elements of turbines, pumps, heat exchangers in the Rankine cycle for power generating equipment with the possibility of design optimi-

zation of the parameters of both elements and the system with subsequent calculation of the flow path of structural elements.

The promising way of using low-grade energy sources is the use of heat recovery converters based on steam turbine plants using organic actuation fluids with the condensation temperature below 100 ° C.

The considered structure of a low-power distributed power generating system takes into account only individual sources and possibilities of northern and inaccessible territories and is determined by the general requirement for heat sources: a relatively low temperature potential, which requires the development and production of special equipment for turbo power generation, determined by the satisfactory possibility of block transportation and installation, as well as minimum maintenance for a long service life. Undoubtedly, low potential, increased safety requirements and a long service life with minimal maintenance make this area of power generation quite losing in terms of energy efficiency with large power generation. However, only such a performance forms a niche of low-grade energy in hard-to-reach subarctic regions, in our opinion. The materials do not consider other elements of renewable energy, although their use is cogeneratively possible.

Библиографические ссылки

1. Fates of heavy organics of bio-oil in hydrotreatment: The key challenge in the way from biomass to biofuel / L. Zhang, X. Hu, C. Li, V. Esmaili, M. Gholizadeh // *Science of the Total Environment* . 2021. Vol. 778, 146321.
2. Economic-environmental analysis of combined heat and power-based reconfigurable microgrid integrated with multiple energy storage and demand response program / M. Hemmati, M. A. Mirzaei, M. Abapour et al. // *Sustainable Cities and Society*. 2021. Vol. 69, 102790.
3. Research and applications of drag reduction in thermal equipment: A review (Review) / W. Gong, J. Shen, W. Dai et al. // *View Correspondence (jump link)*. *International Journal of Heat and Mass Transfer*. 2021. Vol. 172. 121152.
4. Romei A., Binotti M. Off-design performance of closed OTEC cycles for power generation (Article) *View Correspondence (jump link)* // *Renewable Energy*. 2021. Vol. 170. P. 1353–1366.
5. Разработка установок-утилизаторов низкопотенциального тепла на основе органического цикла Ренкина / А. А. Кишкин, Д. В. Черненко, А. А. Ходенков и др. // *Альтернативная энергетика и экология*. 2013. № 14 (136). С. 57–63.
6. Разработка установок-утилизаторов низкопотенциального тепла на основе органического цикла Ренкина / А. А. Кишкин, Д. В. Черненко, А. А. Ходенков и др. // *Альтернативная энергетика и экология*. 2014. № 3 (4). С. 35–36.
7. Проектирование паровых микротурбинных установок малой распределенной энергетики / М. А. Ермаков, В. С. Галимов, Ю. Н. Шевченко и др. // *Сб. материалов Междунар. семинара, проводимого в рамках подготовки IX Междунар. науч.-практ. конф. «Горные территории : приоритетные направления науки Российской Федерации»*. 2018. С. 77–79.
8. Прямолинейное равномерное течение газов с теплоотдачей в энергетических установках летательных аппаратов / М. И. Толстомятов, А. А. Зуев, А. А. Кишкин и др. // *Вестник СибГАУ*. 2012. № 4 (44). С. 134–139.
9. Белоусов В. И., Эрлих Э. Н. Становление геотермальной энергетики Камчатки : проблемы и решения // *Вопросы истории естествознания и техники*. 2015. Т. 36, № 2. С. 306–321.
10. Проектная оптимизация теплотехнических систем, работающих по замкнутому контуру / А. А. Кишкин, А. В. Делков, А. А. Ходенков и др. // *Вестник СибГАУ*. 2012. № 5 (45). С. 34–38.

11. Теплоотдача вращательных течений в турбомашинах на основе двухслойной модели турбулентного пограничного слоя / А. А. Зуев, А. А. Кишкин, М. И. Толстомятов и др. // Вестник СибГАУ. 2012. № 5 (45). С. 127–129.
12. Бутузов В. А., Амерханов Р. А., Григораш О. В. Геотермальное теплоснабжение в мире и в России: состояние и перспективы // Теплоэнергетика. 2018. № 5. С. 45–49.
13. Васильев Ю. С., Амосов Н. Т. Атомные станции малой мощности // Научно-технические ведомости Санкт-Петербургского гос. политехн. ун-та. 2014. № 2 (195). С. 26–34.
14. Сравнительная эффективность использования атомных станций малой мощности в локальных энергосистемах на востоке России / Н. И. Воропай, Б. Г. Санеев, И. Ю. Иванова, А. К. Ижбулдин // Атомные станции малой мощности: новое направление развития энергетики : под ред. акад. РАН А. А. Саркисова. Т. 2. М. : Академ-Принт, 2015. С. 59–72.
15. Численное исследование газодинамики сопел малоразмерных газогенераторов с вытекающими из них струй / И. Э. Иванов, И. А. Крюков, С. А. Шустов // Вестник Самарского государственного аэрокосмического университета. № 1 (43) / 2014. С. 112–122.
16. Пат. 2697274 Российская Федерация, ^{МПК} В09В 3/00. Способ переработки твердых коммунальных и промышленных отходов / Чернорот В. А., Лапшин Б. М., Аброськин В. А. № 2018141008 ; заявл. 21.11.2018 ; опубл. 13.08.2019 Бюл. № 23. 7 с.
17. Пат. 181361 Российская Федерация, ^{МПК} F01D 1/32. Центробежная турбина / Аброськин В. А. № 2017144390 ; заявл. 18.12.2017 ; опубл. 11.07.2018 Бюл. № 20. 7 с.

References

1. Zhang L., Hu X., Li C., Esmaili V., Gholizadeh M. Fates of heavy organics of bio-oil in hydrotreatment: The key challenge in the way from biomass to biofuel. *Science of the Total Environment*. 2021, Vol. 778, No. 146321.
2. Hemmati M., Mirzaei M. A., Abapour M., Zare K., Mohammadi-ivatloo B., Mehrjerdi H., Marzband M. Economic-environmental analysis of combined heat and power-based reconfigurable microgrid integrated with multiple energy storage and demand response program. *Sustainable Cities and Society*. 2021, Vol. 69, No. 102790.
3. Gong W., Shen J., Dai W., Li K., Gong M. Research and applications of drag reduction in thermal equipment: A review (Review). View Correspondence (jump link). *International Journal of Heat and Mass Transfer*. 2021, Vol. 172, No. 121152.
4. Romei A., Binotti M. Off-design performance of closed OTEC cycles for power generation (Article). View Correspondence (jump link). *Renewable Energy*. 2021, Vol. 170, P. 1353–1366.
5. Kishkin A. A., Chernenko D. V., Khodenkov A. A., Delkov A. V., Tanasienko F. V. [Development of low-grade heat recovery units based on the organic Rankin cycle]. *Alternative Energy and ecology*. 2013, No. 14 (136), P. 57–63 (In Russ.).
6. Kishkin A. A., Chernenko D. V., Khodenkov A. A., Delkov A. V., Tanasienko F. V. [Development of low-grade heat recovery units based on the organic Rankin cycle]. *Alternative Energy and ecology*. 2014, No. 3 (4), P. 35–36 (In Russ.).
7. Ermakov M. A., Galimov V. S., Shevchenko Yu. N., Kishkin A. A., Melkozerov M. G. [Design of steam microturbine installations of small distributed power engineering]. *Collection of materials of the International seminar held in preparation for IX International Scientific and Practical Conference Mountainous Territories: Priority Areas and Sciences of the Russian Federation*. 2018, P. 77–79.

8. Tolstopyatov M. I., Zuev A. A., Kishkin A. A., Zhuikov D. A., Nazarov V. P. [Rectilinear uniform flow of gases with heat transfer in power plants of aircraft]. *Vestnik SibSAU*. 2012, No. 4 (44), P. 134–139 (In Russ.).
9. Belousov V. I., Erlikh E. N. [Formation of geothermal energy in Kamchatka: problems and solutions]. *Problems of the history of natural science and technology*. 2015, Vol. 36, No. 2, P. 306–321. (In Russ.)
10. Kishkin A. A., Delkov A. V., Khodenkov A. A., Zuev A. A., Zhuikov D. A. [Design optimization of heat engineering systems operating in a closed loop]. *Vestnik SibSAU*. 2012, No. 5(45), P. 34–38 (In Russ.).
11. Zuev A. A., Kishkin A. A., Tolstopyatov M. I., Zhuikov D. A. [Heat transfer of rotational flows in turbomachines on the basis of a two-layer model of a turbulent boundary layer]. *Vestnik SibSAU*. 2012, No. 5 (45), P. 127–129 (In Russ.).
12. Butuzov V. A., Amerkhanov R. A., Grigorash O. V. Geothermal heat supply in the world and in Russia: state and prospects. *Teploenergetika*. 2018, No. 5, P. 45–49 (In Russ.).
13. Vasiliev Yu. S., Amosov N. T. [Nuclear plants of low power]. *Scientific and technical statements of the St. Petersburg State Polytechnic University*. 2014, No. 2 (195), P. 26–34 (In Russ.).
14. Voropai N. I., Saneev B. G., Ivanova I. Yu., Izbuldin A. K. Comparative efficiency of the use of low-power nuclear power plants in local power systems in the east of Russia. *Nuclear power plants of low power: a new direction of energy development*. Vol. 2. Moscow, Akadem-Print Publ., 2015, P. 59–72.
15. Ivanov I. E., Kryukov I. A., Shustov S. A. [Numerical study of gas dynamics of small-size gas generators and the jets flowing from them]. *Bulletin of the Samara State Aerospace University*. 2014, No. 1 (43), P. 112–122 (In Russ.).
16. Chernorot V. A., Lapshin B. M., Abroskin V. A. *Method of processing solid municipal and industrial waste*. Patent RF, no. 2697274, mpk B09B 3/00 No. 2018141008. 2019.
17. Abroskin V. A. *Centrifugal turbine*. Patent RF, IPC F01D 1/32. No. 2017144390. 2018.

© Аброськин В. А., Чернорот В. А., Кишкин А. А., Делков А. В., Журавлев В. Ю., 2021

Аброськин Василий Алексеевич – директор; ООО «Союз-Энерго». E-mail: megahol64@mail.ru.

Чернорот Владимир Алексеевич – заместитель директора; ООО «Союз-Энерго». E-mail: megahol64@mail.ru.

Кишкин Александр Анатольевич – доктор технических наук, профессор, Сибирский государственный университет науки и технологий имени академика М. Ф. Решетнева. E-mail: spsp99@mail.ru.

Делков Александр Викторович – кандидат технических наук, доцент, доцент кафедры холодильной, криогенной техники и кондиционирования; Сибирский государственный университет науки и технологий имени академика М.Ф. Решетнева. E-mail: delkov-mx01@mail.ru.

Журавлев Виктор Юрьевич – кандидат технических наук, доцент, профессор кафедры двигателей летательных аппаратов; Сибирский государственный университет науки и технологий имени академика М. Ф. Решетнева.

Abroskin Vasily Alekseevich – Director; Soyuz Energo LLC. E-mail: megahol64@mail.ru.

Chernorot Vladimir Alekseevich – Deputy Director; Soyuz Energo LLC. E-mail: megahol64@mail.ru

Kishkin Aleksandr Anatolevich – Dr. Sc., Professor; Reshetnev Siberian State University of Science and Technologies. E-mail: spsp99@mail.ru.

Delkov Aleksandr Viktorovich – Ph. D., associate Professor; Reshetnev Siberian State University of Science and Technologies. E-mail: delkov-mx01@mail.ru.

Zhuravlev Viktor Yurievich – Ph. D. assistant Professor; Reshetnev Siberian State University of Science and Technologies.

УДК 669/713-048/25

Doi: 10.31772/2587-6066-2021-22-2-371-382

Для цитирования: Структурно-фазовое состояние и свойства заэвтектического силумина, обработанного импульсным электронным пучком / Ю. Ф. Иванов, С. П. Ереско, А. А. Клопотов и др. // Сибирский аэрокосмический журнал. 2021. Т. 22, № 2. С. 371–382. Doi: 10.31772/2587-6066-2021-22-2-371-382.

For citation: Ivanov Yu. F., Eresko S. P., Klopotov A. A., Rygina M. E., Petrikova E. A., Teresov A. D. Structural-phase state and properties of hypereutectic silumin treated with a pulsed electron beam. *Siberian Aerospace Journal*. 2021, Vol. 22, No. 2, P. 371–382. Doi: 10.31772/2587-6066-2021-22-2-371-382.

Структурно-фазовое состояние и свойства заэвтектического силумина, обработанного импульсным электронным пучком*

Ю. Ф. Иванов¹, С. П. Ереско^{2**}, А. А. Клопотов³, М. Е. Рыгина^{1,4},
Е. А. Петрикова¹, А. Д. Тересов¹

¹Институт сильноточной электроники СО РАН

Российская Федерация, 634055, г. Томск, просп. Академический, 2/3

²Сибирский государственный университет науки и технологий имени академика М. Ф. Решетнева
Российская Федерация, 660037, г. Красноярск, просп. им. газ. «Красноярский рабочий», 31

³Томский государственный архитектурно-строительный университет
Российская Федерация, 634003, г. Томск, пл. Соляная, 2

⁴Национальный исследовательский Томский политехнический университет
Российская Федерация, 634055, г. Томск, ул. Ленина, 34

**E-mail: eresko07@mail.ru

Силумины заэвтектического состава являются перспективными современными материалами широкого назначения (машиностроение, авиация, приборостроение, медицина и т. д.). Недостатками заэвтектических силуминов, существенно ограничивающих сферу их применения, являются поры и раковины, крупные (порядка 100 мкм) включения вторых фаз пластинчатой и игольчатой формы. В результате выполненных в работе исследований продемонстрирована возможность формирования в поверхностном слое силумина структурно-фазовых состояний, размер и морфология кристаллитов которых может целенаправленно изменяться в пределах от десятков микрометров до десятков нанометров. Выявлены режимы облучения, позволяющие более чем в 5 раз повысить микротвердость (15 Дж/см², 150 мкс, 0,3 с⁻¹, 5 имп.) и более чем в 3 раза повысить износостойкость (50 Дж/см², 150 мкс, 0,3 с⁻¹, 5 имп.) силумина.

Ключевые слова: силумин заэвтектического состава, импульсный электронный пучок, структура, износостойкость, твердость.

Structural-phase state and properties of hypereutectic silumin treated with a pulsed electron beam

Yu. F. Ivanov¹, S. P. Eresko^{2**}, A. A. Klopotov³, M. E. Rygina^{1,4},
E. A. Petrikova¹, A. D. Teresov¹

* Работа выполнена при финансовой поддержке гранта РФФИ (проект № 19-52-04009).

The work was carried out with the financial support of the RFBR grant (project No. 19-52-04009).

¹Institute of High Current Electronics (IHCE) of the Siberian Branch of the Russian Academy of Sciences
2/3, Akademicheskii Av., Tomsk, 634055, Russian Federation

²Reshetnev Siberian State University of Science and Technology
31, Krasnoyarskii rabochii prospekt, Krasnoyarsk, 660037, Russian Federation

³Tomsk State University of Architecture and Building
2, Solyanaya Sq., Tomsk, 6340032, Russian Federation

⁴National Research Tomsk State University
36, Lenin Av., Tomsk, 634050, Russian Federation

**E-mail: eresko07@mail.ru

Hypereutectic silumin composition are promising modern materials of wide application (mechanical engineering, aviation, instrumentation, medicine, etc.). Disadvantages of hypereutectic silumin, significantly limiting their scope of application, are pores and cavities, large (about 100 μm) inclusions of lamellar and needle-shaped second phases. As a result of the studies carried out in this work, the possibility of forming structural-phase states in the surface layer of silumin, the size and morphology of which can purposefully change in the range from tens of micrometers to tens of nanometers, is demonstrated. The irradiation modes that allow more than 5 times to increase the microhardness (15 J/cm², 150 μs , 0.3 s⁻¹, 5 imp.) and more than 3 times to increase the wear resistance (50 J/cm², 150 μs , 0.3 s⁻¹, 5 imp.) of silumin were revealed.

Keywords: hypereutectic silumin, pulsed electron beam, structure, wear resistance, hardness.

Introduction

Silumins belong to a class of aluminum-based materials that are widely used in the aerospace industry. Silumin is an alloy of aluminum and silicon. This alloy is distinguished by its low cost, high corrosion resistance, and good casting properties. The state diagram of the Al-Si system is eutectic. There are hypoeutectic (<12 wt% Si), eutectic (\approx 12 wt% Si), hypereutectic (> 12 wt% Si) silumins. The structure of hypereutectic silumin is represented by eutectic, primary silicon grains and intermetallic compounds based on iron, aluminum and silicon. Hypereutectic silumin has a number of macro- and microdefects arising during casting and crystallization of the alloy: pores and cavities caused by high gas saturation. Most often these defects can be corrected either by using modifying additives or by changing the casting method. Various alloy casting technologies are currently under development that employ intensive cooling [1], quenching [2], as well as alloying [3-5]. These methods require costly additives; casting methods have limitations in shape and size.

Irradiation of silumin with a pulsed electron beam makes it possible to modify the structure and properties of the surface layer without using expensive additives [6–8]. In a number of works [9; 10], performed on silumins of eutectic composition, it is shown that the interaction of an electron beam with the surface of metallic materials due to ultrahigh heating and cooling rates forms a multiphase structure of the nano- and submicron size range. This contributes to an increase in hardness and wear resistance, fatigue life and many other properties of the material.

The aim of this work is to discover and analyze the regularities of the transformation of the structure and properties of hypereutectic silumin exposed to an intense pulsed electron beam of submillisecond duration of exposure.

Material and research technique

The study material was silumin of hypereutectic composition (Al-22 wt.% Si) in cast condition. The alloy was prepared in a shaft-type laboratory electric resistance furnace with silicon carbide heaters in a painted stainless steel crucible. As a charge, we used commercially pure aluminum A7 (GOST 11069-2001 [11]) and silicon Kr0 (GOST 2169-69 [12]). The alloy was made without modifying and refining the liquid metal. The technological process of alloy preparation included the following main operations: loading into the furnace and melting the calculated amount of aluminum, introducing a silicon sample into liquid aluminum (step-

wise) and dissolving it, settling the melt, removing slag, pouring. The melt preparation temperature was 800–850 °C. The melt was poured into a cold aluminum chill mold painted with a fire-resistant paint at a temperature of 820 °C. To measure the temperature of the melt, a chromel-alumel thermocouple (CA) and a direct current potentiometer of the PP type (class 0.5) were used. The resulting castings were rectangular plates 55 × 120 × 20 mm in size (excluding feeding head), from which specimens 15 × 15 × 5 mm in size were cut out for processing with a pulsed electron beam in order to analyze the structural-phase state and properties of silumin. The samples were irradiated with an intense pulsed electron beam on a “SOLO” setup [13]. Irradiation mode: the energy of accelerated electrons is 18 keV, the energy density of the electron beam is 15–50 J/cm², the pulse repetition rate is 0.3 s⁻¹, the duration of the action of the electron beam is 150 μs, the number of irradiation pulses is 3; irradiation was carried out in a residual argon atmosphere at a pressure of 0.02 Pa. The irradiation mode was selected according to thermal calculations [14].

The samples were examined by optical (μVizo-MET-221), scanning (SEM-515 Philips) and transmission (JEM-2100F) electron microscopy. Measuring of microhardness was carried out on the device PMT-3 at a load on an indenter of 0,2 N. Parameter of wear and coefficient of friction were determined on tribometer TRIBOtechnic (condition of dry friction at room temperature, counterbody - ball ИХХ15, diameter 6 mm, track diameter 4 mm, sample speed 2.5 cm/s, indenter load 10 N, number of revolutions 8000).

Research results and their discussion

The structure of the initial hypereutectic silumin is typical for this group of alloys and is characterized by the presence of primary silicon grains up to 100 μm in size, grains of Al-Si eutectics and inclusions of intermetallic phase (Fig. 1).

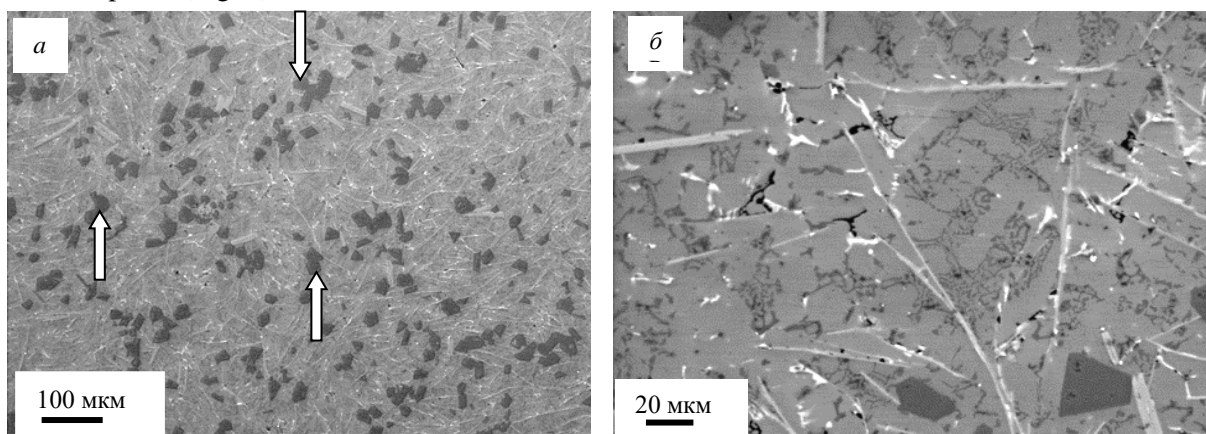


Рис. 1. Структура исходного заэвтектического силумина

Fig. 1. Structure of the initial hypereutectic silumin

The micro-X-ray spectral analysis performed by the "point-by-point" method revealed a substantially heterogeneous distribution of the alloy elemental composition. Silicon grains (Fig. 2, *a*, marked «1»), grains of Al-Si eutectics (Fig. 2, *a*, marked «2»), intermetallic inclusions of different element composition and shape (Fig. 2, *б*) were revealed.

Irradiation of silumin with a pulsed electron beam leads to a significant transformation of the structure of the surface layer of the alloy. Shown in Fig. 3 electron microscopic images illustrate the state of the surface layer of the alloy irradiated in the regime of partial (Fig. 3, *a*, *б*) and complete (Fig. 3, *в*, *г*) dissolution of inclusions of intermetallic compounds and silicon grains. It is clearly seen that in the second case, a homogeneous structure is formed with crystallite sizes varying within a few micrometers. Irradiation of silumin with a pulsed electron beam in the indicated range of energy densities does not lead to a significant change in the elemental composi-

tion of the surface layer; the concentration of alloying and impurity elements varies within the measurement error.

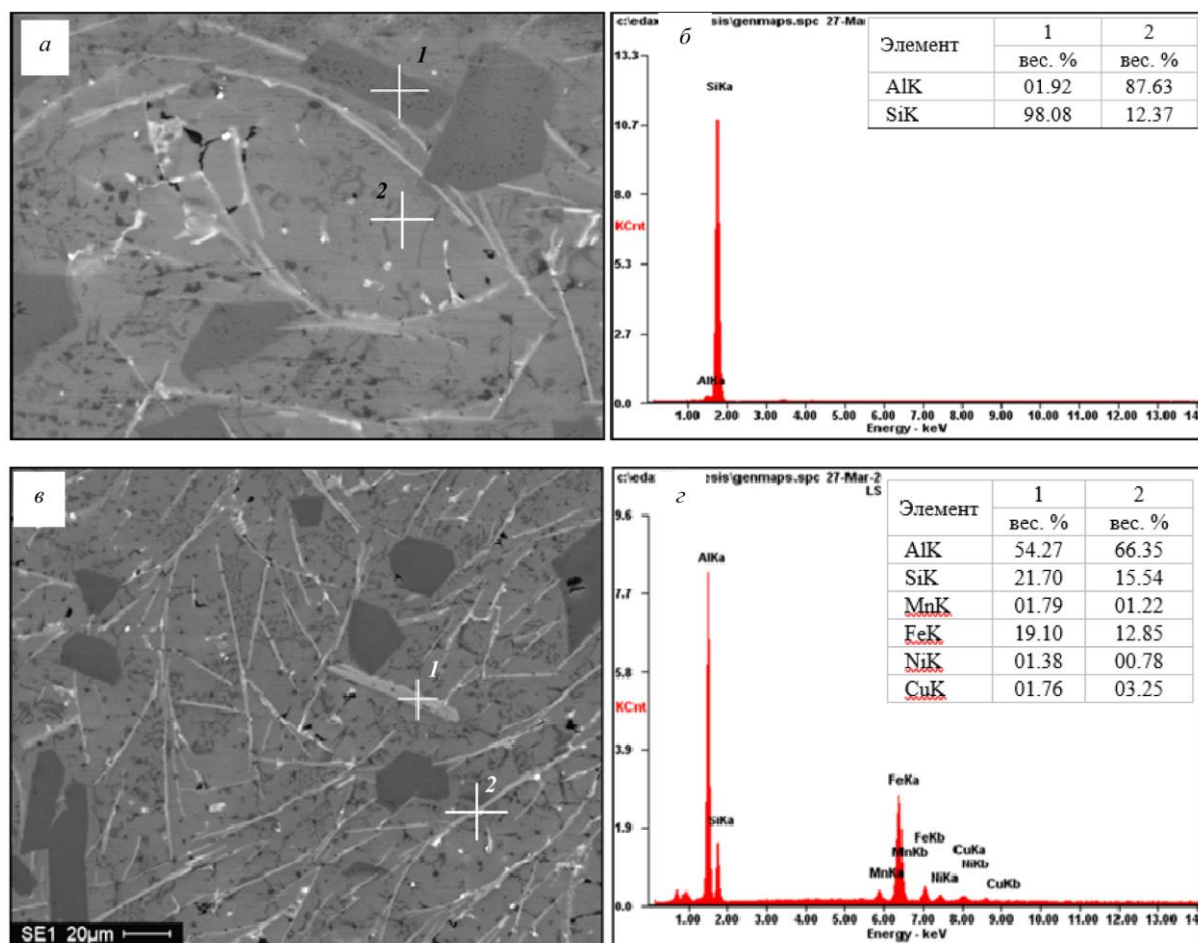


Рис. 2. Электронно-микроскопические изображения структуры силумина в литом состоянии (а, в); энергетические спектры (б, г), полученные с участков, обозначенных значком «+» и цифрой «1» (а, в). В таблицах (б, г), показан элементный состав анализируемых участков силумина

Fig. 2. Electron microscopic images of the structure of silumin in the cast state (a, v); (b, g) show the energy spectra obtained from the areas indicated in (a, v) with a "+" and the number "1". The tables given in (b) and (g) show the elemental composition of the analyzed sections of silumin

The structural-phase state of silumin at the submicro-nanodimensional level was analyzed by transmission electron microscopy. It was found that the pulse electron-beam treatment leads to a radical transformation of the structure of the surface layer of silumin. The high-speed mode of heating, melting, crystallization and cooling, which is realized during pulse electron-beam irradiation [15], leads to the formation of a cellular crystallization structure in the surface layer of the samples (Fig. 4). The size of crystallization cells varies in the range from 200 to 650 nm. The thickness of the modified layer increases with increasing energy density of the electron beam and can reach hundreds of micrometers. Along the boundaries of crystallization cells, inclusions of the second phase are located that form (at an electron beam energy density of up to 30-35 J/cm²) extensive interlayers (Fig. 4, a, б) with a thickness of 30-85 nm. At high values of energy density of electron beam in the surface layer of silumin rounded (globular) particles of the second phase are formed at the borders of cells (Fig. 4, в, arrows indicate the particles). Size of such particles is 100-180 nm. It is important to note that at the energy densities of the electron beam not exceeding 20 J/cm², in the surface layer of silumin, along with cells of high-speed crystallization, there

are primary inclusions of the second phase, formed in the material during casting (Fig. 4, *a*, inclusions are designated by numbers 1 and 2). The sizes of such inclusions can reach tens of micrometers.

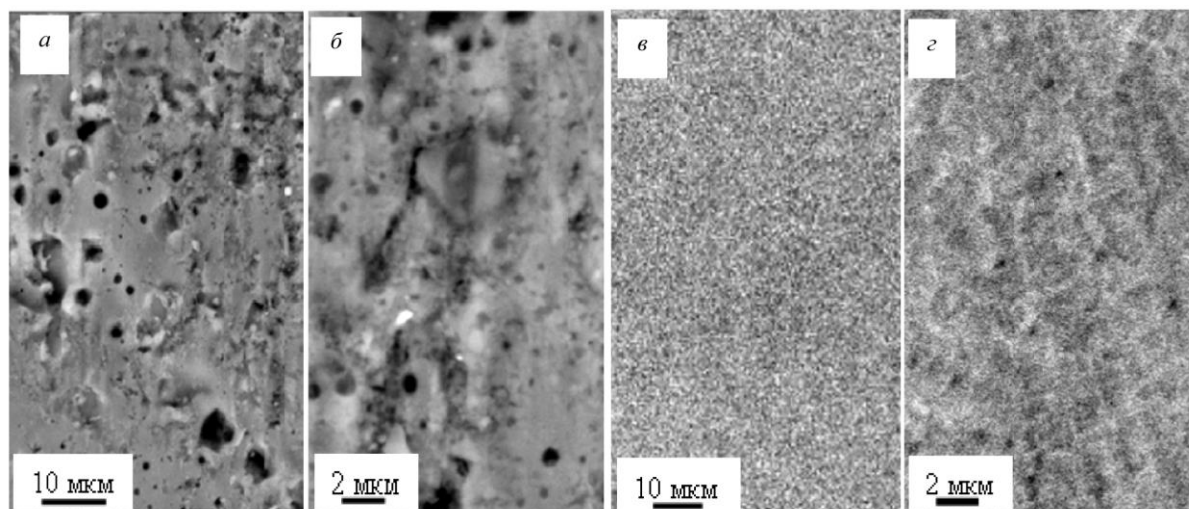


Рис. 3. Структура заэвтектического силумина, облученного импульсным электронным пучком (150 мкс, $0,3 \text{ с}^{-1}$, 3 имп): *a, б* – 15 Дж/см²; *в, з* – 50 Дж/см²

Fig. 3. Structure of hypereutectic silumin irradiated with a pulsed electron beam (150 μs , $0,3 \text{ s}^{-1}$, 3 impulses): *a, б* – 15 J/cm²; *в, з* – 50 J/cm²

It is obvious that such a significant transformation of silumin structure that takes place during irradiation with a pulsed electron beam will lead to changes in mechanical and tribological properties of the material. Indeed, studies of mechanical properties performed by determination of microhardness showed that irradiation of silumin with a pulsed electron beam contributes to hardening of the material (Fig. 5). The best result providing increase of hardness of samples more than in 5 times in comparison with cast state was reached at irradiation of silumin by electron beam with energy density of electron beam 15 J/cm².

Analysis of the structure and phase state of the modified silumin layer gives grounds to conclude that the main factors providing the revealed multiple increase in the microhardness of the samples are the presence of partially dissolved inclusions of silicon and intermetallic compounds of the initial state, as well as the formation of crystallization cells that increase the strength of aluminum grains. and Al-Si eutectics. Complete dissolution of the initial inclusions of the second phase is accompanied by a decrease in the microhardness of silumin.

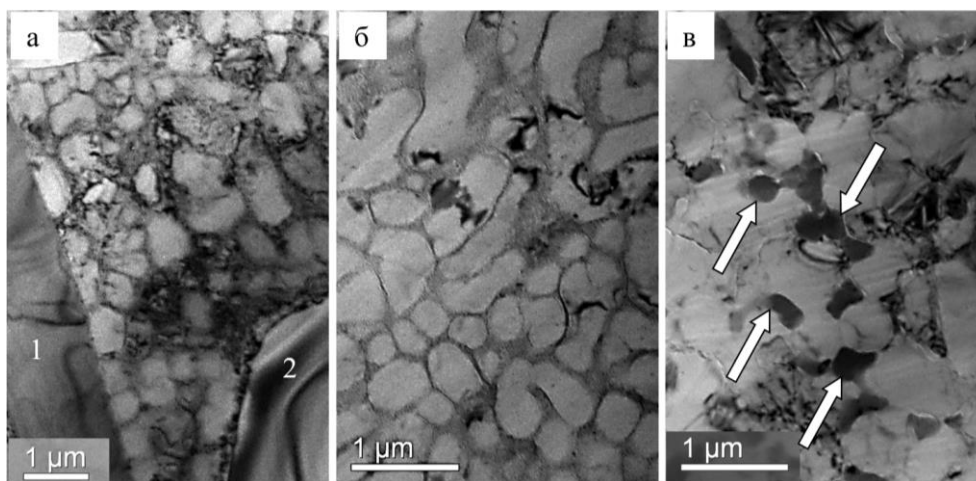


Рис. 4. Электронно-микроскопическое изображение структуры поверхностного слоя образцов силумина, облученных импульсным электронным пучком (150 мкс, $0,3 \text{ с}^{-1}$, 3 имп.): а – 15 Дж/см^2 ; б – 25 Дж/см^2 , в – 40 Дж/см^2 . На (а) цифрами обозначены включения второй фазы микронных размеров, образовавшиеся в процессе литья; на (б) стрелками указаны частицы второй фазы субмикронных размеров, образовавшиеся в результате облучения силумина электронным пучком. Просвечивающая электронная микроскопия

Fig. 4. Electron microscopic image of the structure of the surface layer of silumin samples irradiated with a pulsed electron beam ($150 \mu\text{s}$, $0,3 \text{ s}^{-1}$, 3 pulses): а – 15 J/cm^2 ; б – 25 J/cm^2 , в – 40 J/cm^2 . On (а) the numbers indicate inclusions of the second phase of micron dimensions, formed during the casting process; in (б), arrows indicate the particles of the second phase of submicron sizes, formed as a result of irradiation of silumin with an electron beam. Transmission electron microscopy

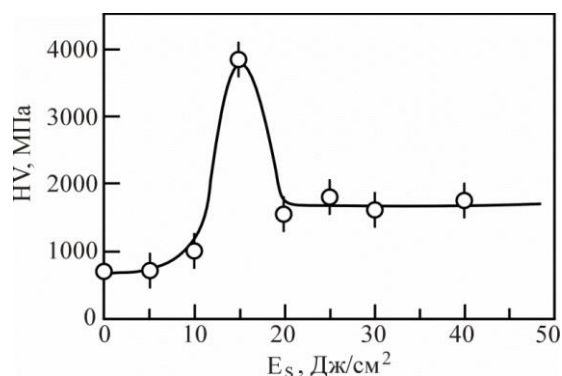


Рис. 5. Зависимость микротвердости силумина, облученного электронным пучком, от плотности энергии пучка электронов (150 мкс, 3 имп., $0,3 \text{ с}^{-1}$)

Fig. 5. Dependence of the microhardness of silumin irradiated with an electron beam on the energy density of the electron beam ($150 \mu\text{s}$, 3 pulses, $0,3 \text{ s}^{-1}$)

The microhardness of the modified layer exceeds the microhardness of the cast state by more than 2 times (Fig. 5).

Облучение силумина сопровождается существенным преобразованием трибологических свойств материала. Установлено, что при увеличении плотности энергии пучка электронов происходит снижение износа (повышение износостойкости) (рис. 6, а) и уменьшение коэффициента трения (рис. 6, б). Основываясь на результатах структурно-фазового анализа силумина, рассмотренных выше, можно заключить, что увеличение износостойкости силумина обусловлено, во-первых,

растворением зерен первичного кремния, являющегося хрупкой фазой, которая в процессе трения выкрашивается и приводит к дополнительному изнашиванию материала. Во-вторых, повторным выделением частиц второй фазы субмикро- наноразмерного диапазона. В-третьих, формированием структуры ячеистой кристаллизации, упрочняющей зерна алюминия и эвтектики Al-Si.

Irradiation of silumin is accompanied by a significant transformation of the tribological properties of the material. It was found that with an increase in the energy density of the electron beam, there is a decrease in wear (increase in wear resistance) (Fig. 6, *a*) and a decrease in the friction coefficient (Fig. 6, *b*). Based on the results of the structural-phase analysis of silumin discussed above, it can be concluded that an increase in the wear resistance of silumin is due, first, to the dissolution of grains of primary silicon, which is a brittle phase, which crumbles during friction and leads to additional wear of the material. Second, it is due to the repeated separation of particles of the second phase of the submicro-nanoscale range and, third, to the formation of a cellular crystallization structure that strengthens the grains of aluminum and Al-Si eutectic.

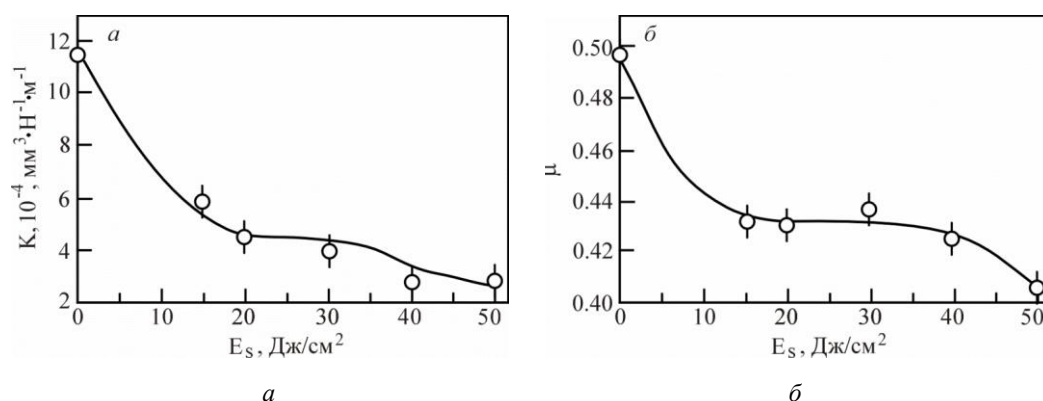


Рис. 6. Зависимость параметра износа (*a*) и коэффициента трения (*б*) силумина, облученного импульсным электронным пучком, от плотности энергии пучка электронов (150 мкс, 3 имп., 0,3 с⁻¹)

Fig. 6. Dependence of the wear parameter (*a*) and the friction coefficient (*b*) of a silumin irradiated with a pulsed electron beam on the energy density of the electron beam (150 μ s, 3 pulses, 0.3 s⁻¹)

Ternary systems Al-Cu-Si, Al-Cu-Fe, Al-Fe-Si and Cu-Fe-Si

On the basis of the literature data, an analysis of the structural features of the ternary diagrams of the Al-Cu-Si, Al-Cu-Fe, Al-Fe-Si and Cu-Fe-Si systems has been carried out.

In the Al-Cu-Si ternary system inside the isothermal triangle, the existence of only one ternary compound based on the *k*-phase was found (prototype Mg, Pearson's symbol *hP2*). A ternary solid solution with a wide homogeneity region based on Cu (Al, Si) is formed in the region of the copper corner [16; 17]. Also in this system, the existence of a phase with a noticeable size homogeneity region based on the γ_1 -phase (Cu₉Al₄), in which the third component Si is well dissolved, is observed. Only on one side of the Al-Cu isothermal triangle is the formation of ternary compounds with narrow regions of homogeneity based on binary compounds.

In [18] the formation of a ternary solid solution with a wide area of homogeneity based on Cu(Al,Fe) in the ternary system Al-Cu-Fe in the area of the copper angle was revealed. The β -Fe_xCu_yAl_z (CsCl, *cP8*) ($0 < x < 1$, $0 < y < 1$, $0.23 < x < 0.7$) phase occupies a significant area in the isothermal triangle [18; 19]. Also within the isothermal triangle, the formation of about six ternary compounds has been established: Ψ -FeCu₂Al₆ (prototype Mg₂₃(Al,Zn)₄₉, Pearson's symbol *cI62*ω-FeCu₂Al₇ (Al₇Cu₂Fe, *tP40*), Φ -FeCu₁₀Al₁₀ (δ -Ni₂Al, *hP5*), τ_2 -FeCu₂Al₇ (Al₇Cu₂Fe, *tP40*), τ_3 -FeCu₁₀Al₇ (Al₇Cu₂Fe, *tP40*), τ_1 -Fe_{12,5}Cu_{25,5}Al₆₂ (Mg₂₃(Al,Zn)₄₉, *cI62*). In addition, on the sides of the Al-Cu and Cu-Fe isothermal triangle up to 9 compounds based on binary compounds with small areas of homogeneity are formed [18; 19].

Basing on the data presented, it can be concluded that in a ternary solid solution with a wide range of homogeneity based on Cu(Al, Si), good dissolution of the fourth component Fe should occur.

In the Al-Fe-Si ternary system in the Fe region of the isothermal triangle angle, there are two regions of a ternary solid solution based on a disordered bcc lattice α -(Fe, Al, Si) and on the basis of a disordered fcc lattice γ -(Fe, Al, Si) [20–22]. The two-component compound FeSi ($P2_13$, $cP8$) dissolves the third component Al well and, as a result, an extended region of homogeneity of the ternary compound $\text{FeSi}_{1-x}\text{Al}_x$ is created. A characteristic feature of this system inside the isothermal triangle is the formation of about 10 intermetallic ternary compounds with narrow regions of homogeneity: τ_1/τ_1 , $\text{Fe}_3\text{Al}_2\text{Si}_3$ ($\text{Fe}_3\text{Al}_2\text{Si}_3$, $aP16$), τ_2 γ - $\text{Fe}_2\text{Al}_5\text{Si}_2$ (mC^*), τ_3 , $\text{Fe}_5\text{Al}_9\text{Si}_5$ (FeAl_2Si , $oC128$), τ_4 , δ - FeAl_3Si_3 (PdGa_5 , $tI24$), τ_5 , $\text{Fe}_2\text{Al}_{7.4}\text{Si}$ ($\text{Fe}_2\text{Al}_{7.4}\text{Si}$, $hP245$), τ_6 , β - $\text{Fe}_2\text{Al}_9\text{Si}_2$ ($\text{Fe}_2\text{Al}_9\text{Si}_2$, $C2/c$), τ_7 , $\text{Fe}_{22}\text{Al}_{40}\text{Si}_{38}$ ($\text{Fe}_2\text{Al}_3\text{Si}_3$, $P2_1/c$), τ_8 , $\text{Fe}_3\text{Al}_2\text{Si}_4$ ($\text{Fe}_3\text{Al}_2\text{Si}_4$, $oC36$), τ_{10} , $\text{Fe}_5\text{Al}_{12}\text{Si}_3$ ($\text{Mn}_3\text{Al}_{10}$, $hP26$).

In the ternary system Cu-Fe-Si, no ternary intermetallic compounds were found inside the isothermal triangle. Only in the region of the Fe angle of the isothermal triangle there is a region of a ternary solid solution based on α -(Fe,Cu,Si) phase [23].

The presented data show that as a result of high-energy exposure in the mode of high-speed melting in the surface layer of the alloy under study, it is possible to form a large number of double, ternary (possibly four-component) compounds based on copper Cu (Al, Si, Fe).

Conclusion

It is shown that irradiation of samples of hypereutectic silumin with a pulsed electron beam makes it possible, depending on the energy density of the electron beam, to form structural-phase states in the surface layer, the crystallite size of which can purposefully vary from tens of micrometers to tens of nanometers. The irradiation mode (15 J/cm², 150 μs , 0.3 s⁻¹, 3 impulses) was revealed, which makes it possible to increase the hardness of the modified material many times (more than 5 times). It was concluded, based on structural and phase studies of silumin, that the condition for a multiple increase in the microhardness of samples is the presence of partially dissolved inclusions of silicon and intermetallic compounds of the initial state, as well as the formation of crystallization cells that increase the strength of aluminum grains and Al-Si eutectic. It was found that an increase in the energy density of the electron beam in the range of 15–50 J/cm² (150 μs , 0.3 s⁻¹, 3 pulses) promotes an increase in wear resistance and a decrease in the friction coefficient of silumin irradiated with a pulsed electron beam. This is due, firstly, to the dissolution of grains of primary silicon, which is a brittle phase, which crumbles during friction and leads to additional wear of the material; secondly, to the repeated separation of particles of the second phase of the submicro-nanoscale range and, thirdly, to the formation of a cellular crystallization structure that strengthens the grains of aluminum and Al-Si eutectic.

Библиографические ссылки

1. Władysław R., Kozuń A., Dębowska K., Pacyniak T. Analysis of Crystallization Process of Intensive Cooled AlSi20CuNiCoMg Alloy // Archives of foundry engineering. 2017. Vol. 17(2). P. 137–144.
2. Марукович Е. А. Стеценко В. Ю. Получение отливок из заэвтектического силумина методом литья закалочным затвердеванием // Литье и металлургия. 2005. № 2(34). P. 142–144.
3. Piatkowska J., Wieszalab R. Tribological Properties of AlSi17Cu5Mg Alloy Modified with CuP Master Alloy with Various Speeds of Friction // Archives of foundry engineering. 2016. Vol. 16. P. 45–48.

4. Szymczak T., Gumienny G., Pacyniak T. Effect of Sr and Sb Modification on the Microstructure and Mechanical Properties of 226 Silumin Pressure Casts // Archives of foundry engineering. 2015. Vol. 15(1). P. 105–108.
5. Roik T. A., Gavrysh O. A., Vitsiuk Y. Y. The Functional Properties Acquired by Antifriction Composites Produced from Silumin Grinding Waste // Powder metallurgy and metal ceramics. 2019. Vol. 57, № 9–10. P. 526–532.
6. Modification of hypereutectic Al–20 wt%Si alloy based on the addition of yttrium and Al–5Ti–1B modifiers mixing melt / Qinglin Li, Binqiang Li, Jianjun Liu et al. // International Journal of Metalcasting. 2019. Vol. 13. P. 367–383.
7. Афанасьев В. К., Прудникова А. Н. Влияние обработки расплава на структуру и прочность промышленного заэвтектического силумина // Вестник ТГУ. 1998. № 3(3). С. 314.
8. Мартюшев Н. В., Зыкова А. П., Башев В. С. Модифицирование сплава марки АК12 частицами ультрадисперсного порошка вольфрама // Обработка металлов (технология, оборудование, инструменты). 2017. № 3 (76). С. 51–58.
9. Модификация структуры и свойств эвтектического силумина электронно-ионно-плазменной обработкой / под ред. А. П. Ласковнева. Минск : Беларус. навука, 2013. 287 с.
10. Электронно-ионно-плазменная модификация поверхности цветных металлов и сплавов / под ред. Н. Н. Коваля и Ю. Ф. Иванова. Томск : НТЛ, 2016. 312 с.
11. ГОСТ 11069–2001. Алюминий первичный. Марки. М. : Изд-во стандартов. 2008. 6 с.
12. ГОСТ 2169–69. Кремний технический. М. : Изд-во стандартов. 2001. 6 с.
13. Коваль Н. Н., Иванов Ю. Ф. Наноструктурирование поверхности металлокерамических и керамических материалов при импульсной электронно-пучковой обработке // Известия вузов. Физика. 2008. Т. 51, № 5. С. 60–70.
14. Численное моделирование температурного поля силумина, облученного интенсивным электронным пучком / Ю. Ф. Иванов, Е. А. Петрикова, О. В. Иванова и др. // Известия вузов. Физика. 2015. Т. 58, № 4. С. 46–51.
15. Модификация поверхностных слоев металлических материалов низкоэнергетическими сильноточными электронными пучками / В. П. Ротштейн, Д. И. Проскуровский, Г. Е. Озур, Ю. Ф. Иванов. Новосибирск : Наука, 2019. 348 с.
16. Ponweiser N., Richter K.W. New investigation of phase equilibria in the system Al-Cu-Si // J. Alloys and Compound. 2012. Vol. 512. P. 252–263.
17. Experimental investigation and thermodynamic modeling of the Al-Cu-Si system / C. Y. He, Y. Du, H. L. Chen et. al. // CALPHAD: Computer Coupling of Phase Diagrams and Thermochemistry. 2009. Vol. 33. P. 200–210.
18. Диаграммы состояния двойных и многокомпонентных систем на основе железа: Справочник / О. А. Банных, П. Б. Будберг, С. П. Алисова и др. М. : Металлургия, 1986. 440 с.
19. Zhang L. M., Lück R. Phase diagram of the Al-Cu-Fe quasicrystal-forming alloy system. III. Isothermal sections // International Journal of Materials Research. 2003. Vol. 94. P. 108–115.
20. A thermodynamic description of the Al-Fe-Si system over the whole composition and temperature ranges via a hybrid approach of CALPHAD and key experiments / Y. Du, J. C. Schuster, Z. K. Liu et. al. // Intermetallics. 2008. Vol. 16. P. 554–570.
21. Dons A. L. AlFeSi-particles in commercial pure aluminum // Zeitschrift für Metallkunde. 1984. Vol. 75. P. 170–174.
22. Miyazaki T., Kozakai T., Tsuzuki T. Phase decomposition of Al-Si-Fe ordered alloys // J. Materials Science. 1986. Vol. 21. P. 2557–2564.

23. Phase equilibria in FeCu-X (X: Co,Cr,Si,V) ternary systems / C. P. Wang, X. J. Liu, I. Ohnuma et. al. // J. Phase Equilibria. 2002. Vol. 23, № 3. P. 236–245.

Refereces

1. Władysław R., Kozuń A., Dębowska K., Pacyniak T. Analysis of Crystallization Process of Intensive Cooled AlSi20CuNiCoMg Alloy. Archives of foundry engineering. 2017. Vol. 17(2). P. 137–144.
2. Marukovich E. A. Stetsenko V. Yu. *Poluchenie-otlivok-iz-zaehvtekticheskogo-silumina-metodom-litya-zakalochnym-zatverdevaniem* [Production of castings from hypereutectic silumin by quenching solidification casting]. Casting and metallurgy. 2005. No. 2(34). P. 142–144.
3. Piatkowskia J., Wieszałab R. Tribological Properties of AlSi₁₇Cu₅Mg Alloy Modified with CuP Master Alloy with Various Speeds of Friction. Archives of foundry engineering. 2016. Vol. 16. P. 45–48.
4. Szymczak T., Gumienny G., Pacyniak T. Effect of Sr and Sb Modification on the Microstructure and Mechanical Properties of 226 Silumin Pressure Casts. Archives of foundry engineering. 2015. Vol. 15(1). P. 105–108.
5. Roik T. A., Gavrysh O. A., Vitsiuk Y. Y. The Functional Properties Acquired by Antifriction Composites Produced from Silumin Grinding Waste. Powder metallurgy and metal ceramics. 2019. Vol. 57, No. 9-10. P. 526–532.
6. Qinglin Li, Binqiang Li, Jianjun Liu, Jinbao Li, Dexue Liu, Yefeng Lan, and Tiandong Xia Modification of hypereutectic Al–20 wt%Si alloy based on the addition of yttrium and Al–5Ti–1B modifiers mixing melt// International Journal of Metalcasting. 2019. Vol. 13. P. 367–383.
7. Afanasyev V. K., Prudnikova A. N. *Vliyanie obrabotki rasplava na strukturu i prochnost' promyshlennogo zaehtekticheskogo silumina* [Effect of melt treatment on the structure and strength of industrial hypereutectic silumin]. Bulletin of TSU. 1998. T. 3(3). P. 314.
8. Martyshev N. V., Zyкова A. P., Bashev V. S. *Modificirovanie splava marki AK12 chasticami ul'tradispersnogo poroshka vol'frama*. [Modification of the AK12 alloy with ultrafine tungsten powder particles] Metal processing (technology, equipment, tools). 2017. No. 3 (76). P. 51–58.
9. *Modifikaciya struktury i svojstv evtekticheskogo silumina elektronno-ionno-plazmennoj obrabotkoj* [Modification of the structure and properties of eutectic silumin by electron-ion-plasma treatment] / edited by A. P. Laskovnev. Minsk, Belarus. navuka, 2013, 287 c.
10. *Elektronno-ionno-plazmennaya modifikaciya poverhnosti cvetnyh metallov i splavov* [Electron-ion-plasma modification of the surface of non-ferrous metals and alloys]. Ed. N. N. Koval and Yu. F. Ivanov. Tomsk, NTL, 2016, 312 p.
11. *GOST 11069–2001. Alyuminij pervichnyj. Marki* [GOST 11069–2001. Primary aluminum. Stamps]. Moscow, Standartinform Publ., 2008, 6 p.
12. *GOST 2169–69. Kremnij tekhnicheskij*. [GOST 2169–69. Technical silicon.] Moscow, Standartinform Publ., 2001, 6 p.
13. Koval N. N., Ivanov Yu. F. Nanostructuring of surfaces of metalloceramic and ceramic materials by electron-beams. *Russian Physics. Journal*. 2008. Vol. 51. P. 505–516.
14. Ivanov Yu. F., Petricova E. A., Ivanova O. V. and et. al. Numerical Simulation of the Temperature Field of Silumin. *Russian Physics. Journal*. 2015. Vol. 58. P. 478–484.
15. Rotshtein V. P., Proskurovsky D. I., Ozur G. E., Ivanov Yu. F. *Modifikaciya poverhnostnykh sloev metallicheskih materialov nizkoenergeticheskimi sil'notochnymi elektronnyimi puchkami*. [Modification of

the surface layers of metallic materials by low-energy high-current electron beams]. Novosibirsk, SB RAS, Nauka, 2019, 348 p.

16. Ponweiser N., Richter K. W. New investigation of phase equilibria in the system Al-Cu-Si. *J. Alloys and Compound*. 2012. Vol. 512. P. 252–263.

17. He C. Y., Du Y., Chen H. L. and et. al. Experimental investigation and thermodynamic modeling of the Al-Cu-Si system. *CALPHAD: Computer Coupling of Phase Diagrams and Thermochemistry*. 2009. Vol. 33. P. 200–210.

18. Bannykh O. A., Budberg P. B., Alisova S. P. and et. al. *Diagrams of the state of dual and multicomponent systems based on iron: Reference* [Diagrammy sostoyaniya dvoynyh i mnogokomponentnyh sistem na osnove zheleza: Spravochnik]. Moscow, Metallurgy, 1986, 440 p.

19. Zhang L. M., Lück R. Phase diagram of the Al-Cu-Fe quasicrystal-forming alloy system. III. Isothermal sections. *International Journal of Materials Research*. 2003. Vol. 94. P. 108–115.

20. Du Y., Schuster J. C., Liu Z. K. and et. al. A thermodynamic description of the Al-Fe-Si system over the whole composition and temperature ranges via a hybrid approach of CALPHAD and key experiments. *Intermetallics*. 2008. Vol. 16. P. 554–570.

21. Dons A. L. AlFeSi – particles in commercial pure aluminum. *Zeitschrift für Metallkunde*. 1984. Vol. 75. P. 170–174.

22. Miyazaki T., Kozakai T., Tsuzuki T. Phase decomposition of Al-Si-Fe ordered alloys. *J. Materials Science*. 1986. Vol. 21. P. 2557–2564.

23. Wang C. P., X. J. Liu, I. Ohnuma and et. al. Phase equilibria in FeCu-X (X: Co, Cr, Si, V) ternary systems. *J. Phase Equilibria*. 2002. Vol. 23. No. 3. P. 236–245.

© Иванов Ю. Ф., Ереско С. П., Клопотов А. А., Рыгина М. Е.,
Петрикова Е. А., Тересов А. Д., 2021

Иванов Юрий Федорович – доктор физико-математических наук, доцент, главный научный сотрудник; лаборатория плазменной эмиссионной электроники Института сильноточной электроники Сибирского отделения Российской академии наук (ИСЭ СО РАН). E-mail: yufi55@mail.ru.

Ереско Сергей Павлович – доктор технических наук, профессор, заслуженный изобретатель Российской Федерации, профессор; Сибирский государственный университет науки и технологий имени академика М. Ф. Решетнева. E-mail: eresko07@mail.ru.

Клопотов Анатолий Анатольевич – доктор физико-математических наук, профессор; Томский государственный архитектурно-строительный университет. E-mail: klopotovaa@tsuab.ru.

Рыгина Мария Евгеньевна – аспирант; Томский политехнический университет; мл. науч. сотр., лаборатория плазменной эмиссионной электроники Института сильноточной электроники Сибирского отделения Российской академии наук (ИСЭ СО РАН). E-mail: L-7755me@mail.ru.

Петрикова Елизавета Алексеевна – мл. науч. сотр.; лаборатория плазменной эмиссионной электроники Института сильноточной электроники Сибирского отделения Российской академии наук (ИСЭ СО РАН). E-mail: petrikova@opee.hcei.tsc.ru.

Тересов Антон Дмитриевич – науч. сотр.; лаборатория плазменной эмиссионной электроники Института сильноточной электроники Сибирского отделения Российской академии наук (ИСЭ СО РАН). E-mail: tad514@yandex.ru.

Ivanov Yuriy Fedorovich – Dr. Sc., assistant professor, senior scientist, main scientific of IHCE RAS, Institute of High Current Electronics (IHCE), Siberian Branch, Russian Academy of Sciences. E-mail: yufi55@mail.ru.

Eresko Sergey Pavlovich – Dr. Sc., Honored Inventor, professor, Siberian State University of Science and Technology. E-mail: eresko07@mail.ru.

Klopotov Anatoly Anatolyevich – Dr. Sc., professor, Tomsk State University of Architecture and Building. E-mail: klopotovaa@tsuab.ru.

Rygina Maria Evgenievna – post-graduate student; Tomsk Polytechnic University, junior researcher, Institute of High Current Electronics (IHCE), Siberian Branch, Russian Academy of Sciences. E-mail: L-7755me@mail.ru.

Petrikova Elizaveta Alekseevna – junior researcher, Institute of High Current Electronics (IHCE), Siberian Branch, Russian Academy of Sciences. E-mail: petrikova@opee.hcei.tsc.ru.

Teresov Anton Dmitrievich – researcher, Institute of High Current Electronics (IHCE), Siberian Branch, Russian Academy of Sciences. E-mail: tad514@yandex.ru.

УДК 538.9

Doi: 10.31772/2712-8970-2021-22-2-383-390

Для цитирования: Назарова З. И., Назаров А. Н. Прогнозирование образования конкурирующих фаз при росте тонких плёнок Cr_2GaC на $\text{MgO}(111)$ // Сибирский аэрокосмический журнал. 2021. Т. 22, № 2. С. 383–390. Doi: 10.31772/2712-8970-2021-22-2-383-390.

For citation: Nazarova Z. I., Nazarov A. N. Prediction of formation of competing phases during the growth of Cr_2GaC THIN FILMS ON $\text{MgO}(111)$. *Siberian Aerospace Journal*. 2021, Vol. 22, No. 2, P. 383–390. Doi: 10.31772/2712-8970-2021-22-2-383-390.

Прогнозирование образования конкурирующих фаз при росте тонких пленок Cr_2GaC на $\text{MgO}(111)$ *

З. И. Назарова^{1, 2**}, А. Н. Назаров^{1, 2}

¹Институт физики имени Л. В. Киренского СО РАН –
обособленное подразделение ФИЦ КНЦ СО РАН

Российская Федерация, 660036, г. Красноярск, Академгородок, 50, стр. 38

²Сибирский федеральный университет

Российская Федерация, 660041, Красноярский край, г. Красноярск, просп. Свободный, 79

**E-mail: jercompany@gmail.com

МАХ-фазы представляют собой семейство тройных слоистых соединений с формальной стехиометрией $M_{n+1}AX_n$ ($n = 1, 2, 3...$), где M – переходный d -металл; A – p -элемент (например, Si , Ge , Al , S , Sn и др.); X – углерод или азот [1]. Слоистые тройные карбиды и нитриды d - и p -элементов (МАХ-фазы) проявляют уникальное сочетание свойств, характерных как для металлов, так и для керамики, что делает их применение перспективным в космической отрасли в качестве различных покрытий. Получение требуемых свойств МАХ-фаз зависит от технологических условий синтеза материала. Для этого необходимо тщательное теоретическое моделирование взаимодействия элементов на границе раздела. Одновременный рост конкурирующих фаз наряду с МАХ-фазой может происходить из-за выгоды образования конкурирующих фаз, а также из-за более низкоэнергетического интерфейса с подложкой по сравнению с МАХ-фазой. В данной работе мы изучаем термодинамическую выгоду конкурирующих фаз и МАХ-фазы Cr_2GaC в зависимости от химического состава потока атомов. Для изучения этих соединений было необходимо рассмотреть систему Cr-Ga-C . Согласно модели эффективной теплоты образования каждую реакцию образования некоторой фазы можно охарактеризовать энтальпией [2]. Для выяснения наиболее выгодных к формированию фаз было необходимо произвести расчёт энтальпии для всех возможных реакций. Таким образом, задача состояла в переборе всех возможных реакций между чистыми элементами, доступными в различных соотношениях, в частности, в соотношении, соответствующем заданной стехиометрии МАХ-фазы, т. е. $\text{Cr:Ga:C}=2:1:1$. Кроме того, считается, что плотность совпадающих узлов [3; 4] для границ раздела между МАХ-фазой, термодинамически выгодными конкурирующими фазами и поверхностью $\text{MgO}(111)$

* Исследования выполняются при финансовой поддержке Российского фонда фундаментальных исследований, Правительства Красноярского края, Красноярского краевого фонда науки в рамках научного проекта № 20-42-240012, Правительства РФ в рамках гранта по созданию лабораторий мирового уровня (соглашение № 075-15-2019-1886).

The research is carried out with the financial support of the Russian Foundation for Basic Research, the Government of the Krasnoyarsk Territory, the Krasnoyarsk Regional Science Foundation in the framework of the scientific project No. 20-42-240012, the Government of the Russian Federation in the framework of the grant for the creation of world-class laboratories (agreement No. 075-15-2019-1886).

показывает роль интерфейса при определении структурного качества тонкой плёнки MAX-фазы, выращенной на MgO(111).

Ключевые слова: MAX материалы, тонкие пленки, конкурирующие фазы, энтальпия образования, хром, галлий, углерод.

Prediction of formation of competing phases during the growth of Cr₂GaC thin films on MgO(111)

Z. I. Nazarova^{1, 2*}, A. N. Nazarov^{1, 2}

¹Kirensky Institute of Physics, Federal Research Center KSC SB RAS
50/38, Akademgorodok, Krasnoyarsk, 660036, Russian Federation

²Siberian Federal University
79, Svobodny Av., Krasnoyarsk, 660041, Russian Federation

*E-mail: jercompany@gmail.com

MAX-phases are a family of ternary layered compounds with the formal stoichiometry $M_{n+1}AX_n$ ($n = 1, 2, 3...$), where M is a transition d-metal; A is a p-element (for example, Si, Ge, Al, S, Sn, etc.); X is carbon or nitrogen [1]. Layered triple carbides and nitrides of d-and p-elements (MAX-phases) exhibit a unique combination of properties characteristic of both metals and ceramics, which makes their application as various coatings in space industry very promising. Obtaining the desired properties of the MAX-phases depends on the technological conditions of material synthesis. This requires thorough theoretical modelling of the elements' interaction at the interface. Concurrent growth of competing phases along with the MAX-phase may occur due to the favorability of competing phases' formation and may also be promoted by lower energy interfaces with the substrate in comparison with a MAX-phase. In this work, we study thermodynamic favorability of competing phases and Cr₂GaC MAX-phase depending on the chemical composition of the atomic flow. To study these compounds, it was necessary to consider the Cr-Ga-C system. According to the effective heat of formation model, each reaction of a certain phase formation can be characterized by enthalpy [2]. To find out the most favorable phases, it was necessary to calculate the enthalpy of all possible reactions. Thus, the task was to sort through all possible reactions between pure elements available in various ratios, in particular, in the ratio corresponding to the given MAX-phase stoichiometry, i.e. Cr:Ga:C=2:1: 1. Moreover, it is considered that the density of near-coincidence sites [3,4] for interfaces between MAX-phase, thermodynamically favourable competing phases and MgO(111) surface shows a role of the interface in the determination of the structural quality of the MAX-phase thin film grown on MgO(111).

Keyword: MAX materials, thin films, competing phases, enthalpy of formation, chromium, gallium, carbon.

Introduction

Currently, one of the most promising areas of research related to the synthesis of new materials is the study of formation processes and physical properties of MAX phases, the family of which is shown in Fig. 1. MAX-phases possess low density, high values of thermal and electrical conductivity, strength, low elastic modulus, excellent corrosion resistance in aggressive liquid media [5–7], resistance to high-temperature oxidation and thermal shock [8–10], and are also easily machined [11; 12], have a high melting point [13] and are quite stable at temperatures up to 1000 °C and above [14].

It is well known that thin films of MAX phases are mainly synthesized applying physical methods, such as magnetron sputtering of pulsed layer deposition. A comprehensive study of magnetic properties requires

high quality magnetic thin films of MAX-phases. Films of the highest quality are defined as single phase, monocrystalline and smooth.

1 18

2 13 14 15 16 17

H Li Be B C N O F Ne

Na Mg 3 4 5 6 7 8 9 10 11 12 Al Si P S Cl Ar

K Ca Sc Ti V Cr Mn Fe Co Ni Cu Zn Ga Ge As Se Br Kr

Rb Sr Y Zr Nb Mo Tc Ru Rh Pd Ag Cd I Sn Sb Te I Xe

Cs Ba Lu Hf Ta W Re Os Ir Pt Au Hg Tl Pb Bi Po At Rn

Fr Ra Lr Unq Unp Unh Uns Uno Une

М = Переходный элемент первых групп
А = Элемент группы А
Х = С или N

Рис. 1. Периодическая таблица элементов, образующих наноламинаты общего состава [2]

Fig. 1. The periodic table of the elements constituting the nanolaminates of general composition [2]

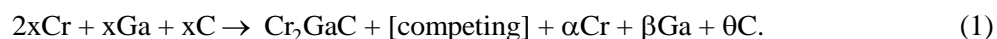
The quality of the resulting films is influenced by such factors as precipitation temperature, pressure, power supplied to magnetrons, i.e., the outgoing / incoming material flow, as well as the choice of substrate. For the synthesis of MAX phases, it is necessary to consider competing binary or ternary phases that are close in composition and / or structure.

The growth of the Cr_2GaC epitaxial film is accompanied by the growth of the Cr_3Ga phase, which is not predicted to be competitive in terms of stoichiometric chemical composition [15]. Substrate, in turn, can radically change the situation, as is observed in the case of Mn_2GaC . Under the same growth conditions, there was no visible signal of the MAX phase on any substrate other than MgO [15].

Thus, our task is to consider the effect of a change in the stoichiometry of the atomic flux on the thermodynamic advantage of phase formation, and also to take into account the role of the interfaces between the substrate and the MAX phase and competing phases.

Results and discussions

In this work, we study the MAX phase of Cr_2GaC . To study this compound, it is necessary to consider the Cr-Ga-C system. The challenge is to consider all possible reactions between pure elements available in varying quantities. Below is an example of the reaction.



In this example, pure elements are available in quantities corresponding to the stoichiometry of the MAX phase, i.e. Cr: Ga: C = 2: 1: 1 on the right-hand side of the equation; the coefficients at the remainder of pure elements are symbolised by Greek letters. The competing phase can be any of seven possible phases in the Cr-Ga-C system: CrGa_4 , Cr_5Ga_6 , CrGa , Cr_3Ga , Cr_3C_2 , Cr_7C_3 , or Cr_{23}C_6 .

The enthalpy of one specific reaction was calculated not only in the case of elements presence in quantities corresponding to the stoichiometry of the MAX-phase, i.e. Cr: Ga: C = 2: 1: 1, but also for all possible ratios.

Due to the large amount of calculations required, it was decided to write a special code in the "Matlab" software package. The outer cycles are the cycles for i, j, k, which mean the atomic fractions of chromium,

gallium and carbon, respectively. When establishing the boundaries of the cycle, it was taken into account that their sum is 1. These are the cycles that are responsible for calculating the enthalpy of each specific reaction, not only in the case of the elements in quantities corresponding to the stoichiometry of the MAX-phase, i.e. Cr: Ga: C = 2: 1: 1, but also for all possible ratios. Each phase was assigned to a corresponding set of three numbers, the first of which means the number of chromium atoms in the formula unit of the compound, the second - the number of gallium atoms, the third – carbon. For example, the set 703 was assigned to the Cr₇C₃ phase, and to the Cr₃Ga – 310 phase was assigned. Thus, the netlist was transformed into a list of sets of numbers, accessing to which in the program code was reduced to accessing certain elements of the matrix. Each set of three digits also had a sequential number, which corresponds to the enthalpy of the encoded phase. The need to separately access each type of incoming into the phase atom was due to the need to calculate the atomic balance in the equation and to search for the largest coefficients for all phases in the right-hand side of the equation. The implementation of the latter in the program code was based on the idea of checking whether it is possible to form any phase in the right-hand side from the remainder of free atoms. By introducing such additional internal cycles, it was found that in some cases the phase coefficients on the right-hand side of the equation are really different from the units, i.e., from how it was written at the beginning when describing the general form of reaction equation (1).

In this paper, three different types of reactions have been considered. The types are determined by the number of different competing phases. The first type contains $C_7^1 = 7$ various reactions with a competing phase; the second type contains $C_7^2 = 21$ a different reaction, with each containing a unique pair of competing phases; the third type contains $C_7^3 = 35$ different reactions, with each containing a unique triple of competing phases. In addition, each reaction can be recorded without the MAX phase on the right side of the equation.

Since the variable parameter in the calculation model was the ratio of the three different pure elements numbers, it was agreed to present the results in the form of ternary diagrams, namely, in the form of a set of three ternary diagrams for each case (for each of the arrows in Scheme 1). Below, only results for the first and second types of reactions in the presence of the MAX-phase on the right side of the equation are given (Fig. 2, 3).

Each point on ternary diagrams in Fig. 2 corresponds to one defined ratio Cr: Ga: C. For this ratio, 7 enthalpies were calculated and compared. Then the most negative value was determined and the point was shown in the color corresponding to the competing phase, the formation of which leads to the greatest energy release. Areas and their boundaries are easily visible on the charts. This allows us to judge, for example, the experimental error in the ratio of the elements number: by comparing the expected and obtained competing phases, it is possible to determine which element was taken in excess. The third diagram (Fig. 2, *б*) shows the difference between the heats of formation of the two most thermodynamically favorable competing phases. It is noteworthy that the leading phases are the same, they only change their areas.

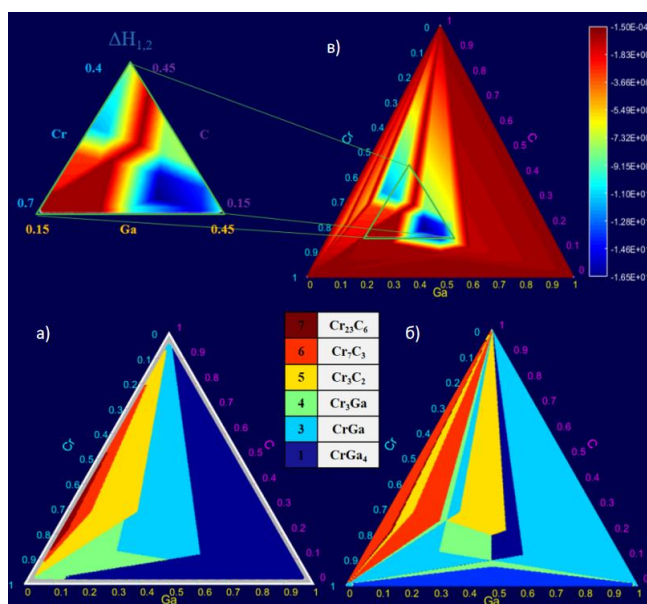


Рис. 2. Диаграммы номеров наиболее выгодных конкурирующих фаз (в случае образования МАХ-фазы и одной конкурирующей фазы):
 а – первый кандидат; б – второй кандидат; в – разница между эффективными теплотами образования (кДж/моль*атом) двух наиболее термодинамически выгодных конкурирующих фаз

Fig. 2. Diagrams of the numbers of the most favorable competing phases (in the case of the formation of the MAX-phase and one competing phase):
 (bottom left) the first candidate; (bottom right) the second candidate; (top right) the difference between the effective heat of formation (kJ/mol*atom) of the two most thermodynamically favourable competing phases

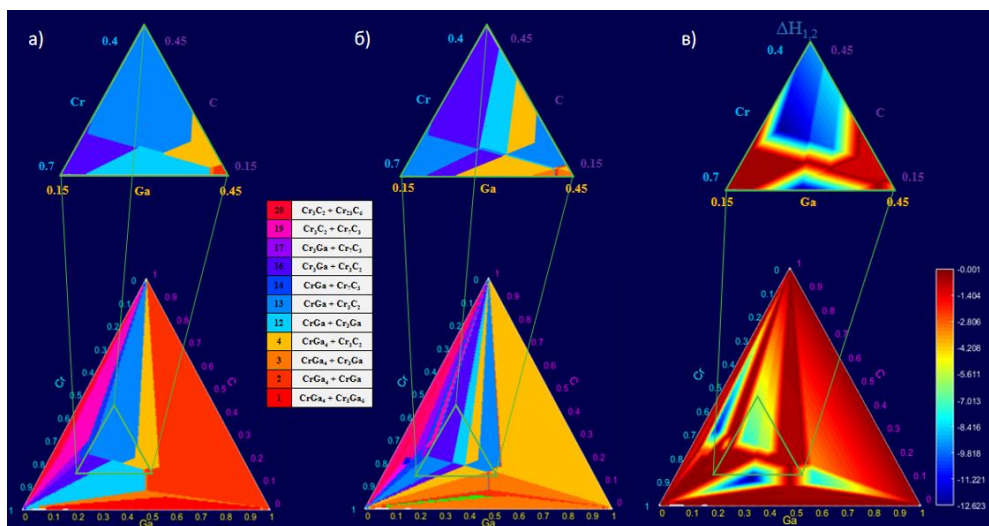


Рис. 3. Диаграммы номеров наиболее выгодных конкурирующих фаз (в случае образования МАХ-фазы и двух конкурирующих фаз):
 а – первый кандидат; б – второй кандидат; в – разница между эффективными теплотами образования (кДж/моль*атом) двух наиболее термодинамически выгодных конкурирующих фаз

Fig. 3. Diagrams of the numbers of the most favorable competing phases (in the case of the formation of the MAX-phase and two competing phases):
 (bottom left) the first candidate; (bottom right) the second candidate; (top right) the difference between the effective heat of formation (kJ/mol*atom) of the two most thermodynamically favourable competing phases

The same was done in the case of two competing phases (Fig. 3), i.e, for the second type of reactions. It can be seen that the group of leading phases remains the same again: CrGa, Cr₃Ga, Cr₃C₂, in this case we are simply dealing with their combinations.

According to the effective heat of formation model [2], one of the most significant factors influencing the formation of phases is: the larger the number of atoms in the unit cell, the more difficult the formation of the phase is (Table 1).

Table 1

Number of atoms in unit cells of different phases

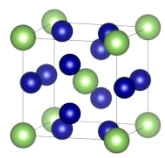
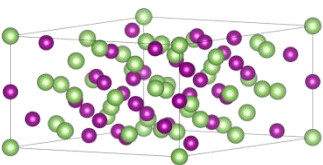
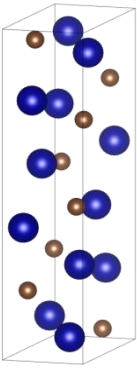
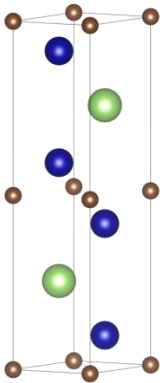
Cr ₃ Ga 21 atoms in unit cell	CrGa 92 atoms in unit cell	Cr ₃ C ₂ 20 atoms in unit cell	Cr ₂ GaC 18 atoms in unit cell
			

Table 2

Orientation relations and the density of near-coincident sites at the interface between the MAX-phase Cr₂GaC and MgO [3;4]

Interface	u11v11w11	U12v12w12	u21v21w21	u22v22w22	h1k1l1	h2k2l2	Density of near-coincident sites, R
MgO Cr ₂ GaC	[011]	[020]	[10-1]	[200]	(-11-1)	(001)	0.0418
MgO CrGa	[0-11]	[11-2]	[-1.578 – 2.989 1.071]	[4.61 1.49 4 0.0]	(-11-1)	(-5.09 2.989 0.507)	0.0545
MgO Cr ₃ Ga	[0-11]	[11-2]	[010]	[001]	(-11-1)	(001)	0.0887

In addition, consideration of the possible interface between CrGa and the surface of magnesium oxide MgO (111) applying the coincident lattice method reveals the preferability of the Cr₃Ga phase over CrGa (Table 2).

Conclusion

During the formation of magnetic thin films of MAX phases, there are only three most thermodynamically favorable phases: CrGa, Cr₃Ga, and Cr₃C₂.

Although the enthalpy of CrGa formation is most negative, according to the coincident lattice method the formation of the Cr₃Ga phase with fewer atoms is more likely in a unit cell, which has been experimentally confirmed [15].

Библиографические ссылки

1. Сметкин А. А., Майорова Ю. К. Свойства материалов на основе МАХ-фаз (обзор) // Вестник Пермского нац. исслед. политехн. ун-та. Машиностроение, материаловедение. 2015. № 17(4). С. 120–138.

2. Pretorius R., Theron C. C., Vantomme, A., Mayer J. W. Compound phase formation in thin film structures // *Critical reviews in solid state and materials sciences*. 1999. No. 24(1), P. 1–62.
3. Tarasov I. A., Visotin M. A., Kuznetzova T. V. et. al. Selective synthesis of higher manganese silicides: a new $Mn_{17}Si_{30}$ phase, its electronic, transport, and optical properties in comparison with Mn_4Si_7 // *J. Mater Sci*. 2018. No. 53. P. 7571–7594. doi: 10.1007/s10853-018-2105-y
4. Visotin M. A., Tarasov I. A., Fedorov A. S. et al. Prediction of orientation relationships and interface structures between α -, β -, γ - $FeSi_2$ and Si phases // *Acta Crystallogr Sect B Struct Sci Cryst Eng Mater*. 2020. No. 76: P. 469–482. doi: 10.1107/S2052520620005727
5. Barsoum M. W., Radovic M. Elastic and mechanical properties of the MAX phases // *Annual review of materials research*. 2011. Vol. 41. P. 195–227.
6. Sun Z. M. Progress in research and development on MAX phases: a family of layered ternary compounds // *International Materials Reviews*. 2011. Vol. 56. No. 3. P. 143–166.
7. Radovic M., Barsoum M. W. MAX phases: bridging the gap between metals and ceramics // *American Ceramics Society Bulletin*. 2013. Vol. 92, No. 3. P. 20–27.
8. Sokol M. et al. On the chemical diversity of the MAX phases // *Trends in Chemistry*. 2019. Vol. 1, No. 2. P. 210–223.
9. Barsoum M. W. MAX phases: properties of machinable ternary carbides and nitrides. John Wiley & Sons, 2013.
10. Dahlqvist M., Alling B., Rosén J. Stability trends of M A X phases from first principles // *Physical Review B*. 2010. Vol. 81, No. 22. P. 220102.
11. Hu C. et al. Nb_4AlC_3 : A new compound belonging to the MAX phases // *Scripta Materialia*. 2007. Vol. 57, No. 10. P. 893–896.
12. Tallman D. J. et al. Effect of neutron irradiation on select MAX phases // *Acta Materialia*. 2015. Vol. 85. P. 132–143.
13. Ingason A. S., Dahlqvist M., Rosén J. Magnetic MAX phases from theory and experiments; a review // *Journal of Physics: Condensed Matter*. 2016. Vol. 28, No. 43. P. 433003.
14. Медведева Н. И., Еняшин А. Н., Ивановский А. Л. Моделирование электронного строения, химической связи и свойств тройного силикокарбида Ti_3SiC_2 // *Журнал структурной химии*. 2011. № 52(4). С. 806.
15. Phase stability of $Cr_{n+1}Ga_n$ MAX phases from first principles and Cr_2GaC thin - film synthesis using magnetron sputtering from elemental targets / A. Petruhins, A. S. Ingason, M. Dahlqvist et al. // *Physica status solidi (RRL) – Rapid Research Letters*. 2013. No. 7(11). P. 971–974.

References

1. Smetkin A. A., Mayorova Yu. K. Properties of materials based on MAX-phases (review). *Bulletin of the Perm National Research Polytechnic University. Mechanical engineering, materials science*. 2015, No. 17 (4), P. 120–138 (In Russ.).
2. Pretorius R., Theron C. C., Vantomme, A., Mayer J. W. Compound phase formation in thin film structures. *Critical reviews in solid state and materials sciences*. 1999, No. 24(1), P. 1–62.
3. Tarasov I. A., Visotin M. A., Kuznetzova T. V. et. al. Selective synthesis of higher manganese silicides: a new $Mn_{17}Si_{30}$ phase, its electronic, transport, and optical properties in comparison with Mn_4Si_7 . *J. Mater Sci*. 2018, No. 53, P. 7571–7594. doi: 10.1007/s10853-018-2105-y
4. Visotin M. A., Tarasov I. A., Fedorov A. S. et al. Prediction of orientation relationships and interface structures between α -, β -, γ - $FeSi_2$ and Si phases. *Acta Crystallogr Sect B Struct Sci Cryst Eng Mater*. 2020, No. 76, P. 469–482. doi: 10.1107/S2052520620005727

5. Barsoum M. W., Radovic M. Elastic and mechanical properties of the MAX phases. *Annual review of materials research*. 2011, Vol. 41, P. 195–227.
6. Sun Z. M. Progress in research and development on MAX phases: a family of layered ternary compounds. *International Materials Reviews*. 2011, Vol. 56, No. 3, P. 143–166.
7. Radovic M., Barsoum M. W. MAX phases: bridging the gap between metals and ceramics. *American Ceramics Society Bulletin*. 2013, Vol. 92, No. 3, P. 20–27.
8. Sokol M. et al. On the chemical diversity of the MAX phases. *Trends in Chemistry*. 2019, Vol. 1, No. 2, P. 210–223.
9. Barsoum M. W. MAX phases: properties of machinable ternary carbides and nitrides. John Wiley & Sons, 2013.
10. Dahlqvist M., Alling B., Rosén J. Stability trends of M A X phases from first principles. *Physical Review B*. 2010, Vol. 81, No. 22, P. 220102.
11. Hu C. et al. Nb₄AlC₃: A new compound belonging to the MAX phases. *Scripta Materialia*. 2007, Vol. 57, No. 10, P. 893–896.
12. Tallman D. J. et al. Effect of neutron irradiation on select MAX phases. *Acta Materialia*. 2015, Vol. 85, P. 132–143.
13. Ingason A. S., Dahlqvist M., Rosén J. Magnetic MAX phases from theory and experiments; a review. *Journal of Physics: Condensed Matter*. 2016, Vol. 28, No. 43, P. 433003.
14. Medvedeva N. I., Enyashin A. N., Ivanovsky A. L. Modeling the electronic structure, chemical bond and properties of the Ti₃SiC₂ ternary silicocarbide. *Journal of Structural Chemistry*. 2011, No. 52 (4), P. 806 (In Russ.).
15. Petruhins A., Ingason A. S., Dahlqvist M. et al. Phase stability of Cr_n+1GaC_n MAX phases from first principles and Cr₂GaC thin - film synthesis using magnetron sputtering from elemental targets. *Physica status solidi (RRL) – Rapid Research Letters*. 2013, No. 7(11), P. 971–974.

© Назарова З. И., Назаров А. Н., 2021

Назаров Александр Николаевич – студент; Сибирский федеральный университет; лаборант; Институт физики имени Л. В. Киренского СО РАН – обособленное подразделение ФИЦ КНЦ СО РАН. E-mail: jercompany@gmail.com.

Назарова Зоя Игоревна – студент; Сибирский федеральный университет; лаборант; Институт физики имени Л. В. Киренского СО РАН – обособленное подразделение ФИЦ КНЦ СО РАН. E-mail: zoyavishni@gmail.com.

Nazarov Alexandr Nikolaevich – student, Siberian Federal University; Laboratory assistant, Kirensky Institute of Physics, Federal Research Center KSC SB RAS. E-mail: jercompany@gmail.com.

Nazarova Zoya Igorevna – student, Siberian Federal University; Laboratory assistant, Kirensky Institute of Physics, Federal Research Center KSC SB RAS. E-mail: jercompany@gmail.com. E-mail: zoyavishni@gmail.com.

UDC 67.02

Doi: 10.31772/2712-8970-2021-22-2-391-397

Для цитирования: Руденко М. С., Михеев А. Е., Гирн А. В. Технология изготовления сотовых заполнителей из полимерных композиционных материалов // Сибирский аэрокосмический журнал. 2021. Т. 22, № 2. С. 391–397. Doi: 10.31772/2712-8970-2021-22-2-391-397.

For citation: Rudenko M. S., Mikheev A. E., Girn A. V. Honeycomb fillers manufacturing technology from polymeric composite materials. *Siberian Aerospace Journal*. 2021, Vol. 22, No. 2, P. 391–397. Doi: 10.31772/2712-8970-2021-22-2-391-397.

Honeycomb fillers manufacturing technology from polymeric composite materials

M. S. Rudenko A. E. Mikheev, A. V. Girn

Reshetnev Siberian State University of Science and Technology
31, Krasnoyarskii rabochii prospekt, Krasnoyarsk, 660037, Russian Federation
E-mail: mister.m.rudenko@gmail.com

The honeycomb filler is an integral part of the spacecraft's sandwich panel. Currently, a honeycomb filler made of aluminum alloys is used. The proposed technology makes it possible to replace the honeycomb filler material from aluminum alloys with polymer composite materials (PCM). The main difference between the developed technology for the production of honeycomb filler by the RTM method is that corrugated tape is glued during the formation of the composite material. This is a separate process in the existing methods for the production of honeycomb cores from PCM. This paper presents the results of creating a prototype of a honeycomb filler by the RTM-method, a technological process has been developed.

Keywords: honeycomb filler, polymer composite material, RTM method.

Технология изготовления сотовых заполнителей из полимерных композиционных материалов

М. С. Руденко, А. Е. Михеев, А. В. Гирн

Сибирский государственный университет науки и технологий имени академика М. Ф. Решетнева
Российская Федерация, 660037, г. Красноярск, просп. им. газ. «Красноярский рабочий», 31
E-mail: mister.m.rudenko@gmail.com

Сотовый заполнитель является неотъемлемой частью трехслойных панелей космических аппаратов. На данный момент используют сотовый заполнитель из алюминиевых сплавов. Предложенная технология позволяет заменить материал сотового заполнителя с алюминиевых сплавов на полимерные композиционные материалы (ПКМ). Основное отличие разработанной технологии изготовления сотового заполнителя RTM-методом заключается в том, что за период формования композиционного материала происходит склейка гофролент. В существующих методах изготовления сотовых заполнителей из ПКМ это является отдельным процессом. В данной работе представлены результаты создания опытного образца сотового заполнителя RTM-методом, разработан технологический процесс.

Ключевые слова: сотовый заполнитель, полимерный композиционный материал, RTM-метод.

Introduction

The three-layer structure (TS) is one of the main power elements of modern spacecraft (SC). TS consists of two load-bearing layers, filler, located between the load-bearing layers, and frame elements. Bearing layers perceive longitudinal loads (tension, compression, shear) in their plane and transverse bending moments. The main feature of three-layer structures with a filler is that as a result of the separation of the bearing layers at a certain distance from each other, a greater ratio of the structure's stiffness to its mass is achieved [1–6].

At the present time, in the elements of SC honeycomb filler from aluminum alloys are most widely used, this is connected with the simplicity of their production and their low cost, but they have disadvantages associated with the strength and physicochemical characteristics [7–12]. Also, polymer composite materials (PCM) are used as a material for honeycomb fillers. At the present moment, there are several technologies for the production of cellular core from PCM:

1) stretching the glued package - the method consists in gluing dry reinforcing layers, stretching them in a technological device to obtain the shape of a honeycomb cell, dipping into a binder, drying and polymerization in an oven. This method can be used to produce a large number of honeycomb products, which are mainly used in aircraft and helicopter construction. The precision characteristics of this honeycomb fillers are not suitable for space technology application;

2) gluing corrugated sheets - the method consists in making a single or double corrugated strip in a hexagonal molding tooling and gluing them together in an oven. This method has low efficiency and requires a lot of auxiliary equipment;

3) the method of volumetric weaving - the method is similar to the method of stretching a glued package with the difference that the honeycomb package is formed not by gluing sheets, but by weaving on a Jaccard shuttle loom. As a result, the layers are fastened together by interweaving the threads along the lines in a checkerboard pattern, depending on the layer [13–15].

Experimental part

The aim of the work is to develop a process diagram and technology for manufacturing a honeycomb filler from PCM using the RTM (Resin Transfer Molding) method. The RTM method consists in placing a dry reinforcing filler in a special sealed mold, the inner surfaces of which repeat the outer surface of the product (in the impregnation of the resin filler under pressure), and polymerization in the mold. The RTM method has the following advantages in comparison with other methods: the ability to manufacture parts of complex shapes; tight dimensional tolerance; mechanical properties are comparable to autoclave molding; high performance.

A scheme is proposed and a technological process for manufacturing a honeycomb filler from PCM is developed (Fig. 1).

Reinforcing material 2 (Fig. 2) is cut out according to the size of the product, taking into consideration the curvature of the cellular strip. Dry reinforcing material 2 (fiberglass, carbon fiber) is laid on the hexagonal surface 1. The first layer of fiber 2 is pressed by rigid hexagonal rods 3. The next layer of fiber 2 is laid on top and similarly pressed by rods 3. This is repeated until the structure is fully loaded. The last layer is pressed by the lid to the hexagonal surface 4.

In order to reduce the internal stress of the dry reinforcing material during installation, it is molded in such a way as to tightly contact the hexagonal surface. This happens until the snap-in is fully loaded. The structure is closed with side covers and sealed, then a binder is fed into it under pressure, which impregnates the fibers.

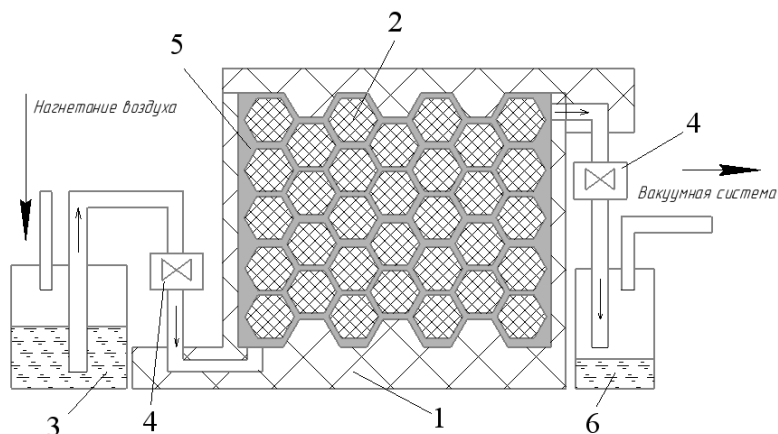


Fig. 1. Scheme of manufacturing a honeycomb filler from PCM by the RTM method:
1 – structure body; 2 – hexagonal rod; 3 – a container with a binder; 4 – locking device; 5 – zone of impregnation of dry reinforcing material with a binder; 6 –reservoir for excess binder

Рис. 1. Схема изготовления сотового заполнителя из ПКМ методом RTM:
1 – корпус конструкции; 2 – гексагональный стержень; 3 – емкость со связующим; 4 – запорное устройство; 5 – зона пропитки сухого армирующего материала связующим; 6 – ёмкость для излишек связующего

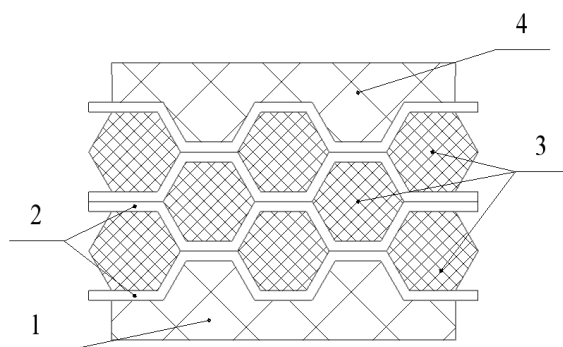


Fig. 2. Laying scheme for dry reinforcing material:
1, 4 – hexagonal surfaces; 2 – reinforcing material; 3 – hexagonal rods

Рис. 2. Схема укладки сухого армирующего материала:
1, 4 – шестигранные поверхности; 2 – армирующий материал; 3 – гексагональные стержни

For the production of a prototype of a honeycomb filler, technological equipment was designed and constructed (Fig. 3), which consists of a body, side covers and a set of hexagonal rods (inserts). The design of the equipment should ensure:

- 1) rigidity and strength;
- 2) hermitisation the internal cavity;
- 3) anti-adhesive properties.

The snap-in was made on a «Hercules 2018» 3D printer. Printing material: PETG plastic. Nozzle diameter 0.5 mm. Layer height 0.15 mm.

The following materials were selected for the prototype of the honeycomb filler:

– reinforcing material - glass fabric T-11 (GOST 19170-2001);

– binders – epoxy resin ED-20 (GOST 10587–84) with cold hardening agent ETAL-45 (TU 2257-045-18826195-01).

The technological process of manufacturing a prototype consists of the following stages:

Application of a layer of release wax to the tooling to ensure anti-adhesive properties.

Cutting out the reinforcing material.

Laying reinforcing material into the body of the tooling with pressure with hexagonal rods.

Installation of the top and two side covers.

Rig-in sealing.

Connection of a vacuum system for supplying epoxy resin to the tooling.

Preparing the resin and feeding it under pressure into the structure.

Polymerization time of the resin in the rig-in (24 hours).

Removal of the honeycomb block from the tooling structure.

Processing on a grinding machine to remove excess resin from the ends of the product.

Removing the hex rods from the honeycomb block, finishing.

As a result, a prototype of a honeycomb filler was manufactured (Fig. 4), which confirms the realizability of the technology.

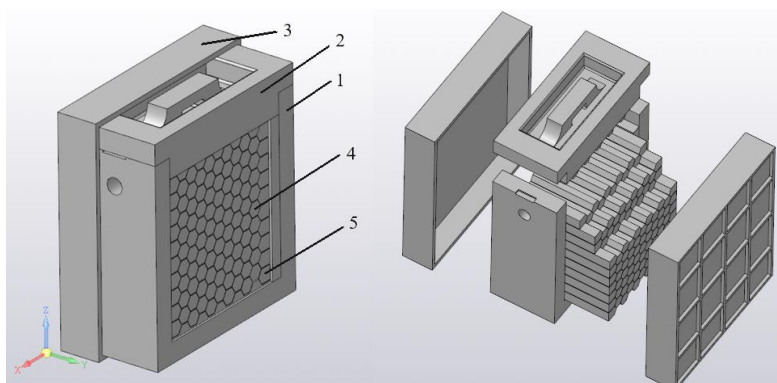


Fig. 3. Technological rig-in:

1 – tooling body; 2 – top cover; 3 – side cover; 4 – hexagonal rod; 5 – side bar

Рис. 3. Технологическая оснастка:

1 – корпус оснастки; 2 – верхняя крышка; 3 – боковая крышка;
4 – гексагональный стержень; 5 – боковой стержень

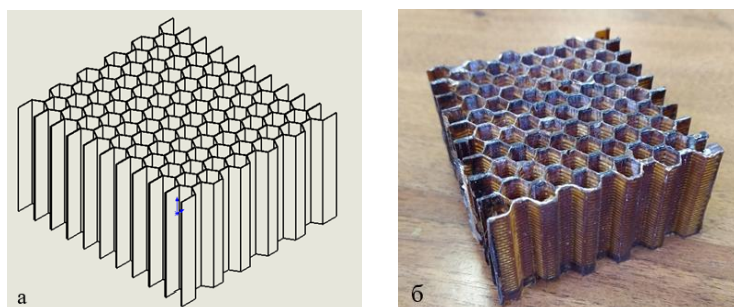


Fig. 4. PCM honeycomb filler:

a – model; b – prototype

Рис. 4. Сотовый наполнитель из ПКМ:

a – модель; *б* – опытный образец

The characteristics of the prototype are presented in the table. The mass of the prototype is 45.03 g; the volume mass is 220 kg/m³.

The characteristics of the prototype

The Characteristics	The prototype
Cell Form	Hexagon
HF Size	
- length, mm	73
- width, mm	70
- height, mm	40
Cell size	8
Weight, g	45,03
Volume, m ³	2·10 ⁻⁴
Bulk weight, kg / m ³	220,15
Filler weight, g	21,834
Volume fraction of the filler, %	38

Conclusion

The results of the work show that the proposed method can be used to produce honeycomb fillers not only with a hexagonal cell, but also with many different variations of shapes. The shape and size of the cell will depend only on the shape and size of the insert. When using the technology of stretching a cellular package, it is impossible to achieve this.

It is also possible to produce honeycomb fillers with different curvature and install embedded elements at the molding stage, thereby not gluing them into the finished detail.

As a result, the technology for manufacturing cellular fillers from polymer composite materials by the RTM method is developed. This method can be adapted for the mass production of industrial products.

References

1. Panin V. F., Gladkov Yu. A. *Konstruktsii s zapolnitelem* [Constructions with filler]. Moscow, Mashinostroenie Publ., 1991, 272 p.
2. Khaliulin V. I., Shapaev I. I. *Tekhnologiya proizvodstva kompozitnykh izdeliy* [Technology of production of composite products]. Kazan', Izd-vo Kazan. gos. tekhn. un-ta Publ., 2003.
3. Achilles Petras Design of Sandwich Structures: Doct. Diss. 1998. P. 5–7.
4. Grabin B. V. *Inzhenernye osnovy konstruirovaniya kosmicheskikh apparatov* [Engineering bases of spacecraft design]. Moscow, MAI Publ., 2018, 255 p.
5. Testodov N. A., Nagovitskin V. N., Permyakov M. Yu. [The use of three-layer honeycomb structures in spacecraft]. *Vestnik SibSAU*. 2016, Vol. 17, No. 1, P. 200–211 (In Russ.).
6. Endogur A. I., Vainberg M. V., Ierusalimsky K. M. *Sotovye konstruktsii: Vybory parametrov i proektirovaniye* [Cellular structures: choice of parameters and design]. Moscow, Mashinostroenie Publ., 1986, 192 p.
7. Melnikov D. A., Petrov A. P., Gromova A. A. et al. [Calculation of the ratio of the components of the prepreg brand VPS-53/120, determination of the physical-mechanical and operational characteristics of fiberglass]. *TRUDY VIAM*. 2019, No. 1 (73), P. 92–104 (In Russ.).
8. Urakova A. S., Nagovitsin V. N. [Application of cellular panels in satellite technology]. *Reshetnevskie chteniya* [Reshetnev readings]. 2018, P. 179–180 (In Russ.).

9. Minakov V. T., Postnov V. I., Shchvets N. I. et al. [Features of manufacturing three-layer honeycomb panels with a polymer filler of hot curing]. *Aviatsionnye materialy i tekhnologii*. 2009, No. 4 (12), P. 15–18 (In Russ.).
10. Zlotenko V. V., Ishenina N. N. [Features of mechanical processing of aluminum honeycomb structures] *Vestnik SibSAU*. 2005, No. 6, P. 209–211 (In Russ.).
11. Slivinsky, V. I., Tkachenko, G. V., Slivinsky M. V. [Efficacy of cell structures in aircraft]. *Vestnik SibSAU*. 2005, No. 6, P. 169–173 (In Russ.).
12. A. A. Ivanov, S. M. Kashin, V. I. *Semenov Novoe pokolenie sotovykh zapolniteley dlya aviatsionno-kosmicheskoy tekhniki* [New generation of cell aggregates for aerospace engineering]. Moscow, Energoatomizdat Publ., 2000, 584 p.
13. Pershin A. M. [Computational study of static stability of cellular aggregates made of composite materials]. *Vestnik Samarskogo gosudarstvennogo aerokosmicheskogo universiteta*. 2014, No. 5 (47), chast' 1, P. 118–123 (In Russ.).
14. Kryukov A. M., Volkova V. S., Murashkin Yu. G. et al. *Sposob izgotovleniya sotovykh zapolniteley* [Method of manufacturing honeycomb fillers]. Patent RF, No. 2651012, 2018.
15. Kryukov A. M., Volkova V. S., Murashkin Yu. G. et al. *Sposob izgotovleniya trekhslonnykh paneley slozhnoy krivizny* [Method of manufacturing three-layer panels of complex curvature]. Patent RF, No. 2680571, 2018.

Библиографические ссылки

1. Панин В. Ф., Гладков Ю. А. Конструкции с заполнителем: справочник. М.: Машиностроение, 1991. 272 с.
2. Халиулин В. И., Шапаев И. И. Технология производства композитных изделий: учеб. пособие Казань: Изд-во Казан. гос. техн. ун-та, 2003.
3. Achilles Petras Design of Sandwich Structures: dissertation, Doctor of Philosophy. Cambridge University Engineering Department. 1998. P. 5–7.
4. Грабин Б. В. Инженерные основы конструирования космических аппаратов / под ред. д-ра техн. наук, проф. О. М. Алифанова. М.: МАИ, 2018. 255 с.
5. Тестоедов Н. А., Наговицкий В. Н., Пермяков М. Ю. Применение трехслойных сотовых конструкций в космических аппаратах // Вестник СибГАУ. 2016. Т. 17, № 1. С. 200–211.
6. Ендогур А. И., Вайнберг М. В., Иерусалимский К. М. Сотовые конструкции: выбор параметров и проектирование. М.: Машиностроение, 1986. 192 с.
7. Расчет соотношения компонентов препрега марки ВПС-53/120, определение физико-механических и эксплуатационных характеристик стеклопластика / Д. А. Мельников, А. П. Петров, А. А. Громова и др. // ТРУДЫ ВИАМ. 2019. № 1 (73). С. 92–104.
8. Уракова А. С., Наговицин В. Н. Применение сотовых панелей в спутниковой технике // Решетневские чтения. 2018. С. 179–180.
9. Особенности изготовления трехслойных сотовых панелей с полимерным заполнителем горячего отверждения / В. Т. Минаков, В. И. Постнов, Н. И. Щвец. и др. // Авиационные материалы и технологии. 2009. № 4 (12). С. 15–18.
10. Злотенко В. В., Ишенина Н. Н. Особенности механической обработки алюминиевых сотовых конструкций // Вестник СибГАУ. 2005. № 6. С. 209–211.
11. Сливинский В. И., Ткаченко Г. В., Сливинский М. В. Эффективность применения сотовых конструкций в летательных аппаратах // Вестник СибГАУ. 2005. № 6. С. 169–173.

12. Иванов А. А., Кашин С. М., Семенов В. И. Новое поколение сотовых заполнителей для авиационно-космической техники. М.: Энергоатомиздат, 2000. 584 с.
13. Першин А. М. Расчётное исследование статической устойчивости сотовых заполнителей из композиционных материалов // Вестник Самарского гос. аэрокосмич. ун-та. 2014. № 5 (47). Ч. 1. С. 118–123.
14. Патент № 2651012 Российская Федерация, МПК В32В 3/12 (2006.01). Способ изготовления сотовых заполнителей / А. М. Крюков, В. С. Волкова, Ю. Г. Мурашкин и др. ; заявитель АО «Обнинское научно-производственное предприятие «Технология» им. А. Г. Ромашина». № 2017108041; заявл. 10.03.2017; опубл. 18.02.2018. 9 с.
15. Патент № 2680571 Российская Федерация, МПК Е04С 2/24 (2006.01), В32В 3/12 (2006.01). Способ изготовления трехслойных панелей сложной кривизны / А. М. Крюков, В. С. Волкова, Ю. Г. Мурашкин и др. ; заявитель АО «Обнинское научно-производственное предприятие «Технология» им. А. Г. Ромашина». – № 2018112189; заявл. 04.04.2018; опубл. 22.02.2019. 8 с.

© Руденко М. С., Михеев А. Е., Гирн А. В., 2021

Руденко Михаил Сергеевич – ассистент; Сибирский государственный университет науки и технологий имени академика М. Ф. Решетнева. E-mail: mister.m.rudenko@gmail.com.

Михеев Анатолий Егорович – доктор технических наук, профессор; Сибирский государственный университет науки и технологий имени академика М. Ф. Решетнева. E-mail: michla@mail.ru.

Гирн Алексей Васильевич – кандидат технических наук, доцент; Сибирский государственный университет науки и технологий имени академика М. Ф. Решетнева. E-mail: girn007@gmail.com.

Rudenko Mikhail Sergeevich – Assistant; Reshetnev Siberian State University of Science and Technology. E-mail: mister.m.rudenko@gmail.com.

Mikheev Anatoly Yegorovich – Dr. Sc., Professor; Reshetnev Siberian State University of Science and Technology. E-mail: michla@mail.ru.

Girn Alexey Vassilyevich – Cand. Sc., Associate Professor; Reshetnev Siberian State University of Science and Technology. E-mail: girn007@gmail.com.

УДК 537.6

Doi: 10.31772/2712-8970-2021-22-2-398-405

Для цитирования: Яковлев И. А. Сравнение магнитной анизотропии поликристаллической и монокристаллической пленок Fe_3Si // Сибирский аэрокосмический журнал. 2021. Т. 22, № 2. С. 398–405. Doi: 10.31772/2712-8970-2021-22-2-398-405.

For citation: Yakovlev I. A. The magnetic anisotropy comparison of polycrystalline and single-crystal Fe_3Si films. *Siberian Aerospace Journal*. 2021, Vol. 22, No. 2, P. 398–405. Doi: 10.31772/2712-8970-2021-22-2-398-405.

Сравнение магнитной анизотропии поликристаллической и монокристаллической пленок Fe_3Si^*

И. А. Яковлев

Институт физики имени Л. В. Киренского СО РАН –
обособленное подразделение ФИЦ КНЦ СО РАН
Российская Федерация, 660036, г. Красноярск, Академгородок, 50, стр. 38
E-mail: yia@iph.krasn.ru

Постоянное совершенствование высокотехнологичных приборов требует от науки постоянного развития технологий и поиска новых материалов. На сегодняшний день развитие области магнетизма достигло очень широких знаний, что позволило создать и изучить множество искусственных ферромагнитных материалов, которые уже сейчас активно применяются в науке и технике. Последние научные знания показывают, что один и тот же материал в различном состоянии может проявлять разные электрические, магнитные свойства. Так в современных приборах активно применяются тонкие магнитные пленки. Физические процессы в тонких пленках протекают иначе, чем в массивных материалах. В результате пленочные элементы имеют характеристики, отличные от характеристик массивных образцов и позволяют наблюдать эффекты, не свойственные массивным образцам. Пленка – это тонкий слой связанного конденсированного вещества, толщина которого сравнивается с расстоянием действия поверхностных сил; представляет собой термодинамически стабильную или метастабильную часть гетерогенной системы «пленка – подложка». Дальнейшее изучение пленочных структур привело к созданию и исследованию многослойных магнитных систем. В таких структурах возможно присутствие как слоев различных ферромагнитных материалов, так и неферромагнитных прослоек, а свойства многослойных систем могут значительно отличаться от свойств любого из компонентов системы. Для практики эти материалы также имеют множество применений, в том числе, радиосвязь и геологоразведка. В нашем эксперименте методом молекулярно-лучевой эпитаксии при совместном осаждении Fe и Si синтезированы ферромагнитные тонкие пленки силицида Fe_3Si . На подложке $\text{SiO}_2/\text{Si}(111)$ была получена поликристаллическая пленка силицида, а на $\text{Si}(111)7\times7$ – монокристаллическая. Структура была исследована с помощью дифракции отраженных быстрых электронов непосредственно в процессе роста. Методом ферромагнитного резонанса была изучена магнитная анизотропия полученных образцов. Установлено, что поликристаллическая пленка характеризуется одноосной магнитной анизотропией, которая составляет 13.42 Э и формируется в

* Автор статьи выражает благодарность Беляеву Борису Афанасьевичу (ИФ СО РАН) за проведенные измерения на сканирующем спектрометре ферромагнитного резонанса.

The author expresses his gratitude to Boris Afanasyevich Belyaev (Kirensky Institute of Physics SB RAS) for the measurements performed on a scanning ferromagnetic resonance spectrometer.

следствие «косого» напыления. А магнитная анизотропия для монокристаллической пленки Fe_3Si формируется в большей степени внутренними магнитокристаллическими силами.

Ключевые слова: магнитная анизотропия, ферромагнитные пленки, Fe_3Si , молекулярно-лучевая эпитаксия.

The magnetic anisotropy comparison of polycrystalline and single-crystal Fe_3Si films

I. A. Yakovlev

Kirensky Institute of Physics, Federal Research Center KSC SB RAS
50/38, Akademgorodok, Krasnoyarsk, 660036, Russian Federation
E-mail: yia@iph.krasn.ru

High-tech devices improvement requires development of technology and search for new materials from science. Currently, the development of the magnetism research field has reached a very broad knowledge, making it possible to create and study a variety of artificial ferromagnetic materials, which are already actively used in science and technology. The latest scientific knowledge shows that the same material in different states can exhibit different electrical and magnetic properties. Thus, thin magnetic films are actively used in modern devices. Physical processes in thin films proceed differently than in bulk materials. As a result, the film elements have characteristics that differ from those of bulk samples and make it possible to observe effects that are not characteristic of bulk samples. A film is a thin layer of a bound condensed substance, the thickness of which is compared with the distance of surface forces action; it is a thermodynamically stable or metastable part of a heterogeneous film-substrate system. Further research of film structures led to the creation and study of multilayer magnetic systems. In such structures, the presence of both various ferromagnetic materials layers and non-ferromagnetic interlayers is possible, and the multilayer systems properties can differ significantly from the properties of any system components. These materials also have many practical applications, including radio communications and geological exploration. In our experiment, ferromagnetic thin films of Fe_3Si silicide were synthesized by molecular beam epitaxy with co-deposition of Fe and Si. A polycrystalline silicide film was obtained on a $\text{SiO}_2/\text{Si}(111)$ substrate, and a single-crystal film – on $\text{Si}(111)7\times7$. The structure was investigated using the diffraction of reflected fast electrons directly during the growth process. The magnetic anisotropy of the obtained samples was studied applying the method of ferromagnetic resonance. It was found that the polycrystalline film is characterized by uniaxial magnetic anisotropy, which is 13.42 Oe and is formed as a result of “oblique” deposition, whereas the magnetic anisotropy for a single-crystal Fe_3Si film is formed to a greater extent by internal magnetocrystalline forces.

Keywords: magnetic anisotropy, ferromagnetic films, Fe_3Si , molecular beam epitaxy.

Introduction

One of the key issues for realizing spintronic applications is the production of high-quality epitaxial ferromagnets with high spin polarization on semiconductor substrates. Hybrid structures consisting of alternating metallic and semiconducting layers are of great interest for modern spintronic devices. Important aspects of the layered material system applicability are stable magnetism in close proximity to interfaces and a suitable states density at the Fermi level, which, however, are highly dependent on the interface structure. Spin polarization indicates its quality for transport devices.

Iron-based systems are also of interest in the scientific community. Spin injection of more than 30% was measured for Fe / GaAs (001) [1], as well as 10 % for Fe₃Si / GaAs (001) [2; 3]. Since the atomically clean GaAs (110) surface is not reconstructed [4], epitaxial growth is possible for both Fe and quasi-Geusler Fe₃Si, for which the lattice mismatch amounts to only 0.1 % [5].

Silicide Fe₃Si is a ferromagnetic material that can be a promising candidate for the injection of spin-polarized electrons from a ferromagnet into a semiconductor [2]. For Fe₃Si / GaAs heterostructures, the structural, transport, and magnetic properties have been studied [6–9]. For epitaxial Fe₃Si films grown on GaAs (001) by MBE, the magnetotransport properties were studied mainly by applying a current along the hard magnetization axis, i.e, along the [110] crystallographic axis, which is the direction of easy cleavage for GaAs (100) [10].

Numerous studies show that depending on the crystal structure of the interface films in layers, the same material has different properties, which determines their future use, as well as the development of technologies for their synthesis and processing. The anisotropic magnetoresistance for Fe₃Si showed that the resistivity in a field perpendicular to the current was greater than the resistivity in a field parallel to the current. It is known that in single crystals the direction of the current and magnetization relative to the crystal axes affects the behavior of the magnetoresistance [11].

Crystals orientation in thin magnetic films is closely related to both their physical and magnetic properties. Textured magnetic materials often exhibit much better characteristics such as easy magnetization, high magnetostriction and excellent squareness in the B – H magnetization loop, flux density plot, B, for various magnetic field strengths, H [12–15]. This information makes it possible to create microelectronic devices, including radio communications, with higher accuracy and sensitivity for practical use.

In our work, we investigated the magnetic properties, including the in-plane magnetic anisotropy, for Fe₃Si silicide films with polycrystalline and single-crystal structures.

Experiment

Polycrystalline and epitaxial Fe₃Si films were obtained applying molecular beam epitaxy with the joint deposition of iron and silicon. For the films obtained, the magnetic anisotropy was studied using the method of ferromagnetic resonance (FMR), the contributions of unidirectional, uniaxial, cubic, and hexagonal anisotropies to the resulting value were determined, as well as the high-frequency (microwave) magnetic characteristics of all the films under study: the width of the ferromagnetic resonance line, the effective saturation magnetization, and the values of ferromagnetic resonance for a given pumping frequency.

The synthesis of the samples was carried out in an "Anagara" ultrahigh-vacuum molecular-beam epitaxy unit, with the base vacuum of 1.3×10^{-8} Pa. The deposition was carried out by the method of thermal evaporation from effusion Knudsen cells from two sources simultaneously, the so-called coprecipitation, of iron and silicon in atomic proportions

Fe: Si = 3:1. The film formation process was monitored by the method of high-energy reflected electron diffraction (RHEED).

Crystalline structure

In the course of the experiment, a polycrystalline Fe₃Si film with a thickness of 40 nm was obtained. It was synthesized at room temperature on a Si (111) substrate coated with a SiO₂ oxide layer about 1.5 nm thick. Fig. 1 shows a RHEED pattern for this structure.

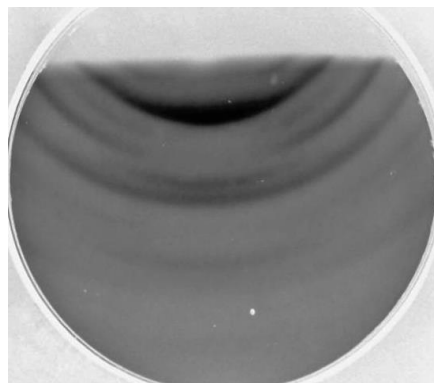


Рис. 1. Картина ДОБЭ от пленки Fe_3Si на $\text{SiO}_2/\text{Si}(111)$

Fig. 1. RHEED pattern on $\text{Fe}_3\text{Si}/\text{SiO}_2/\text{Si}(111)$

The obtained diffraction pattern contains reflections in the form of concentric Debye rings, as well as sectors of the rings. This geometry of the diffraction pattern corresponds to a polycrystalline structure with a certain texture.

Fig. 2 shows the diffraction pattern of reflected fast electrons from Fe_3Si films 40 nm thick, obtained on a 7×7 Si (111) substrate at room temperature.

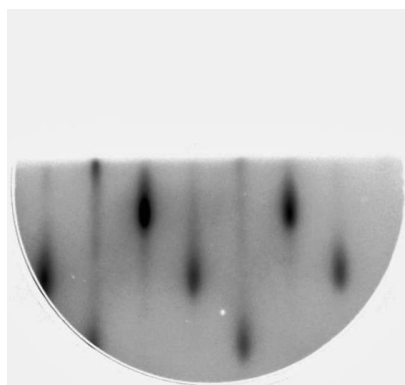


Рис. 2. Картина ДОБЭ от пленки $\text{Fe}_3\text{Si}/\text{Si}(111)7 \times 7$

Fig. 2. RHEED pattern on $\text{Fe}_3\text{Si}/\text{Si}(111)7 \times 7$

This diffraction pattern contains reflections in the form of points elongated in the vertical direction. This geometry of the pattern corresponds to a single-crystal structure of a film with an island surface morphology. The analysis of the diffraction data also shows that Fe_3Si films on Si (111) 7×7 are formed epitaxially.

Study of magnetic anisotropy

For both films, the magnetic anisotropy was investigated by the method of ferromagnetic resonance. Fig. 3 shows the angular dependences of the ferromagnetic resonance field, obtained on a scanning ferromagnetic resonance spectrometer at the pump frequency 3.329 GHz [16].

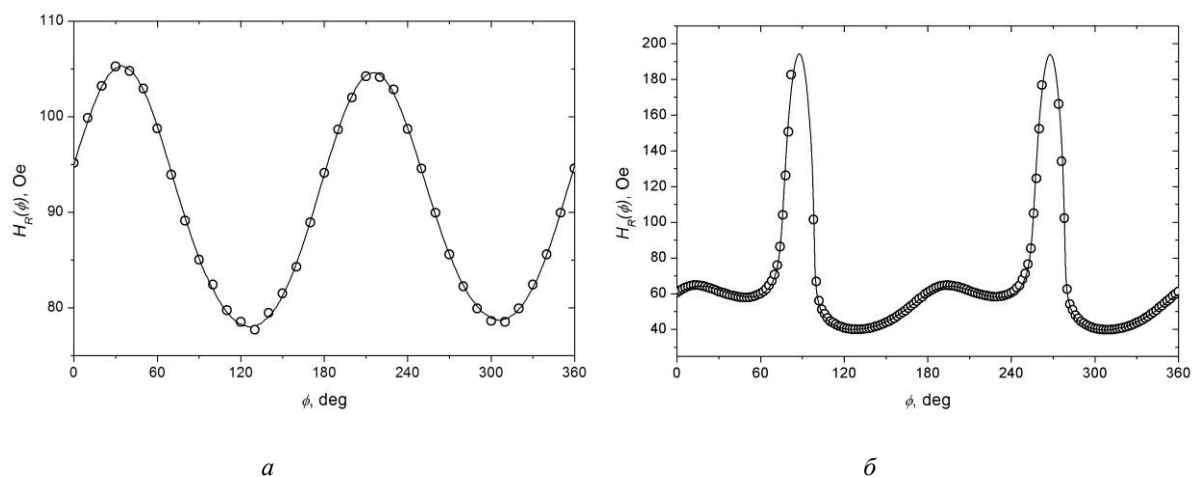


Рис. 3. Угловые зависимости поля ферромагнитного резонанса для поликристаллической пленки Fe_3Si (а); монокристаллической пленки Fe_3Si (б) (круг – экспериментальные данные, линия – расчетная кривая)

Fig. 3. The angular dependences of the ferromagnetic resonance field for polycrystalline Fe_3Si film (a); a single-crystal Fe_3Si film (b) (circle – experimental data, line – calculated curve)

According to this dependence, based on the phenomenological model, the following characteristics for the obtained film were calculated applying the iterative technique [17] (Table 1): effective saturation magnetization M_s , unidirectional anisotropy field H_{k1} , uniaxial anisotropy field H_{k2} , and cubic anisotropy field H_{k4} . Based on the ferromagnetic resonance data the FMR line width in the direction of the easy magnetization axis ΔH_{ema} was also determined (Table 1).

Table 1

Magnetic characteristics of films Fe_3Si

	$\text{Fe}_3\text{Si}/\text{SiO}_2/\text{Si}(111)$	$\text{Fe}_3\text{Si}/\text{Si}(111)7 \times 7$
	Polycrystalline	Single-crystal
M_s, Hs	1235,5	1227,2
H_{k1}, Oe	0,48	0,17
H_{k2}, Oe	13,42	73,16
H_{k4}, Oe	0,23	310,58
$\Delta H_{\text{ОЛН}}, \text{Oe}$	33,5	7,7

Based on the data analysis, it was found that the polycrystalline film is to a greater extent characterized only by uniaxial anisotropy, which is approximately 28 times higher than other components. The formation of predominantly uniaxial anisotropy is most likely caused by the deposition of the material at the angle to the substrate surface, the so-called "oblique" deposition [18].

For a single-crystal Fe_3Si film on Si (111) 7×7 , the same magnetic characteristics as for polycrystalline samples were determined (Table 1), but according to the method [19] adapted for single-crystal structures.

From the data obtained (Table 1), it can be seen that the single-crystal film is dominated by the cubic magnetic anisotropy H_{k4} , which is more than four times greater than the uniaxial component H_{k2} . This fact shows and justifies our film to possess a single-crystal structure. In turn, the uniaxial anisotropy for a single-crystal Fe_3Si is more than 5 times stronger than for a polycrystalline sample. To determine the exact nature of such differences, additional studies of the structural and magnetic properties of all elements of our sample are required. However, most likely, this is caused by the several factors: misorientation of the substrate surface, "oblique" deposition, and internal forces in a single crystal.

Conclusion

Poly- and single-crystal Fe₃Si silicide films on Si (111) substrates were obtained by molecular beam epitaxy. The magnetic anisotropy was studied applying the method of ferromagnetic resonance. It was found that the polycrystalline film is characterized by uniaxial magnetic anisotropy, which is 13.42 Oe and is formed as a result of "oblique" deposition, while the magnetic anisotropy for a single-crystal Fe₃Si film is formed mostly by internal magnetocrystalline forces. The presented results show that by varying the crystal structure of one material, it is possible to change its magnetic properties and, therefore, employ in various applications, for example, in spintronic devices or sensors of weak magnetic fields.

Библиографические ссылки

1. Spin injection across (110) interfaces: Fe/GaAs(110) spin-light-emitting diodes / C. H. Li, G. Kioseoglou, O. M. J. van 't Erve, A. Petrou // *Applied Physics Letters*. 2004. Vol.85, No. 9. P. 1544–1548.
2. Spin injection from Fe₃Si into GaAs / A. Kawaharazuka, M. Ramsteiner, J. Herfort, H.-P. Schonherr // *Applied Physics Letters*. 2004. Vol. 85, No. 16. P. 3492–3494.
3. Herper H. C., Entel P. Interface structure and magnetism of Fe₃Si/GaAs(110) multilayers: An ab-initio study // *Philosophical Magazine*. 2008. Vol. 88, No. 18-20. P. 2699–2707.
4. Qian G.-X., Martin R., Chadi J. First-principles calculations of atomic and electronic structure of the GaAs(110) surface // *Physical review. B (Condensed matter)*. 1988. Vol. 37, No. 3. P. 1303–1307.
5. A comparative study of (Fe, Fe₃Si)/GaAs and Heusler/MgO for spintronics applications / A. Grunebohm, M. Siewert, H. C. Herper et al. // *Journal of Physics: Conference Series*. 2010. Vol. 200. P. 072038.
6. Magnetic properties of epitaxial single crystal ultrathin Fe₃Si films on GaAs (001) / S. H. Liou, S. S. Malhotra, J. X. Shen et al. // *Journal of Applied Physics*. 1993. Vol. 73, No. 10. P. 6766–6768.
7. Transport and magnetic properties of Fe₃Si epitaxial films / H. Vinzelberg, J. Schumann, D. Elefant et al. // *Journal of Applied Physics*. 2008. Vol. 104, No. 9. P. 093707–093707.
8. Order-driven contribution to the planar Hall effect in Fe₃Si thin films / M. Bowen, K.-J. Friedland, J. Herfort et al. // *Physical Review B*. 2005. Vol. 71, No. 17. P.172401.
9. Spin and orbital magnetism in ordered Fe_(3±δ)Si_(1∓δ) binary Heusler structures: Theory versus experiment / K. Zakeri, S. J. Hashemifar, J. Lindner et al. // *Physical Review B*. 2008. Vol. 77, No. 10. P. 104430.
10. Structural, magnetic, electronic, and spin transport properties of epitaxial Fe₃Si/GaAs(001) / A. Ionescu, T. Trypiniotis, H. Garcia-Miquel et al. // *Physical Review B*. 2005. Vol. 71, No. 9. P. 094401.
11. Strong crystal anisotropy of magneto-transport property in Fe₃Si epitaxial film / H. Y. Hung, S. Y. Huang, P. Chang et al. // *Journal of Crystal Growth*. 2011. Vol. 323. P. 372–375.
12. Hong J. Thickness-dependent magnetic anisotropy in ultrathin FeCo/Cu(001) films // *Physical Review. B.(Condensed matter)*. 2006. Vol. 74. P. 172408
13. Arai K. I., Ohoka Y., Wakui Y. Preparation and magnetic properties of anodic oxide magnetic films // *Electronics and Communications in Japan. (Part II Electronics)*. 1989. Vol. 72, No. 5. P. 81–88.
14. Liu X., Shiozaki Y., Morisako A. Magnetization reversal mechanism of ultra thin Nd₂Fe₁₄B films with perpendicular magnetic anisotropy // *Journal of Applied Physics*. 2008. Vol. 103. P. 07E104.

15. Texture and magnetic properties of Fe thin films fabricated by field-sputtering vs field-annealing / S. J. Park, C.-H. Liu, H. S. Kim et al. // *Thin Solid Films*. 2015. Vol. 594. P. 178–183.
16. Диагностика тонкопленочных структур методом ферромагнитного резонанса : учеб. пособие / Беляев Б. А., Волошин А. С., Изотов А. В. и др. Красноярск, Сибирский федер. ун-т, 2011. 104 с.
17. Belyaev B. A., Izotov A. V., Leksikov A. A. Magnetic imaging in thin magnetic films by local spectrometer of ferromagnetic resonance // *IEEE Sensors Journal*. 2005. Vol. 5, No. 2. P. 260–267.
18. Uniaxial magnetic anisotropy in Pd/Fe bilayers on Al₂O₃ (0001) induced by oblique deposition / C.-S. Chi, B.-Y. Wang, W.-F. Pong et al. // *Journal of Applied Physics*. 2012, Vol. 111. P. 123918.
19. Belyaev B. A., Izotov A. V. FMR Study of the anisotropic properties of an epitaxial Fe₃Si film on a Si(111) Vicinal Surface // *JETP Letters*. 2016. Vol. 103, No. 1. P. 41–45.

References

1. Li C. H., Kioseoglou G., J. van 't Erve O. M., Petrou A. Spin injection across (110) interfaces: Fe/GaAs(110) spin-light-emitting diodes. *Applied Physics Letters*. 2004, Vol. 85, No. 9, P. 1544–1548.
2. Kawaharazuka A., Ramsteiner M., Herfort J., Schonherr H.-P. Spin injection from Fe₃Si into GaAs. *Applied Physics Letters*. 2004, Vol. 85, No. 16, P. 3492–3494.
3. Herper H. C., Entel P. Interface structure and magnetism of Fe₃Si/GaAs(110) multilayers: An ab-initio study. *Philosophical Magazine*. 2008, Vol. 88, No. 18-20, P. 2699–2707.
4. Qian G.-X., Martin R., Chadi J. First-principles calculations of atomic and electronic structure of the GaAs(110) surface. *Physical review. B (Condensed matter)*. 1988, Vol. 37, No. 3, P. 1303–1307.
5. Grunebohm A., Siewert M., Herper H. C., Gruner M. E., Entel P. A comparative study of (Fe, Fe₃Si)/GaAs and Heusler/MgO for spintronics applications. *Journal of Physics: Conference Series*. 2010, Vol. 200, P. 072038.
6. Liou S. H., Malhotra S. S., Shen J. X., Hong M., Kwo J., Chen H.-C., Mannaerts J. P. Magnetic properties of epitaxial single crystal ultrathin Fe₃Si films on GaAs (001). *Journal of Applied Physics*. 1993, Vol. 73, No. 10, P. 6766–6768.
7. Vinzelberg H., Schumann J., Elefant D., Arushanov E., Schmidt O. G. Transport and magnetic properties of Fe₃Si epitaxial films. *Journal of Applied Physics*. 2008, Vol. 104, No. 9, P. 093707–093707.
8. Bowen M., Friedland K.-J., Herfort J., Schönherr H.-P., Ploog K. H. Order-driven contribution to the planar Hall effect in Fe₃Si thin films. *Physical Review B*. 2005, Vol. 71, No. 17, P. 172401.
9. Zakeri K., Hashemifar S. J., Lindner J., Barsukov I., Meckenstock R., Kratzer P., Frait Z., Farle M. Spin and orbital magnetism in ordered Fe_(3±δ)Si_(1∓δ) binary Heusler structures: Theory versus experiment. *Physical Review B*. 2008, Vol. 77, No. 10, P. 104430.
10. Ionescu A., Trypiniotis T., Garcia-Miquel H., Vickers M. E., Dalgliesh R. M., Langridge S., Bugoslavsky Y., Miyoshi Y., Cohen L. F. Structural, magnetic, electronic, and spin transport properties of epitaxial Fe₃Si/GaAs(001). *Physical Review B*. 2005, Vol. 71, No. 9, P. 094401.
11. Hung H. Y., Huang S. Y., Chang P., Lin W. C., Liu Y. C., Lee S. F., Hong M., Kwo J. Strong crystal anisotropy of magneto-transport property in Fe₃Si epitaxial film. *Journal of Crystal Growth*. 2011, Vol. 323, P. 372–375.
12. Hong J. Thickness-dependent magnetic anisotropy in ultrathin FeCo/Cu(001) films. *Physical Review. B.(Condensed matter)*. 2006, Vol. 74, P. 172408
13. Arai K. I., Ohoka Y., Wakui Y. [Preparation and magnetic properties of anodic oxide magnetic films]. *Electronics and Communications in Japan. (Part II Electronics)*. 1989, Vol. 72, No. 5, P. 81–88.

14. Liu X., Shiozaki Y., Morisako A. Magnetization reversal mechanism of ultra thin $\text{Nd}_2\text{Fe}_{14}\text{B}$ films with perpendicular magnetic anisotropy. *Journal of Applied Physics*. 2008, Vol. 103, P. 07E104.
15. Park S. J., Liu C.-H., Kim H. S., Park N. J., Jin S., Han J. H. Texture and magnetic properties of Fe thin films fabricated by field-sputtering vs field-annealing. *Thin Solid Films*. 2015, Vol. 594, P. 178–183.
16. Belyaev B. A., Voloshin A. S., Izotov A. V. et al. *Diagnostika tonkoplenochnykh struktur metodom ferromagnitnogo rezonansa : uchebnoe posobie* [Thin-film structures investigation by the ferromagnetic resonance: a tutorial]. Krasnoyarsk, Siberian Federal University, 2011, 104 p.
17. Belyaev B. A., Izotov A. V., Leksikov A. A. Magnetic imaging in thin magnetic films by local spectrometer of ferromagnetic resonance. *IEEE Sensors Journal*. 2005, Vol. 5, No. 2, P. 260–267.
18. Chi C.-S., Wang B.-Y., Pong W.-F., Ho T.-Y., Tsai C.-J., Lo F.-Y., Chern M.-Y., Lin W.-C. Uniaxial magnetic anisotropy in Pd/Fe bilayers on Al_2O_3 (0001) induced by oblique deposition. *Journal of Applied Physics*. 2012, Vol. 111, P. 123918.
19. Belyaev B. A., Izotov A. V. FMR Study of the anisotropic properties of an epitaxial Fe_3Si film on a Si(111) Vicinal Surface. *JETP Letters*. 2016, Vol. 103, No. 1, P. 41–45.

© Яковлев И. А., 2021

Яковлев Иван Александрович – кандидат физико-математических наук, научный сотрудник, Институт физики имени Л. В. Киренского Сибирского отделения Российской академии наук – обособленное подразделение ФИЦ КНЦ СО РАН. E-mail: yia@iph.krasn.ru.

Yakovlev Ivan Aleksandrovich – candidate of physical and mathematical sciences, researcher, Kirensky Institute of Physics, Federal Research Center KSC SB RAS. E-mail: yia@iph.krasn.ru.
